

BRUNA CRISTINA DOS SANTOS CRUZ

**EFFECTS OF PROBIOTIC VSL#3 AND SYNBIOTIC VSL#3 ASSOCIATED WITH
YACON-BASED PRODUCT (PBY) ON GUT MICROBIOTA AND ON THE
DEVELOPMENT OF INTESTINAL DISEASES IN MICE**

Thesis submitted to the Science of Nutrition
Graduate Program of the Universidade Federal
de Viçosa in partial fulfillment of the
requirements for the degree of *Doctor
Scientiae*.

Adviser: Maria do Carmo Gouveia Peluzio

Co-advisers: Célia Lucia de Luces F. Ferreira
Leandro Licursi de Oliveira
Lisiane Lopes da Conceição

**VIÇOSA - MINAS GERAIS
2022**

**Ficha catalográfica elaborada pela Biblioteca Central da Universidade
Federal de Viçosa - Campus Viçosa**

T

Cruz, Bruna Cristina dos Santos, 1988-
C957e Effect of probiotic VSL#3 and synbiotic VSL#3 associated
2022 with yacon-based product (PBY) on gut microbiota and on the
development of intestinal diseases in mice: Effect of probiotic
and synbiotic on gut microbiota and on the development of
intestinal diseases in mice / Bruna Cristina dos Santos Cruz. –
Viçosa, MG, 2022.

1 tese eletrônica (249 f.): il. (algumas color.).

Inclui anexos.

Orientador: Maria do Carmo Gouveia Peluzio.

Tese (doutorado) - Universidade Federal de Viçosa,
Departamento de Nutrição e Saúde, 2022.

Inclui bibliografia.

DOI: <https://doi.org/10.47328/ufvbbt.2022.025>

Modo de acesso: World Wide Web.

1. Reto - Câncer. 2. Intestinos - Microbiologia.
3. Probióticos. 4. Simbióticos. I. Peluzio, Maria do Carmo
Gouveia, 1958-. II. Universidade Federal de Viçosa.
Departamento de Nutrição e Saúde. Programa de Pós-Graduação
em Ciência da Nutrição. III. Título.

CDD 22. ed. 616.99435

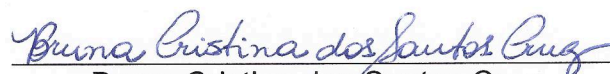
BRUNA CRISTINA DOS SANTOS CRUZ

**EFFECTS OF PROBIOTIC VSL#3 AND SYMBIOTIC VSL#3 ASSOCIATED WITH
YACON-BASED PRODUCT (PBY) ON GUT MICROBIOTA AND ON THE
DEVELOPMENT OF INTESTINAL DISEASES IN MICE**

Thesis submitted to the Science of Nutrition
Graduate Program of the Universidade
Federal de Viçosa in partial fulfillment of the
requirements for the degree of *Doctor
Scientiae*.

APPROVED: January 17, 2022.

Assent:



Bruna Cristina dos Santos Cruz

Author



Maria do Carmo Gouveia Peluzio

Adviser

ACKNOWLEDGEMENTS

To God for the gift of life, health, wisdom and strength to move forward!

To my parents, João and Lucia, for their support, prayers and teachings.

To my siblings, Beatriz and Hebert, for their affection and companionship.

To my nephews, Mariana and Lucas, for making me dream and look for better days!

To Thyago, for his understanding, patience and encouragement.

To my advisor, Profa. Maria do Carmo Gouveia Peluzio, for all her teachings over the years, for her trust, friendship and for making the development of this work viable.

To all my friends and research partners at the Nutritional Biochemistry Laboratory, new and old, who welcomed me and made my daily life lighter: Toninho, Nando, Letícia, Kelly, Milena, Rafaela, Lisiane, Sandra, Mariana Moura, Anderson, Andressa, Mariana Albuquerque and Iasmin.

To my co-supervisors, Célia, Leandro and Lisiane for their guidance and availability.

To the employees, members and partners of the Experimental Nutrition Laboratory (DNS-UFV), Experimental Pathology Laboratory (DBA-UFV), Vegetable Processing Laboratory (DTA-UFV), Lactic Culture Laboratory (Bioagro-UFV), Molecular Immunovirology Laboratory (LIVM-UFV), and Laboratory of Biochemical Analyzes (DBB-UFV), Biomolecules Nucleus, and Microscopy Nucleus (UFV).

To the board members, Professors Célia, Tiago, Vinícius, and Damiana, for their availability and valuable contributions.

To the Universidade Federal de Viçosa, for being my window to the world!

To the Conselho Nacional de Desenvolvimento Científico e Tecnológico (CNPq), for granting the scholarship.

To the Fundação de Amparo à Pesquisa do Estado de Minas Gerais (FAPEMIG) for the financial support.

This study was financed in part by the Coordenação de Aperfeiçoamento de Pessoal de Nível Superior – Brasil (CAPES) – Finance Code 001.

BIOGRAPHY

Bruna Cristina dos Santos Cruz, daughter of João Martins dos Santos Cruz and Maria Lúcia dos Santos Cruz, was born on October 7, 1988, in the city of Guiricema - Minas Gerais. In March 2009, she joined the Nutrition course at the Universidade Federal de Viçosa (UFV), obtaining the title of Nutritionist on January 21, 2014. In March of the same year she started the Multiprofessional Residency course in Oncology at the National Cancer Institute (INCA-RJ), ending in February 2016. During this period, she completed a postgraduate degree in Phytotherapy and Clinical and Sports Supplementation, at Universidade Estácio de Sá. In March 2016, she started the Masters in Nutrition Science, at the UFV, ending in February 2018.

ABSTRACT

CRUZ, Bruna Cristina dos Santos, D.Sc., Universidade Federal de Viçosa, January, 2022. **Effects of probiotic VSL#3 and synbiotic VSL#3 associated with yacon-based product (PBY) on gut microbiota and on the development of intestinal diseases in mice.** Adviser: Maria do Carmo Gouveia Peluzio. Co-advisers: Célia Lúcia de Luces Fortes Ferreira, Leandro Licursi de Oliveira and Lisiane Lopes da Conceição.

Intestinal diseases, including colorectal cancer (CRC) and inflammatory bowel diseases (IBD) have high prevalence and mortality rates worldwide. Although there is a genetic component associated with the etiology of these diseases, the participation of environmental and lifestyle-related factors in their development has been increasingly demonstrated. Changes in the composition and activity of the intestinal microbiota, which may be associated, for example, with inadequate feeding, seem to contribute to the increased risk of development of both CRC and IBD. Thus, it is increasing and justifiable the search for food or no-food compounds, that can reestablish the balance of the microbiota and modify the intestinal microenvironment, reducing the risk of diseases. The use of probiotics and prebiotics, isolated or combined (synbiotic), is one of the main strategies for targeted modulation of the microbiota, either by adding specific microorganisms or by conferring a selective advantage on resident microorganisms. The general objective of this study was to investigate the effects of probiotic VSL#3 and synbiotic VSL#3 associated with yacon-based product (PBY), on the modulation of the gut microbiota and its influence on the development of precursor lesions of CRC and on the manifestations of colitis-associated carcinogenesis (CAC). For this, two distinct experiments were conducted: in *Experiment 1*, wild C57BL6/J mice received, for 13 consecutive weeks, the probiotic multispecies VSL#3 isolated (probiotic group - PRO) or associated with PBY (synbiotic group - SYN) and were induced to colorectal carcinogenesis with 1,2-dimethylhydrazine (DMH). In *Experiment 2*, knockout mice for interleukin-10 (IL-10^{-/-}), a spontaneous colitis model, were induced to carcinogenesis with DMH and received the synbiotic VSL#3 + PBY for the same period. In *Manuscript 1 (Published)* (Experiment 1), our aim was to evaluate the effects of probiotic and synbiotic on the composition of the intestinal microbiota and their influence on the development of precursor lesions of CRC. It was observed that both the use of probiotic and synbiotic

modified the composition of the microbiota; changes in the microbiota of the control group were also observed, confirming that carcinogenesis itself alters the resident microbial community. The precursor lesions of CRC were significantly reduced in the SYN group, but not in the PRO group. This outcome is possibly associated with changes in the intestinal microenvironment induced by microbiota modulation in the SYN group, such as significant reduction of inflammatory response in the colon, reduction of the activity of the pro-carcinogenic enzyme β -glucuronidase, and increase in short-chain fatty acids (SCFA). *Manuscript 2 (Published)* (Experiment 1) sought to investigate possible mechanisms of action associated or that could explain the results obtained in Article 1. Thus, the effects of probiotic and synbiotic on oxidative stress and intestinal permeability were investigated. Probiotic and synbiotic have antioxidant activity *in vitro*. Both PRO and SYN groups had lower concentrations of oxidation products, manlondialdehyde and protein carbonyl, compared to the control group. The activity of the antioxidant enzyme catalase was higher in the SYN group compared to the others. It was also observed an increase in the depth crypts in the PRO and SYN groups, which corroborates the reduction in intestinal permeability (measured by urinary lactulose excretion) in these groups. *Manuscript 3 (Submitted)* (Experiment 1) evaluated the effect of probiotic and synbiotic on the functional metabolic pathways of the microbiota and on the expression of genes associated with colorectal carcinogenesis. The SYN group showed a highly differentiated intestinal community based on the MetaCyc pathways. Of the 351 predicted functional pathways, 222 differed between groups. Most of them were enriched in the SYN group, namely: amino acid biosynthesis pathways, small molecule biosynthesis pathways, carbohydrate degradation pathways, and fermentation pathways. In addition, synbiotic was able to stimulate the anti-inflammatory immune response and reduce gene expression of PCNA and c-myc. As demonstrated in these studies, the use of the synbiotic VSL#3 + PBY significantly reduced the incidence of precursor lesions of CRC and down-regulated the expression of genes associated with carcinogenesis. We believe that these findings are the result of the synbiotic influence on the composition and activity of the intestinal microbiota, notably through reduced inflammatory response, improved oxidative stress, reduced pro-carcinogenic enzyme activity, increased SCFA and reduced permeability intestinal. *Manuscript 4 (Published)* (Experiment 2) aimed to evaluate the effect of the synbiotic VSL#3 + PBY in a colitis-associated carcinogenesis (CAC) model. Preservation of intestinal architecture, increased activity of antioxidant

enzymes superoxide dismutase and catalase, and AGCC concentrations, especially butyrate, were observed. Regarding the composition of the intestinal microbiota, we highlight that the microbiota of the experimental model used was characterized by a restricted biodiversity, with a limited number of bacterial genera representing the total microbial community. This finding has been consistently demonstrated in cases of cancer in experimental models and in humans, and in IBD patients. In Manuscript 5 (Submission process) (Experiment 2), we investigate the effects of the synbiotic VSL#3 and PBV on the intestinal inflammatory response, expression of genes associated with colorectal carcinogenesis, β -glucuronidase enzyme activity, functional metabolic pathways of the microbiota, and production of fecal fatty acids. Lower expression of p53 and c-myc in the synbiotic group compared to control group was observed. Similarly, IL-17 levels were also lower. There was also an increase in IL-4 in the synbiotic group compared to negative control. The principal component analysis revealed a poorly differentiated intestinal community based on MetaCyc pathways. These findings support the similarity in predicted metabolic pathways between groups. There was also a reduction in the activity of the β -glucuronidase enzyme and an increase in short-chain fatty acids in the synbiotic group. Thus, it is suggested that the synbiotic could be a novel potential health-protective natural agent against CAC.

Keywords: Colorectal cancer. Inflammatory bowel disease. Gut microbiota. Probiotic. Prebiotic. Synbiotic.

RESUMO

CRUZ, Bruna Cristina dos Santos, D.Sc., Universidade Federal de Viçosa, janeiro de 2022. **Efeitos do probiótico VSL#3 e do simbiótico VSL#3 associado ao produto à base de yacon (PBY) na microbiota intestinal e no desenvolvimento de doenças intestinais em camundongos.** Orientadora: Maria do Carmo Gouveia Peluzio. Coorientadores: Célia Lúcia de Luces Fortes Ferreira, Leandro Licursi de Oliveira e Lisiane Lopes da Conceição.

As doenças intestinais, dentre elas o câncer colorretal (CCR) e as doenças inflamatórias intestinais (DII), apresentam altas taxas de prevalência e mortalidade no mundo. Embora exista um componente genético associado à etiologia dessas enfermidades, cada vez mais tem sido demonstrada a participação de fatores ambientais e relacionadas ao estilo de vida no desenvolvimento das mesmas. As alterações na composição e na atividade da microbiota intestinal, que podem estar associadas, por exemplo, à alimentação inadequada, parecem contribuir para o aumento do risco de desenvolvimento tanto do CCR quanto das DII. Assim, é crescente e justificável a busca por compostos alimentares ou não, que possam reestabelecer o equilíbrio da microbiota e modificar o microambiente intestinal, reduzindo o risco de doenças. O uso de probióticos e prebióticos, isolados ou combinados (simbiótico), é uma das principais estratégias de modulação direcionada da microbiota, seja pela adição de microrganismos específicos ou por conferir vantagem seletiva aos microrganismos residentes. O objetivo geral deste estudo foi investigar os efeitos do probiótico VSL#3 e do simbiótico VSL#3 associado ao produto à base de yacon (PBY), na modulação da microbiota intestinal e sua influência no desenvolvimento de lesões precursoras do CCR e nas manifestações da carcinogênese associada à colite (CAC). Para isso, foram conduzidos dois experimentos distintos: no *Experimento 1*, camundongos C57BL6/J selvagens receberam, por 13 semanas consecutivas, o probiótico multiespécies VSL#3 isolado (grupo probiótico - PRO) ou associado ao PBY (grupo simbiótico - SYN) e foram induzidos à carcinogênese colorretal com 1,2-dimetilhidrazina (DMH). Já no *Experimento 2*, camundongos nocautes para interleucina-10 (IL-10^{-/-}), um modelo de colite espontânea, foram induzidos à carcinogênese com DMH e receberam o simbiótico VSL#3 + PBY pelo mesmo período. No *Artigo 1 (Publicado)* (Experimento

1), nosso objetivo foi avaliar os efeitos do probiótico e do simbiótico na composição da microbiota intestinal e sua influência no desenvolvimento de lesões precursoras do CCR. Foi observado que, tanto o uso do probiótico quanto do simbiótico modificaram a composição da microbiota; também foram observadas modificações na microbiota do grupo controle, confirmando que a carcinogênese em si altera a comunidade microbiana residente. As lesões precursoras do CRC foram reduzidas significativamente no grupo SYN, mas não no grupo PRO. Esse desfecho possivelmente está associado às modificações no microambiente intestinal, induzidas pela modulação da microbiota no grupo SYN, como a redução significativa da resposta inflamatória no cólon, a redução da atividade da enzima pró-carcinogênica β -glucuronidase, e o aumento dos ácidos graxos de cadeia curta (AGCC). O *Artigo 2 (Publicado)* (Experimento 1) buscou averiguar possíveis mecanismos de ação associados ou que pudessem explicar os resultados obtidos no Artigo 1. Assim, foram investigados os efeitos do probiótico e do simbiótico no estresse oxidativo e na permeabilidade intestinal. Foi demonstrado que o probiótico e o simbiótico possuem atividade antioxidante *in vitro*. Ambos os grupos PRO e SYN apresentaram menores concentrações dos produtos de oxidação, malondialdeído (MDA) e proteína carbonilada (PC), comparados ao grupo controle. A atividade da enzima antioxidante catalase (CAT) foi maior no grupo SYN comparado ao demais. Observou-se ainda, aumento da profundidade das criptas intestinais nos grupos PRO e SYN, o que corrobora a redução da permeabilidade intestinal (medida pela excreção de lactulose urinária) nesses grupos. No *Artigo 3 (Submetido)* (Experimento 1) foi avaliado o efeito do probiótico e do simbiótico nas vias metabólicas funcionais da microbiota e na expressão de genes associados à carcinogênese colorretal. O grupo SYN apresentou a comunidade intestinal altamente diferenciada com base nas vias MetaCyc. Das 351 vias funcionais previstas, 222 diferiram entre os grupos, sendo a maioria enriquecidas no grupo SYN, a saber: vias de biossíntese de aminoácidos, vias de biossíntese de pequenas moléculas, vias de degradação de carboidratos e vias de fermentação. Além disso, o simbiótico foi capaz de estimular a resposta imune anti-inflamatória e reduzir a expressão gênica de PCNA e c-myc. Como demonstrado nestes estudos, o uso do simbiótico VSL#3 + PBY reduziu significativamente a incidência de lesões precursoras do CCR e regulou negativamente a expressão de genes associados à carcinogênese. Acreditamos que esses achados sejam resultantes da influência do simbiótico sobre a composição e a atividade da microbiota intestinal, notavelmente

por meio da redução da resposta inflamatória, melhora do estresse oxidativo, redução da atividade de enzima pró-carcinogênica, aumento dos AGCC e redução da permeabilidade intestinal. O Artigo 4 (Publicado) (Experimento 2), teve como objetivo avaliar o efeito do simbiótico VSL#3 + PBY em um modelo de carcinogênese associado à colite (CAC). Foi observado a preservação da arquitetura intestinal, o aumento da atividade das enzimas antioxidantes SOD e CAC, e das concentrações dos AGCC, especialmente o butirato. Em relação à composição da microbiota intestinal, destacamos que o modelo experimental utilizado foi caracterizado por uma biodiversidade restrita, com um número limitado de gêneros bacterianos representando a comunidade microbiana total. Este achado é consistentemente demonstrado em casos de câncer em modelos experimentais e em humanos, e em pacientes com DII. No Artigo 5 (*Em processo de submissão*) (*Experimento 2*), investigamos os efeitos do simbiótico VSL # 3 e PBY na resposta inflamatória intestinal, na expressão de genes associados à carcinogênese colorretal, na atividade da enzima β -glucuronidase, nas vias metabólicas funcionais da microbiota e na produção de ácidos graxos fecais. Foi observada menor expressão de p53 e c-myc no KOSYN em comparação com o grupo controle. Da mesma forma, os níveis de IL-17 também foram menores. Houve um aumento de IL-4 no KOSYN em comparação com o controle negativo. A análise de componentes principais revelou uma comunidade intestinal pouco diferenciada com base nas vias MetaCyc. Esses achados corroboram a similaridade nas vias metabólicas preditas entre os grupos. Também houve redução da atividade da enzima β -glucuronidase e aumento dos AGCC no grupo simbiótico. Assim, sugere-se que o simbiótico pode ser um novo agente natural potencial protetor da saúde contra o CAC.

Palavras-chave: Cancer colorretal. Doença inflamatória intestinal. Microbiota intestinal. Probiótico. Prebiótico. Simbiótico.

LIST OF ILLUSTRATIONS

Manuscript 1

Figure 1. Effect of probiotic and synbiotic on (A) fecal pH, and (B) fecal score in C57BL/6J mice. Data are expressed as the mean \pm SD (n=15/group). Statistical differences between groups were analyzed by ANOVA test. (*) $p < 0.05$. CON, AIN-93M diet; PRO, AIN-93M diet and probiotic VSL#3®; SYN, AIN-93M diet with PBV and probiotic VSL#3®..... 44

Figure 2. Photomicrograph of the colon of C57BL/6J mice induced to colorectal carcinogenesis with DMH, stained with 0.1% methylene blue. (a) normal crypts; (b) ACF with two aberrant crypts (indicated by the arrow)..... 45

Figure 3. Effect of probiotic and synbiotic on colon cytokine profile in C57BL/6J mice. Data are expressed as the mean \pm SD (n= 6 or 7/group). Statistical differences between groups were analyzed by ANOVA test. (*) $p < 0.05$. CON, AIN-93M diet; PRO, AIN-93M diet and probiotic VSL#3®; SYN, AIN-93M diet with PBV and probiotic VSL#3®..... 46

Figure 4. Effect of probiotic and synbiotic on bacterial enzyme activity β -glucuronidase in C57BL/6J mice. Data are expressed as the mean \pm SD (n=7/group). Statistical differences between groups were analyzed by ANOVA test. (*) $p < 0.05$. CON, AIN-93M diet; PRO, AIN-93M diet and probiotic VSL#3®; SYN, AIN-93M diet with PBV and probiotic VSL#3®..... 47

Figure 5. Effect of probiotic and synbiotic on fecal concentrations of short-chain fatty acids, (A) acetate, (B) propionate e (C) butyrate, before (t_0), during (t_1 , t_2), and after (t_3) intervention..... 48

Figure 6. Box and whisker plots comparing species richness (A) and diversity between (B and C) the different groups (CON, PRO, and SYN) before (t_0) and after (t_3) their respective intervention. Horizontal bold lines show the median values. The bottom and top of the boxes show the 25th and the 75th percentiles, respectively. The whiskers

extend up to the most extreme points within 1.5 times the interquartile ranges (IQR). Different letters indicate significant differences between groups (Tukey's test, $p < 0.05$)..... 49

Figure 7. Principal coordinate analysis (PCoA) based on (A) Weighted and (B) Un-weighted UniFrac distances for CON, PRO and SYN before (t_0) and after (t_3) their respective intervention. PERMANOVA with 99,999 permutations was used to detect significant differences between microbial communities (dissimilarity) of different exper-imental groups..... 50

Figure 8. Relative abundance distribution of major phyla (A), families (B), and genera (C) across the groups CON, PRO and SYN in two different time-points (t_0 and t_3). Only families and genera with relative abundance greater than 0.05% were shown. The taxa were sorted by the decreasing order of average relative abun-dance..... 53

Figure 9. A Venn diagram showing the number of differentially abundant genera (Fold change ≥ 2 ; FDR $p < 0.05$) associated with each group (CON, PRO, and SYN) at the time-points t_0 and t_1 . Green and red values indicate, respectively, an increase or a reduction in the relative abundance of a certain genus observed after the intervention in the different groups..... 54

Figure 10. Canonical correspondence analysis (CCA) performed on the most abundant OTUs (relative abundance $\geq 0.05\%$) at the family (A) and genus (B) levels, shorty-chain fatty acids (SCFA) (acetate, butyrate, and propionate) and fecal pH. Green lines indicate the direction and magnitude of measurable variables (SCFA and fecal pH) associated with community structures. Ellipses, colored according to the group, as-sume a bivariate normal distribution and estimate a region where 95% of population points are expected to fall..... 57

Supplementary Figure 1. Phylum level composition in mice feces observed in CON, PRO and SYN groups before (t_0) and after (t_3) their respective intervention. Color-coded bar plots show the mean bacterial proportion (%). Only phyla with significant differences are shown (FDR < 0.05)..... 79

Supplementary Figure 2. Column bar graph of *Firmicutes/Bacteroidetes* ratios CON, PRO and SYN groups at the time-points *t0* (before the experimental period) and *t1* (end of the experimental period)..... 80

Supplementary Figure 3. Family level composition in mice feces observed in CON, PRO and SYN groups before (*t0*) and after (*t1*) their respective intervention. Color-coded bar plots show the mean bacterial proportion (%). Only families with significant differences are shown (FDR < 0.05)..... 91

Manuscript 2

Figure 1. Effect of probiotic and synbiotic on (a) cecum weight, (b) colon weight, and (c) colon length in a colorectal carcinogenesis model. The data were expressed as mean \pm SD (n = 15/group). Statistical difference between groups was analyzed by Anova test or Kruskal–Wallis test. (*) p < 0.05. CON, AIN-93 M diet; PRO, AIN-93 M diet and probiotic VSL#3; SYN, AIN-93 M diet with PBV and probiotic VSL#3..... 104

Figure 2. Effect of probiotic and synbiotic on intestinal morphometry in a colorectal carcinogenesis model. (a) Crypt depth, (b) submucosa layer, (c) muscularis layer, and (d) external muscularis layer. The data were expressed as mean \pm SD (n = 7/group). Statistical difference between groups was analyzed by Anova test or Kruskal-Wallis test. (*) p < 0.05. CON, AIN-93 M diet; PRO, AIN-93 M diet and probiotic VSL#3; SYN, AIN-93 M diet with PBV and probiotic VSL#3..... 105

Figure 3. Effect of probiotic and synbiotic on histopathological score in a colorectal carcinogenesis model. (a) Total histopathological score, (b) histopathological score parameters, and (c) illustrative photomicrography of the colon of mice induced to carcinogenesis colorectal stained with hematoxylin-eosin (HE). Orange arrow: extensive area of inflammatory infiltrate (submucosa); red arrow: preserved colonic crypts and damaged crypt transition area; green arrow: preserved crypts and epithelium (scale bars, 100 μ m). The data were expressed as mean \pm SD (n = 7/group). Statistical difference between groups was analyzed by Anova test or Kruskal–Wallis test. (*) p <

0.05. CON, AIN-93 M diet; PRO, AIN-93 M diet and probiotic VSL#3; SYN, AIN-93 M diet with PBY and probiotic VSL#3..... 106

Figure 4. Effect of probiotic and synbiotic on biochemical markers in a colorectal carcinogenesis model. (a) aspartate aminotransferase, (b) alanine aminotransferase, (c) alkaline phosphatase, (d) gamma-glutamyl transferase, (e) area, (f) creatinine, and (g) albumin. The data were expressed as mean \pm SD (n = 15/group). Statistical difference between groups was analyzed by Anova test or Kruskal–Wallis test..... 108

Manuscript 3

Figure 1. Principal Component Analysis (PCA) based on the normalized abundance of predicted MetaCyc pathways across the different groups (CON, PRO and SYN)..... 134

Figure 2. Heatmap (A) of the predicted functional categories (MetaCyc pathways) obtained from fecal microbiota of C57BL6 mice after the different interventions. Only statistically significant features were considered (222 metabolic pathways in total). Functional level extended error bar chart profile between the groups PRO and SYN (B), as well as CON vs SYN (C)..... 135

Figure 3. Taxonomic contributors at the family level identified in fecal samples of C57BL6 mice determined by FishTaco (A). The bar on the top-right of Y axis represents SYN-associated families driving the enrichment in the functional module, whereas the bar on the top-left of Y axis indicates SYN-associated families attenuating functional shift. The bar on the bottom-right of Y axis represents families depleted in the SYN group driving functional shift, whereas the bar on the bottom-left of Y axis shows families depleted in the SYN group attenuating functional shift. White diamonds represent family-based functional shift scores. (B) Overlapped stacked bar chart of SYN-associated families and genera driving the enrichment of selected KO pathways in fecal samples across the groups CON, PRO and SYN..... 136

Figure 4. Effect of probiotic and synbiotic on gene expression in C57BL/J mice induced to colorectal tumorigenesis. (A) c-myc, (B) p53, (C) PCNA, and (D) caspase-3. Gene expression was calculated in relation to the constitutive GAPDH gene and presented as a relative variation of the control group. The data are expressed as mean \pm SD (n=6 or 7/group). Statistical difference between groups were analyzed by ANOVA test or Kruskal-Wallis test, (*) p < 0.05. CON, AIN-93M diet; PRO, AIN-93M diet and probiotic VSL#3; SYN, AIN-93M diet with PBY and probiotic VSL#3..... 137

Figure 5. Effect of probiotic and synbiotic on cytokine profile in colon tissue in C57BL/J mice induced to colorectal tumorigenesis. (A) IL-4/IFN, (B) IL-4/IL-10, (C) IFN/IL-10, (D) IL-10/IL-6, and (E) IL-10/TNF. The data are expressed as mean \pm SD (n=6 or 7/group). Statistical difference between groups were analyzed by ANOVA test or Kruskal-Wallis test, (*) p < 0.05. CON, AIN-93M diet; PRO, AIN-93M diet and probiotic VSL#3; SYN, AIN-93M diet with PBY and probiotic VSL#3..... 139

Figure 6. Effect of probiotic and synbiotic on fecal concentrations of branched chain fatty acids in C57BL/J mice induced to colorectal tumorigenesis. (A) isobutyric, (B) valeric, and (C) isovaleric. The data are expressed as mean \pm SD (n=7/group). Statistical difference between groups were analyzed by ANOVA test or Kruskal-Wallis test, (*) p < 0.05. CON, AIN-93M diet; PRO, AIN-93M diet and probiotic VSL#3; SYN, AIN-93M diet with PBY and probiotic VSL#3..... 140

Manuscript 4

Figure 1. Experimental timeline for colitis-associated colorectal carcinogenesis model with synbiotic administration. Carcinogenesis was initiated with eight injections of DMH (20 mg/kg), once a week. The VSL#3® was administered via gavage (10⁹ CFU/day) and the PBY added to the standard diet throughout the experiment. After thirteen weeks, IL-10-deficient mice were sacrificed and tissues and feces were harvested..... 170

Figure 2. Effect of synbiotic on (A) dietary intake, (B) body weight and (C) food efficiency (CFE) in colitis-associated carcinogenesis model. *p-value lesser than 0.05 using Student's t-test between control (KOCON) and synbiotic-treated group (KO-SYN)..... 176

Figure 3. Effect of synbiotic on disease activity index (DAI) in colitis-associated carcinogenesis model. *p-value lesser than 0.05 using Student's t-test between control (KOCON) and synbiotic-treated group (KOSYN)..... 177

Figure 4. Effect of synbiotic on intestinal morphometry in colitis-associated carcinogenesis model. (A) crypt depth, (B) submucosa, (C) muscularis, (D) external muscularis, and (E) illustrative photomicrography of the intestinal morphometry. Red arrow: measure of crypt depth; blue arrow: muscularis layer; orange arrow: external muscularis layer (scale bars, 100 μ m). *p-value lesser than 0.05 using Student's t-test between control (KOCON) and synbiotic-treated group (KOSYN)..... 178

Figure 5. Effect of synbiotic on histopathological score in colitis-associated carcinogenesis model. (A) histopathological score, (B) components of histopathological score, and (C) illustrative photomicrography of the colon of IL-10-deficient mice, stained with Hematoxylin-Eosin (HE). Orange arrow: preserved crypts and epithelium; black arrow: infiltration in the submucosa; red arrow: preserved colonic crypts and damaged crypt transition area; green arrow: extensive area of damaged crypts (scale bars, 100 μ m). *p-value lesser than 0.05 using Student's t-test between control (KOCON) and synbiotic-treated group (KO-SYN).....179

Figure 6. Effect of synbiotic on liver concentrations of (A) MDA, malondialdehyde, and (B) CP, carbonylated protein, and on antioxidants enzymes expression (C) SOD, superoxide dismutase, (D) CAT, catalase, and (E) GST, glutathione-S-transferase in colitis-associated carcinogenesis model. *p- value lesser than 0.05 using Student's t-test between control (KOCON) and synbiotic-treated group (KO-SYN)..... 180

Figure 7. Microbiome characterization before (*t0*) and after (*t1*) using the synbiotic in colitis-associated carcinogenesis model. (A) Multidimensional scaling (MDS), (B) Shannon Index, (C) Simpson Index, and (D) Chao-1 Index. Red and blue colors represent the control group before and after treatment, respectively. Green and cyan colors represent the synbiotic group before and after the treatment..... 182

Figure 8. Relative abundance (%) of Phylum, Family and Genus levels before (*t0*) and after (*t1*) use the synbiotic in colitis-associated carcinogenesis model..... 182

Manuscript 5

Figure 1. Effect of synbiotic VSL#3 + PBV on (A) food intake, and (B) body weight in colitis-associated carcinogenesis model. The data were expressed as mean \pm SD. Statistical differences between groups were analyzed by *ANOVA test*, (*) $p < 0.05$. KONEG, AIN-93M diet, without induction with DMH; KOCON, AIN-93M diet, induced with DMH; KOSYN, AIN-93M diet with PBV and probiotic VSL#3, induced with DMH..... 216

Figure 2. Effect of synbiotic VSL#3 + PBV on gene expression in colitis-associated carcinogenesis model. (A) p53, (B) c-myc, (C) PCNA, and (D) caspase-3. Gene expression was calculated in relation to the constitutive GAPDH gene and presented as a relative variation of the control group. The data are expressed as mean \pm SD. Statistical difference between groups were analyzed by *ANOVA test* or *Kruskal-Wallis test*, (*) $p < 0.05$. KONEG, AIN-93M diet, without induction with DMH; KOCON, AIN-93M diet, induced with DMH; KOSYN, AIN-93M diet with PBV and probiotic VSL#3, induced with DMH..... 217

Figure 3. Effect of synbiotic VSL#3 + PBV on cytokine profile in colon tissue in colitis-associated carcinogenesis model. (A) IL-2, (B) IL-4, (C) IL-6, (D) IL-17, and (E) TNF. The data are expressed as mean \pm SD. Statistical difference between groups were analyzed by *ANOVA test* or *Kruskal-Wallis test*, (*) $p < 0.05$. KONEG, AIN-93M diet, without induction with DMH; KOCON, AIN-93M diet, induced with DMH; KOSYN, AIN-93M diet with PBV and probiotic VSL#3, induced with DMH..... 219

Figure 4. Principal Component Analysis (PCA) based on the normalized abundance of predicted MetaCyc pathways across the different groups (KONEG, KOCON, and KOSYN)..... 220

Figure 5. Predicted functional categories (MetaCyc pathways) obtained from the fecal microbiota of IL-10^{-/-} mice after intervention. Only statistically significant features were considered (10 metabolic pathways in total, with significant *post hoc*). Functional level extended error bar chart profile between the groups KONEG, KOCON and KOSYN..... 221

Figure 6. Effect of synbiotic VSL#3 + PBY on β -glucuronidase activity in colitis-associated carcinogenesis model. The data were expressed as mean \pm SD. Statistical differences between groups were analyzed by *ANOVA test*, (*) $p < 0.05$. KONEG, AIN-93M diet, without induction with DMH; KOCON, AIN-93M diet, induced with DMH; KOSYN, AIN-93M diet with PBY and probiotic VSL#3, induced with DMH..... 222

Figure 7. Effect of synbiotic VSL#3 + PBY on fecal concentrations of fatty acids after (*t0*) and before (*t1*) intervention in colitis-associated carcinogenesis model. The data were expressed as mean \pm SD. Statistical differences between groups were analyzed by *paired t-test* or *Wilcoxon test*, (*) $p < 0.05$. KONEG, AIN-93M diet, without induction with DMH; KOCON, AIN-93M diet, induced with DMH; KOSYN, AIN-93M diet with PBY and probiotic VSL#3, induced with DMH..... 223

Figure 8. Effect of synbiotic VSL#3 + PBY on fecal pH in colitis-associated carcinogenesis model. Data were expressed as mean \pm SD. Statistical differences between groups were analyzed by *ANOVA test*, (*) $p < 0.05$. KONEG, AIN-93M diet, without induction with DMH; KOCON, AIN-93M diet, induced with DMH; KOSYN, AIN-93M diet with PBY and probiotic VSL#3, induced with DMH..... 224

Supplementary Material 1. Functional level box plot chart profile between the groups KONEG, KOCON, and KOSYN..... 240

LIST OF TABLES

Manuscript 1

Table 1. Effects of probiotic and synbiotic on DMH-induced ACF in the colon of C57BL/6 mice.....	45
--	----

Manuscript 2

Table 1. Composition of experimental diets.....	97
---	----

Table 2. Effect of probiotic and synbiotic on oxidation products and antioxidant enzymes activity in C57BL/6 mice	111
---	-----

Manuscript 3

Table 1. qRT-PCR murine primer sequences used in this study.....	132
--	-----

Manuscript 4

Table 1. Composition of AIN-93M diet for control and synbiotic diet.....	175
--	-----

Table 2. Effect of synbiotic on the production of faecal short-chain fatty acids in colitis-associated colorectal cancer model.....	183
---	-----

Manuscript 5

Table 1. Centesimal composition and oligofructanos content of the yacon-based product (PBY).....	210
--	-----

LIST OF ACRONYMS AND ABBREVIATIONS

AAI	Radical Scavenging Activity
AC	Aberrant Crypts
ACF	Aberrant Crypt Foci
ALT	Alanine Aminotransferase
ANOVA	Analysis of Variance
AST	Aspartate Aminotransferase
ASV	Amplicon Sequence Variants
CAC	Colitis-Associated Cancer
CAT	Catalase
CBA	Cytometric Bead Array
CCA	Canonical Correspondence Analysis
CD	Crohn's Disease
CFE	Coefficient of Food Efficiency
CFU	Colony-Forming Unit
CON	Control Group
CP	Carbonylated Protein
CRC	Colorectal Cancer
DAI	Disease Activity Index
DMH	1,2-Dimethylhydrazine
DNA	Deoxyribonucleic Acid
DPPH	1,1-Diphenyl-2-Picrylhydrazyl
DSS	Dextran Sulfate Sodium
EC	Enzyme Commission
EDTA	Ethylenediaminetetraacetic Acid
FDR	False Discovery Rate
FishTaco	Functional Shifts' Taxonomic Contributors
FOS	Fructooligosaccharides
GAE	Gallic Acid Equivalent
GGT	Gamma-Glutamyl Transferase
GST	Glutathione-S-Transferase
HE	Hematoxylin-Eosin
HPLC	High-Performance Liquid Chromatography

IBD Inflammatory Bowel Disease
IFN Interferon
IL Interleukin
IL-10^{-/-} Interleukin-10-*Knockout* Mice
KEGG Kyoto Encyclopedia of Genes and Genomes
KOCON Interleukin-10-*Knockout* Control Group
KONE Interleukin-10-*Knockout* Negative Control Group
KOSYN Interleukin-10-*Knockout* Synbiotic Group
LAB Lactic Acid Bacteria
MDA Malondialdehyde
MDS Multidimensional Scaling
MetaCyc Metabolic Pathway Database
NLR NOD-like
OTU Operational Taxonomic Unit
PBY Yacon-Based Product
PCNA Proliferating Cell Nuclear Antigen
PCoA Principal Coordinate Analysis
PICRUSt2 Phylogenetic Investigation of Communities by Reconstruction of Unobserved States
PRO Probiotic Group
RF Free Radicals
ROS Rective Oxygen Species
rRNA Ribosomal Ribonucleic Acid
RT-qPCR Quantitative Real-Time Polymerase Chain Reaction
SCFA Short-Chain Fatty Acids
SD Standard Deviation
SOD Superoxide Dismutase
SRA Sequence Read Archive
SYN Synbiotic Group
TNBS Trinitrobenzene Sulfonic Acid
TNF Tumor Necrosis Factor
UC Ulcerative Colitis

SUMMARY

1. INTRODUCTION	23
1.1 References	26
2. OBJECTIVES	29
2.1 General objective	29
2.2 Specifics objectives	29
3. HYPOTESIS	32
4. RESULTS	33
4.1 MANUSCRIPT 1. Synbiotic VSL#3 and yacon-based product modulate the intestinal microbiota and prevent the development of pre-neoplastic lesions in a colorectal carcinogenesis model	33
4.2 MANUSCRIPT 2. Evaluation of the efficacy of probiotic VSL#3 and synbiotic VSL#3 and yacon-based product in reducing oxidative stress and intestinal permeability in mice induced to colorectal carcinogenesis	92
4.3 MANUSCRIPT 3. Synbiotic modulates intestinal microbiota metabolic pathways and inhibits DMH-induced colon tumorigenesis through c-myc and PCNA suppression	124
4.4 MANUSCRIPT 4. Use of the synbiotic VSL#3 and yacon-based concentrate attenuates intestinal damage and reduces the abundance of <i>Candidatus Saccharimonas</i> in a colitis-associated carcinogenesis model	164
4.5. MANUSCRIPT 5. Modulation of metabolic pathways in the intestinal microbiota and on the expression of genes related to tumorigenesis in a colitis-associated carcinogenesis model, using synbiotic VSL#3 and yacon-based product (PBY)	206
5. GENERAL CONCLUSIONS	246
6. ATTACHMENT	247

1. INTRODUCTION

Intestinal diseases are those that affect any segment of the intestine (small or large intestine), from the duodenum to the rectum. The term encompasses acute or chronic conditions and covers a wide range of diseases including constipation, diverticular disease, irritable bowel syndrome, intestine cancer, and inflammatory bowel diseases. Among these diseases, colorectal cancer (CRC) has a worrying epidemiological condition, due to its high incidence, prevalence and mortality rates worldwide (Wijnands et al., 2021).

Over 1.8 million new CRC cases and 881,000 deaths were estimated in 2018, accounting for about 1 in 10 cancer cases and deaths in the world. Overall, CRC ranks third in terms of incidence but second in terms of mortality. Incidence rates are about 3-fold higher in transitioned versus transitioning countries; however, with average case fatality higher in lower human development index settings, there is less variation in the mortality rates (Bray et al., 2018).

There are a large number of factors that play a direct role in driving the polyp - CRC sequence, including, but not limited to, gene mutations, epigenetic alterations, and local inflammatory changes. The polyp to cancer progression sequence was proposed in the seminal and classic tumor progression model of Fearon and Vogelstein and involves a step that initiates the formation of benign neoplasms (adenomas and sessile serrated polyps); followed by a step that promotes the progression to more histologically advanced neoplasms; and then a step that transforms the tumors to invasive carcinoma (Fearon & Vogelstein, 1990; Grady & Markowitz, 2015).

Chronic inflammation of the intestinal epithelium is positively associated with cancer development, and although there are several mechanisms by which inflammation could induce epithelial damage, only a few of those point to a direct source of the DNA lesions necessary for cellular transformation and cancer initiation. The oxidant environment created by activated inflammatory cells in the intestinal epithelium has been associated with carcinogenesis. The colitis-associated cancer (CAC) is a complication of chronic intestinal inflammation (Irrazabal, Thakur, Croitoru & Martin, 2021). It is estimated that patients with colonic inflammatory bowel disease (IBD) have a 1.7-fold increased risk of CRC (Lutgens et al., 2013).

More recently, in addition to genetic and epigenetic risk factors, environmental factors, especially the Western diet and gut microbiota, have been implicated in the genesis of CRC and CAC. In fact, depending on the structure of the microbial community, the microbiota can favor mucosal permeability alterations, bacterial translocation, and activation of the immune system, leading to chronic inflammation (Aprile et al., 2021).

Although there is no consensus on whether changes in the microbiota precede the development of precursor lesions of CRC or not, several studies have demonstrated changes in the composition of the intestinal microbiota in individuals with CRC (Ranjbar et al, 2021; Prosberg et al. 2016). In these cases, enrichment of bacterial species *Streptococcus gallolyticus*, *Fusobacterium nucleatum*, *Escherichia coli*, *Bacteroides fragilis* and *Enterococcus faecalis*, and depletion of taxa short-chain fatty acids (SCFA)-producing, such as the species *Faecalibacterium prausnitzii*, *Clostridium butyricum* and *Butyrivibrio fibrisolvens* the genera Roseburia and Eubacterium, and the families Lachnospiraceae and Ruminococcaceae were observed (Wu et al. 2013; Wang et al. 2011; Balamurugan et al. 2008; Chen et al. 2014).

Thus, knowledge of the intestinal microbiota in health and disease has been useful in two aspects: the first as a possible diagnostic tool - the identification of specific microbial signatures can help in the screening of individuals at high risk of CRC development; second, the composition and functionality of the microbiota can be modulated by intrinsic and extrinsic factors, can be modified as part of CRC preventive strategies.

In this sense, the search for compounds that can modify the microbiota and mitigate the development of CRC is growing. Among these compounds, probiotics and prebiotics, or the combination of both (synbiotics), have received prominence. Classically, probiotics are defined as "live microorganisms that, when administered in adequate amounts, confer benefits to the health of the host" (Hill et al., 2014). Its use is an attempt at targeted modulation of the intestinal microbiota, notably through the addition of specific probiotic strains. On the other hand, prebiotics, which are "substrates that confer health benefits used selectively by host microorganisms", are another strategy of targeted modulation of the microbiota, which aims to confer a selective advantage on resident microorganisms (Gibson et al., 2017).

Several bacterial species are considered probiotic, with lactic acid bacteria (LAB), in particular members of the genera *Lactobacillus* and *Bifidobacterium*, being the most used ones. VSL#3 is a mix of probiotic bacteria, which includes strains of distinct taxa such as *Lactobacillus*, *Bifidobacterium*, and *Streptococcus*, widely used in studies of IBD (Liu et al. 2019; Chung et al. 2017; Rossi et al. 2014). Based on these studies, VSL#3 demonstrated an interesting anti-inflammatory activity and the ability to increase beneficial bacterial species in the colon, however, there is no information on the power to prevent colorectal carcinogenesis.

Yacon (*Smallanthus sonchifolius*) is a tuberous root, considered a prebiotic food due to its high content of fructooligosaccharides (FOS) and inulin, in addition to being rich in phenolic compounds (Russo et al. 2015). Notwithstanding the protective effects of yacon intake on colorectal carcinogenesis having been demonstrated in previous experimental studies (Grancieri et al. 2017; Moura et al. 2012), special attention was given to pre neoplastic lesion development and SCFA production.

This study elucidated, for the first time, that the synbiotic formulation composed of the probiotic VSL # 3 and the yacon-based product (PBY) modifies the composition and activity of the intestinal microbiota, consequently, altering the risk of CRC and CAC. Attenuation of intestinal inflammation, control of cell proliferation, reduction of oxidative stress, improvement in barrier function, increase in SCFA, are some of the outcomes potentially influenced by the modulation of the intestinal microbiota.

1.1 References

Aprile, F., Bruno, G., Palma, R., Mascellino, M. T., Panetta, C., Scalese, G., Oliva, A., Severi, C., & Pontone, S. (2021). Microbiota Alterations in Precancerous Colon Lesions: A Systematic Review. *Cancers*, *13*(12), 3061. <https://doi.org/10.3390/cancers13123061>

Balamurugan R, Rajendiran E, George S, Samuel GV, Ramakrishna BS (2008) Real-time polymerase chain reaction quantification of specific butyrate-producing bacteria, *Desulfovibrio* and *Enterococcus faecalis* in the feces of patients with colorectal cancer. *J Gastroenterol Hepatol* 23(8 Pt 1):1298-1303. doi:10.1111/j.1440-1746.2008.05490.x

Bray, F., Ferlay, J., Soerjomataram, I., Siegel, R. L., Torre, L. A., & Jemal, A. (2018). Global cancer statistics 2018: GLOBOCAN estimates of incidence and mortality worldwide for 36 cancers in 185 countries. *CA: a cancer journal for clinicians*, *68*(6), 394–424. <https://doi.org/10.3322/caac.21492>

Chen L, Wang W, Zhou R, Ng SC, Li J, Huang M, Zhou F, Wang X, Shen B, A Kamm M, Wu K, Xia B (2014) Characteristics of fecal and mucosa-associated microbiota in chinese patients with inflammatory bowel disease. *Md Med J* 93(8):e51

Chung EJ, Do EJ, Kim SY, Cho EA, Kim DH, Pak S, Hwang SW, Lee HJ, Byeon JS, Ye BD, Yang DH, Park SH, Yang SK, Kim JH, Myung SJ (2017) Combination of metformin and VSL#3 additively suppresses western-style diet induced colon cancer in mice. *Eur J Pharmacol* 794:1-7

Fearon, E. R., & Vogelstein, B. (1990). A genetic model for colorectal tumorigenesis. *Cell*, *61*(5), 759–767. [https://doi.org/10.1016/0092-8674\(90\)90186-i](https://doi.org/10.1016/0092-8674(90)90186-i)

Gibson, G. R., Hutkins, R., Sanders, M. E., Prescott, S. L., Reimer, R. A., Salminen, S. J., Scott, K., Stanton, C., Swanson, K. S., Cani, P. D., Verbeke, K., & Reid, G. (2017). Expert consensus document: The International Scientific Association for Probiotics and Prebiotics (ISAPP) consensus statement on the definition and scope of

prebiotics. *Nature reviews. Gastroenterology & hepatology*, 14(8), 491–502. <https://doi.org/10.1038/nrgastro.2017.75>

Grady, W. M., & Markowitz, S. D. (2015). The molecular pathogenesis of colorectal cancer and its potential application to colorectal cancer screening. *Digestive diseases and sciences*, 60(3), 762–772. <https://doi.org/10.1007/s10620-014-3444-4>

Grancieri M, Costa NMB, Vaz Tostes MDG, de Oliveira DS, Nunes LDC, Marcon LDN, Viana ML (2017) Yacon flour (*Smallanthus sonchifolius*) attenuates intestinal morbidity in rats with colon cancer. *J Funct Foods* 37. <https://doi.org/10.1016/j.jff.2017.08.039>

Hill C, Guarner F, Reid G, Gibson GR, Merenstein DJ, Pot B, Morelli L, Canani RB, Flint HJ, Salminen S, Calder PC, Sanders ME (2014) Expert consensus document: The international scientific association for probiotics and prebiotics consensus statement on the scope and appropriate use of the term probiotic. *Nat Rev Gastroenterol Hepatol* 11: 506-514

Irrazabal, T., Thakur, B. K., Croitoru, K., & Martin, A. (2021). Preventing Colitis-Associated Colon Cancer With Antioxidants: A Systematic Review. *Cellular and molecular gastroenterology and hepatology*, 11(4), 1177–1197. <https://doi.org/10.1016/j.jcmgh.2020.12.013>

Liu XJ, Yu R, Zou KF (2019) Probiotic mixture VSL#3 alleviates dextran sulfate sodium-induced colitis in mice by downregulating T follicular helper cells. *Curr Med Sci* 39(3):371-378. doi: 10.1007/s11596-019-2045-z

Lutgens, M. W., van Oijen, M. G., van der Heijden, G. J., Vleggaar, F. P., Siersema, P. D., & Oldenburg, B. (2013). Declining risk of colorectal cancer in inflammatory bowel disease: an updated meta-analysis of population-based cohort studies. *Inflammatory bowel diseases*, 19(4), 789–799. <https://doi.org/10.1097/MIB.0b013e31828029c0>

Moura NA, Caetano BF, Sivieri K, Urbano LH, Cabello C, Rodrigues MA, Barbisan LF (2012) Protective effects of yacon (*Smallanthus sonchifolius*) intake on experimental colon carcinogenesis. *Food Chem Toxicol* 50:2902-10. doi: 10.1016/j.fct.2012.05.006

Prosberg M, Bendtsen F, Vind I, Petersen AM, Gluud LL (2016) The association between the gut microbiota and the inflammatory bowel disease activity: a systematic review and meta-analysis. *Scand J Gastroenterol* 1-9

Ranjbar, M., Salehi, R., Haghjooy Javanmard, S., Rafiee, L., Faraji, H., Jafarpor, S., Ferns, G. A., Ghayour-Mobarhan, M., Manian, M., & Nedaeinia, R. (2021). The dysbiosis signature of *Fusobacterium nucleatum* in colorectal cancer-cause or consequences? A systematic review. *Cancer cell international*, 21(1), 194. <https://doi.org/10.1186/s12935-021-01886-z>

Rossi G, Pengo G, Caldin M, Palumbo Piccionello A, Steiner JM, Cohen ND, Jergens AE, Suchodolski JS (2014) Comparison of microbiological, histological, and idiopathic inflammatory bowel disease. *PLoS One* 10;9(4):e94699. doi: 10.1371/journal.pone.0094699

Russo D, Valentão P, Andrade PB, Fernandez EC, Milella L (2015) Evaluation of antioxidant, antidiabetic and anticholinesterase activities of *Smallanthus sonchifolius* landraces and correlation with their phytochemical profiles. *Int J Mol Sci* 16(8), 17696-17718. <https://doi.org/10.3390/ijms160817696>

Wang T, Cai G, Qiu Y, Fei N, Zhang M, Pang X, Jia W, Cai S, Zhao L (2011) Structural segregation of gut microbiota between colorectal cancer patients and healthy volunteers. *ISME J*. doi:10.1038/ismej.2011.109

Wijnands, A. M., de Jong, M. E., Lutgens, M., Hoentjen, F., Elias, S. G., Oldenburg, B., & Dutch Initiative on Crohn and Colitis (ICC) (2021). Prognostic Factors for Advanced Colorectal Neoplasia in Inflammatory Bowel Disease: Systematic Review and Meta-analysis. *Gastroenterology*, 160(5), 1584–1598. <https://doi.org/10.1053/j.gastro.2020.12.036>

2. OBJECTIVES

2.1 General objective

To investigate the effects of probiotic VSL#3 and/or synbiotic VSL#3 associated with the yacon-based product (PBY) on the gut microbiota and its influence on the development of precursor lesions of colorectal cancer and on the manifestations of colitis-associated carcinogenesis *in vivo*.

2.2 Specifics objectives

Manuscript 1

- To evaluate the pH and fecal characteristics after administration of the probiotic and synbiotic;
- To quantify aberrant crypt foci (CRC precursor lesions) after administration of the probiotic and synbiotic;
- To analyze the profile of cytokines in the colon after administration of the probiotic and synbiotic;
- To evaluate the activity of the β -glucuronidase enzyme after administration of the probiotic and synbiotic;
- To quantify faecal short-chain fatty acids (SCFA), before and after administration of the probiotic and synbiotic;
- To evaluate the composition of the intestinal microbiota before and after administration of the probiotic and synbiotic.

Manuscript 2

- To evaluate the antioxidant capacity of probiotic VSL#3 and synbiotic VSL#3 + PBY *in vitro*;
- To determine the concentrations of the total phenolic compounds in PBY;
- To assess the influence of probiotic and synbiotic on body weight and food intake of mice;

- To evaluate the influence of probiotic and synbiotic on colon morphometry and histopathological changes;
- To quantify serum markers (aspartate aminotransferase, alanine aminotransferase, alkaline phosphatase, gamma-glutamyl transferase, urea, and creatinine) after using the probiotic and synbiotic;
- To determine urinary lactulose concentrations after administration of the probiotic and synbiotic;
- To evaluate the activity of hepatic and cecal antioxidant enzymes (catalase, superoxide dismutase and glutathione) and the concentrations of oxidation products (malondialdehyde and protein carbonyl) after administration of the probiotic and synbiotic.

Manuscript 3

- Evaluate the effects of probiotic and synbiotic on the metabolic pathways of the intestinal microbiota;
- Quantify the expression of genes related to colorectal carcinogenesis;
- Determine the profile of cytokines in the colon after administration of the probiotic and synbiotic;
- Determine the concentrations of branched chain fatty acids (BCFA) after administration of the probiotic and synbiotic.

Manuscript 4

- To assess the influence of synbiotic on body weight and food intake;
- To quantify serum markers (albumin, urea, and creatinine) after administration of the synbiotic;
- To evaluate the effects of synbiotic in the manifestations of colitis throughout the experimental period;
- To evaluate the influence of synbiotic on colon morphometry and histopathological changes;
- To evaluate the activity of liver antioxidant enzymes and the concentrations of oxidation products after administration of the synbiotic;

- To evaluate the composition of the intestinal microbiota before and after using the synbiotic.

Manuscript 5

- To assess the influence of synbiotic on body weight and food intake of mice;
- To quantify the expression of genes related to colorectal carcinogenesis;
- To determine the profile of cytokines in the spleen and colon after administration of the synbiotic;
- To evaluate the effects of probiotic and synbiotic on the metabolic pathways of the intestinal microbiota;
- To evaluate the activity of the β -glucuronidase enzyme;
- To determine the concentrations of short-chain fatty acids before and after using synbiotic;
- To evaluate the pH and fecal characteristics after using the synbiotic.

3. HYPOTESIS

-The use of probiotic VSL#3 and the synbiotic VSL#3 associated with the yacon-based product (PBY) modify the composition and activity of the intestinal microbiota and, as a result, will reduce the risk of developing colorectal cancer precursor lesions and mitigate the manifestations of colitis-associated carcinogenesis.

-The combination of probiotic plus prebiotic brings additional benefits to the balance of the intestinal microbiota and will improve overall parameters when compared to the use of probiotic alone.

4. RESULTS

4.1 MANUSCRIPT 1

Manuscript published in **Applied Microbiology and Biotechnology** (Impact Factor: 4,813) (Attachment 1)

Synbiotic VSL#3 and yacon-based product modulate the intestinal microbiota and prevent the development of pre-neoplastic lesions in a colorectal carcinogenesis model.

Bruna Cristina dos Santos Cruz¹, Vinícius da Silva Duarte², Alessio Giacomini², Viviana Corich², Sérgio Oliveira de Paula³, Lilian da Silva Fialho⁴, Valéria Monteze Guimarães⁵, Célia Lúcia de Lucas Fortes Ferreira⁶, Maria do Carmo Gouveia Peluzio¹

¹Nutritional Biochemistry Laboratory, Department of Nutrition and Health, Universidade Federal de Viçosa, Avenida P. H. Rolfs, Campus Universitário S/N, Viçosa, Minas Gerais CEP: 36570-900, Brazil

²Department of Agronomy, Food, Natural Resources, Animals and Environment (DAFNAE), University of Padova, Legnaro, Italy

³Immunovirology Laboratory, Department of Biology, Universidade Federal de Viçosa, Viçosa, Minas Gerais, Brazil

⁴Biochemical Analysis Laboratory, Department of Biochemistry and Molecular Biology, Universidade Federal de Viçosa, Viçosa, Minas Gerais, Brazil

⁵Biochemical Analysis Laboratory, Department of Biochemistry and Molecular Biology, Universidade Federal de Viçosa, Viçosa, Minas Gerais, Brazil

⁶Institute of Biotechnology Applied to Agriculture & Livestock (Bioagro), Universidade Federal de Viçosa, Viçosa, Minas Gerais, Brazil

Received: 10 June 2020/Revised: 6 August 2020/Accepted: 26 August 2020

Published online 09 September 2020

<https://doi.org/10.1007/s00253-020-10863-x>

Abstract

Colorectal cancer is a public health problem, with dysbiosis being one of the risk factors due to its role in intestinal inflammation. Probiotics and synbiotics have been used in order to restore the microbiota balance and to prevent colorectal carcinogenesis. We aimed to investigate the effects of the probiotic VSL#3[®] alone or in combination with a yacon-based prebiotic concentrate on the microbiota modulation and its influence on colorectal carcinogenesis in an animal model. C57BL/6J mice were divided into three groups: control (control diet), probiotic (control diet + VSL#3[®]), and synbiotic (yacon diet + VSL#3[®]). The diets were provided for 13 weeks and, from the third one, all animals were subjected to induction of colorectal cancer precursor lesions. Stool samples were collected to evaluate organic acids, feces pH, β -glucuronidase activity, and microbiota composition. The colon was used to count pre-neoplastic lesions and to determine the cytokines. The microbiota composition was influenced by the use of probiotic and synbiotic. Modifications were also observed in the abundance of bacterial genera with respect to the control group, which confirms the interference of carcinogenesis in the microbiota. Pre-neoplastic lesions were reduced by the use of the synbiotic, but not with the probiotic. The protection provided by the synbiotic can be attributed to the modulation of the intestinal inflammatory response, to the inhibition of a pro-carcinogenic enzyme, and to the production of organic acids. The modulation of the composition and activity of the microbiota contributed to beneficial changes in the intestinal microenvironment, which led to a reduction in carcinogenesis.

Key points:

- Synbiotic reduces the incidence of colorectal cancer precursor lesions.
- Synbiotic modulates the composition and activity of intestinal microbiota.
- Synbiotic increases the abundance of butyrate-producing bacteria.

Keywords: gut microbiota; probiotic; prebiotic; synbiotic; colorectal cancer

Introduction

Colorectal cancer (CRC) is a public health problem worldwide, with 1.8 million new cases and almost 861,000 deaths reported in 2018 (IARC 2019). Colorectal carcinogenesis is characterized by a series of morphological changes of the intestinal epithelium, with the formation of precursor lesions of CRC, such as aberrant crypt foci (ACF), which can progress to invasive adenomas and carcinomas (Calderwood et al. 2016; Armaghany et al. 2012). The ACF study has become an important marker for understanding the pathogenesis of CRC and represents a challenge for cancer screening and surveillance in the early stages, in addition to being proposed to identify new chemopreventive agents (Newell and Heddle 2004).

Sporadic CRC, that is, not associated with heredity, is diagnosed in approximately 70 to 87% of the cases, indicating the existence of other important risk factors for the development of the disease (Frank et al. 2017; Johnson et al. 2013). The intestinal microbiota, defined as a complex community of microorganisms that coexist in close association with the host, has gained prominence in the pathogenesis of CRC (Mori et al. 2018; Jie et al. 2017; Coughnoux et al. 2014).

Although there is no consensus on the composition of the intestinal microbiota during the development and progression of CRC, the percentage of some bacterial species such as *Streptococcus bovis*, *Bacteroides fragilis*, *Enterococcus faecalis*, *Fusobacterium nucleatum*, and *Escherichia coli* was related to CRC occurrence (Gagnière et al. 2016). According to the “passenger-driver” hypothesis, intestinal bacteria called “drivers” induce damage to epithelial DNA, cause inflammation, increase cell proliferation, and produce genotoxic substances that contribute to tumorigenesis. Then, “passenger” bacteria begin to colonize the intestine, with growth advantages in the tumor microenvironment. Both have roles in CRC progression (Tjalsma et al. 2012).

On the other hand, several studies have investigated chemopreventive agents that could restore the intestinal microbiota balance and thereby reduce the CRC risk. Probiotics and prebiotics have been used for this purpose, alone or combined (Hill et al. 2014; Verma and Shukla 2014). Synbiotic is defined as the association between probiotic and prebiotic components (e.g., fructooligosaccharides and inulin) that work synergistically improving the colonization and survivability of beneficial microorganisms (Shinde et al. 2020; Kearney and Gibbons 2018). It has been reported

that the greatest effects of synbiotic supplementation in the gastrointestinal (GI) tract include local inflammation reduction, modulation of the immune response, improvement of the intestinal barrier, compound production with anticarcinogenic activity, and oxidative stress improvement (Cruz et al. 2020).

Several bacterial species are considered probiotic, with lactic acid bacteria (LAB), in particular members of the genera *Lactobacillus* and *Bifidobacterium*, being the most used ones. VSL#3[®] is a mix of probiotic bacteria, which includes strains of distinct taxa such as *Lactobacillus*, *Bifidobacterium*, and *Streptococcus*, widely used in studies of inflammatory bowel diseases (Liu et al. 2019; Chung et al. 2017; Rossi et al. 2014; Arthur et al. 2013; Uronis et al. 2011; Reiff et al. 2009). Based on these studies, VSL#3[®] demonstrated an interesting anti-inflammatory activity and the ability to increase beneficial bacterial species in the colon; however, there is no information on the power to prevent colorectal carcinogenesis.

Yacon (*Smallanthus sonchifolius*) is a tuberous root, considered a prebiotic food due to its high content of fructooligosaccharides (FOS) and inulin, in addition to being rich in phenolic compounds (Russo et al. 2015). Notwithstanding the protective effects of yacon intake on colorectal carcinogenesis having been demonstrated in previous experimental studies (Grancieri et al. 2017; Moura et al. 2012), special attention was given to pre neoplastic lesion development and short-chain fatty acid (SCFA) production. In the present study, the effects of yacon concentrate combined with the probiotic VSL#3[®], an unprecedented synbiotic formulation, were evaluated in terms of gut microbial composition and immunological response, as well as organic acid production and their influence on CRC development.

Here, we hypothesize that the prophylactic administration of the probiotic VSL#3[®] alone or combined with a yacon based prebiotic concentrate (PBY) could be able to modulate the composition and metabolism of the intestinal microbiota and, consequently, reduce the CRC risk at the early stages. Thus, the present study aimed to investigate the effects of the probiotic and synbiotic product on the intestinal microbiota modulation and its influence on the development of precursor lesions of CRC in an experimental animal model.

Material and Methods

Probiotics

The commercial probiotic VSL#3[®] (Sigma-Tau Pharmaceuticals, Gaithersburg, USA) was used. VSL#3[®], according to company's claim, contains eight bacterial strains, namely *Streptococcus thermophilus* BT01, three bifidobacteria (*Bifidobacterium breve* BB02, *Bifidobacterium animalis* subsp. *lactis* BL03, *Bifidobacterium animalis* subsp. *lactis* BI04) and four lactobacilli (*Lactobacillus acidophilus* BA05, *Lactobacillus plantarum* BP06, *Lactobacillus paracasei* BP07, *Lactobacillus helveticus* BD08). The commercial lyophilized formulation, in sachets containing 450 billion viable bacteria was used. The product was kept refrigerated and reconstituted in distilled water immediately before administration.

The animals (probiotic and synbiotic groups) received 0.1 mL of the probiotic by orogastric gavage, in the morning, for five days a week, for 13 weeks (Arthur et al. 2013). The animals of the control group received 0.1 mL of autoclaved tap water. The volume was adjusted to provide a daily supply of 2.25×10^9 colony-forming unit (CFU)/animal, based on the daily intake of about 10^9 CFU for an adult of 70 kg (Uronis et al. 2011; Zavisic et al. 2012; Dai et al. 2013).

Yacon-based product (PBY) and synbiotic

The processing of yacon-based product (PBY) can not be detailed due to ongoing patent application (PI 1106621-0). PBY sufficient to provide 6% of FOS and inulin (Paula et al. 2012) was added to the standard diet of the AIN-93M rodents (Reeves et al. 1993), in order to provide the benefits of fructan consumption without promoting toxicity or adverse effects. Considering that 100 g of PBY contains 23.6 g of FOS and inulin, 25.4 g of PBY was added to every 100 g of diet. Carbohydrate, protein and fiber contents were adjusted so that the experimental diets had a similar composition. The diets were prepared as pellets and stored at -20°C. The synbiotic was composed of the probiotic VSL#3[®] and the PBY, source of the prebiotics, FOS and inulin.

Animals, diets and experimental design

Forty-five male C57BL6/J mice, healthy, eight weeks old and body weight of approximately 22 g were obtained from the Central Bioterium at the Biological

Sciences and Health Center at Federal University of Viçosa, Minas Gerais, Brazil. The animals were collectively allocated in polypropylene cages, containing five mice each. Animals were kept under controlled conditions, at a temperature of $22 \pm 2^\circ\text{C}$ and humidity of 60-70% with a 12 h light/dark cycle.

After the acclimation period (one week) during which they received a commercial diet and water, the animals were randomly assigned to three experimental groups:

- 1) Control group (CON, n=15): AIN-93M diet and water (0.1 mL), via orogastric gavage, for 13 weeks;
- 2) Probiotic group (PRO, n=15): AIN-93M diet and probiotic VSL#3[®] (2.25×10^9 CFU/0.1 mL), via orogastric gavage, for 13 weeks;
- 3) Synbiotic group (SYN, n=15): modified AIN-93M diet containing PBY (6% FOS and inulin) and probiotic VSL#3[®] (2.25×10^9 CFU/0.1 mL), via orogastric gavage, for 13 weeks.

Diet and water were provided ad libitum throughout the experimental period. From the third experimental week, the protocol for the induction of preneoplastic lesions (ACF) in the colon was introduced for all. The colon carcinogen 1,2-dimethylhydrazine (DMH) (Sigma-Aldrich, Saint Louis, USA) was prepared in 0.9% saline solution containing 1 mM ethylenediamine tetraacetic acid (EDTA) and 10 mM sodium citrate, pH 8 (Newell and Heddle 2004). A dose of 20 mg/kg body weight was injected intraperitoneally (0.1 mL), once a week, for eight consecutive weeks (Gomides et al. 2014).

At the end of the experimental period (13 weeks), the animals were anesthetized with 3% isoflurane (Isoflorine[®], Cristalia, Itapira, Brazil) and blood samples collected from the retro-orbital sinus. The mice were sacrificed by cervical dislocation. The colon was resected, washed with cold 0.1 M phosphate-buffered saline (PBS, pH 7.2), sliced in small fragments and snap-frozen in nitrogen liquid and then stored at -80°C .

All experimental procedures using animals were performed following the Directive 2010/63/EU, in compliance with the ethical principles for animal experimentation. The study protocol was approved by the Ethics Committee of the Federal University of Viçosa (CEUA/UFV, protocol n° 08/2017. Approval: May 9, 2017).

Body weight and dietary intake

To evaluate the physiological effects of the administration of probiotics and synbiotic in terms of weight loss or gain, the animals were weighed weekly on a digital semi-analytical scale. Dietary intake was measured daily and was calculated by the difference from the amount of diet offered (g) and the remaining amount (g) in the successive day.

Feces collection and feces characteristics

The feces of each animal (n=15 mice/group) were harvested four times: *t0*, end of the first experimental week; *t1*, fourth experimental week, after the first ACF induction; *t2*, tenth experimental week, last ACF induction; and *t3*, last experimental week. To obtain samples, individual cages were previously cleaned and sanitized and a single mouse was kept there until a sufficient amount of feces were spontaneously expelled. Samples were kept at -80°C for further analysis.

Fecal samples collected during the last week (*t3*) were used to evaluate pH and fecal scores. For each animal, an aliquot of feces was diluted in distilled water (1:10), homogenized, and the pH was measured with a duly calibrated digital pH meter (Ultra Basic UB-10®, Hexis, Jundiaí, Brazil) in a temperature-controlled room after an adequate amount of time for pH stabilization (Bedani et al. 2011).

To assess the fecal score, a visual inspection was carried out, and each sample received a score according to its characteristics. The following ranking was considered: (1) firm or normal feces consistency; (2) viscous non-diarrhea feces; (3) watery feces characteristic of diarrhea (De Freitas et al. 2006, with modifications).

Aberrant crypt foci (ACF) count

Colonic ACF were analyzed using the method proposed by Bird and Good (2000). The colon was removed, cut along the longitudinal axis and flushed with saline solution 0.1 M, pH 7 (n=7 mice/group). Each colon was fixed in Karnovsky solution for 24 h and transferred to ethyl alcohol solution (70%) until analysis. The colon was cut into three sections with equal length (namely proximal, middle and distal) and stained with 0.1% methylene blue solution (Vetec®, Duque de Caxias, Brazil) for 4 min. Then, ACF were observed using a light microscope (Zeiss®, Primo Star, Oberkochen, Germany). ACF were identified as elevated focal lesions with multiple aberrant crypts

(AC), with thickened lining epithelium and increased luminal opening relative to normal adjacent mucosa (Bird and Good 2000). Counting was performed by two trained evaluators.

Analysis of cytokines profile

Pro- and anti-inflammatory cytokines were simultaneously determined by the Cytometric Bead Array (CBA) mouse Th1/Th2/Th17 cytokine Kit (BD Biosciences, San Jose, USA) in a BD FACSVerser Flow cytometry, following manufacturer's instructions. Colon samples (100 to 200 mg; n=6 or 7 mice/group) were ground using a tissue homogenizer (T10 basic UltraTurrax, IKA®, Rio de Janeiro, Brazil) in PBS buffer (pH 7.0), centrifuged (10,000 g, for 10 min at 4 °C) and the supernatant recovered. The beads were diluted with the diluent solution and distributed in microtubes. Twenty-five µL of the sample and 17 µL of the detector solution were added to each microtube, followed by incubation for 2 h. Subsequently, 1 mL of the washing solution was added, followed by centrifugation (1,800 g, for 5 min at 4°C), and discarded part of the supernatant (approximately 800 µL). The remaining volume was used for the measurement on the flow cytometer. The standard curve was built from the most concentrated solution (top standard). The data was processed using the FCAP Array 3.0 (FCAP Array Software BD Biosciences, California, USA) and the results were expressed in pg/g of tissue.

Evaluation of β -glucuronidase activity

To evaluate the β -glucuronidase enzyme activity, stool samples collected in the last experimental week (*t3*) were used. The enzymatic activity was evaluated according to De Moreno et al. (2005), with the modifications described below. For the preparation of enzymatic extract, stool samples (n=7 mice/group) were homogenized in distilled water (1:30) with the aid of a homogenizer (T10 basic UltraTurrax, IKA®, Rio de Janeiro, Brazil), for 1 minute, on ice. Then, samples were sonicated (Branson 1210 Ultrasonic, Marshall Scientific LLC, Hampton, USA), on ice, by 3 bursts of 2 min each (1 min interval between each burst) and then centrifuged (10,000 g, for 15 min at 4°C). The supernatant was collected. All enzymatic assays were carried out in phosphate

buffer, 200 mM, pH 6.5 at 37°C in triplicate and the mean values calculated. Relative standard deviations of measurements were below 5%. The enzymatic reaction contained 65 µL buffer; 25 µL *p*-nitrophenyl β-D-glucuronide 4 mM (pNPG, Sigma-Aldrich, Saint Louis, USA) and 10 µL enzymatic extract. The samples were incubated at 37°C for 3h. Absorbance was measured at 410 nm and the amount of *p*-nitrophenol released assessed by a standard curve. One enzyme activity unit (U) was defined as the amount of enzyme which released a µmol of the *p*-nitrophenol per hour under assay conditions.

Fecal short-chain fatty acids (SCFA) quantification

The concentration of SCFA was determined in stool samples (n=7 mice/group) collected at four times (*t*₀, *t*₁, *t*₂ and *t*₃), as described above. Quantification was performed according to Smiricky-Tjardes et al. (2003) with some modifications. Approximately 50 mg of feces were vortexed with deionized water (950 µL) and incubated in ice for 30 min, followed by homogenization in vortex every 5 min. Samples were centrifuged at 10,000 g, for 30 min at 4°C three times and the supernatant was collected and filtered through a 0.45 µm membrane filter. The SCFA were measured by high-performance liquid chromatography (HPLC) (Shimadzu®, Quito, Japan) using an Aminex HPX 87H column at 32°C, with acidified water (H₂SO₄, 0.005 M) as the eluent at a flow rate of 0.6 mL/min. The products were detected and quantified by an ultraviolet detector (SPD-20A VP) at 210 nm. Standard curves of acetic, propionic and butyric acid were constructed (Supelco®, Darmstadt, Germany). Results were expressed in µmol/g of feces.

DNA extraction

Mice fecal samples (250 mg; n=5 mice/group) were harvested at the end of the first experimental week (*t*₀) and after the intervention period (*t*₃). Total genomic DNA (gDNA) was extracted using the PowerSoil DNA isolation kit (Mo Bio, Carlsbad, USA) following the manufacturer's instructions. Total genomic DNA (gDNA) concentration and purity were determined via 260/280 and 260/230 absorbance ratios measured on the NanoDrop 2000c (Thermo Fisher Scientific, Waltham, USA).

DNA sequencing

After stool DNA extraction, samples of five different animals composing each experimental group at the time-points t_0 and t_3 (30 samples) were randomly collected and sent for Next-Generation Sequencing (NGS) at Eurofins (Eurofins Genomics Germany GmbH, Ebersberg, Germany). To assess the gut microbial profile, the hypervariable region V3-V5 of the bacterial 16S rRNA genes were PCR amplified, amplicon libraries generated using the Nextera XT DNA Library Preparation Kit (Illumina Inc, San Diego, USA) and sequenced with the Illumina MiSeq desktop sequencer producing 300 bp paired-end (PE) reads.

Bioinformatic analyses

Sequence data were analyzed with the CLC Genomics Workbench software (v.12.0.2, QIAGEN Bioinformatics, Hilden, Germany) using the Microbial genomics module plugin as described by Treu et al. (2018). Briefly, quality filtering, operational taxonomic unit (OTU) clustering, taxonomical assignment (Greengenes v13_8 database), biodiversity indicators (alpha and beta diversity indices) determination were performed using default parameters. When appropriate, the OTU consensus sequence of the most relevant taxa was manually verified using MEGABLAST (Database: 16S ribosomal RNA sequences) to improve the taxonomical assignment. Raw reads were deposited in the Sequence Read Archive (SRA) database (<http://www.ncbi.nlm.nih.gov/sra>) under the BioProject PRJNA625308.

For diversity analysis, data were rarefied to the minimum library size (18,039 sequences) when appropriate. The Shannon, Chao 1 and Simpson indices were calculated for each experimental group (CON, PRO, and SYN) at the time-points t_0 and t_3 and compared using ANOVA with Tukey's multiple comparisons test in GraphPad Prism 7 (GraphPad Software LLC, La Jolla, CA). In terms of bacterial community structure (beta diversity analysis), gut microbial dissimilarities among the groups were assessed by PERMANOVA with 99,999 permutations using Unweighted and Weighted UniFrac diversity metrics. Principal coordinate analysis (PCoA) was chosen as the ordination method to explore and visualize the data.

The abundance and comparison of specific taxa were carried out with STAMP (Parks et al. 2014) using Kruskal-Wallis H-test analysis and Benjamini-Hochberg FDR

as a multiple test correction method. Lastly, canonical correspondence analysis (CCA) was performed with PAST v3.25 (Hammer et al. 2001).

Statistical analysis

Statistical processing and analysis were performed using the Statistical Package for the Social Sciences 20.0 (SPSS Software IBM, Chicago, USA) and graphs were constructed using GraphPad Prism 7 (GraphPad Software LLC, La Jolla, CA). The normality of variables was determined by the Shapiro-Wilk test. The mean values of the three groups (CON, PRO, SYN) were compared by one-way analysis of variance (ANOVA) followed by Bonferroni multiple comparison post hoc test, for parametric data. For non-parametric data, the Kruskal Wallis test was applied, complemented by Dunn's multiple comparison test. The paired *t*-test or Wilcoxon test was used to compare the pre-and post-treatment. Correlations between continuous variables were determined by Pearson's (parametric data) or Spearman (non-parametric data) correlation. Differences were considered significant at $p < 0.05$. All results were expressed as mean \pm standard deviation (SD).

Results

Effect of probiotics and synbiotic on mice body weight and dietary intake

The mice groups started the experimental period with homogeneous body weight and, after thirteen weeks, there were no significant differences among the experimental groups. This result indicates that the consumption of the probiotic VSL#3[®] and synbiotic VSL#3[®] + PBY did not interfere with body weight gain. Similarly, there were no significant differences among the groups concerning dietary intake regardless of the experimental week. However, when the total dietary intake per week was taken into consideration (i.e., CON + PRO + SYN), a significant reduction in dietary consumption in the third experimental (after DMH injection) week was observed and was significant when compared to the 1st (2.73 g \pm 0.15 g x 4.06 g \pm 0.05 g; $p = 0.000$), 2nd (2.73 g \pm 0.15 g x 3.46 g \pm 0.15 g; $p = 0.018$), 11th (2.73 g \pm 0.15 g x 3.70 g \pm 0.17 g; $p = 0.000$) and 12th (2.73 g \pm 0.15 g x 3.73 g \pm 0.20 g; $p = 0.000$) experimental weeks (Supplemental Fig. S1).

Effect of probiotic and synbiotic on pH and feces characteristics

Feces characteristics were evaluated in order to verify the possible interferences of probiotic and synbiotic on feces production and intestinal transit. The use of the synbiotic reduced the fecal pH compared to the control diet (Fig. 1a). Fecal pH was positively correlated to the total ACF ($r=0.584$; $p = 0.011$). Predominantly, the fecal score of the synbiotic group was classified as 1 (33.3%; feces with normal consistency), and 2 (40.0%; viscous non-diarrhea feces) (Fig. 1b).

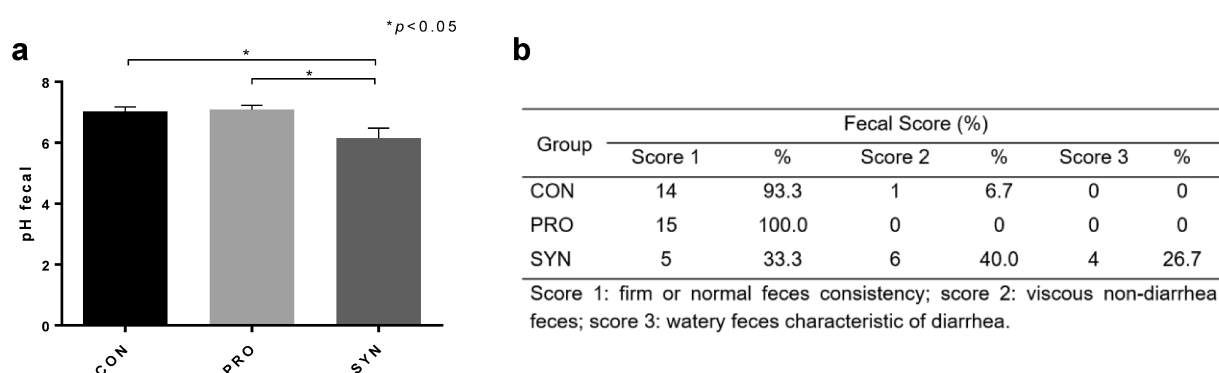


Figure 1. Effect of probiotic and synbiotic on (A) fecal pH, and (B) fecal score in C57BL/6J mice. Data are expressed as the mean \pm SD ($n=15$ /group). Statistical differences between groups were analyzed by ANOVA test. (*) $p < 0.05$. CON, AIN-93M diet; PRO, AIN-93M diet and probiotic VSL#3[®]; SYN, AIN-93M diet with PBY and probiotic VSL#3[®].

Effects of probiotic and synbiotic on colonic ACF in mice

ACF incidence was identified in all the experimental groups. The foci consisted predominantly of up to three aberrant crypts (AC) each, which indicates an early stage of precancerous lesions. The AC were wider and exhibited slit-like apertures compared to the circular appearance of normal crypts (Fig. 2). Synbiotic administration reduced the incidence of total ACF by 38.1% compared to the CON group (Table 1). In the segment analysis of the colon, we observed that the SYN group presented a lower ACF count in the proximal and medial regions, compared to the CON group. In the distal colon, there was no difference among the groups. These results demonstrate that the synbiotic was able to reduce the development of pre-neoplastic lesions in the

colon of mice. The mean number of AC was significantly higher in the CON group, indicating a greater multiplicity of pre-neoplastic lesions. The mortality rate in the groups was 0%.

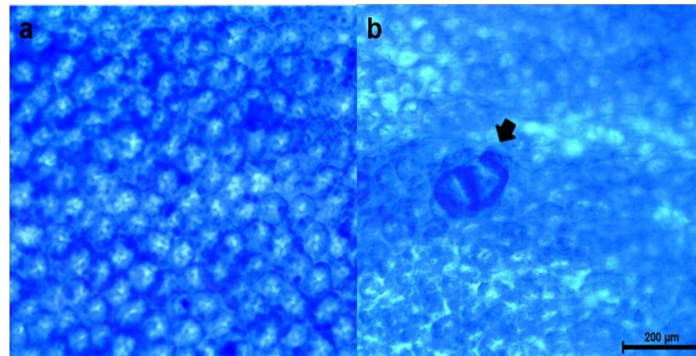


Figure 2. Photomicrograph of the colon of C57BL/6J mice induced to colorectal carcinogenesis with DMH, stained with 0.1% methylene blue. (a) normal crypts; (b) ACF with two aberrant crypts (indicated by the arrow).

Table 1. Effects of probiotic and synbiotic on DMH-induced ACF in the colon of C57BL/6 mice.

Number of ACF	CON	PRO	SYN	<i>P</i>
<i>ACF total</i>	48.7 ± 9.3 ^a	39.1 ± 5.1 ^{a,b}	30.1 ± 5.6 ^b	0.001 [#]
Proximal colon	18.8 ± 5.8 ^a	14.3 ± 3.6 ^{a,b}	10.7 ± 5.7 ^b	0.029 [*]
Medial colon	17.0 ± 7.5 ^a	11.1 ± 3.5 ^{a,b}	7.4 ± 4.1 ^b	0.013 [*]
Distal colon	12.8 ± 5.3	13.7 ± 4.5	12.0 ± 5.1	0.817 [*]
<i>AC total</i>	68.3 ± 10.8 ^a	50.6 ± 4.6 ^b	41.1 ± 7.7 ^b	0.000 [*]
<i>AC/ACF</i>	1.36 ± 0.14	1.35 ± 0.09	1.42 ± 0.23	0.681 [*]

ACF: aberrant crypt foci. AC: aberrant crypt. Data are expressed as the mean ± SD (n=7/group). Statistical difference between groups were analyzed by ANOVA^(*) test or Kruskal-Wallis test^(#), with *p*<0.05. Different letters in the same line indicate statistical difference. CON, AIN-93M diet; PRO, AIN-93M diet and probiotic VSL#3[®]; SYN, AIN-93M diet with PBY and probiotic VSL#3[®].

Effects of probiotic and synbiotic on cytokine profile in colon tissue

The cytokines IL-2, IL-4, IL-6, IL-10, IL-17, TNF and IFN- γ were measured in colon tissue by flow cytometry (Fig. 3). Animals receiving the synbiotic displayed an increase of the interleukin (IL)-2 in colonic homogenates compared to the control group (Fig. 3a), while the increase in interleukin (IL)-4 levels was observed in both

PRO and SYN groups (Fig. 3b). Lastly, the levels of the pro-inflammatory cytokine, tumor necrosis factor (TNF), was significantly lower in the SYN group when compared to the other groups (Fig. 3f). There were no significant differences among the levels of IL-6, IL-10, IL-17 and IFN- γ (Fig. 3c-e,g).

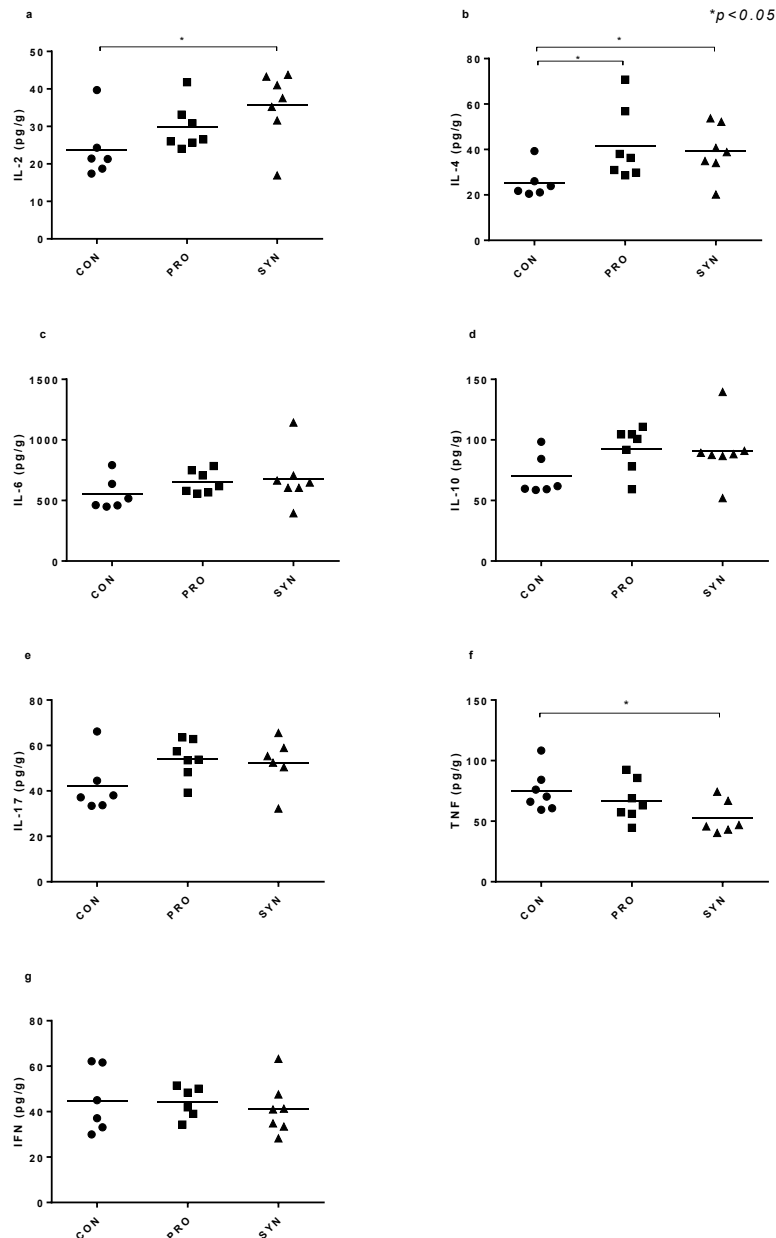


Figure 3. Effect of probiotic and synbiotic on colon cytokine profile in C57BL/6J mice. Data are expressed as the mean \pm SD (n= 6 or 7/group). Statistical differences between groups were analyzed by ANOVA test. (*) $p < 0.05$. CON, AIN-93M diet; PRO, AIN-93M diet and probiotic VSL#3[®]; SYN, AIN-93M diet with PBY and probiotic VSL#3[®].

Effects of probiotic and synbiotic on β -glucuronidase enzyme activity

Animals receiving the synbiotic displayed a significant reduction in β -glucuronidase enzyme activity when compared to the control group (Fig. 4). The PRO group activity did not differ from the other groups.

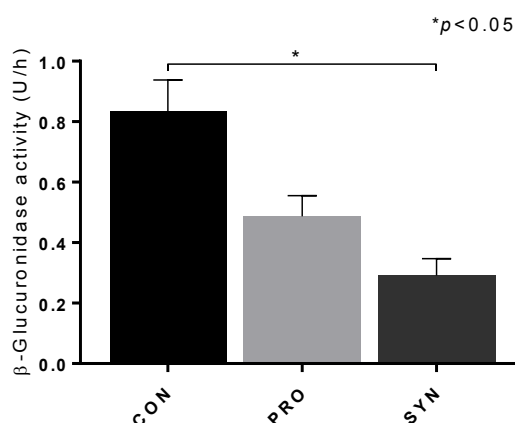


Figure 4. Effect of probiotic and synbiotic on bacterial enzyme activity β -glucuronidase in C57BL/6J mice. Data are expressed as the mean \pm SD (n=7/group). Statistical differences between groups were analyzed by ANOVA test. (*) $p < 0.05$. CON, AIN-93M diet; PRO, AIN-93M diet and probiotic VSL#3[®]; SYN, AIN-93M diet with PBY and probiotic VSL#3[®].

Effects of probiotic and synbiotic on the fecal concentration of SCFA

The SCFA profile of acetate, propionate, and butyrate was evaluated in fecal samples collected at time t_0 , t_1 , t_2 , and t_3 . SCFA concentrations varied widely between groups (Fig. 5). In general, the inter-group analysis showed that the animals in the SYN group had higher concentrations of acetic, propionic and butyric acids at all times (t_0 , t_1 , t_2 , t_3), compared to the CON and PRO groups (except for propionic acid at t_2 , in which there were no significant differences between groups) (differences not indicated in the graphs). The CON and PRO groups did not differ from each other.

We emphasize that when intra-group analysis ($t_0 \times t_3$) was performed, a reduction in acetic and butyric acids levels in the CON and PRO groups was observed throughout the experiment (Fig. 5a,c), as well as a reduction of propionic acid in the PRO group (Fig. 5b). On the other hand, the SYN group was able to maintain the concentrations of all SCFA throughout the experimental period. Total

ACF incidence was negatively correlated to the concentration of total SCFA ($r = -0.797$; $p = 0.000$).

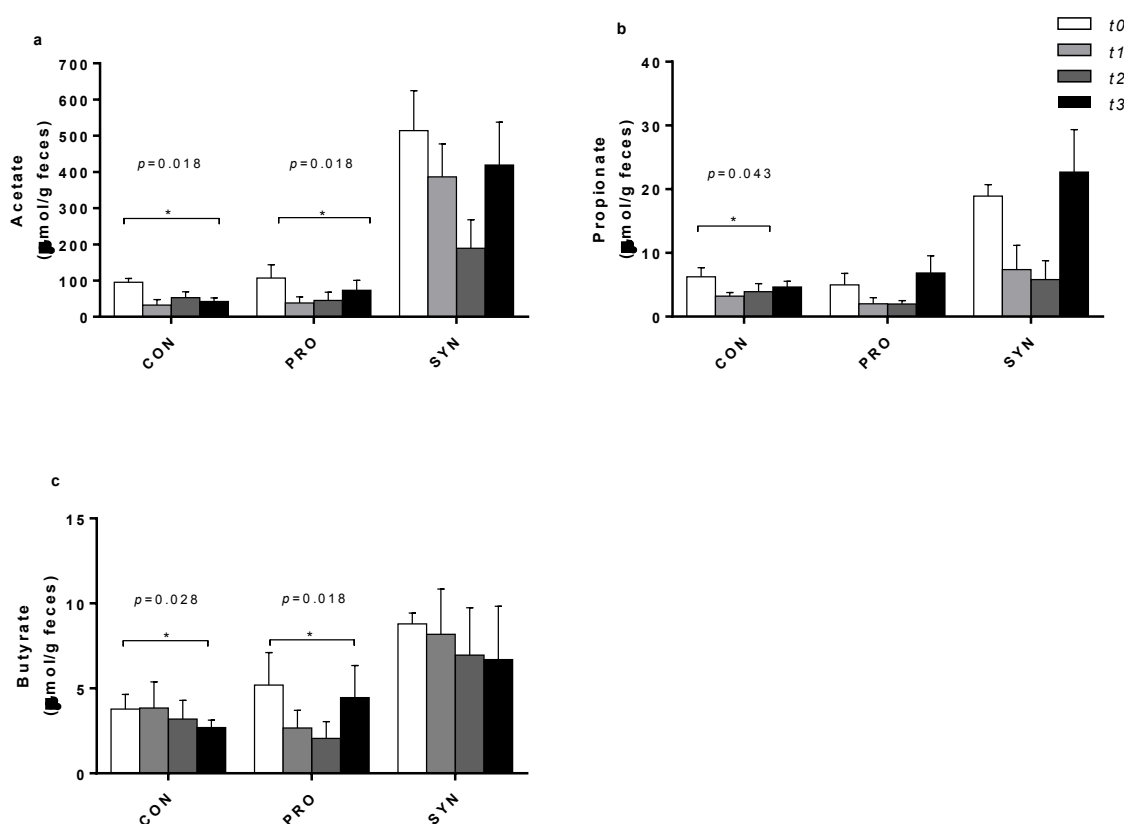


Figure 5. Effect of probiotic and synbiotic on fecal concentrations of short-chain fatty acids, (A) acetate, (B) propionate e (C) butyrate, before (t_0), during (t_1 , t_2), and after (t_3) intervention.

Bioinformatic analysis and microbiota profiling

Conducting a deep amplicon sequencing of the V3-V5 hypervariable region of the 16S rRNA genes, a total of 1,181,027 sequences with a length of 254 bp were obtained. After the removal of low quality and chimeric sequences from 30 data sets (6 groups, $n = 5$), a total of 725,924 high-quality reads, with an average of 24,197 ($\pm 2,876$) sequences for each sample, were assigned to 2,275 predicted OTUs ($\geq 97\%$ similarity). The number of OTUs per sample ranged from 307 to 597 (Supplemental Table S1).

Considering the analysis of alpha diversity, Shannon's entropy and Phylogenetic diversity curves reached a plateau and were used to estimate the depth

of sequencing in this study (Supplemental Table S2). These results suggest that sequencing covered most of the microbial diversity and that the majority of bacterial phylotypes were sampled.

Alpha and beta diversity

Alpha diversities were compared among the groups by Shannon and Simpson indices, whereas the Chao 1 index was used to evaluate bacterial richness (Fig. 6a-c). There was no statistically significant difference in terms of bacterial diversity among the groups before probiotics or synbiotic administration ($p > 0.05$). However, after the intervention ($t3$), the Shannon index of SYN $t3$ (5.97 ± 0.54) was significantly higher than PRO $t3$ (4.77 ± 0.45 ; $p = 0.0242$). With regards to bacterial richness, there was no significant difference among the groups ($p > 0.05$).

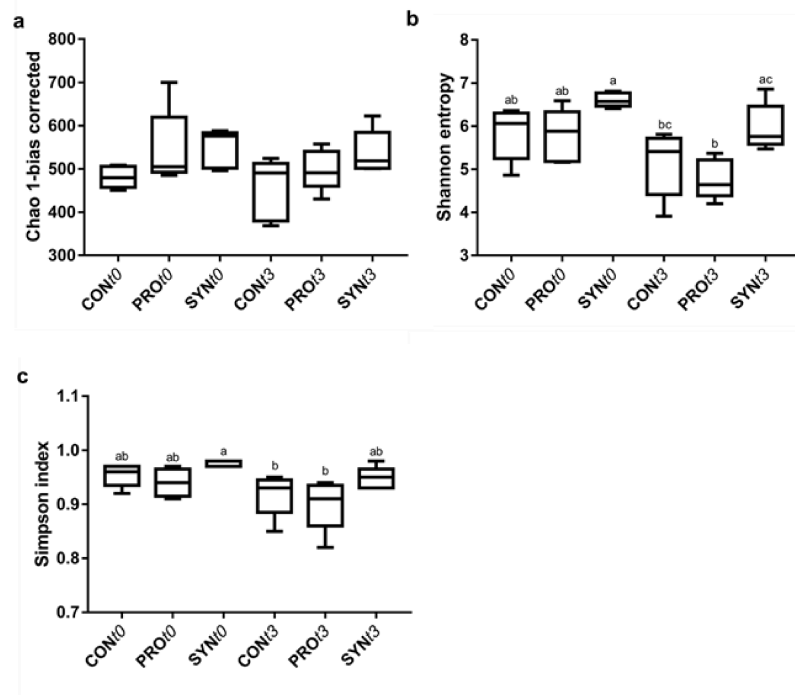
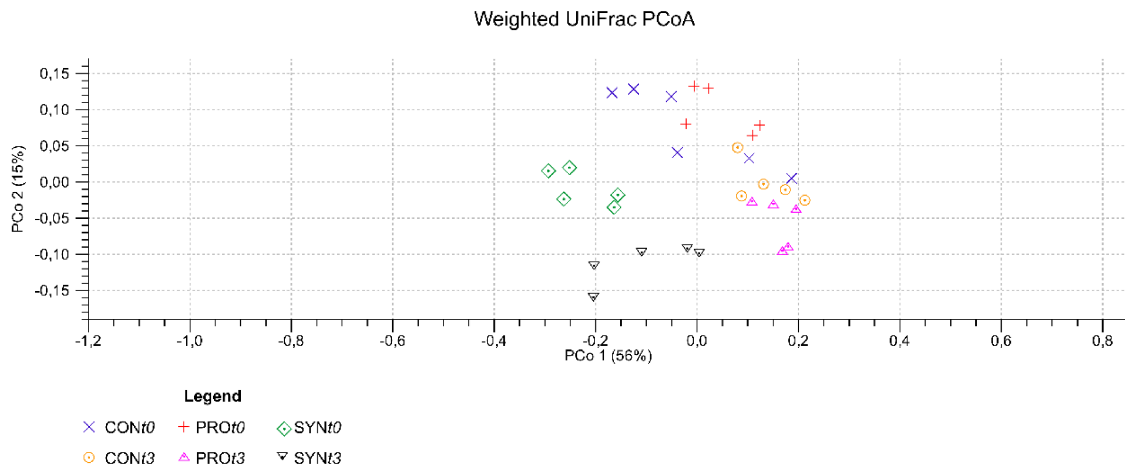


Figure 6. Box and whisker plots comparing species richness (A) and diversity between (B and C) the different groups (CON, PRO, and SYN) before ($t0$) and after ($t3$) their respective intervention. Horizontal bold lines show the median values. The bottom and top of the boxes show the 25th and the 75th percentiles, respectively. The whiskers extend up to the most extreme points within 1.5 times the interquartile ranges (IQR). Different letters indicate significant differences between groups (Tukey's test, $p < 0.05$).

The fecal bacterial community structures of animals fed with probiotic or synbiotic before and after colon carcinogenesis induction with DMH were assessed by the Unweighted and Weighted UniFrac distance metrics. As depicted in Fig. 7a and 7b, scatter plot of the Principal Coordinate Analysis (PCoA) using both distance metrics, revealed that SYN groups significantly clustered separately from CON and PRO (PERMANOVA Weighted UniFrac: $p = 0.00001$, Pseudo-f statistic = 8.97; PERMANOVA Unweighted UniFrac: $p = 0.00001$, Pseudo-f statistic = 8.21). In fact, after performing pairwise comparisons to evaluate microbiota composition similarities among the groups it was observed that, except for CON t_0 vs. PRO t_0 (PERMANOVA Unweighted UniFrac: $p = 0.10$, Pseudo-f statistic = 2.35; PERMANOVA Weighted UniFrac: $p = 0.39$, Pseudo-f statistic = 0.91) and CON t_3 vs. PRO t_3 (PERMANOVA Weighted UniFrac: $p = 0.22$, Pseudo-f statistic = 1.48), all the groups showed significant differences ($p < 0.05$) in the bacterial community structure (Supplemental Table S3). In total, Unweighted and Weighted UniFrac components (PCoA 1 and PCoA 2) accounted, respectively, for 61% and 71% of the total variance.

A



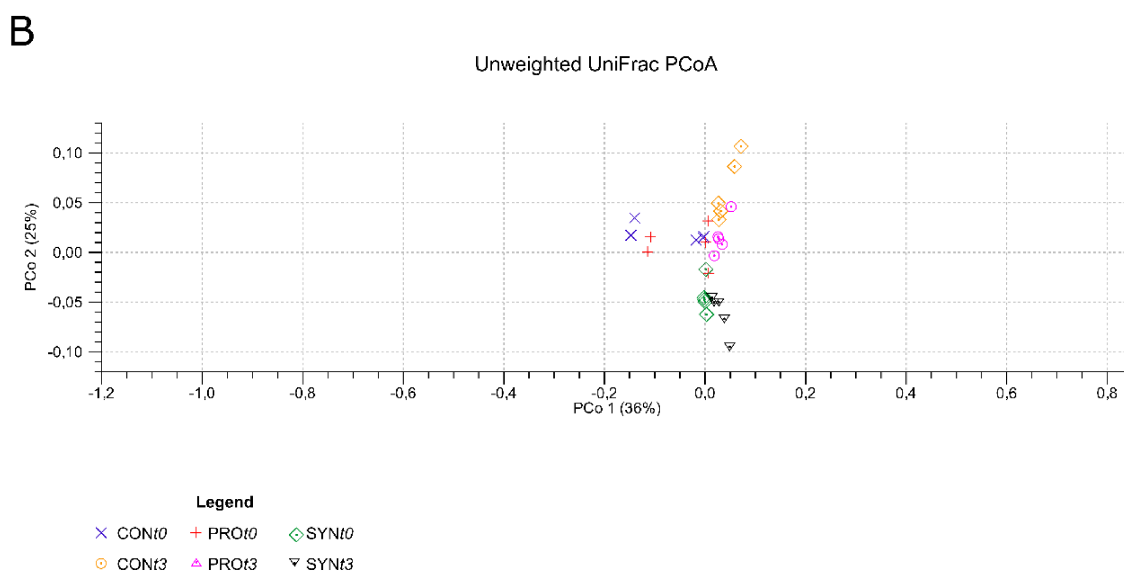


Figure 7. Principal coordinate analysis (PCoA) based on (A) Weighted and (B) Unweighted UniFrac distances for CON, PRO and SYN before (t_0) and after (t_3) their respective intervention. PERMANOVA with 99,999 permutations was used to detect significant differences between microbial communities (dissimilarity) of different experimental groups.

Bacterial community before and after the use of probiotics and synbiotic

Phylum level

The relative distributions of bacteria at the phylum, family and genus level identified by 16S rRNA gene amplicon sequencing are reported in Fig. 8a-c. The prevalent bacterial phyla among all groups were Firmicutes (75%), Proteobacteria (11%), Bacteroidetes (6%), Deferribacteres (2%), and TM7 (1%) (Fig. 8a; Supplemental Fig. S2). At the end of the experimental period (t_3), the phylum Firmicutes was significantly more abundant in CONt3 ($p < 0.01$; 0.3-fold) and PROt3 ($p < 0.01$; 0.3-fold) when compared to CONt0 and PROt0 groups, respectively. There was no significant difference in the relative abundance of Firmicutes between SYNt0 and SYNt3 ($p = 0.52$), however, a significant reduction of this taxon was observed in SYNt3 when compared to CONt3 ($p < 0.001$; 0.2-fold). With regards to Bacteroidetes, a significantly lower abundance of this phylum was observed after intervention in all groups when compared to CONt0 (CONt3: $p < 0.05$, 1.5-fold; PROt3: $p < 0.02$, 1.8-

fold; SYNt3: $p = 0.05$, 1.3-fold). Except for the group CONt3, a significant reduction was also observed for the phylum Proteobacteria in relation to CONt0 after the intervention (PROt3: $p = 3.47 \times 10^{-3}$, 1.5-fold; SYNt3: $p = 0.012$, 0.8-fold). The ratio of Firmicutes-to-Bacteroidetes (F/B) was also calculated and an augmented F/B ratio was observed between CONt0 and PROt3 (ANOVA, Dunn; $p = 0.030$) (Supplemental Fig. S3).

Family level

At the family level, 50 bacterial taxa were identified in total. After considering only the most abundant OTUs (relative abundance higher than 0.05% in at least one sample), 23 families accounted for more than 99.6% of the total sequences in each group. Among them, *Lactobacillaceae* was the most abundant family in the CON and PRO groups, whereas *Lachnospiraceae* was the most prevalent in the SYN groups (Fig. 8b; Supplemental Fig. S4).

Concerning the microbial changes after the intervention, a significant increase in the relative abundance of the family *Lachnospiraceae* was observed in the group SYNt3 when compared to CONt3 ($p < 0.01$; 1.7-fold) and PROt3 ($p < 0.01$, 1.8-fold) (Supplemental Fig. S4a).

Regarding *Clostridiaceae* and *Turicibacteraceae*, these families were found to be significantly more abundant in CONt3 and PROt3 (*Clostridiaceae*, $p < 0.01$; *Turicibacteraceae*, $p < 0.001$) in comparison to CONt0 and PROt0, respectively (Supplemental Fig. S4b and S4c). Interestingly, the relative abundance of *Clostridiaceae* increased proportionally in both groups (~1.5-fold), whereas the abundance of *Turicibacteraceae* increased by 5 and 6.7-fold in CONt3 and PROt3, respectively.

Lastly, except for SYNt3, the relative abundance of the bacterial taxon *Desulfovibrionaceae* significantly diminished in all groups after the intervention when compared to their corresponding groups at the time-point t_0 (CONt3, $p < 0.05$, 1-fold; PROt3, $p < 0.01$, 1.5-fold) (Supplemental Fig. S4d). With regards to the family *Helicobacteraceae*, a significant decrease of abundance was noticed in the groups PROt3 ($p < 0.05$, 2-fold) and SYNt3 ($p < 0.05$, 1.1-fold) when compared to their corresponding groups at the time-point t_0 (Supplemental Fig. S4e).

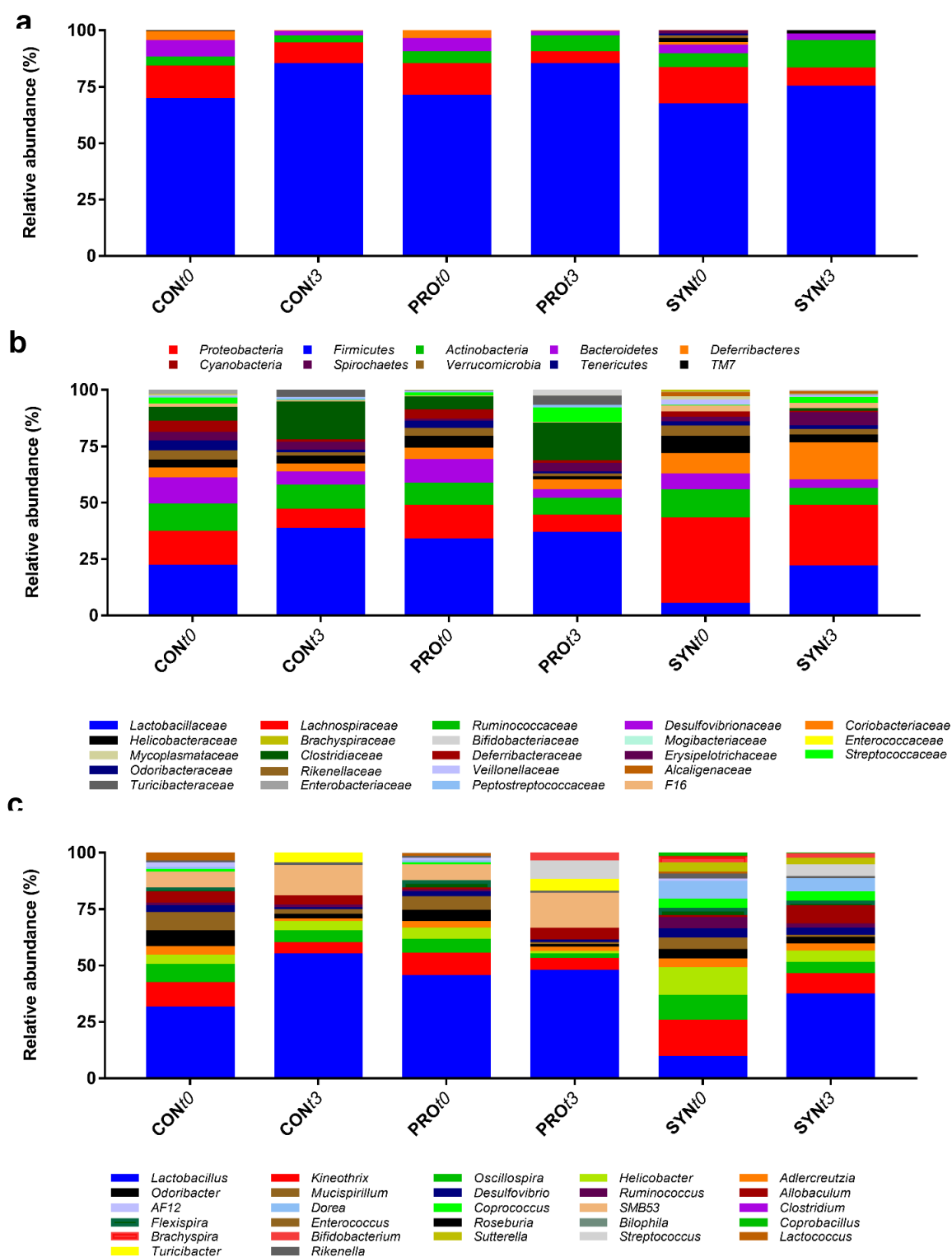


Figure 8. Relative abundance distribution of major phyla (A), families (B), and genera (C) across the groups CON, PRO and SYN in two different time-points (t_0 and t_3). Only families and genera with relative abundance greater than 0.05% were shown. The taxa were sorted by the decreasing order of average relative abundance.

Genus level

In total, 66 bacterial taxa were assigned to the genus level. After defining the most abundant genera (relative abundance higher than 0.05% in at least one sample), 27 OTUs were selected and accounted for more than 99.3% of the total sequences in each group. *Lactobacillus* was the most abundant microorganism in the groups CONt3, PROt3, and SYNt3, whereas *Kineothrix* dominated the group SYNt0 (Fig. 8c). In order to understand the microbial changes before and after the use of probiotics and synbiotic, a differential abundance analysis was conducted. As depicted in Fig. 9, the PRO group presented the highest number of microorganisms among the groups in which the relative abundance changed significantly (Fold change ≥ 2 ; FDR $p < 0.05$). Common to all groups involved in this study, a higher relative abundance of *Turicibacter* with a concomitant reduction of *Lactococcus* was observed after the intervention.

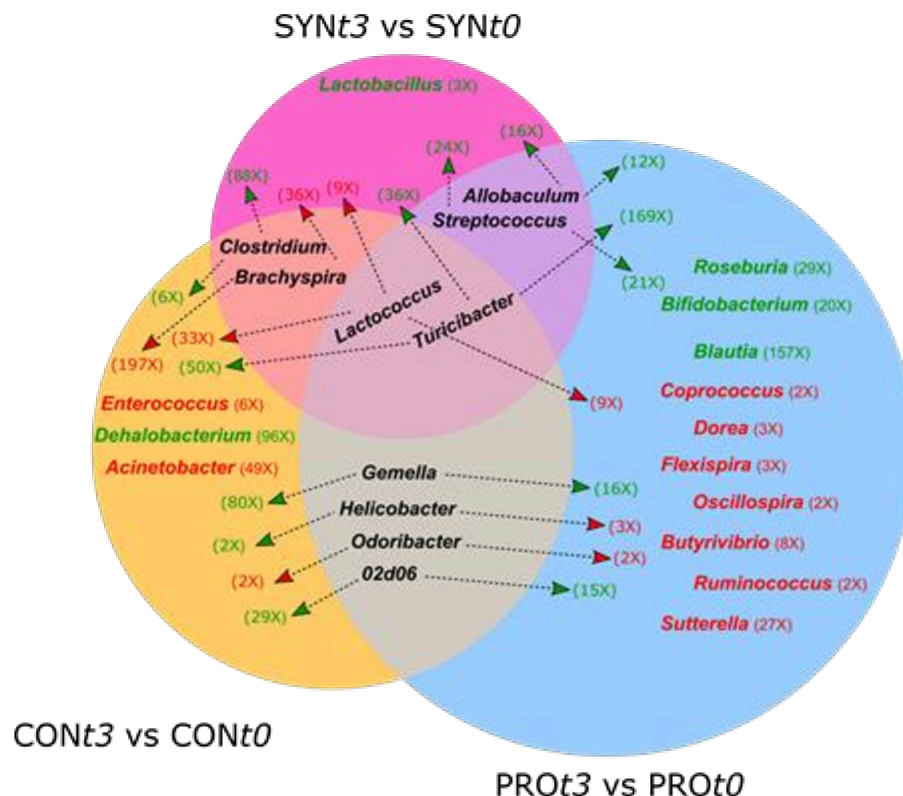


Figure 9. A Venn diagram showing the number of differentially abundant genera (Fold change ≥ 2 ; FDR $p < 0.05$) associated with each group (CON, PRO, and SYN) at the time-points t_0 and t_1 . Green and red values indicate, respectively, an increase or a

reduction in the relative abundance of a certain genus observed after the intervention in the different groups.

The intra-group comparison revealed a lower abundance of *Enterococcus* (6-fold) and *Acinetobacter* (49-fold) in CONt3, whereas the relative abundance of *Dehalobacterium* was enhanced by 96-fold. In PROt3, an impressive increase in the relative abundance of beneficial microorganisms such as *Bifidobacterium* (20-fold), *Roseburia* (29-fold) and *Blautia* (157-fold) was noticed. On the contrary, a reduced abundance of *Coprococcus* (2-fold), *Dorea* (3-fold), *Flexispira* (3-fold), *Oscillospira* (2-fold), *Ruminococcus* (2-fold), *Butyrivibrio* (8-fold) and *Sutterella* (27-fold) was observed. Regarding the SYNt3 group, the taxon *Lactobacillus* increased by 3-fold.

The taxa *Gemella*, *Helicobacter* and *02d06* increased in CONt3 by 80, 2 and 29-fold, respectively, whereas *Odoribacter* was reduced by 2-fold. The higher relative abundance of *Gemella* (16-fold) and *02d06* (15-fold) was also observed in PROt3, however *Odoribacter* (2-fold) and *Helicobacter* (3-fold) were less abundant in this group. An increase of *Clostridium* (CONt3, 6-fold; SYNt3, 88-fold) was followed by a reduction of *Brachyspira* (CONt3, 197-fold; SYNt3, 36-fold). Lastly, a mutual increase in the abundance of *Allobaculum* (PROt3, 12-fold; SYNt3, 16-fold) and *Streptococcus* (PROt3, 21-fold; SYNt3, 24-fold) was detected.

Correlation analysis

Canonical correspondence analysis (CCA) was used to investigate relationships between bacterial community structure at the family and genus level, the amount of the short-chain fatty acids (SCFA) acetate, butyrate and propionate, and fecal pH. A negative correlation was observed between the production of propionate ($r = -0.69$, $p = 0.0056$) and butyrate ($r = -0.76$, $p = 0.0015$), and fecal pH. At family level, *Lachnospiraceae* (propionate: $r = 0.56$, $p = 0.0340$; butyrate: $r = 0.59$, $p = 0.0223$; acetate: $r = 0.63$, $p = 0.0141$), *Veillonellaceae* (propionate: $r = 0.82$, $p = 0.0003$; butyrate: $r = 0.82$, $p = 0.0003$; acetate: $r = 0.61$, $p = 0.0174$) and *Alcaligenaceae* (propionate: $r = 0.61$, $p = 0.0185$; butyrate: $r = 0.82$, $p = 0.0003$; acetate: $r = 0.75$, $p = 0.0019$) were positively correlated with SCFA production (Fig. 10a). The family *Erysipelotrichaceae*, a known butyrate-producing group, was positively correlated with butyrate ($r = 0.62$, $p = 0.0152$) and acetate ($r = 0.59$, $p = 0.0242$) production.

On the contrary, the taxa *Clostridiaceae* (propionate: $r = -0.63$, $p = 0.0139$; butyrate: $r = -0.68$, $p = 0.0063$; acetate: $r = -0.72$, $p = 0.0033$), *Peptostreptococcaceae* (propionate: $r = -0.56$, $p = 0.0308$; butyrate: $r = -0.83$, $p = 0.0003$; acetate: $r = -0.67$, $p = 0.0078$) and *Turicibacteraceae* (propionate: $r = -0.60$, $p = 0.0197$; butyrate: $r = -0.74$, $p = 0.0021$; acetate: $r = -0.75$, $p = 0.0020$) were negatively correlated with SCFA production (Fig. 10a).

Focusing at the genus level, seven genera were found to be positively correlated with increased levels of SCFA (Fig. 10b). Family *Lachnospiraceae*: *Dorea* (propionate: $r = 0.61$, $p = 0.0175$; butyrate: $r = 0.62$, $p = 0.0164$; acetate: $r = 0.78$, $p = 0.0010$), *Coprococcus* (propionate: $r = 0.52$, $p = 0.0470$; butyrate: $r = 0.65$, $p = 0.0105$; acetate: $r = 0.78$, $p = 0.0012$) and *Kineothrix* (acetate: $r = 0.60$, $p = 0.0202$); Family *Alcaligenaceae*: *Sutterella* (propionate: $r = 0.66$, $p = 0.0106$; butyrate: $r = 0.80$, $p = 0.0004$; acetate: $r = 0.83$, $p = 0.00004$); and family *Erysipelotrichaceae*: *Coprobacillus* (butyrate: $r = 0.75$, $p = 0.0020$; acetate: $r = 0.76$, $p = 0.0011$). Although the taxon *Ruminococcaceae* was not significantly associated with SCFA production taking into consideration the relative abundance of the most abundant families as above mentioned, *Oscillospira* (propionate: $r = 0.62$, $p = 0.0161$) and *Ruminococcus* (propionate: $r = 0.54$, $p = 0.0418$; butyrate: $r = 0.55$, $p = 0.0370$; acetate: $r = 0.65$, $p = 0.0109$) were found to be positively correlated with increased values of SCFA. As depicted in Fig. 10b, both taxa were positively correlated with the SCFA measured in the group SYNt1.

Discussion

The use of probiotics isolated or associated to prebiotics (synbiotic) to promote intestinal health has gained prominence in the scientific literature (Tandon et al. 2019). Previous studies demonstrated the protective effect of probiotics and varied combinations of synbiotics in preventing colorectal cancer and other intestinal diseases (Lee et al. 2018; Gavresea et al. 2018). Current evidence suggests that the composition and metabolic activity of the intestinal microbiota are a key variable in this process (Wu et al. 2013; Yu 2018).

associated with community structures. Ellipses, colored according to the group, assume a bivariate normal distribution and estimate a region where 95% of population points are expected to fall.

It was observed that the use of the synbiotic increased fecal humidity and viscosity, with alteration in fecal pH. The presence of soluble fibers present in the yacon retains water, increasing the humidity in the feces. In addition, the bacterial fermentation favors the reduction of fecal pH, leading to water retention in the intestinal lumen in order to preserve intraluminal osmotic pressure (De Nadai Marcon et al. 2019; Le Blay et al. 1999). Thus, we believe that the change in the consistency of feces is probably related to the synbiotic administration and not to the induction of carcinogenesis.

The aberrant crypt foci (ACF) were used as a morphological marker of colorectal carcinogenesis, as previously described (Islam et al. 2015). The present study demonstrated a 38.1% reduction in ACF in the SYN group compared to the CON group ($p = 0.001$). As expected, the total count of aberrant crypt (AC) was significantly higher in the CON group compared to the others.

The ACF in the PRO and SYN groups were predominantly composed of one or two aberrant crypts (data not shown). The ACF containing a single crypt are classified as quiescent or senescent. These ACF can reenter the proliferation cycle and develop bifurcations (proliferative ACF) or disappear via apoptosis (Tsukamoto et al. 1999). The use of probiotic and synbiotic limited the development of proliferative ACF (with multiple crypts), suggesting a possible action in apoptosis or even in the reversal of ACF into normal crypts since the ACF are potentially reversible lesions (Bird and Good 2000).

The regulation of genes expression involved in cell proliferation, differentiation and apoptosis is one of the mechanisms suggested to be responsible for the antitumor effect of probiotics and synbiotics (Cruz et al. 2020; Reis et al. 2017), although it is not completely clear how each probiotic and synbiotic acts specifically on gene expression. We hypothesize that the additional protection afforded by the synbiotic can be explained, at least in part, by the increase in butyrate production in this group. Butyrate is a potential modulator of the Wnt/ β -catenin signaling pathway; in colonic tumorigenesis the Wnt pathway is constitutively activated, resulting in the overexpression of several oncogenes (Cheng et al. 2019; Uchiyama et al. 2016).

Tumor development and progression are favored in chronically inflamed tissues, in which an increase in the secretion of pro-inflammatory cytokines is observed, such as IL-1 β , IL-6, IL-8, IL-17, IL-12 and TNF (tumor necrosis factor), along with a reduction of anti-inflammatory cytokines, such as IL-10 and TGF- β (transforming growth factor beta) (Reis et al. 2017; Zhu et al. 2013; Pagès et al. 2010). This fact justifies, for example, the increased risk of CRC in individuals with inflammatory bowel diseases. During carcinogenesis, the tissue inflammatory response reflects an attempt by the immune system itself to eradicate the tumor (cancer immunoediting), which seems paradoxical, since inflammation stimulates tumor progression (Hanahan and Weinberg 2000; Fouad and Aanei 2017; Qian and Pollard 2010; Karnoub et al. 2007).

In this sense, the probiotic VSL#3[®] and the synbiotic VSL#3[®] + PBV were used to attenuate the inflammatory process initiated with the induction of carcinogenesis and, thus, to mitigate tumor development. Microorganisms and their metabolites interact with cells of the immune system, through binding to receptors, such as Toll-like (TLR) and NOD-like (NLR). As a consequence, immune and intestinal cells begin to secrete cytokines to regulate the innate and adaptive immune response, with an increase in the anti-inflammatory response (Corthésy et al. 2007; Delcenserie et al. 2008; Maldonado Galdeano et al. 2015; Igarashi et al. 2017).

In the present study, a significant increase in IL-2 was observed in the SYN group compared to the CON group. A similar result was demonstrated by Štofilová et al. (2015), after administration of the synbiotic *L. plantarum* and inulin in an experimental model of DMH-induced carcinogenesis. IL-2 has effects on the regulation of immune cells, and its concentration is inversely correlated with tumor size (Jacouton et al. 2019). *Lactobacillus casei* appears to have an important effect on IL-2 secretion (Hoyer et al. 2008). Interestingly, after the consumption of VLS#3[®] + PBV there was a 3-fold increase in the abundance of members of the genus *Lactobacillus*.

We also observed an increase in IL-4 (Th2 pattern) in the PRO and SYN groups. Studies using probiotic (Sivieri et al. 2008) and yacon (Delgado et al. 2012; Velez et al. 2013) supplementation have also obtained similar results in experimental models. The increase in IL-4 occurs concomitantly with the TLR4 expression, which results in the improvement of the innate immune response and antitumor defense (Velez et al. 2013; Nakamura et al. 2004).

TNF is another cytokine that plays an important role in carcinogenesis and that was influenced by the use of the synbiotic VSL#3[®] + PBV (significantly reduced

compared to the CON group). Studies that evaluated TNF concentrations show discordant results, with either an increase or decrease in TNF after the use of probiotic or synbiotic (Sivieri et al. 2008; Bassaganya-Riera et al. 2012; Talero et al. 2015; Lee et al. 2015; Štofilová et al. 2015).

Although TNF can activate apoptosis pathways, which would be interesting in controlling tumorigenesis, high concentrations of TNF have been associated with a higher prevalence of colorectal adenomas (Cabal-Hierro and O'Dwyer 2017; Park et al. 2014; Engstrom et al. 2014; Kim et al. 2008). Thus, we believe that changes in cytokine concentrations, promoted mainly by the synbiotic, may have contributed to an early antitumor response.

The assessment of bacterial enzyme activity is often used to demonstrate changes related to dietary intervention in the colon and to provide additional information on its effect on the intestinal microbiota modulation (De Preter et al. 2008). Bacterial enzymes such as β -glucuronidase, nitroreductase and azoreductase are involved in the conversion of pro-carcinogens into carcinogens in the colon, with the release of cytotoxic and genotoxic metabolites (Chandel et al. 2019; Uccello et al. 2012). Therefore, interventions that result in the lower activity of these enzymes may be a strategy for preventing colorectal carcinogenesis.

In this study, we used the DMH drug to induce precursor lesions of CRC. DMH is classified as a pro-carcinogen, which needs metabolic activation to become an active carcinogen. Activation occurs mainly in the liver, where DMH is oxidized to azomethane and later to azoxymethane, which in turn is N-hydroxylated to methylazoxymethanol (Štofilová et al. 2015; Perše et al. 2011). In the liver, methylazoxymethanol can be conjugated with glucuronic acid and secreted through the bile duct into the intestine. The intestinal bacteria that show β -glucuronidase activity are able to hydrolyze the complex formed in the liver, with the release of azoxymethane (an active carcinogen), triggering carcinogenesis in the colon (Zhu et al. 2013; Arthur et al. 2011).

Bacterial strains commonly used as probiotics, such as organisms belonging to the lactic acid bacteria group, must not produce β -glucuronidase or show a low enzymatic activity (Son et al. 2017). For instance, microorganisms classified into the genera *Bifidobacterium* and *Lactobacillus* have been displayed a minimal β -

glucuronidase activity, unlike the obligate anaerobes *Bacteroides* spp., *Eubacterium* spp. and *Clostridium* spp.) (Anuradha et al. 2005; Nakamura et al. 2002).

Reduction of enzyme activity after the use of probiotic and synbiotic has been demonstrated in experimental models and studies with humans (Mohania et al. 2013; Verma et al. 2013; Chang et al. 2012; Dominici et al. 2014; Villarini et al. 2008; Hatakka et al. 2008). In our study, β -glucuronidase activity decreased in the PRO group; however, a significant difference was observed only in the SYN group. The presence of fructooligosaccharides and inulin in the synbiotic possibly contributed to these results, since these substrates selectively stimulate the growth of bifidobacteria (Roberfroid 2005; Hijova et al. 2014; De Preter et al. 2008).

The changes in the microbiota after the use of the probiotic and synbiotic corroborate our findings. An increase in the genus *Bifidobacterium* was observed in the PRO and SYN groups, as well as a significant enrichment of the genus *Lactobacillus* in the SYN group. Additionally, β -glucuronidase producing bacteria such as *Flavobacterium* spp., *Bacteroides* spp. and *Corynebacterium* spp., (Tryland and Fiksdal 1998), were not identified in this study by using 16S rRNA gene amplicon sequencing.

Dysbiosis associated with CRC is characterized by the depletion of SCFA-producing bacteria (Wu et al. 2013). Bacteria metabolize fibers, resistant starch and fructooligosaccharides to SCFA, which strengthen the intestinal barrier through the production of mucins, antimicrobial peptides and cell junction proteins (Scheppach and Weiler 2004; Lin et al. 2018). It is common to observe an inverse correlation between SCFA concentrations and the incidence of precursor lesions and tumors in the colon (Worthley et al. 2009), as also demonstrated in this study. Butyrate-producing bacteria receive special attention, since butyrate acts as an inhibitor of histone deacetylase, regulating the expression of oncogenes, and stimulates the secretion of anti-inflammatory cytokines (Farrokhi et al. 2019; Kumar et al. 2012; Sokol et al. 2009).

The acetate, propionate and butyrate concentrations varied throughout the experiment. In general, the lowest concentrations of SCFA were observed during the period of DMH administration, between the third and tenth experimental weeks (t_1 and t_2). These results suggest that in addition to the availability of fermentable substrates, other factors, such as the administration of the carcinogen, may have influenced the intestinal microbiota metabolism. However, we emphasize that the SYN group was the

only one capable of maintaining the concentrations of all SCFA compared to the initial time (t_0 x t_3).

Previous studies have shown the reduction of butyrate-producing microorganisms in individuals with inflammatory bowel diseases and CRC, such as the species *Faecalibacterium prausnitzii*, *Clostridium butyricum* and *Butyrivibrio fibrisolvens*; the genera *Roseburia* and *Eubacterium*, and the families *Lachnospiraceae* and *Ruminococcaceae* (Wu et al. 2013; Wang et al. 2011; Balamurugan et al. 2008; Chen et al. 2014; Ohkawara et al. 2005). Our results are in agreement with previous findings and it is worth mentioning that genera positively correlated to SCFA production were depleted in the CON and PRO groups, however, a higher relative abundance of these genera was observed in the SYN group.

Based on the canonical correspondence analysis (CCA), a positive correlation between the concentration of SCFA and the abundance of the families *Lachnospiraceae*, *Veillonellaceae*, *Alcaligenaceae* and *Erysipelotrichaceae* was observed. On the contrary, an inverse correlation between the families *Clostridiaceae*, *Peptostreptococcaceae* and *Turicibacteraceae* and SCFA levels was noticed. Although commonly found as a low abundant taxon in the intestinal microbiota, the genus *Clostridium* (family *Clostridiaceae*) is an important butyrate producer (Chen et al. 2020) and had its abundance considerably increased after the synbiotic intervention.

At the genus level, there was a positive correlation between *Dorea*, *Coprococcus*, *Kineothrix*, *Sutterella*, *Coprobacillus*, *Oscillospira*, *Ruminococcus* and the SCFA levels. All these genera were identified in greater proportions in the SYN group, which explains the higher concentrations of SCFA total in this group.

It is also suggested that SCFA protects against CRC indirectly by decreasing the intestinal pH. The correlation between CRC risk and fecal pH has been demonstrated previously (Chandel et al. 2019; Chang et al. 2012). The acidification of the colonic content limits the colonization of pathogenic bacteria. In the present study, we observed a positive correlation between the incidence of ACF and fecal pH, and an inverse correlation between propionate and butyrate concentrations and fecal pH.

Given the probable involvement of the intestinal microbiota in the origin and progression of the CRC, and the advances in culture-independent microbial profiling techniques, several studies have been seeking specific microbial signatures that can assist in the screening and surveillance of the CRC. Bacterial species such as

Streptococcus gallolyticus, *F. nucleatum*, *E. coli*, *B. fragilis* and *E. faecalis* have a high prevalence in individuals with CRC compared to the healthy population, while the genera such as *Roseburia*, *Clostridium*, *Faecalibacterium* and *Bifidobacterium* may be depleted (Saus et al. 2019; Goodwin et al. 2011; Wu et al. 2009).

The *Firmicutes/Bacteroidetes* (F/B) ratio can be considered an important marker of intestinal dysbiosis. In general, individuals with pre-neoplastic lesions or tumors, present a decrease in the proportion of F/B, and *Actinobacteria*, concomitantly to the expansion of the phylum *Proteobacteria* (Mori et al. 2018; Lu et al. 2016). Although the *Firmicutes/Bacteroidetes* ratio apparently increased at the end of the experiment (t3), a significant difference was identified only between the CONt0 and PROt3 groups.

In general, the use of the probiotic VSL#3® and the synbiotic VSL#3® + PBY promoted remarkable changes in gut microbiota composition and might be a consequence of the availability of fermentable substrates, as demonstrated in this study. There were an increase and maintenance throughout the experiment in the abundance of the genera present in a mix of probiotic used (*Lactobacillus*, *Bifidobacterium* and *Streptococcus*), unlike other genera. Changes in the metabolic activity of the microbiota, such as the increase in the production of organic acids, were also observed. We emphasize that the relative abundance of some bacterial genera was also altered in the CON group, which indicates that exposure to the chemical carcinogen is capable of influencing the microbiota composition.

In conclusion, the synbiotic VSL#3® in combination with PBY showed additional benefits compared to the use of VSL#3® alone, which culminated in a significant reduction in the precursor lesions of CRC. We hypothesize that this result is linked to changes in the composition and metabolic activity of the intestinal microbiota. The modulation of the intestinal inflammatory response, the inhibition of pro-carcinogenic enzymes and the production of SCFA can be considered important targets of synbiotics in CRC prevention. The enrichment of potentially pathogenic microorganisms and the reduction of SCFA-producing species may represent a specific microbial signature of CRC. Understanding the dynamic changes of the microbiota from health to disease can assist in the development of diagnostic tools based on the fecal microbial structure.

Acknowledgments Our work was supported by the National Council of Technological and Scientific Development (CNPq), Coordination for the Improvement of Higher

Education Personnel (CAPES), and Foundation for the Support to the Researches in Minas Gerais (Fapemig).

Author contribution statement BCSC, MCGP, and CLLFF conceived and designed the research. BCSC, VSD, and LSF conducted the experiments. AG, VC, VMG, SOP, and MCGP contributed new reagents or analytical tools. BCSC, VSD, and LSF analyzed data. BCSC wrote the manuscript. All authors read and approved the manuscript.

Compliance with ethical standards

Conflict of interest All authors declare that they have no conflict of interest.

Ethical approval All experimental protocols were approved by the Ethics Committee in Animal Experimentation of the Federal University of Viçosa (n° 08/2017, date of approval: May 09, 2017), under the guidelines of the European Community (Directive 2010/63/EU).

References

Anuradha S, Rajeshwari K (2005) Probiotics in health and disease. *J Ind Acad Clin Med* 6:67-72

Armaghany T, Wilson JD, Chu Q, Mills G (2012) Genetic alterations in colorectal cancer. *Gastrointest Cancer Res* 5:19-27

Arthur J, Jobin C (2011) The struggle within: microbial influences on colorectal cancer. *Inflamm Bowel Dis* 17:396-409

Arthur JC, Gharaibeh RZ, Uronis JM, Perez-Chanona E, Sha W, Tomkovich S, Mühlbauer M, Fodor AA, Jobin C (2013) VSL#3 probiotic modifies mucosal microbial composition but does not reduce colitis-associated colorectal cancer. *Sci Rep* 3:2868. doi: 10.1038

Balamurugan R, Rajendiran E, George S, Samuel GV, Ramakrishna BS (2008) Real-time polymerase chain reaction quantification of specific butyrate-producing bacteria, *Desulfovibrio* and *Enterococcus faecalis* in the feces of patients with colorectal cancer. *J Gastroenterol Hepatol* 23(8 Pt 1):1298-1303. doi:10.1111/j.1440-1746.2008.05490.x

Bassaganya-Riera J, Viladomiu M, Pedragosa M, De Simone C, Hontecillas R (2012) Immunoregulatory mechanisms underlying prevention of colitis-associated colorectal cancer by probiotic bacteria. *Plos One* 7:e34676

Bedani R, Pauly-Silveira ND, Cano VSP, Valentini SR, Valdez GF, Rossi EA (2011) Effect of ingestion of soy yogurt on intestinal parameters of rats fed on a beef-based animal diet. *Braz J Microbiol* 42(3), 1238-1247. <http://dx.doi.org/10.1590/S1517-83822011000300050>

Bird RP, Good CK (2000) The significance of aberrant crypt foci in understanding the pathogenesis of colon cancer. *Toxicol Lett* 15;112-113:395-402. doi: 10.1016/s0378-4274(99)00261-1

Cabal-Hierro L, O'Dwyer PJ (2017) TNF signaling through RIP1 kinase enhances SN38-induced death in colon adenocarcinoma. *Mol Cancer Res* 15(4). doi: 10.1158/1541-7786.MCR-16-0329

Calderwood AH, Lasser KE, Roy HK (2016) Colon adenoma features and their impact on risk of future advanced adenomas and colorectal cancer. *World J Gastrointest Oncol* 15:826-834. <https://doi.org/10.4251/wjgo.v8.i12.826>

Chandel D, Sharma M, Chawla V, Sachdeva N, Shukla G (2019) Isolation, characterization and identification of antigenotoxic and anticancerous indigenous probiotics and their prophylactic potential in experimental colon carcinogenesis. *Sci Rep* 9:14769. <https://doi.org/10.1038/s41598-019-51361-z>

Chang JH, Shim YY, Cha SK, Reaney MJT, Chee KM (2012) Effect of *Lactobacillus acidophilus* KFRI342 on the development of chemically induced precancerous growths in the rat colon. *J Med Microbiol* 61(pt 3):361-368

Chen D, Jin D, Huang S, Wu J, Xu M, Liu T, Dong W, Liu X, Wang S, Zhong W, Liu Y, Jiang R, Piao M, Wang B, Cao H (2020) *Clostridium butyricum*, a **butyrate**-producing probiotic, inhibits intestinal tumor development through modulating Wnt signaling and gut microbiota. *Cancer Lett* 28;469:456-467. doi: 10.1016/j.canlet.2019.11.019

Chen L, Wang W, Zhou R, Ng SC, Li J, Huang M, Zhou F, Wang X, Shen B, A Kamm M, Wu K, Xia B (2014) Characteristics of fecal and mucosa-associated microbiota in chinese patients with inflammatory bowel disease. *Md Med J* 93(8):e51

Cheng X, Xu X, Chen D, Zhao F, Wang W (2019) Therapeutic potential of targeting the Wnt/ β -catenin signaling pathway in colorectal cancer. *Biomed Pharmacother* 110:473-481. doi: 10.1016/j.biopha.2018.11.082

Chung EJ, Do EJ, Kim SY, Cho EA, Kim DH, Pak S, Hwang SW, Lee HJ, Byeon JS, Ye BD, Yang DH, Park SH, Yang SK, Kim JH, Myung SJ (2017) Combination of metformin and VSL#3 additively suppresses western-style diet induced colon cancer in mice. *Eur J Pharmacol* 794:1-7

Corthésy B, Gaskins HR, Mercenier A (2007) Cross-talk between probiotic bacteria and the host immune system. *J Nutr* 137:781-790

Cougnoux A, Dalmaso G, Martinez R, Buc E, Delmas J, Gibold L, Sauvanet P, Darcha C, Déchelotte P, Bonnet M, Pezet D, Wodrich H, Darfeuille-Michaud A, Bonnet R (2014) Bacterial genotoxin colibactin promotes colon tumour growth by inducing a senescence-associated secretory phenotype. *Gut* 63,1932-1942. doi: 10.1136/gutjnl-2013-305257

Cruz BCS, Sarandy MM, Messias AC, Gonçalves RV, Ferreira CLLF, Peluzio MCG (2020) Preclinical and clinical relevance of probiotics and synbiotics in colorectal carcinogenesis: a systematic review. *Nutr Rev* <https://doi.org/10.1093/nutrit/nuz087>

Dai C, Zheng CQ, Meng FJ, Zhou Z, Sang LX, Jiang M (2013) VSL#3 probiotics exerts the anti-inflammatory activity via PI3k/Akt and NF-kappaB pathway in rat model of DSS-induced colitis. *Mol Cell Biochem* 374:1-11

De Freitas LS, Lopes DC, De Freitas AF, Carneiro JDC, Corassa A, Pena SDM, Costa LF (2006) Effects of feeding organic acids for piglets from 21 to 49 days old. *Rev Bras de Zootec* 35, 1711–1719. <https://doi.org/10.1590/S1516-35982006000600019>

de Moreno de LeBlanc A, Perdigon G (2005) Reduction of β -glucuronidase and nitroreductase activity by yoghurt in a murine colon cancer model. *Biocell* 29:15-24

De Nadai Marcon L, Moraes LFS, Cruz BCS, Teixeira MDO, Bruno TCV, Ribeiro, IE, Messias AC, Ferreira CLLF, Oliveira LL, Peluzio MCG (2019) Yacon (*Smallanthus sonchifolius*)-based product increases fecal short-chain fatty acids and enhances regulatory T cells by downregulating ROR γ t in the colon of BALB/c mice. *Journal of Functional Foods* 55, 333-342.

De Preter V, Hamer HM, Windey K, Verbeke K (2011) The impact of pre- and/or probiotics on human colonic metabolism: does it affect human health? *Mol Nutr Food Res* 55, 4657

De Preter V, Raemen H, Cloetens L, Houben E, Rutgeerts P, Verbeke K (2008) Effect of dietary intervention with different pre- and probiotics on intestinal bacterial enzyme activities. *Eur J Clin Nutr* 62(2):225-231

Delcenserie V, Martel D, Lamoureux M, Amiot J, Boutin Y, Roy D (2008) Immunomodulatory effects of probiotics in the intestinal tract. *Curr Issues Mol Biol* 10:37-54

Delgado GT, Thomé R, Gabriel DL, Tamashiro WM, Pastore GM (2012) Yacon (*Smallanthus sonchifolius*)-derived fructooligosaccharides improves the immune parameters in the mouse. *Nutr Res* 32:884-892. doi: 10.1016/j.nutres.2012.09.012

Dominici L, Villarini M, Trotta F, Federici E, Cenci G, Moretti M (2014) Protective effects of probiotic *Lactobacillus rhamnosus* IMC501 in mice treated with PhIP. *J Microbiol Biotechnol* 24:371-378

Engstrom A, Erlandsson A, Delbro D, Wijkander J (2014) Conditioned media from macrophages of M1, but not M2 phenotype, inhibit the proliferation of the colon cancer cell lines HT-29 and CACO-2. *Int J Oncol* 44:385-392

Farrokhi AS, Mohammadlou M, Abdollahi M, Eslami M, Yousefi B (2019) Histone deacetylase modifications by probiotics in colorectal cancer. *J Gastrointest Canc* doi.org/10.1007/s12029-019-00338-2

Fouad YA, Aanei C (2017) Revisiting the hallmarks of cancer. *Am J Cancer Res* 7(5):1016-1036 doi: www.ajcr.us /ISSN:2156-6976/ajcr0053932

Frank C, Sundquist J, Yu H, Hemminki A, Hemminki, K (2017) Concordant and discordant familial cancer: familial risks, proportions and population impact. *Int J.Cancer* 140:1510-1516

Gagnière J, Raisch J, Veziat J, Barnich N, Bonnet R, Buc E, Bringer MA, Pezet D, Bonnet M (2016) Gut microbiota imbalance and colorectal cancer. *World J Gastroenterol* 22, 501-518. <https://doi.org/10.3748/wjg.v22.i2.501>

Gavresea F, Vagianos C, Korontzi M, Sotiropoulou G, Dadioti P, Triantafillidis JK, Papalois AE (2018) Beneficial effect of synbiotics on experimental colon cancer in rats. *Turk J Gastroenterol* 29: 494-501

Gomides AFF, de Paula SO, Gonçalves RV, de Oliveira LL, Ferreira CL de LF, Comastri DF, Peluzio MCG (2014) Prebiotics prevent the appearance of aberrant crypt foci (ACF) in the colon of BALB/c mice for increasing the gene expression of p16 protein. *Nutr Hosp* 30: 883-890

Goodwin AC, Destefano Shields CE, Wu S, Huso DL, Wu X, Murray-Stewart TR, Hacker-Prietz A, Rabizadeh S, Woster PM, Sears CL, Casero RA (2011) Polyamine

catabolism contributes to enterotoxigenic *Bacteroides fragilis*-induced colon tumorigenesis. Proc Natl Acad Sci 108:15354–15359. doi: 10.1073/pnas.1010203108

Grancieri M, Costa NMB, Vaz Tostes MDG, de Oliveira DS, Nunes LDC, Marcon LDN, Viana ML (2017) Yacon flour (*Smallanthus sonchifolius*) attenuates intestinal morbidity in rats with colon cancer. J Funct Foods 37. <https://doi.org/10.1016/j.jff.2017.08.039>

Hammer Ø, Harper DAT, Ryan PD (2001) PAST: Paleontological Statistics Software Package for Education and Data Analysis. Palaeontologia Electronica 4(1), 9. http://palaeo-electronica.org/2001_1/past/issue1_01.htm

Hanahan D, Weinberg RA (2000) The hallmarks of cancer. Cell 7;100(1):57-70

Hatakka K, Holma R, El-Nezami H, Suomalainen T, Kuisma M, Saxelin M, Poussa T, Mykkänen H, Korpela R (2008) The influence of *Lactobacillus rhamnosus* LC705 together with *Propionibacterium freudenreichii* ssp. *shermanii* JS on potentially carcinogenic bacterial activity in human colon. Int J Food Microbiol 128:406-410

Hijova E, Szabadosova V, Strojny L, Bomba A (2014) Changes chemopreventive markers in colorectal cancer development after inulin supplementation. Bratisl Lek Listy 115 (2). doi: 10.4149/BLL_2014_016

Hill C, Guarner F, Reid G, Gibson GR, Merenstein DJ, Pot B, Morelli L, Canani RB, Flint HJ, Salminen S, Calder PC, Sanders ME (2014) Expert consensus document: The international scientific association for probiotics and prebiotics consensus statement on the scope and appropriate use of the term probiotic. Nat Rev Gastroenterol Hepatol 11: 506-514

Hoyer KK, Doms H, Barron L, Abbas AK (2008) Interleukin-2 in the development and control of inflammatory disease. Immunol Rev 226:19-28. doi: 10.1111/j.1600-065X.2008.00697.x

Igarashi M, Nakae H, Matsuoka T, Takahashi S, Hisada T, Tomita J, Koga Y (2017) Alteration in the gastric microbiota and its restoration by probiotics in patients with

functional dyspepsia. *BMJ Open Gastroenterol* 1:e000144. doi: 10.1136/bmjgast-2017-000144

International Agency for Research Cancer (IARC) Cancer Today. <https://gco.iarc.fr/today/>. Access: March 16, 2020

Islam A, Gallaher DD (2015) Wheat type (class) influences development and regression of colon cancer risk markers in rats. *Nutr Cancer* 67, 1285-1294

Jacouton E, Michel ML, Torres-Maravilla E, Chain F, Langella P, Bermúdez-Humarán LG (2019) Elucidating the immune-related mechanisms by which probiotic strain *Lactobacillus casei* BL23 displays anti-tumoral properties. *Front Microbiol* 11;9:3281. doi: 10.3389/fmicb.2018.03281

Jie Z, Xia H, Zhong SL, Feng Q, Li S, Liang S, Zhong H, Liu Z, Gao Y, Zhao H, Zhang D, Su Z, Fang Z, Lan Z, Li J, Xiao L, Li J, Li R, Li X, Li F, Ren H, Huang Y, Peng Y, Li G, Wen B, Dong B, Chen JY, Geng QS, Zhang ZW, Yang H, Wang J, Wang J, Zhang X, Madsen L, Brix S, Ning G, Xu X, Liu X, Hou Y, Jia H, He K, Kristiansen K (2017) The gut microbiome in atherosclerotic cardiovascular disease. *Nat Commun* 8, 845

Johnson CM, Wei C, Ensor JE, Smolenski DJ, Amos CI, Levin B, Berry DA (2013) Meta-analyses of colorectal cancer risk factors. *Cancer Causes Control* 24:1207-1222

Karnoub AE, Weinberg RA (2007) Chemokine networks and breast cancer metastasis. *Breast Dis* 26:75-85

Kearney SM, Gibbons SM (2018) Designing synbiotics for improved human health. *Microb Biotechnol* 11(1):141-144. doi: 10.1111/1751-7915.12885

Kim S, Keku TO, Martin C, Galanko J, Woosley JT, Schroeder JC, Satia JA, Halabi S, Sandler RS (2008) Circulating levels of inflammatory cytokines and risk of colorectal adenomas. *Cancer Res* 68:323-328

Kumar M, Nagpal R, Verma V, Kumar A, Kaur N, Hemalatha R, Gautam SK, Singh S (2012) Probiotic metabolites as epigenetic targets in the prevention of colon cancer. *Nutr Rev* 71:23-34

Le Blay G, Michel C, Blottière HM, Cherbut C (1999). Prolonged intake of fructooligosaccharides induces a short-term elevation of lactic acid-producing bacteria and a persistent increase in cecal butyrate in rats. *J Nutr* 129(12): 2231-2235. <https://doi.org/10.1093/jn/129.12.2231>

Lee HA, Kim H, Lee KW, Park KY (2015) Dead nano-sized *Lactobacillus plantarum* inhibits azoxymethane/dextran sulfate sodium-induced colon cancer in Balb/c mice. *J Med Food* 18:1400-1405

Lee HL, Park MH, Song JK, Jung YY, Kim Y, Kim KB, Hwang DY, Yoon do Y, Song MJ, Han SB, Hong JT (2016) Tumor growth suppressive effect of IL-4 through p21-mediated activation of STAT6 in IL-4R α overexpressed melanoma models. *Oncotarget* 26; 7(17): 23425-23438

Lin C, Cai X, Zhang J, Wang W, Sheng Q, Hua H, Zhou X (2018) Role of gut microbiota in the development and treatment of colorectal cancer. *Digestion* 1-7. <https://doi.org/10.1159/000494052>

Liu XJ, Yu R, Zou KF (2019) Probiotic mixture VSL#3 alleviates dextran sulfate sodium-induced colitis in mice by downregulating T follicular helper cells. *Curr Med Sci* 39(3):371-378. doi: 10.1007/s11596-019-2045-z

Lu Y, Chen J, Zheng J, Hu G, Wang J, Huang C, Lou L, Wang X, Zeng Y (2016) Mucosal adherent bacterial dysbiosis in patients with colorectal adenomas. *Sci Rep* 6: 26337. doi: 10.1038/srep26337

Maldonado Galdeano C, Novotny Nuñez I, Carmuega E, de Moreno de LeBlanc A, Perdigón G (2015) Role of probiotics and functional foods in health: gut immune stimulation by two probiotic strains and a potential probiotic yoghurt. *Endocr Metab Immune Disord Drug Targets* 15, 37-45. doi: 10.2174/1871530314666141216121349

Mohania D, Kansal VK, Sagwal R, Shah D (2013) Anticarcinogenic effect of probiotic Dahi and piroxicam on DMH-induced colorectal carcinogenesis in Wistar rats. *Am J Cancer Ther Pharmacol* 1:1-17

Mori G, Rampelli S, Orena BS, Rengucci C, De Maio G, Barbieri G, Passardi A, Casadei Gardini A, Frassinetti GL, Gaiarsa S, Albertini AM, Ranzani GN, Calistri D, Pasca MR (2018) Shifts of faecal microbiota during sporadic colorectal carcinogenesis. *Sci Rep* 9;8(1):10329. doi: 10.1038/s41598-018-28671-9

Moura NA, Caetano BF, Sivieri K, Urbano LH, Cabello C, Rodrigues MA, Barbisan LF (2012) Protective effects of yacon (*Smallanthus sonchifolius*) intake on experimental colon carcinogenesis. *Food Chem Toxicol* 50:2902-10. doi: 10.1016/j.fct.2012.05.006

Nakamura J, Kubota Y, Miyaoka M, Saitoh T, Mizuno F, Benno Y (2002) Comparison of four microbial enzymes in *Clostridia* and *Bacteroides* isolated from human feces. *Microbiol Immunol* 46, 487-490

Nakamura Y, Nosaka S, Suzuki M, Nagafuchi S, Takahashi T, Yajima T, Takenouchi-Ohkubo N, Iwase T, Moro I (2004) Dietary fructooligosaccharides up-regulate immunoglobulin A response and polymeric immunoglobulin receptor expression in intestines of infant mice. *Clin Exp Immunol* 137(1):52-58

Newell L, Heddle, JA (2004) The potent colon carcinogen, 1,2-dimethylhydrazine induced mutations primarily in the colon. *Mutat Res* 564:1-7

Ohkawara S, Furuya H, Nagashima K, Asanuma N, Hino T (2005) Oral administration of *Butyrivibrio fibrisolvens*, a butyrate-producing bacterium, decreases the formation of aberrant crypt foci in the colon and rectum of mice. *J Nutr* 135(12):2878-2883

Pagès F, Galon J, Dieu-Nosjean MC, Tartour E, Sautès-Fridman C, Fridman WH (2010) Immune infiltration in human tumors: a prognostic factor that should not be ignored. *Oncogene* 29: 1093-1102

Park ES, Yoo JM, Yoo HS, Yoon DY, Yun YP, Hong J (2014) IL-32 gamma enhances TNF-alpha-induced cell death in colon cancer. *Mol Carcinog* 53Suppl 1:E23-35

Parks DH, Tyson GW, Hugenholtz P, Beiko RG (2014) STAMP: statistical analysis of taxonomic and functional profiles. *Bioinformatics* 1;30(21):3123-3124. doi: 10.1093/bioinformatics/btu494

Paula HAA, Martins JFL, Sartori SSR, Castro ASB, Abranches MV, Rafael VC, Ferreira CLLF (2012) The yacon product PBY: Which is the best dose to evaluate the functionality of this new source of prebiotic fructans? *Functional Foods Forum Probiotics*, Turku, Finland

Perše M, Cerar A (2011) Morphological and molecular alterations in 1,2 dimethylhydrazine and azoxymethane induced colon carcinogenesis in rats. *J Biomed Biotechnol* 2011:1-14

Prosberg M, Bendtsen F, Vind I, Petersen AM, Gluud LL (2016) The association between the gut microbiota and the inflammatory bowel disease activity: a systematic review and meta-analysis. *Scand J Gastroenterol* 1-9

Qian BZ, Pollard JW (2010) Macrophage diversity enhances tumor progression and metastasis. *Cell* 141:39-51

Reeves PG, Nielsen FH, Fahey GC Jr (1993) AIN-93 purified diets for laboratory rodents: final report of the American Institute of Nutrition ad hoc writing committee on the reformulation of the AIN-76A rodent diet. *J Nut* 1939-1951

Reiff C, Delday M, Rucklidge G, Reid M, Duncan G, Wohlgemuth S, Hörmannspurger G, Loh G, Blaut M, Collie-Duguid E, Haller D, Kelly D (2009) Balancing inflammatory, lipid, and xenobiotic signaling pathways by VSL#3, a biotherapeutic agent, in the treatment of inflammatory bowel disease. *Inflamm Bowel Dis* 15(11):1721-36. doi: 10.1002/ibd.20999

Reis SA, Conceição LL, Siqueira NP, Rosa DD, Silva LL, Peluzio MCG (2017) Review of the mechanisms of probiotic actions in the prevention of colorectal cancer. *Nutr Res* 37:1-19. <http://dx.doi.org/10.1016/j.nutres.2016.11.009>

Roberfroid MB (2005) Introducing inulin-type fructans. *Br J Nutr* 93, S13–S25

Rossi G, Pengo G, Caldin M, Palumbo Piccionello A, Steiner JM, Cohen ND, Jergens AE, Suchodolski JS (2014) Comparison of microbiological, histological, and immunomodulatory parameters in response to treatment with either combination therapy with prednisone and metronidazole or probiotic VSL#3 strains in dogs with idiopathic inflammatory bowel disease. *PLoS One* 10;9(4):e94699. doi: 10.1371/journal.pone.0094699

Russo D, Valentão P, Andrade PB, Fernandez EC, Milella L (2015) Evaluation of antioxidant, antidiabetic and anticholinesterase activities of *Smallanthus sonchifolius* landraces and correlation with their phytochemical profiles. *Int J Mol Sci* 16(8), 17696-17718. <https://doi.org/10.3390/ijms160817696>

Saus E, Iraola-Guzmana S, Willis JR, Brunet-Vegac A, Gabaldon T (2019) Microbiome and colorectal cancer: roles in carcinogenesis and clinical potential. *Mol Aspects Med* 69:93-106. <https://doi.org/10.1016/j.mam.2019.05.001>

Scheppach W, Weiler F (2004) The butyrate story: old wine in new bottles? *Curr Opin Clin Nutr Metab Care* 7(5):563-567

Shinde T, Perera AP, Vemuri R, Gondalia SV, Beale DJ, Karpe AV, Shastri S, Basheer W, Southam B, Eri R, Stanley R (2020) Synbiotic supplementation with prebiotic green banana resistant starch and probiotic *Bacillus coagulans* spores ameliorates gut inflammation in mouse model of inflammatory bowel diseases. *Eur J Nutr*. doi: 10.1007/s00394-020-02200-9

Sivieri K, Spinardi-Barbisan ALT, Barbisan LF, Bedani R, Pauly ND, Carlos IZ, Benzatti F, Vendramini RC, Rossi EA (2008) Probiotic *Enterococcus faecium* CRL

183 inhibit chemically induced colon cancer in male wistar rats. *Eur Food Res Technol* 228:231-237

Smiricky-Tjardes MR, Grieshop CM, Flickinger EA, Bauer LL, Fahey GC Jr (2003) Dietary galactooligosaccharides affect ileal and total tract nutrient digestibility, ileal and fecal bacterial concentrations, and ileal fermentative characteristics of growing pigs. *Anim Sci J* 81, 2535-2545

Sokol H, Seksik P, Furet JP, Firmesse O, Nion-Larmurier I, Beaugerie L, Cosnes J, Corthier G, Marteau P, Doré J (2009) Low counts of *Faecalibacterium prausnitzii* in colitis microbiota. *Inflamm Bowel Dis* 15(8):1183-1189

Son SH, Jeon HL, Yang SJ, Sim MH, Kim YJ, Lee NK, Paik HD (2017) Probiotic lactic acid bacteria isolated from traditional Korean fermented foods based on β -glucosidase activity. *Food Sci Biotechnol* 14;27(1):123-129. doi: 10.1007/s10068-017-0212-1

Štofilová J, Szabadosová V, Hrčková G, Salaj R, Bertková I, Hijová E, Strojny L, Bomba A (2015) Co-administration of a probiotic strain *Lactobacillus plantarum* LS/07 CCM7766 with prebiotic inulin alleviates the intestinal inflammation in rats exposed to N,N-dimethylhydrazine. *Int Immunopharmacol* 24(2), 361-368 <https://doi.org/10.1016/j.intimp.2014.12.022>

Talero E, Bolivar S, Ávila-Román J, Alcaide A, Fiorucci S, Motilva V (2015) Inhibition of chronic ulcerative colitis associated adenocarcinoma development in mice by VSL#3. *Inflamm Bowel Dis* 21:1027-1037. doi:10.1097/MIB.0000000000000346

Tandon D, Haque MM, Gote M, Jain M, Bhaduri A, Dubey AK, Mande SS (2019) A prospective randomized, double-blind, placebo-controlled, dose response relationship study to investigate efficacy of fructo-oligosaccharides (FOS) on human gut microflora. *Sci Rep* 2;9(1):5473

Tjalsma H, Boleij A, Marchesi JR, Dutilh BE (2012) A bacterial driver-passenger model for colorectal cancer: beyond the usual suspects. *Nat Rev Microbiol* 10, 575–582. <https://doi.org/10.1038/nrmicro2819>

Treu L, Kougias PG, De Diego-Díaz B, Campanaro S, Bassani I, Fernández-Rodríguez J, Angelidaki I (2018) Two-year microbial adaptation during hydrogen-mediated biogas upgrading process in a serial reactor configuration. *Bioresour Technol* doi: 10.1016/j.biortech.2018.05.070

Tryland I, Fiksdal L (1998) Enzyme characteristics of beta-D-galactosidase- and beta-D-glucuronidase-positive bacteria and their interference in rapid methods for detection of waterborne coliforms and *Escherichia coli*. *Appl Environ Microbiol* 64:1018-1023

Tsukamoto T, Kozaki K, Nishikawa Y, Yamamoto M, Fukami H, Inoue M, Wakabayashi K, Tatematsu M (1999) Development and distribution of 2-amino-1-methyl-6-phenylimidazo[4,5-b]pyridine (PhIP)-induced aberrant crypt foci in the rat large intestine. *Jpn J Cancer Res* 90, 720-725

Uccello M, Malaguarnera G, Basile F, D'agata V, Malaguarnera M, Bertino G, Vacante M, Drago F, Biondi A (2012) Potential role of probiotics on colorectal cancer prevention. *BMC Surg* 12(suppl 1):S35

Uchiyama K, Sakiyama T, Hasebe T, Musch MW, Miyoshi H, Nakagawa Y, He TC, Lichtenstein L, Naito Y, Itoh Y, Yoshikawa T, Jabri B, Stappenbeck T, Chang EB (2016) **Butyrate** and bioactive proteolytic form of Wnt-5a regulate colonic epithelial proliferation and spatial development. *Sci Rep* 26;6:32094. doi: 10.1038/srep32094

Uronis JM, Arthur JC, Keku T, Fodor A, Carroll IM, Cruz ML, Appleyard CB, Jobin C (2011) Gut microbial diversity is reduced by the probiotic VSL#3 and correlates with decreased TNBS-induced colitis. *Inflamm Bowel Dis* 17:289-297

Velez E, Castillo N, Mesón O, Grau A, Bonet MEB, Perdigón G (2013) Study of the effect exerted by fructo-oligosaccharides from yacon (*Smallanthus sonchifolius*) root flour in an intestinal infection model with *Salmonella* Typhimurium. *Br J Nutr* 109:1971-1979. doi: 10.1017/S0007114512004230

Verma A, Shukla G (2013) Probiotics *Lactobacillus rhamnosus* GG, *Lactobacillus acidophilus* suppresses DMH-induced procarcinogenic fecal enzymes and preneoplastic aberrant crypt foci in early colon carcinogenesis in Sprague Dawley rats. *Nutr Cancer* 65:84-91. [http://doi: 10.1080/01635581.2013](http://doi:10.1080/01635581.2013)

Verma A, Shukla G (2014) Synbiotic (*Lactobacillus rhamnosus* + *Lactobacillus acidophilus* + inulin) attenuates oxidative stress and colonic damage in 1,2-dimethylhydrazine dihydrochloride-induced colon carcinogenesis in Sprague-Dawley rats: a long-term study. *Eur J Cancer Prev* 23(6):550-559

Villarini M, Caldini G, Moretti M, Trotta F, Pasquini R, Cenci G (2008) Modulatory activity of a *Lactobacillus casei* strain on 1,2-dimethylhydrazine-induced genotoxicity in rats. *Environ Mol Mutagen* 49(3):192-9. doi: 10.1002/em.20367

Wang T, Cai G, Qiu Y, Fei N, Zhang M, Pang X, Jia W, Cai S, Zhao L (2011) Structural segregation of gut microbiota between colorectal cancer patients and healthy volunteers. *ISME J*. doi:10.1038/ismej.2011.109

Worthley DL, Le Leu RK, Whitehall VL, Conlon M, Christophersen C, Belobrajdic D, Mallitt KA, Hu Y, Irahara N, Ogino S, Leggett BA, Young GP (2009) A human, double-blind, placebo-controlled, crossover trial of prebiotic, probiotic, and synbiotic supplementation: effects on luminal, inflammatory, epigenetic, and epithelial biomarkers of colorectal cancer. *Am J Clin Nutr* 90:578-586

Wu N, Yang X, Zhang R, Li J, Xiao X, Hu Y, Chen Y, Yang F, Lu N, Wang Z, Luan C, Liu Y, Wang B, Xiang C, Wang Y, Zhao F, Gao FG, Wang S, Li L, Zhang H, Zhu B (2013) Dysbiosis signature of fecal microbiota in colorectal cancer patients. *Microb Ecol* 66:462-470 doi:10.1007/s00248-013-0245-9

Wu S, Rhee KJ., Albesiano E, Rabizadeh S, Wu X, Yen HR, Huso DL, Brancati FL, Wick E, McAllister F, Housseau F, Pardoll DM, Sears CL (2009) A human colonic commensal promotes colon tumorigenesis via activation of T helper type 17 T cell responses. *Nat Med* 15:1016–1022. doi: 10.1038/nm.2015

Yu LCH (2018) Microbiota dysbiosis and barrier dysfunction in inflammatory bowel disease and colorectal cancers: exploring a common ground hypothesis. *J Biomed Sci* 25:79. <https://doi.org/10.1186/s12929-018-0483-8>

Zaviscic G, Petricevic S, Radulovic Z, Begovic J, Golic N, Topisirovic L, Strahinic I (2012) Probiotic features of two oral *Lactobacillus* isolates. *Braz J Microbiol* 43, 418-428. doi: 10.1590/S1517-838220120001000050

Zhu Q, Gao R, Wu W, Qin H (2013) The role of gut microbiota in the pathogenesis of colorectal cancer. *Tumor Biol* 34:1285-1300

SUPPLEMENTARY MATERIAL

Supplemental Table S1 - Number of OTUs per sample.

IDs	Raw reads	Length after trimming	Reads after trimming	Filtered or chimeric reads	Reads in OTUs	% Assigned	Alpha Diversity				Good's Coverage
							Number of OTUs	Simpson's index	Shannon Entropy	Chao 1-bias corrected	
CONt0_1	40883	254	36305	12063	24242	66.77%	402	0.92	4.86	464.05	0.87
CONt0_2	39926	254	35737	11654	24083	67.39%	444	0.95	5.63	503.54	0.88
CONt0_3	42692	254	38065	13920	24145	63.43%	435	0.97	6.36	479.62	0.91
CONt0_4	39809	254	35489	11889	23600	66.50%	401	0.97	6.25	450.40	0.89
CONt0_5	39818	254	35637	12305	23332	65.47%	446	0.96	6.06	508.66	0.88
CONt3_1	31777	254	28598	8164	20434	71.45%	307	0.85	3.91	368.69	0.83
CONt3_2	35545	254	31709	11158	20551	64.81%	456	0.94	5.62	524.10	0.87
CONt3_3	40177	254	36130	12572	23558	65.20%	463	0.95	5.81	501.37	0.92
CONt3_4	34805	254	30807	9713	21094	68.47%	345	0.92	4.91	390.60	0.88
CONt3_5	41942	254	37772	12433	25339	67.08%	434	0.93	5.41	490.86	0.88
PROt0_1	41144	254	37174	11763	25411	68.36%	437	0.96	6.08	499.61	0.87
PROt0_2	40220	254	35852	11889	23963	66.84%	447	0.94	5.88	505.24	0.88
PROt0_3	38665	254	34819	10647	24172	69.42%	422	0.91	5.16	485.12	0.87
PROt0_4	34868	254	34057	8804	25253	74.15%	450	0.92	5.20	539.16	0.84
PROt0_5	38519	254	37667	9982	27685	73.50%	573	0.97	6.59	699.94	0.82
PROt3_1	27827	254	27178	6589	20589	75.76%	376	0.93	5.06	489.61	0.77
PROt3_2	37069	254	36223	9684	26539	73.27%	477	0.94	5.37	557.54	0.86
PROt3_3	37785	254	36814	10862	25952	70.49%	417	0.90	4.57	491.10	0.85
PROt3_4	28930	254	28214	7114	21100	74.79%	397	0.91	4.64	523.73	0.76
PROt3_5	36232	254	32346	10755	21591	66.75%	385	0.82	4.20	430.77	0.89
SYNt0_1	41408	254	40313	13013	27300	67.72%	500	0.98	6.57	588.12	0.85
SYNt0_2	30424	254	29609	10415	19194	64.82%	497	0.98	6.73	579.12	0.86
SYNt0_3	49993	254	44064	16668	27396	62.17%	521	0.98	6.81	575.73	0.90
SYNt0_4	44875	254	40123	13983	26140	65.15%	458	0.97	6.41	507.90	0.90
SYNt0_5	39194	254	34494	13151	21343	61.87%	442	0.97	6.52	495.96	0.89
SYNt3_1	40655	254	36029	11860	24169	67.08%	472	0.93	5.47	518.65	0.91
SYNt3_2	52162	254	46331	14985	31346	67.66%	501	0.95	5.76	546.14	0.92
SYNt3_3	53972	254	47701	17505	30196	63.30%	597	0.98	6.86	622.19	0.96
SYNt3_4	36510	254	32123	11168	20955	65.23%	432	0.93	5.69	500.94	0.86
SYNt3_5	43201	254	38504	13252	25252	65.58%	458	0.95	6.06	501.90	0.91

Supplemental Table S2 – Alpha diversity.

		Total number of OTUs																				
Sample		1.0	1641.0	3281.0	4920.0	6560.0	8200.0	9840.0	11480.0	13119.0	14759.0	16399.0	18039.0	19678.0	21318.0	22958.0	24598.0	26238.0	27877.0	29517.0	31157.0	
CONt0	402.10	CONt0	1.00	151.31	209.04	246.45	278.03	299.61	317.76	334.66	347.88	359.93	370.76	380.83	388.38	395.35	402.10					
CONt0	444.43	CONt0	1.00	188.45	249.96	290.97	319.72	343.09	361.87	378.73	392.32	403.49	413.83	422.55	430.41	438.84	444.43					
CONt0	435.26	CONt0	1.00	207.61	265.29	301.73	328.60	349.56	366.05	378.55	391.82	400.85	410.03	417.64	424.49	429.80	435.26					
CONt0	400.56	CONt0	1.00	190.92	244.64	277.09	300.23	318.29	333.77	346.87	356.77	366.36	375.16	382.37	389.19	395.32	400.56					
CONt0	446.35	CONt0	1.00	206.11	262.69	300.78	326.92	350.96	368.16	382.61	395.78	407.45	415.73	424.59	433.21	439.80	446.35					
PROt0	436.53	PROt0	1.00	196.02	251.64	286.58	314.59	334.80	351.12	366.54	379.95	390.09	399.03	408.30	416.15	423.47	430.88	436.53				
PROt0	446.71	PROt0	1.00	209.30	267.17	302.88	331.46	352.58	369.84	385.14	397.77	408.40	417.39	426.75	434.76	440.37	446.71					
PROt0	421.97	PROt0	1.00	173.88	236.06	274.18	302.97	324.33	342.08	357.28	369.85	382.44	392.17	400.23	408.07	415.68	421.97					
PROt0	450.41	PROt0	1.00	176.71	234.76	273.96	304.44	327.73	348.86	365.77	380.10	393.93	406.13	416.37	425.67	434.85	443.18	450.41				
PROt0	572.56	PROt0	1.00	246.42	320.24	365.71	399.68	425.64	449.09	466.20	485.32	498.15	511.83	523.59	534.88	546.04	554.75	564.00	572.56			
SYNt0	500.48	SYNt0	1.00	234.22	296.21	335.23	363.51	384.18	403.01	416.92	431.38	442.46	453.76	463.38	471.39	479.86	487.60	493.78	500.48			
SYNt0	496.53	SYNt0	1.00	246.84	315.89	359.91	389.88	414.00	433.27	450.95	464.54	476.13	487.27	496.53								
SYNt0	520.90	SYNt0	1.00	244.37	313.11	353.91	384.73	408.26	426.90	441.52	456.54	466.62	477.79	486.88	494.80	502.63	509.09	515.03	520.90			
SYNt0	458.03	SYNt0	1.00	212.60	273.41	312.41	339.63	359.46	376.51	391.38	403.14	414.36	424.15	432.69	439.50	446.35	452.20	458.03				
SYNt0	442.16	SYNt0	1.00	230.97	289.15	326.26	351.60	371.33	386.68	399.31	409.87	419.11	427.85	435.23	442.16							
CONt3	307.33	CONt3	1.00	109.59	154.04	186.99	211.84	231.79	246.92	260.02	272.22	282.15	291.85	299.64	307.33							
CONt3	455.53	CONt3	1.00	195.45	263.41	308.49	340.18	364.45	383.96	400.84	415.21	427.90	437.66	446.74	455.53							
CONt3	462.66	CONt3	1.00	201.64	269.76	311.78	342.73	367.24	386.03	401.47	413.62	425.58	436.45	443.34	451.01	457.55	462.66					
CONt3	344.71	CONt3	1.00	143.77	195.51	228.82	255.72	274.19	291.05	302.88	313.60	322.58	331.02	338.02	344.71							
CONt3	433.92	CONt3	1.00	183.72	246.94	284.78	314.56	336.04	352.78	368.15	380.36	390.07	399.70	408.09	416.43	423.45	428.54	433.92				
PROt3	376.43	PROt3	1.00	141.57	192.15	227.56	255.98	278.84	300.88	316.88	329.63	343.77	356.56	366.37	376.43							
PROt3	477.15	PROt3	1.00	177.76	244.45	289.26	322.01	347.75	368.97	388.37	401.47	415.56	427.39	437.38	447.07	455.78	464.26	470.63	477.15			
PROt3	417.08	PROt3	1.00	141.74	203.66	246.89	275.75	302.07	322.55	338.46	353.77	365.25	377.54	387.53	396.67	403.75	410.99	417.08				
PROt3	397.06	PROt3	1.00	133.64	188.85	230.85	259.56	286.59	305.95	326.70	343.57	359.22	373.10	385.76	397.06							
PROt3	385.47	PROt3	1.00	148.25	207.59	245.28	275.18	297.93	316.46	331.44	343.58	354.24	363.99	371.98	379.33	385.47						
SYNt3	471.62	SYNt3	1.00	203.63	272.88	314.57	347.00	370.54	390.52	407.04	420.85	430.75	441.47	450.57	459.32	465.51	471.62					
SYNt3	501.00	SYNt3	1.00	206.99	271.95	313.74	343.63	369.22	387.37	404.37	418.00	431.24	442.71	451.16	459.18	467.22	474.53	480.86	486.63	491.93	496.44	501.00
SYNt3	597.43	SYNt3	1.00	272.61	354.48	404.79	441.33	469.07	490.63	508.08	524.32	536.81	547.12	557.89	565.21	573.70	578.84	584.15	588.99	593.21	597.43	
SYNt3	432.15	SYNt3	1.00	202.01	262.64	301.42	329.88	349.54	368.88	383.56	395.82	406.83	416.30	424.68	432.15							
SYNt3	458.08	SYNt3	1.00	216.97	277.19	313.59	342.80	364.43	381.20	394.79	407.40	418.25	426.65	434.63	442.78	447.57	452.73	458.08				

Supplemental Table S2 – Alpha diversity (*cont.*).

		Simpson's Index																			
Sample		1.00	1641.00	3281.0	4920.0	6560.0	8200.0	9840.0	11480.0	13119.0	14759.0	16399.0	18039.0	19678.0	21318.0	22958.0	24598.0	26238.0	27877.0	29517.0	31157
CONt0	0.92	CONt0	0.00	0.92	0.92	0.92	0.92	0.92	0.92	0.92	0.92	0.92	0.92	0.92	0.92	0.92					
CONt0	0.95	CONt0	0.00	0.95	0.95	0.95	0.95	0.95	0.95	0.95	0.95	0.95	0.95	0.95	0.95	0.95					
CONt0	0.97	CONt0	0.00	0.97	0.97	0.97	0.97	0.97	0.97	0.97	0.97	0.97	0.97	0.97	0.97	0.97					
CONt0	0.97	CONt0	0.00	0.97	0.97	0.97	0.97	0.97	0.97	0.97	0.97	0.97	0.97	0.97	0.97	0.97					
CONt0	0.96	CONt0	0.00	0.96	0.96	0.96	0.96	0.96	0.96	0.96	0.96	0.96	0.96	0.96	0.96	0.96					
PROt0	0.96	PROt0	0.00	0.96	0.96	0.96	0.96	0.96	0.96	0.96	0.96	0.96	0.96	0.96	0.96	0.96	0.96				
PROt0	0.94	PROt0	0.00	0.94	0.94	0.94	0.94	0.94	0.94	0.94	0.94	0.94	0.94	0.94	0.94	0.94					
PROt0	0.91	PROt0	0.00	0.91	0.91	0.91	0.91	0.91	0.91	0.91	0.91	0.91	0.91	0.91	0.91	0.91					
PROt0	0.92	PROt0	0.00	0.92	0.92	0.92	0.92	0.92	0.92	0.92	0.92	0.92	0.92	0.92	0.92	0.92	0.92				
PROt0	0.97	PROt0	0.00	0.97	0.97	0.97	0.97	0.97	0.97	0.97	0.97	0.97	0.97	0.97	0.97	0.97	0.97	0.97			
SYNt0	0.98	SYNt0	0.00	0.97	0.98	0.98	0.98	0.98	0.98	0.98	0.98	0.98	0.98	0.98	0.98	0.98	0.98	0.98			
SYNt0	0.98	SYNt0	0.00	0.98	0.98	0.98	0.98	0.98	0.98	0.98	0.98	0.98	0.98								
SYNt0	0.98	SYNt0	0.00	0.98	0.98	0.98	0.98	0.98	0.98	0.98	0.98	0.98	0.98	0.98	0.98	0.98	0.98	0.98			
SYNt0	0.97	SYNt0	0.00	0.97	0.97	0.97	0.97	0.97	0.97	0.97	0.97	0.97	0.97	0.97	0.97	0.97	0.97				
CONt3	0.85	CONt3	0.00	0.85	0.85	0.85	0.85	0.85	0.85	0.85	0.85	0.85	0.85	0.85							
CONt3	0.94	CONt3	0.00	0.94	0.94	0.94	0.94	0.94	0.94	0.94	0.94	0.94	0.94	0.94							
CONt3	0.95	CONt3	0.00	0.95	0.95	0.95	0.95	0.95	0.95	0.95	0.95	0.95	0.95	0.95	0.95	0.95					
CONt3	0.92	CONt3	0.00	0.92	0.92	0.92	0.92	0.92	0.92	0.92	0.92	0.92	0.92	0.92							
CONt3	0.93	CONt3	0.00	0.93	0.93	0.93	0.93	0.93	0.93	0.93	0.93	0.93	0.93	0.93	0.93	0.93	0.93				
PROt3	0.93	PROt3	0.00	0.93	0.93	0.93	0.93	0.93	0.93	0.93	0.93	0.93	0.93	0.93							
PROt3	0.94	PROt3	0.00	0.93	0.93	0.93	0.94	0.93	0.93	0.94	0.94	0.94	0.94	0.94	0.94	0.94	0.94	0.94			
PROt3	0.90	PROt3	0.00	0.90	0.90	0.90	0.90	0.90	0.90	0.90	0.90	0.90	0.90	0.90	0.90	0.90	0.90				
PROt3	0.91	PROt3	0.00	0.91	0.91	0.91	0.91	0.91	0.91	0.91	0.91	0.91	0.91	0.91							
PROt3	0.82	PROt3	0.00	0.82	0.82	0.82	0.82	0.82	0.82	0.82	0.82	0.82	0.82	0.82	0.82						
SYNt3	0.93	SYNt3	0.00	0.93	0.93	0.93	0.93	0.93	0.93	0.93	0.93	0.93	0.93	0.93	0.93	0.93					
SYNt3	0.95	SYNt3	0.00	0.95	0.95	0.95	0.95	0.95	0.95	0.95	0.95	0.95	0.95	0.95	0.95	0.95	0.95	0.95	0.95	0.95	0.95
SYNt3	0.98	SYNt3	0.00	0.98	0.98	0.98	0.98	0.98	0.98	0.98	0.98	0.98	0.98	0.98	0.98	0.98	0.98	0.98	0.98	0.98	0.98
SYNt3	0.93	SYNt3	0.00	0.93	0.93	0.93	0.93	0.93	0.93	0.93	0.93	0.93	0.93	0.93							
SYNt3	0.95	SYNt3	0.00	0.95	0.95	0.95	0.95	0.95	0.95	0.95	0.95	0.95	0.95	0.95	0.95	0.95	0.95				

Supplemental Table S2 – Alpha diversity (*cont.*).

Shannon Entropy																							
Sample			1.0	1641.0	3281.0	4920.0	6560.0	8200.0	9840.0	11480.0	13119.0	14759.0	16399.0	18039.0	19678.0	21318.0	22958.0	24598.0	26238.0	27877.0	29517.0	31157.0	
CONt0	4.86	CONt0	0.00	4.74	4.79	4.81	4.83	4.84	4.84	4.85	4.85	4.85	4.86	4.86	4.86	4.86	4.86						
CONt0	5.63	CONt0	0.00	5.48	5.55	5.58	5.59	5.60	5.61	5.62	5.62	5.62	5.63	5.63	5.63	5.63	5.63						
CONt0	6.36	CONt0	0.00	6.21	6.27	6.30	6.32	6.33	6.34	6.34	6.35	6.35	6.35	6.35	6.35	6.36	6.36						
CONt0	6.25	CONt0	0.00	6.11	6.17	6.21	6.21	6.22	6.23	6.24	6.24	6.24	6.24	6.25	6.25	6.25	6.25						
CONt0	6.06	CONt0	0.00	5.90	5.97	6.01	6.02	6.04	6.04	6.05	6.05	6.05	6.05	6.06	6.06	6.06	6.06						
PROt0	6.08	PROt0	0.00	5.93	6.00	6.03	6.05	6.06	6.06	6.07	6.07	6.08	6.08	6.08	6.08	6.08	6.08	6.08					
PROt0	5.88	PROt0	0.00	5.73	5.80	5.82	5.84	5.85	5.85	5.86	5.87	5.87	5.87	5.87	5.87	5.88	5.88						
PROt0	5.16	PROt0	0.00	5.00	5.08	5.10	5.12	5.13	5.13	5.14	5.15	5.15	5.15	5.15	5.15	5.16	5.16						
PROt0	5.20	PROt0	0.00	5.05	5.11	5.13	5.16	5.17	5.17	5.18	5.18	5.18	5.19	5.19	5.19	5.19	5.19	5.20					
PROt0	6.59	PROt0	0.00	6.40	6.48	6.51	6.54	6.55	6.56	6.56	6.57	6.57	6.58	6.58	6.58	6.58	6.58	6.58	6.59				
SYNt0	6.57	SYNt0	0.00	6.40	6.48	6.51	6.53	6.54	6.55	6.55	6.56	6.56	6.56	6.57	6.57	6.57	6.57	6.57	6.57				
SYNt0	6.73	SYNt0	0.00	6.56	6.63	6.67	6.69	6.70	6.71	6.72	6.72	6.72	6.73	6.73									
SYNt0	6.81	SYNt0	0.00	6.62	6.70	6.74	6.76	6.77	6.78	6.78	6.79	6.79	6.80	6.80	6.80	6.80	6.80	6.80	6.81				
SYNt0	6.41	SYNt0	0.00	6.24	6.32	6.35	6.37	6.38	6.38	6.39	6.39	6.40	6.40	6.40	6.40	6.40	6.41						
SYNt0	6.52	SYNt0	0.00	6.36	6.44	6.47	6.49	6.49	6.50	6.50	6.51	6.51	6.52	6.52	6.52								
CONt3	3.91	CONt3	0.00	3.81	3.85	3.87	3.89	3.90	3.90	3.90	3.90	3.91	3.91	3.91	3.91								
CONt3	5.62	CONt3	0.00	5.45	5.53	5.57	5.58	5.59	5.60	5.60	5.61	5.61	5.61	5.62	5.62								
CONt3	5.81	CONt3	0.00	5.64	5.73	5.76	5.78	5.79	5.79	5.80	5.80	5.80	5.81	5.81	5.81	5.81	5.81						
CONt3	4.91	CONt3	0.00	4.80	4.85	4.87	4.89	4.89	4.90	4.90	4.90	4.91	4.91	4.91	4.91								
CONt3	5.41	CONt3	0.00	5.26	5.33	5.36	5.37	5.38	5.39	5.39	5.40	5.40	5.41	5.41	5.41	5.41	5.41	5.41					
PROt3	5.06	PROt3	0.00	4.95	5.00	5.01	5.03	5.04	5.05	5.05	5.05	5.06	5.06	5.06									
PROt3	5.37	PROt3	0.00	5.22	5.29	5.31	5.33	5.34	5.34	5.36	5.36	5.36	5.36	5.36	5.37	5.37	5.37	5.37	5.37				
PROt3	4.57	PROt3	0.00	4.43	4.50	4.52	4.53	4.54	4.55	4.55	4.55	4.56	4.56	4.56	4.57	4.57	4.57	4.57					
PROt3	4.64	PROt3	0.00	4.52	4.57	4.60	4.61	4.61	4.62	4.63	4.63	4.63	4.63	4.64	4.64								
PROt3	4.20	PROt3	0.00	4.08	4.13	4.15	4.17	4.18	4.19	4.19	4.19	4.19	4.20	4.20	4.20	4.20							
SYNt3	5.47	SYNt3	0.00	5.30	5.38	5.41	5.43	5.43	5.45	5.45	5.46	5.46	5.46	5.47	5.47	5.47	5.47						
SYNt3	5.76	SYNt3	0.00	5.60	5.66	5.69	5.71	5.72	5.73	5.74	5.74	5.74	5.74	5.75	5.75	5.75	5.75	5.75	5.75	5.75	5.76	5.76	5.76
SYNt3	6.86	SYNt3	0.00	6.64	6.74	6.78	6.81	6.81	6.82	6.83	6.84	6.84	6.84	6.84	6.85	6.85	6.85	6.85	6.85	6.85	6.86	6.86	6.86
SYNt3	5.69	SYNt3	0.00	5.55	5.62	5.64	5.66	5.67	5.68	5.68	5.69	5.69	5.69	5.69	5.69								
SYNt3	6.06	SYNt3	0.00	5.90	5.98	6.00	6.02	6.03	6.04	6.05	6.05	6.06	6.06	6.06	6.06	6.06	6.06	6.06					

Supplemental Table S2 – Alpha diversity (*cont.*).

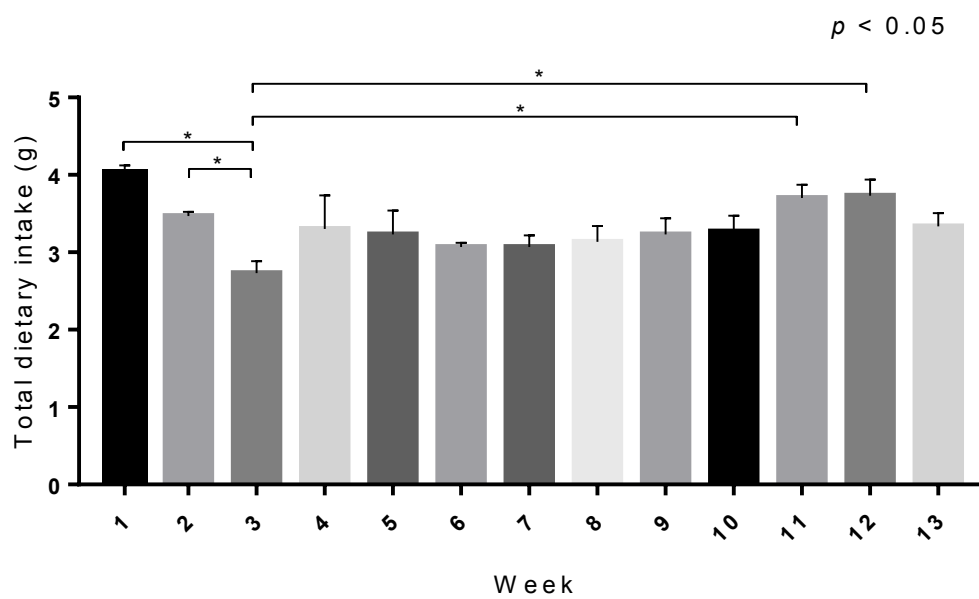
		Chao 1 bias-corrected																				
Sample		1.0	1641.0	3281.0	4920.0	6560.0	8200.0	9840.0	11480.0	13119.0	14759.0	16399.0	18039.0	19678.0	21318.0	22958.0	24598.0	26238.0	27877.0	29517.0	31157.0	
CONt0	464.05	CONt0	1.00	263.89	335.96	364.36	398.92	400.99	419.94	431.14	437.10	445.86	446.45	457.88	457.80	464.07	464.05					
CONt0	503.54	CONt0	1.00	298.31	361.14	400.31	426.73	447.38	461.89	471.79	480.79	486.72	488.44	491.83	495.64	501.84	503.54					
CONt0	479.62	CONt0	1.00	300.50	361.93	398.56	420.75	440.00	448.88	452.64	462.20	466.38	470.68	474.11	477.29	476.95	479.62					
CONt0	450.40	CONt0	1.00	282.11	332.71	358.89	380.29	399.93	417.09	423.39	430.80	435.23	443.84	444.35	446.85	450.17	450.40					
CONt0	508.66	CONt0	1.00	300.39	365.00	408.55	426.66	450.57	463.85	477.09	482.69	488.24	488.29	493.22	499.12	505.68	508.66					
PROt0	499.61	PROt0	1.00	292.71	346.15	387.00	414.94	429.85	444.25	462.29	478.51	479.04	481.91	491.82	494.04	498.55	501.01	499.61				
PROt0	505.24	PROt0	1.00	301.00	367.48	401.06	433.45	450.72	459.71	468.13	479.63	483.56	485.98	496.49	501.59	502.54	505.24					
PROt0	485.12	PROt0	1.00	277.54	344.03	378.52	407.03	426.42	437.92	445.63	455.68	464.34	469.61	471.19	477.24	480.54	485.12					
PROt0	539.16	PROt0	1.00	278.68	349.39	399.70	428.00	449.53	468.27	484.13	495.06	507.16	509.01	516.19	523.18	527.20	532.15	539.16				
PROt0	699.94	PROt0	1.00	371.06	444.53	491.35	527.08	554.79	578.35	598.11	617.85	634.26	647.14	657.22	667.89	676.55	684.20	693.87	699.94			
SYNt0	588.12	SYNt0	1.00	337.63	390.62	433.60	463.62	482.95	505.46	521.51	538.42	546.60	557.36	567.63	573.04	579.88	587.76	586.01	588.12			
SYNt0	579.12	SYNt0	1.00	360.05	432.07	473.02	492.63	517.51	531.45	542.63	555.21	563.52	571.79	579.12								
SYNt0	575.73	SYNt0	1.00	363.38	429.44	458.79	483.38	507.91	520.73	532.63	546.62	550.78	559.60	564.57	570.40	573.76	574.52	575.81	575.73			
SYNt0	507.90	SYNt0	1.00	312.06	374.64	413.13	437.11	452.57	462.70	478.19	483.51	492.17	497.87	502.55	502.81	505.90	504.29	507.90				
SYNt0	495.96	SYNt0	1.00	326.42	377.87	415.31	436.67	454.73	467.22	475.72	480.29	482.62	487.02	490.54	495.96							
CONt3	368.69	CONt3	1.00	207.20	251.77	285.56	314.61	332.17	340.55	344.61	355.45	358.82	361.95	365.19	368.69							
CONt3	524.10	CONt3	1.00	320.06	389.81	428.49	448.35	469.94	483.26	493.51	501.12	511.01	512.08	519.36	524.10							
CONt3	501.37	CONt3	1.00	322.13	396.70	428.25	445.64	459.20	470.77	477.65	483.55	492.42	498.25	498.40	499.97	503.08	501.37					
CONt3	390.60	CONt3	1.00	242.97	298.26	321.33	341.30	353.88	363.94	368.86	375.91	381.03	385.33	385.68	390.60							
CONt3	490.86	CONt3	1.00	288.12	353.46	383.89	404.76	428.65	435.68	450.94	460.48	461.44	470.00	478.20	481.68	486.81	488.96	490.86				
PROt3	489.61	PROt3	1.00	255.04	309.01	349.85	387.49	406.02	427.88	440.92	447.27	463.49	478.20	484.60	489.61							
PROt3	557.54	PROt3	1.00	300.84	380.22	420.80	446.65	461.94	482.58	497.18	503.84	514.96	525.38	530.62	538.43	542.93	549.43	553.87	557.54			
PROt3	491.10	PROt3	1.00	277.12	335.24	376.97	395.77	410.42	422.70	436.12	448.37	454.02	464.06	471.66	479.34	482.68	485.23	491.10				
PROt3	523.73	PROt3	1.00	257.76	327.14	382.31	404.83	436.32	449.78	470.84	490.07	499.04	511.38	515.34	523.73							
PROt3	430.77	PROt3	1.00	263.58	326.35	350.15	374.43	388.90	400.54	410.06	418.12	424.49	431.06	430.85	431.65	430.77						
SYNt3	518.65	SYNt3	1.00	319.10	388.68	428.49	456.06	476.08	487.54	494.80	502.50	501.56	503.33	509.38	515.87	516.05	518.65					
SYNt3	546.14	SYNt3	1.00	322.24	389.03	427.30	451.60	475.30	488.84	502.80	513.65	520.51	528.75	533.70	535.81	540.14	542.76	544.61	545.49	545.66	545.84	546.14
SYNt3	622.19	SYNt3	1.00	407.39	481.41	531.18	563.24	576.96	596.43	598.19	608.56	613.62	616.93	622.27	621.44	627.01	624.67	624.75	623.92	622.19	622.19	
SYNt3	500.94	SYNt3	1.00	310.75	369.40	399.72	425.44	441.54	458.59	468.99	477.92	485.17	490.58	495.20	500.94							
SYNt3	501.90	SYNt3	1.00	318.41	378.93	411.43	435.72	451.19	464.32	473.44	479.15	485.98	485.06	490.75	494.56	495.29	498.97	501.90				

Supplemental Table S2 – Alpha diversity (*cont.*).

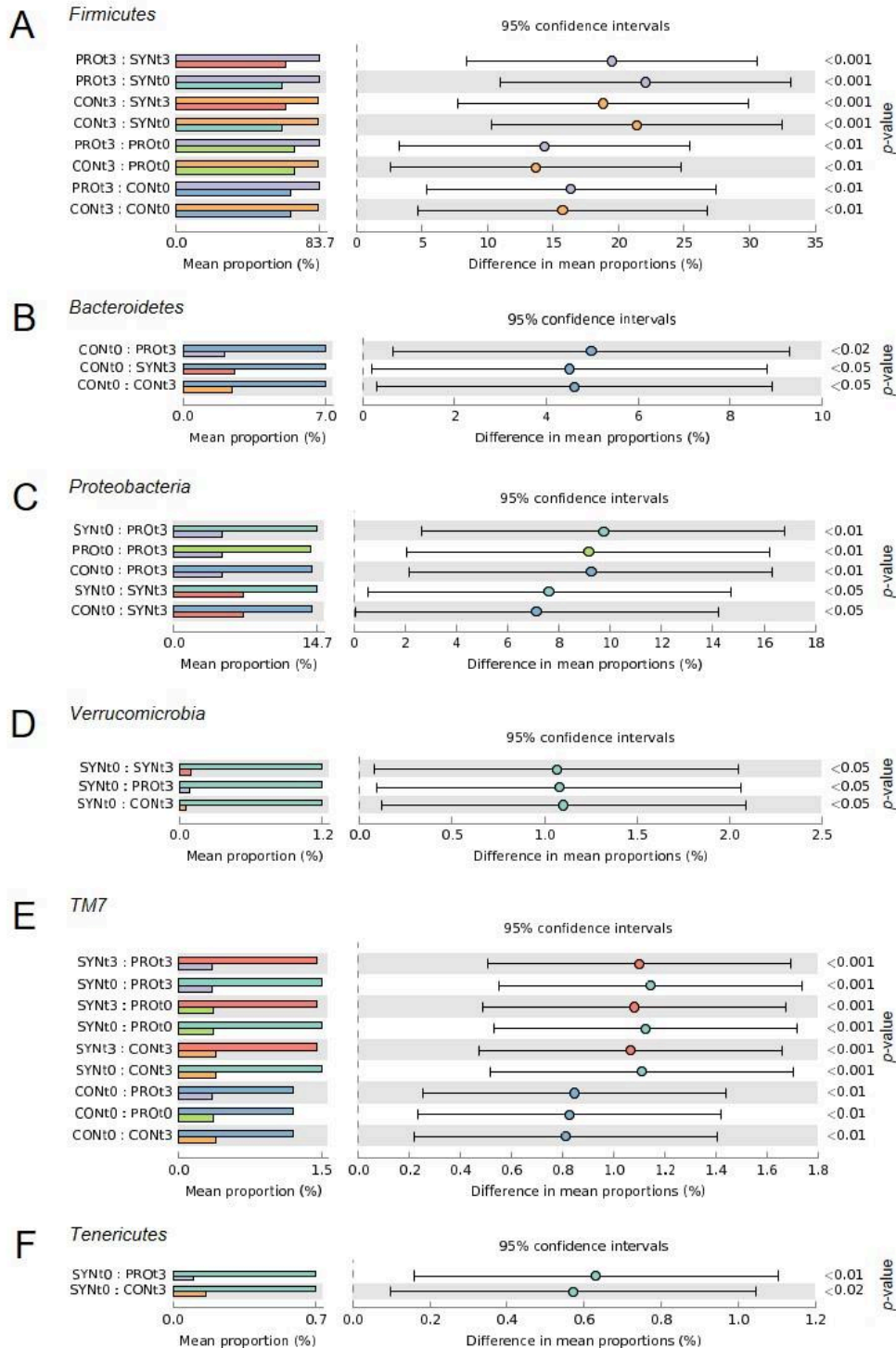
		Phylogenetic diversity																					
Sample		1.0	1641.0	3281.0	4920.0	6560.0	8200.0	9840.0	11480.0	13119.0	14759.0	16399.0	18039.0	19678.0	21318.0	22958.0	24598.0	26238.0	27877.0	29517.0	31157.0		
CONt0	9.31	CONt0	0.59	8.18	8.68	8.87	9.00	9.08	9.13	9.20	9.21	9.25	9.27	9.29	9.30	9.30	9.31						
CONt0	9.36	CONt0	0.53	8.51	8.85	9.04	9.14	9.21	9.25	9.28	9.30	9.32	9.34	9.35	9.35	9.35	9.36						
CONt0	8.17	CONt0	0.38	7.40	7.67	7.86	7.97	8.02	8.06	8.09	8.11	8.12	8.14	8.15	8.16	8.16	8.17						
CONt0	8.12	CONt0	0.36	7.49	7.76	7.85	7.92	7.96	8.01	8.03	8.05	8.07	8.08	8.10	8.12	8.12	8.12						
CONt0	9.22	CONt0	0.41	8.56	8.87	8.95	8.97	9.04	9.09	9.12	9.13	9.15	9.17	9.20	9.21	9.22	9.22						
PROt0	8.48	PROt0	0.43	7.51	7.97	8.14	8.25	8.31	8.33	8.38	8.39	8.40	8.42	8.43	8.45	8.46	8.47	8.48					
PROt0	8.46	PROt0	0.48	7.42	7.98	8.14	8.21	8.24	8.30	8.33	8.32	8.37	8.38	8.42	8.44	8.44	8.46						
PROt0	9.00	PROt0	0.56	8.26	8.73	8.82	8.89	8.92	8.94	8.95	8.97	8.97	8.98	8.98	8.99	9.00	9.00						
PROt0	9.33	PROt0	0.51	8.37	8.86	9.03	9.16	9.19	9.23	9.26	9.29	9.30	9.30	9.32	9.32	9.32	9.32	9.33					
PROt0	9.71	PROt0	0.48	9.25	9.53	9.61	9.67	9.68	9.69	9.70	9.70	9.70	9.70	9.70	9.71	9.71	9.71	9.71	9.71	9.71			
SYNt0	9.46	SYNt0	0.47	9.00	9.28	9.37	9.41	9.43	9.44	9.45	9.45	9.45	9.46	9.46	9.46	9.46	9.46	9.46	9.46	9.46			
SYNt0	9.42	SYNt0	0.33	8.37	8.97	9.17	9.28	9.33	9.36	9.39	9.40	9.41	9.41	9.42									
SYNt0	9.32	SYNt0	0.39	8.63	9.03	9.13	9.18	9.21	9.22	9.23	9.25	9.26	9.27	9.27	9.28	9.29	9.30	9.31	9.32				
SYNt0	9.42	SYNt0	0.42	8.55	8.89	9.01	9.11	9.17	9.21	9.24	9.26	9.30	9.32	9.34	9.35	9.37	9.40	9.42					
SYNt0	9.35	SYNt0	0.22	8.23	8.55	8.81	8.99	9.07	9.14	9.20	9.23	9.28	9.31	9.33	9.35								
CONt3	8.35	CONt3	0.56	5.73	6.65	7.25	7.53	7.72	7.94	8.05	8.16	8.24	8.28	8.32	8.35								
CONt3	8.92	CONt3	0.49	7.88	8.42	8.58	8.69	8.76	8.80	8.82	8.84	8.88	8.89	8.90	8.92								
CONt3	9.00	CONt3	0.47	8.11	8.44	8.63	8.68	8.73	8.80	8.86	8.89	8.92	8.94	8.96	8.98	9.00	9.00						
CONt3	8.47	CONt3	0.54	6.90	7.55	7.89	8.06	8.18	8.24	8.30	8.34	8.37	8.40	8.44	8.47								
CONt3	8.95	CONt3	0.50	7.83	8.35	8.54	8.67	8.73	8.76	8.82	8.84	8.85	8.88	8.89	8.90	8.92	8.95	8.95					
PROt3	8.97	PROt3	0.63	8.03	8.56	8.74	8.84	8.88	8.92	8.94	8.94	8.96	8.96	8.97	8.97								
PROt3	9.21	PROt3	0.45	8.07	8.61	8.80	8.93	9.00	9.03	9.07	9.09	9.12	9.13	9.15	9.17	9.17	9.18	9.20	9.21				
PROt3	9.46	PROt3	0.53	7.77	8.41	8.72	8.89	9.03	9.12	9.18	9.21	9.26	9.32	9.35	9.39	9.42	9.43	9.46					
PROt3	9.16	PROt3	0.59	7.57	8.19	8.55	8.68	8.81	8.94	8.94	9.04	9.08	9.10	9.14	9.16								
PROt3	9.26	PROt3	0.55	7.65	8.36	8.68	8.86	8.95	9.03	9.09	9.15	9.18	9.22	9.25	9.26	9.26							
SYNt3	9.19	SYNt3	0.47	8.02	8.55	8.82	8.90	9.01	9.08	9.11	9.13	9.16	9.16	9.17	9.18	9.19	9.19						
SYNt3	9.38	SYNt3	0.36	8.23	8.76	8.93	9.06	9.13	9.18	9.21	9.23	9.26	9.28	9.28	9.30	9.32	9.33	9.33	9.35	9.35	9.35	9.37	9.38
SYNt3	9.49	SYNt3	0.34	8.56	8.95	9.12	9.20	9.25	9.30	9.33	9.35	9.38	9.39	9.41	9.42	9.43	9.46	9.45	9.47	9.48	9.49		
SYNt3	8.88	SYNt3	0.57	8.05	8.44	8.61	8.70	8.74	8.79	8.82	8.83	8.85	8.86	8.87	8.88								
SYNt3	9.08	SYNt3	0.40	8.13	8.52	8.70	8.81	8.89	8.94	8.96	8.99	9.01	9.01	9.03	9.04	9.06	9.06	9.08					

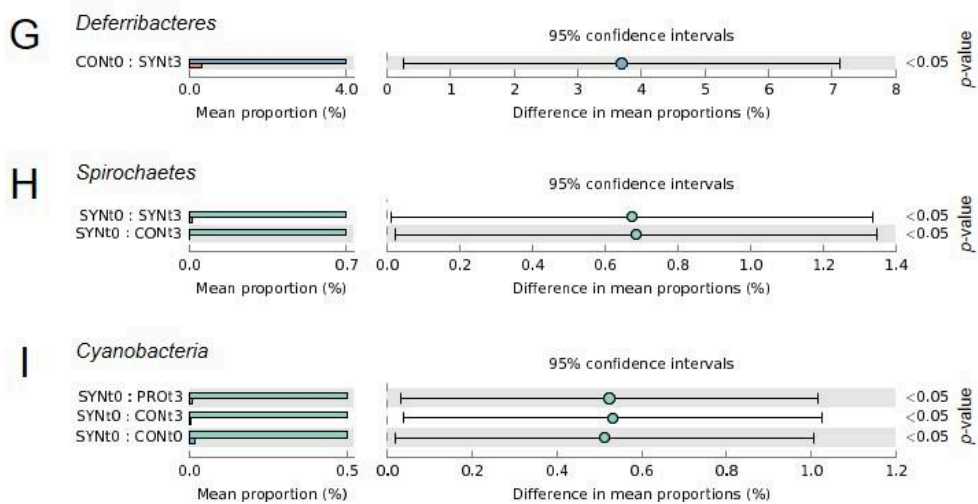
Supplemental Table S3 – Beta diversity.

PERMANOVA analysis (Unweighted UniFrac)				PERMANOVA analysis (Weighted UniFrac)			
Variable	Groups	Pseudo-f statistic	<i>p</i> -value	Variable	Groups	Pseudo-f statistic	<i>p</i> -value
B	CONt3, PROt0, PROt3, CONt0, SYNt0, SYNt3	8.21	0.0001	B	CONt3, PROt0, PROt3, CONt0, SYNt0, SYNt3	8.97	0.0001
Group 1	Group 2	Pseudo-f statistic	<i>p</i> -value	Group 1	Group 2	Pseudo-f statistic	<i>p</i> -value
PROt0	SYNt0	6.29	<u>0.01</u>	PROt0	SYNt0	11.99	<u>0.01</u>
PROt0	CONt3	8.06	<u>0.01</u>	PROt0	CONt3	5.36	<u>0.02</u>
SYNt0	CONt3	19.23	<u>0.01</u>	SYNt0	CONt3	19.17	<u>0.01</u>
PROt0	CONt0	2.35	0.10	PROt0	CONt0	0.91	0.39
SYNt0	CONt0	7.20	<u>0.01</u>	SYNt0	CONt0	5.51	<u>0.01</u>
CONt3	CONt0	8.14	<u>0.01</u>	CONt3	CONt0	4.23	<u>0.06</u>
PROt0	PROt3	4.15	<u>0.01</u>	PROt0	PROt3	11.51	<u>0.01</u>
SYNt0	PROt3	13.45	<u>0.01</u>	SYNt0	PROt3	23.28	<u>0.01</u>
CONt3	PROt3	3.94	<u>0.03</u>	CONt3	PROt3	1.48	0.22
CONt0	PROt3	8.89	<u>0.01</u>	CONt0	PROt3	6.95	<u>0.02</u>
PROt0	SYNt3	8.85	<u>0.01</u>	PROt0	SYNt3	12.53	<u>0.01</u>
SYNt0	SYNt3	3.97	<u>0.02</u>	SYNt0	SYNt3	4.20	<u>0.02</u>
CONt3	SYNt3	16.34	<u>0.01</u>	CONt3	SYNt3	14.23	<u>0.01</u>
CONt0	SYNt3	11.39	<u>0.01</u>	CONt0	SYNt3	4.93	<u>0.01</u>
PROt3	SYNt3	10.51	<u>0.01</u>	PROt3	SYNt3	16.71	<u>0.01</u>

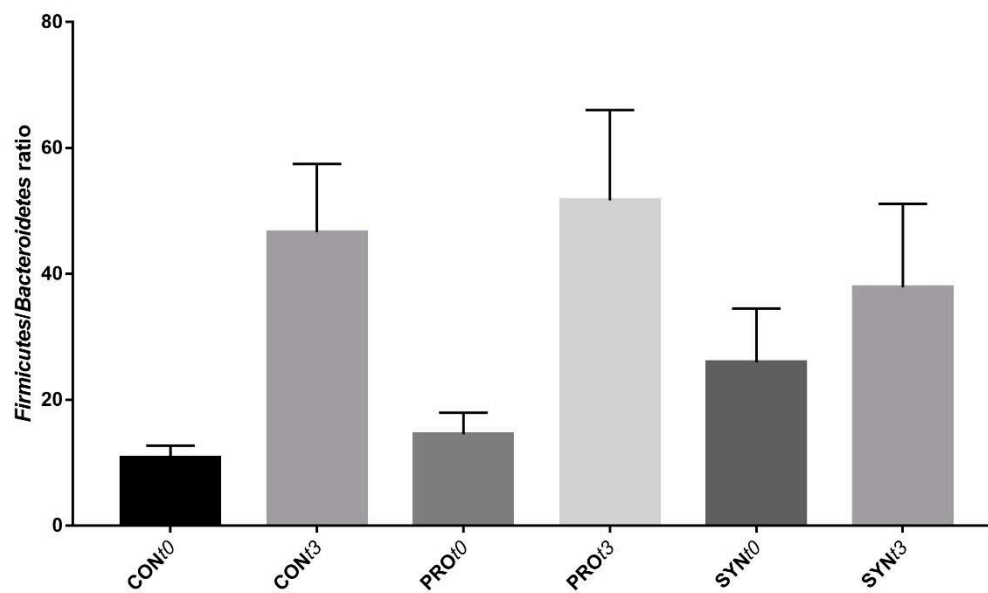
Supplemental Figure S1 – Total dietary intake per week. (*) $p < 0.05$.

Supplemental Figure S2 – Phylum level composition in mice feces observed in CON, PRO and SYN groups before (t_0) and after (t_3) their respective intervention. Color-coded bar plots show the mean bacterial proportion (%). Only phyla with significant differences are shown (FDR < 0.05).

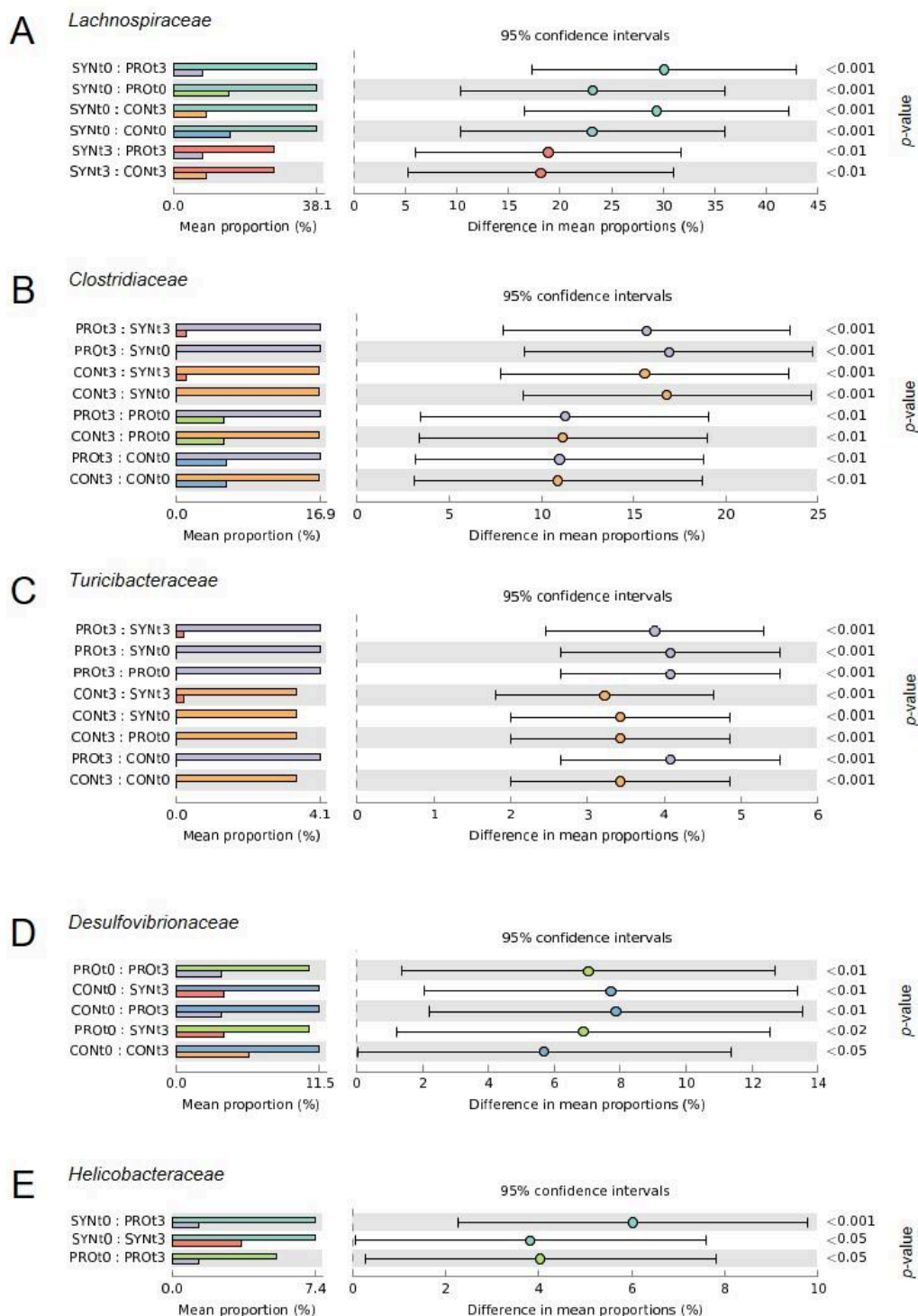


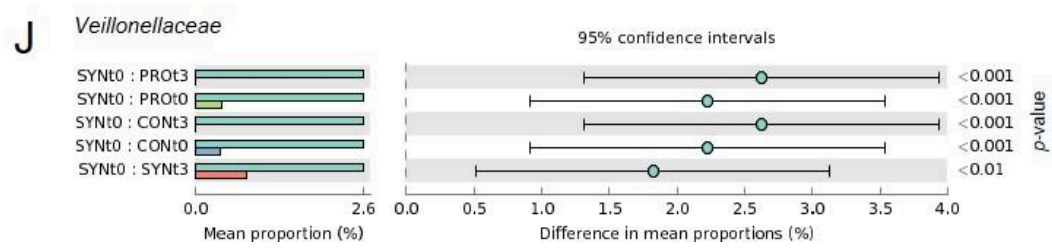
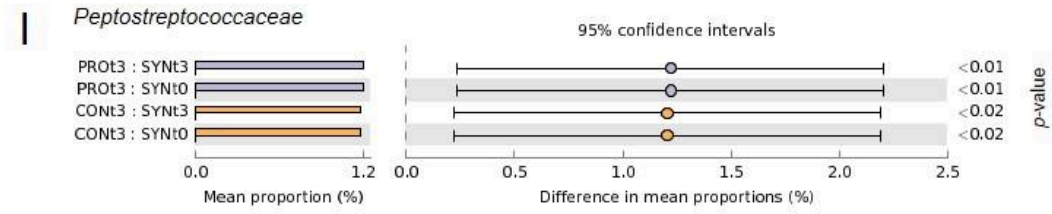
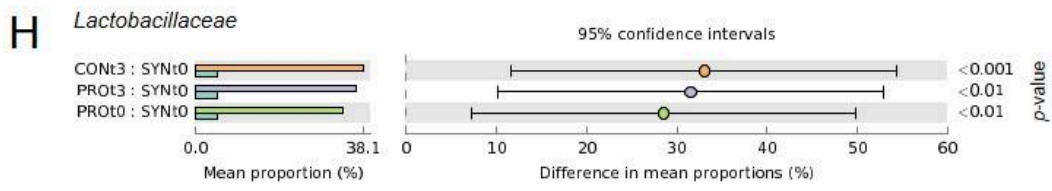
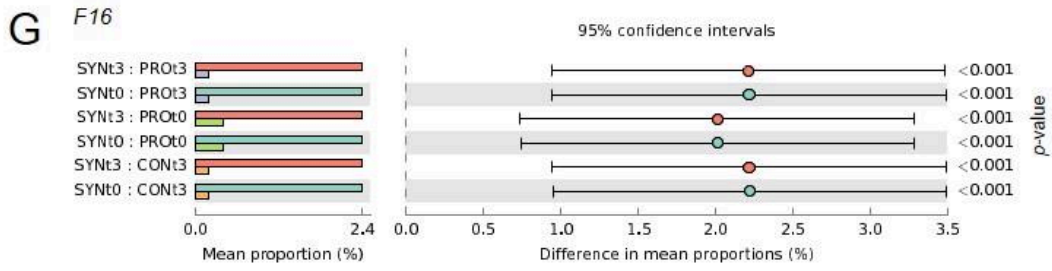
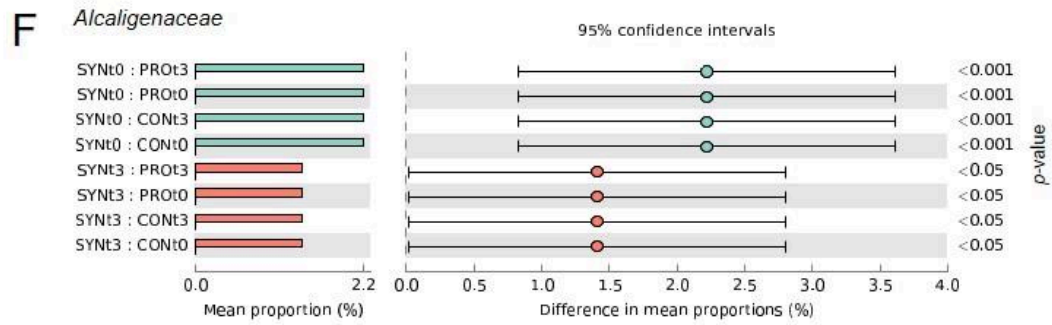


Supplemental Figure S3 – Column bar graph of *Firmicutes/Bacteroidetes* ratios CON, PRO and SYN groups at the time-points t_0 (before the experimental period) and t_1 (end of the experimental period).



Supplemental Figure S4 – Family level composition in mice feces observed in CON, PRO and SYN groups before (t_0) and after (t_1) their respective intervention. Color-coded bar plots show the mean bacterial proportion (%). Only families with significant differences are shown (FDR < 0.05).





4.2 MANUSCRIPT 2

Manuscript published in **Journal of Food Science** (Impact Factor: 3.167) (Attachment 2)

Evaluation of the efficacy of probiotic VSL#3 and synbiotic VSL#3 and yacon-based product in reducing oxidative stress and intestinal permeability in mice induced to colorectal carcinogenesis.

Bruna Cristina dos Santos Cruz¹, Luís Fernando de Sousa Moraes², Letícia De Nadai Marcon¹, Kelly Aparecida Dias¹, Leonardo Borges Murad³, Mariáurea Matias Sarandy⁴, Lisiane Lopes da Conceição¹, Reggiani Vilela Gonçalves⁵, Célia Lúcia de Lucas Fortes Ferreira⁶, Maria do Carmo Gouveia Peluzio¹

¹Nutritional Biochemistry Laboratory, Department of Nutrition and Health. Universidade Federal de Viçosa - UFV, Viçosa, Minas Gerais, Brazil.

²Experimental and Dietetic Nutrition Laboratory, Department of Nutrition. Federal University of Pernambuco - UFPE, Recife, Pernambuco, Brazil

³Brazilian National Cancer Institute, Rio de Janeiro, Brazil.

⁴Department of General Biology, Federal University of Viçosa, Viçosa, Minas Gerais, Brazil.

⁵Experimental Pathology Laboratory, Department of Animal Biology, Universidade Federal de Viçosa - UFV, Viçosa, Minas Gerais, Brazil.

⁶Institute of Biotechnology Applied to Agriculture & Livestock (Bioagro), Universidade Federal de Viçosa - UFV, Viçosa, Minas Gerais, Brazil.

Received 8 November 2020/Revised 18 February 2021

Accepted 20 February 2021

DOI: 10.1111/1750-3841.15690

Abstract

The objective of the present study was to evaluate the effect of probiotic VSL#3 isolated or associated with a yacon-based product (synbiotic) on oxidative stress modulation and intestinal permeability in an experimental model of colorectal carcinogenesis. Forty-five C57BL/6J mice were divided into three groups: control (standard diet AIN-93M); probiotic (standard diet AIN-93M and multispecies probiotic VSL#3, 2.25×10^9 CFU), and synbiotic (standard diet AIN-93M with yacon-based product, 6% fructooligosaccharides and inulin, and probiotic VSL#3, 2.25×10^9 CFU). The experimental diets were provided for 13 weeks. The probiotic and the yacon-based product showed antioxidant activity, with the percentage of DPPH radical scavenging equal to $69.7 \pm 0.4\%$ and $74.3 \pm 0.1\%$, respectively. These findings contributed to reduce hepatic oxidative stress: the control group showed higher concentration of malondialdehyde (1.8-fold, $p=0.007$ and 1.5-fold, $p=0.035$) and carbonylated protein (2-fold, $p=0.008$ and 5.6-fold, $p=0.000$) compared to the probiotic and synbiotic groups, respectively. Catalase enzyme activity increased 1.43-fold ($p=0.014$) in synbiotic group. The crypt depth increased 1.2-fold and 1.4-fold with the use of probiotic and synbiotic, respectively, compared to the control diet ($p=0.000$). These findings corroborate the reduction in intestinal permeability in the probiotic and synbiotic groups, as measured by the percentage of urinary lactulose excretion (CON: $0.93 \pm 0.62\%$ x PRO: $0.44 \pm 0.05\%$, $p=0.048$; and CON: $0.93 \pm 0.62\%$ x SYN: $0.41 \pm 0.12\%$, $p=0.043$). In conclusion, the probiotic and synbiotic showed antioxidant activity, which contributed to the reduction of oxidative stress markers. In addition, they protected the mucosa from damage caused by chemical carcinogen and reduced intestinal permeability.

Keywords: colorectal neoplasm, beneficial bacteria, yacon, intestinal barrier, oxidative damage.

Practical Application: The relationship between intestinal health and the occurrence of various organic disorders, has been demonstrated in many studies. The use of probiotics and prebiotics is currently one of the main targets for modulation of intestinal health. We demonstrated that use of a commercial mix of probiotic bacteria (VSL#3) isolated or associated with a yacon-based prebiotic, rich in fructooligosaccharides and inulin, is able to reduce the oxidative stress and intestinal permeability in a colorectal

carcinogenesis model. These compounds have great potential to be used as a food supplement, or as ingredients in the development of food products.

Introduction

Colorectal cancer (CRC) is a public health problem due to its high incidence and mortality rates worldwide. It is the third type of cancer most diagnosed and the second with the highest mortality. Only in 2020, there are projected to be 147,950 cases newly diagnosed of CRC in the United States (104,610 cases of colon cancer and 43,340 cases of rectal cancer) (Siegel et al., 2020; Bray et al., 2018).

Colorectal carcinogenesis is a complex process, driven by the progressive accumulation of genetic and epigenetic modifications, with activation of oncogenes and inactivation of tumor suppressor genes, that lead to dysregulation of apoptosis, differentiation and cell proliferation (Greenman et al., 2007). Among the morphological changes that occur in the mucosa of the colon, it is initially observed the formation of aberrant crypt foci (ACF), which are putative pre-neoplastic lesions (Khare, Chaudhary, Bissonnette & Carroll, 2009; Bird & Good, 2000).

Changes in the intestinal microenvironment, such as increased oxidative stress and the imbalance of the intestinal microbiota, precede the development of pre-neoplastic lesions and contribute to the progression of the CRC. Together, these disorders result in DNA damage, genetic mutations, endotoxemia, chronic inflammation, and increased intestinal permeability (Jahani-Sherafat et al., 2018).

Currently, specific bacterial genera and non-digestible compounds capable of modulating oxidative stress and microbiota have been deeply studied (Lucas, Barnich, & Nguyen, 2017; Gagnière et al., 2016). An inverse association between the consumption of probiotics, prebiotics and the incidence of CRC has been demonstrated (Oh et al., 2020; Kich et al., 2016).

Probiotics are classically defined as “live microorganisms that, when administered in adequate amounts, confer a health benefit on the host”, and usually include the genera *Bifidobacterium* and *Lactobacillus* (Hill et al., 2014), whereas prebiotics comprise the indigestible food ingredients fermented by gut microorganisms, that serve as selective substrate for their growth; include non-digestible carbohydrates, polyphenols and polyunsaturated fatty acids (Green et al., 2020; Gibson et al., 2017). Synbiotics, in turn, are defined as the association between probiotic and prebiotic, that

work synergistically in the colonization and survivability of beneficial microorganisms in colon; it is suggested that their use is more effective in preventing colorectal carcinogenesis than the use of probiotic or prebiotic separately (Roberfroid, 2007; Rafter et al., 2007).

VSL#3 is a commercial probiotic composed of eight bacterial species. This probiotic has a protective effect on intestinal barrier function, which is one of the important factors for treating multiple chronic diseases (Cheng, et al., 2020). Studies have demonstrated the beneficial effects of VSL#3 on mechanical barrier function and control of inflammatory bowel diseases (Dai et al., 2012; Corridoni et al., 2012; Gionchetti et al., 2007), however, the evidence in the CRC is still insufficient.

Yacon (*Smallanthus sonchifolius*) is a tuberous root, source of fructooligosaccharides (FOS), which are inulin-type prebiotic fructans linked by β 2-1 bonds with low degrees of polymerization, and inulin (Verediano et al., 2020). The yacon-based product (PBY) is a concentrate produced with yacon *in natura* and which has higher concentrations of prebiotics FOS and inulin when compared to fresh root (Rodrigues et al., 2011). Recently, the ability of PBY to reduce oxidative stress, reduce damage to intestinal crypts and increase the production of short-chain fatty acids (SCFA), particularly butyrate, in a colorectal carcinogenesis model was demonstrated (De Nadai Marcon et al., 2020; De Nadai Marcon et al., 2019).

Although studies show the benefits of using probiotics and prebiotics in the function of the intestinal barrier and control of oxidative stress, these effects are not clear in CRC. Here, we hypothesize that the prophylactic administration of the multispecies probiotic VSL#3 alone or as part of the novel synbiotic formulation VSL#3+PBY (considering its additional beneficial effects), could be able to regulate intestinal barrier function and oxidative stress in the early stages of colorectal carcinogenesis. Thus, the present study aimed to investigate the effects of the probiotic VSL#3 and synbiotic VSL#3 + PBY on oxidative stress modulation and intestinal permeability in mice induced to colorectal carcinogenesis. Together, these data will contribute to elucidate the different pathways involved in the possible mechanisms of protection of probiotics and synbiotics.

Materials and Methods

Probiotic

A commercial probiotic VSL#3[®] (Sigma Tau Pharmaceuticals, Inc.; acquired in 2016, valid 04/2018, lot number 604094) was acquired lyophilized, in sachets containing 450 billion viable bacteria, kept refrigerated throughout the experimental period, and reconstituted in water daily before administration. VSL#3 contains eight bacterial species: *Bifidobacterium breve*, *Bifidobacterium infantis*, *Bifidobacterium longum*, *Lactobacillus acidophilus*, *Lactobacillus bulgaricus*, *Lactobacillus casei*, *Lactobacillus plantarum* and *Streptococcus thermophilus*. The probiotic VSL#3 was administered at a dosage of 2.25×10^9 CFU/animal/day based on daily intake of about 10^9 CFU for an adult of 70 kg (Uronis et al., 2011). It is suggested that this dose is sufficient to increase intestinal health, in addition to ensuring a minimum count of 10^6 g⁻¹ of bacteria in feces (Sarao et al., 2017; Zhang et al., 2016). Similar doses were observed in studies that used the probiotic VSL#3 to prevent or treatment of inflammatory bowel disease and colitis-associated cancer (Chang et al., 2012; Bassaganya et al., 2012; Mohania et al., 2013).

Synbiotic

The synbiotic was composed of the probiotic VSL#3 and the yacon-based product (PBY). PBY is a concentrated yacon-based product, rich in prebiotics FOS and inulin. PBY was produced as described by Rodrigues et al. (2011). Briefly, the yacon root is sanitized, peeled, fractionated into smaller pieces and completely crushed. After, it is taken to an open steam boiler to be concentrated until it reaches, approximately, 60°Bx (Patent Request: PI 1106621-0). The centesimal composition of PBY was determined according to the AOAC methodology (AOAC, 1997); FOS and inulin contents were determined by high performance liquid chromatography (HPLC).

PBY was added to the standard rodent diet AIN-93M (Reeves, Nielsen, & Fahey, 1993) to provide 6% FOS and inulin (Paula et al., 2012). This dose was defined based on previous studies in human and animal models, where several beneficial effects were observed, such as: modulation of the immune system, reduction of constipation, increased integrity of crypts and production of SCFA, without causing diarrhea (De Nadai Marcon et al., 2020; De Nadai Marcon et al., 2019; Sant'Anna et al., 2018).

Considering that 100 g of PBY contains 23.6 g of FOS and inulin, 25.4 g of PBY was added to every 100 g of standard diet (Table 1). For comparison purposes, the conversion of the PBY dose to humans was calculated using the body surface area normalization method (Reagan-Shaw, Nihal & Ahmad, 2008). In our study, the average daily diet consumption was 4 g per mouse, which is equivalent to 1016 mg of PBY daily for an adult mouse of approximately 28 g (or 36.2 g PBY/kg body mass/day). Taking into account the average weight of an adult human is 70 kg, the equivalent average daily consumption per day for humans is 205.9 g, amount viable for consumption. In addition, because it is a concentrated product, PBY has advantages over yacon *in natura*: longer shelf life, FOS and inulin stable for longer, regardless of seasonality and higher concentration of nutrients.

Carbohydrate, protein and fiber contents were adjusted so that the experimental diets had a similar composition. The diets were prepared as pellets and stored at -20°C.

Table 1. Composition of experimental diets.

Ingredients (g 100g ⁻¹)	AIN-93M	AIN-93M with PBY (6% FOS + inulin)
Cornstarch	33.20	28.55
Casein	16.50	16.40
Dextrinized starch	15.50	15.50
Sucrose	10.00	5.20
Soybean oil	4.00	4.00
Microfine cellulose	6.40	0.00
PBY*	0.00	25.40
Mineral mix	3.50	3.50
Vitamin mix	1.00	1.00
L-Cystine	0.18	0.18
Choline bitartrate	0.25	0.25
Energy density (kcal/g)	3.37	3.19

PBY: Yacon-based product. Centesimal composition and digestible content of carbohydrate, FOS and inulin on PB (100g of product): fructose: 9.4g; glucose: 6.45g; sucrose: 3.05g; FOS: 17.65g; inulin: 5.95; total carbohydrate: 42.49g; fibers: 1.64g; humidity: 37.20g; ashes: 1.55g; lipids: 0.04g; protein: 2.51g.

***In vitro* antioxidant activity of VSL#3 and PB**

In vitro antioxidant capacity of VSL#3 and PB were evaluated by the 2,2-diphenyl-1-picrylhydrazyl (DPPH) radical scavenger method (Brand-Williams,

Cuvelier, & Berset, 1995). DPPH radical is captured by antioxidants in the sample, causing a decrease in absorbance that can be directly monitored in a spectrophotometer. Briefly, 1.5 mL of DPPH (methanolic solution) was added to 100 μ L of probiotic stock solution. The samples were homogenized in a vortex mixer for 1 min and left to stand for 30 min in the dark. For the evaluation of PBYP, 5 g of the product was homogenized in 30 mL of distilled water and then filtered with a filter paper. The analysis was performed as described above. DPPH radical scavenging activity (% AAI) was calculated by the equation: $\%AAI = [100 - (A_{\text{sample}} - A_{\text{blank}}) / (A_{\text{control}}) \times 100]$, where A = absorbance at 517 nm. The samples were analyzed in triplicate.

Total phenolic content of PBYP

Total phenolic content of PBYP was determined using the Folin-Ciocalteu method (Mau, Lin, & Chen, 2002). The absorbance was measured at 760 nm using a Multiskan GO Microplate Spectrophotometer (Thermo Fisher Scientific, USA). Results were expressed as milligram of gallic acid equivalent (GAE) per gram of dry weight of PBYP (mg GAE/g dw PBYP). The samples were analyzed in triplicate.

Biological assay

Animals and experimental design

Forty-five male C57BL6/J mice, healthy, eight weeks old and body weight of approximately 22 g, were obtained from the Central Bioterium at the Biological Sciences and Health Center at Federal University of Viçosa, Minas Gerais, Brazil. The animals were collectively allocated in polypropylene cages, containing five mice each. Animals were kept under controlled conditions, at a temperature of $22 \pm 2^\circ$ C and humidity of 60-70% with a 12 h light/dark cycle.

After a week of acclimatization, with free access to commercial diet (Purina[®]) and water, animals were divided according to body weight into three different groups (n=15/group), to receive the following interventions, for 13 weeks, as previously described by Cruz et al., (2020a):

- 1) Control group (CON): standard diet AIN-93M and 0.1 mL of water, via orogastric gavage;

- 2) Probiotic group (PRO): standard diet AIN-93M and 0.1 mL of probiotic VSL#3 (2.25×10^9 CFU/animal), via orogastric gavage;
- 3) Synbiotic group (SYN): modified AIN-93M diet, with PBY (6% FOS and inulin) and 0.1 mL of probiotic VSL#3 (2.25×10^9 CFU/animal), via orogastric gavage.

The interventions described above were started in the first experimental week. Standard and modified diets were offered *ad libitum*, and gavages administered in the morning, for five days a week (Arthur et al., 2013). From the third experimental week, the protocol for the induction of pre-neoplastic lesions (ACF) of colorectal cancer was initiated. All animals received an intraperitoneal injection of the colon carcinogen 1,2-dimethylhydrazine (DMH) (Sigma-Aldrich, Saint Louis, USA), 20 mg/kg body weight, once a week, for eight consecutive weeks (Gomides et al., 2014; Newell & Heddle, 2004).

After the end of the experimental period (13 weeks), the animals were anesthetized with 3% isoflurane (Isoflorine[®], Cristalia, Itapira, Brazil) and sacrificed by cervical dislocation. Organs and tissues were collected, washed with cold 0.1 M phosphate-buffered saline (PBS, pH 7.2) and weighed. Cecum, liver and serum were stored at -80°C. Colon was fixed with Carson's formalin for histological analysis.

All experimental procedures were performed following the Directive 2010/63/EU, in compliance with the ethical principles for animal experimentation. The study protocol was approved by the Ethics Committee of the Federal University of Viçosa (CEUA/UFV, protocol n° 08/2017. Approval: May 9, 2017).

Body weight and food intake

The animals were weighed weekly on a digital semi-analytical scale. Food intake was measured daily and was calculated by the difference from the amount of diet offered (g) and the remaining amount (g). The coefficient of food efficiency (CFE) was calculated by the equation: $CFE = \text{weight gain (g)}/\text{total diet consumption (g)}$.

Colonic morphometry and histopathological score

Fragments of the colon were fixed with Carson's formalin for 24 hours (Carson, Martin & Lynn, 1973). Slides of seven animals/group, containing ten non-consecutive

sections (5 mm thick cuts) were stained with hematoxylin-eosin, and about 20 photos of each slide were obtained (Leica Microsystems®, Inc.) to assess intestinal morphometry and histopathological score. Crypt depth, thickness of the submucosa, muscularis and external muscularis layers were measured using the Image Pro Plus 4.5 software.

Histopathological score was calculated by the sum of the following criteria: crypt damage (score 0: none; 1: basal 1/3; 2: basal 2/3; 3: only surface epithelium intact; 4: complete loss of crypt and epithelium), severity of inflammation (score 0: none; 1: slight; 2: moderate; 3: severe) and injury depth (score 0: none; 1: mucosal; 2: mucosal and submucosal; 3: transmural) (Dieleam et al., 1994). The assessment was carried out by two examiners, independently.

Biochemical analysis

After collection, the blood was centrifuged at 870 x g at 4°C for 10 min. Serum markers aspartate aminotransferase (AST), alanine aminotransferase (ALT), alkaline phosphatase, gamma-glutamyl transferase (GGT), urea and creatinine were quantified by colorimetric assay as recommended by the manufacturer of the kits (Bioclin®, Inc.). The measurements were performed in the BS-200 analyzer (Mindray®, Inc.).

Intestinal permeability

The analysis of intestinal permeability was based on the urinary excretion of lactulose and mannitol (Jin et al., 2008). Briefly, in the last experimental week, the animals were fasted for 12 hours and received orogastric gavage (0.2 mL) with a solution containing 11.8 mg of lactulose and 8.9 mg of mannitol. Subsequently, the animals were fasted for another six hours and urine samples were collected for 24 hours and frozen at -80°C. For analysis, the urine was thawed at room temperature, warmed in a 56°C water bath for 10 min, centrifuged at 9,720 x g for 7 min and filtered in a 0.22 µm membrane filter. The urinary concentration of lactulose and mannitol was determined by HPLC (Shimadzu®, Quito, Japan) using a wave length of 220 nm, 300 mm x 7.8 mm diameter column, flow rate of 1 mL/min, pressure 54 Kgf and acidified water (H₂SO₄, 0.005M) as the mobile phase. The results were expressed as percentage of sugar excretion.

Analysis of oxidation products and activity of antioxidant enzymes in hepatic and cecal tissues

Liver and cecum samples were weighed (150 mg) and homogenized in 1.5 mL of cold PBS (pH 7.4) using an Ultra-Turrax homogenizer (T10 basic UltraTurrax, IKA®, Brazil). The homogenate was centrifuged at $10,000 \times g$ for 10 min at 4°C. The supernatant was used for enzyme analysis, catalase (CAT) (Dieterich et al., 2000), superoxide dismutase (SOD) (Aebi, 1984; Buege & Aust, 1978) and glutathione-S-transferase (GST) (Habig & Jakoby, 1981); and for oxidation biomarkers assessment, malondialdehyde (MDA) (Wallin et al., 1993) and carbonyls protein (CP) (Levine et al., 1990). The results were normalized by total protein concentration of supernatant (Lowry et al., 1951).

Statistical analysis

Statistical processing and analysis were performed using the Statistical Package for the Social Sciences 20.0 (SPSS Software IBM, Chicago, USA), and graphs were constructed using GraphPad Prism 7 (GraphPad Software LLC, La Jolla, CA). The normality of variables was determined by the Shapiro-Wilk test. The mean values of the three groups were compared by one-way analysis of variance (ANOVA) followed by Bonferroni multiple-comparison post hoc test, for parametric data. For non-parametric data, the Kruskal-Wallis test was applied, complemented by Dunn's multiple comparison test. $p < 0.05$ was considered to be statistically significant and the data are expressed as the mean \pm standard deviation (SD).

Results and Discussion

***In vitro* antioxidant activity and total phenolics**

Oxidative stress results from excess free radicals (FR), such as reactive oxygen species (ROS), and can cause damage to lipids, proteins and DNA. Although most organisms are able to deal with RF, the imbalance between production and elimination contributes to the development of diseases, including cancer. Thus, there is a growing

search for natural antioxidant compounds for health promotion and disease prevention. (Schieber & Chandel, 2014).

The antioxidant activity *in vitro* and *in vivo* of probiotics and prebiotics has been demonstrated for decades. In the present study, it was observed that probiotic VSL#3 has a high capacity to capture DPPH radicals (%AAI = $69.7 \pm 0.4\%$). Kim et al., (2020) evaluated the *in vitro* antioxidant capacity of several isolated probiotics, and obtained a percentage of DPPH radical capture ranging between $22.2 \pm 2.4\%$ to $38.2 \pm 1.6\%$. These results suggest that the use of multispecies probiotic, such as VSL#3, has potentiated antioxidant effects.

The antioxidant mechanisms of action of probiotics have not been fully clarified. However, it is described that probiotics can act on the redox status of the host through their ability to: chelate metal ions; stimulate the antioxidant system of the host, in addition to having its own antioxidant enzyme system; produce metabolites with antioxidant activity, such as glutathione, and butyrate; mediate antioxidant signaling pathways, such as Nrf2-Keap1-ARE, NFkB, MAPK, and PKC; regulate enzymes that produce ROS; and regulate the intestinal microbiota, controlling excessive proliferation of harmful bacteria that cause endotoxin and significant oxidative stress (Wang et al., 2017).

For PBY, used in synbiotic formulation, the percentage of capture of the DPPH radical was $74.3 \pm 0.1\%$. PBY contains flavonoids and phenolics compounds, which exhibit antioxidant and anti-inflammatory properties (Khajehei et al., 2018). These compounds protect biomolecules, such as DNA, against the damage caused by FR, reducing the risk of tumor development (Shahidi & Yeo, 2018).

The concentration of total phenolic compounds in PBY was 627.6 mg/L (mg GAE/100g total solids). It is described that yacon roots have about 200mg of phenolic compounds per 100g of fresh matter (Gusso, Mattanna & Richards, 2015). Because it is a concentrated product, PBY has considerably higher concentrations of total phenolics. The demonstration of the *in vitro* antioxidant activity of the probiotic VSL#3 and PBY corroborates the beneficial results obtained in the evaluation of oxidative stress *in vivo*.

***In vivo* study**

Body weight, food intake and anatomical characteristics

The animals were weighed weekly to verify the influence of probiotic and synbiotic on body weight gain or loss. Similarly, food intake was evaluated daily. Body weight did not differ significantly between groups at the end of 13 experimental weeks (CON = 24.9±1.3g; PRO = 25.4±1.5g; SYN = 25.2±1.4g; p=0.647).

Similar result was demonstrated by Leu et al., (2010), where animals that were induced to colorectal carcinogenesis and received probiotic or synbiotic did not show significant differences in body weight. This result indicates that the consumption of the probiotic VSL#3 or synbiotic VSL#3+PBY does not interfere with body weight. The similarity of weight can be justified by food intake, which also did not differ between groups in the last experimental week (CON=3.8±0.6g; PRO=4.1±0.6g; SYN=3.9±0.4g; p=0.781), as well as the CFE (CON=0.007±0.005; PRO=0.012±0.008; SYN=0.010±0.005; p=0.604).

However, was observed a significant increase in cecum weight in the group that received the synbiotic when compared to the CON (1.8-fold; p=0.000) and PRO (1.5-fold; p=0.000) groups, as well as colon weight (CON = 1.5-fold, p=0.000; PRO = 1.3-fold, p=0.000) (Figure 1A-C). These data corroborate previously published studies (Pattananandecha et al., 2016; Chang et al., 2012), including one that also used PBY (De Nadai Marcon et al., 2019). According to the study's authors, the fermentation of FOS and inulin present in PBY leads to the production of metabolites that stimulate the proliferation of healthy cells, such as butyrate, which is the main source of energy for colonocytes (De Nadai Marcon et al., 2019). In fact, we previously demonstrated the significant increase in SCFA and butyrate production in the group that received the synbiotic VSL#3+PBY (Cruz et al., 2020a).

The trophic effect of butyrate reflects the increase in the weight of the cecum and colon and contributes to the maintenance and integrity of the mucosa. These findings are confirmed by changes in colon morphometry and reduced intestinal permeability.

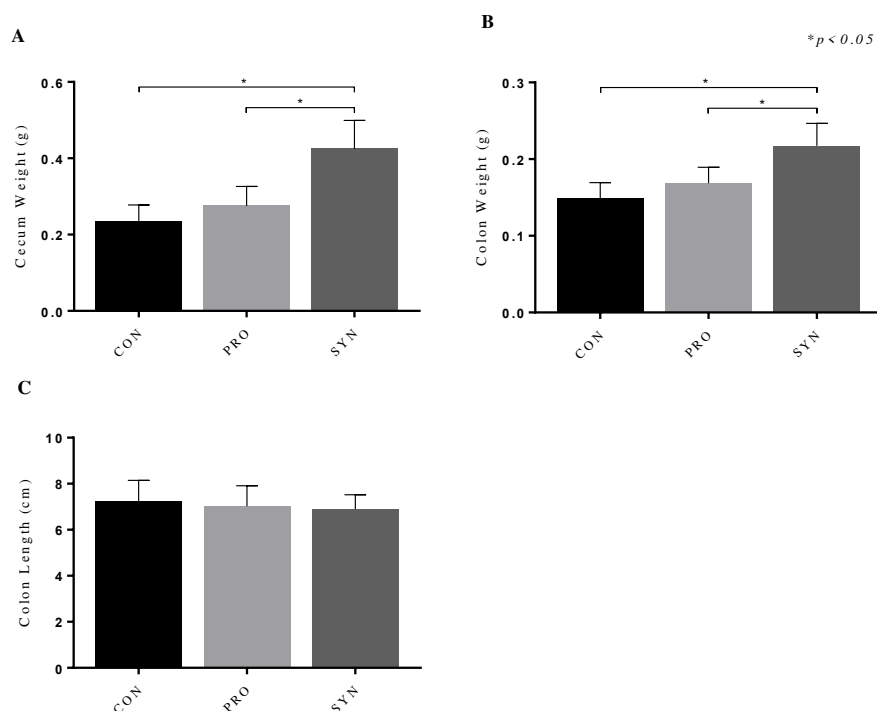


Figure 1. Effect of probiotic and synbiotic on (a) cecum weight, (b) colon weight, and (c) colon length in a colorectal carcinogenesis model. The data were expressed as mean \pm SD (n = 15/group). Statistical difference between groups was analyzed by Anova test or Kruskal-Wallis test. (*) p < 0.05. CON, AIN-93 M diet; PRO, AIN-93 M diet and probiotic VSL#3; SYN, AIN-93 M diet with PBY and probiotic VSL#3

Colonic morphometry and histopathological score

Colon morphometry was influenced by probiotic and synbiotic use. The crypt depth increased 1.2-fold (p=0.000) and 1.4-fold (p=0.000) with the use of probiotic and synbiotic, respectively, compared to the CON group. The use of the synbiotic has a greater influence on the crypt depth, since there was also a significant difference when compared to the PRO group (1.1-fold; p=0.000) (Figure 2A). Interestingly, the submucosal layer decreased 1.2-fold (p=0.025) in the PRO group and 1.3-fold (p=0.000) in the SYN group. (Figure 2B). In the muscularis layer, a significant increase (p=0.000) was observed only in the PRO group (1.5-fold and 1.3-fold compared to the CON and SYN groups, respectively); the CON and SYN groups did not differ (Figure 2C). Regarding the external muscularis layer, there was an increase in the PRO (1.5-

fold; $p=0.001$) and SYN (1.3-fold; $p=0.000$) groups compared to the CON group (Figure 2D).

The increase in the colon layers in the SYN group justifies the difference in weight observed in this tissue, compared to the other groups (Figure 1B). Among the benefits of yacon, there is an increase in the crypts depth, with reduced intestinal permeability (De Moura et al., 2012). According to Leu et al., (2010), the increase in crypts depth is conditioned to the presence of fermentable substrates in the diet, such as FOS and inulin, since animals that receive restricted diets in prebiotics have smaller crypts.

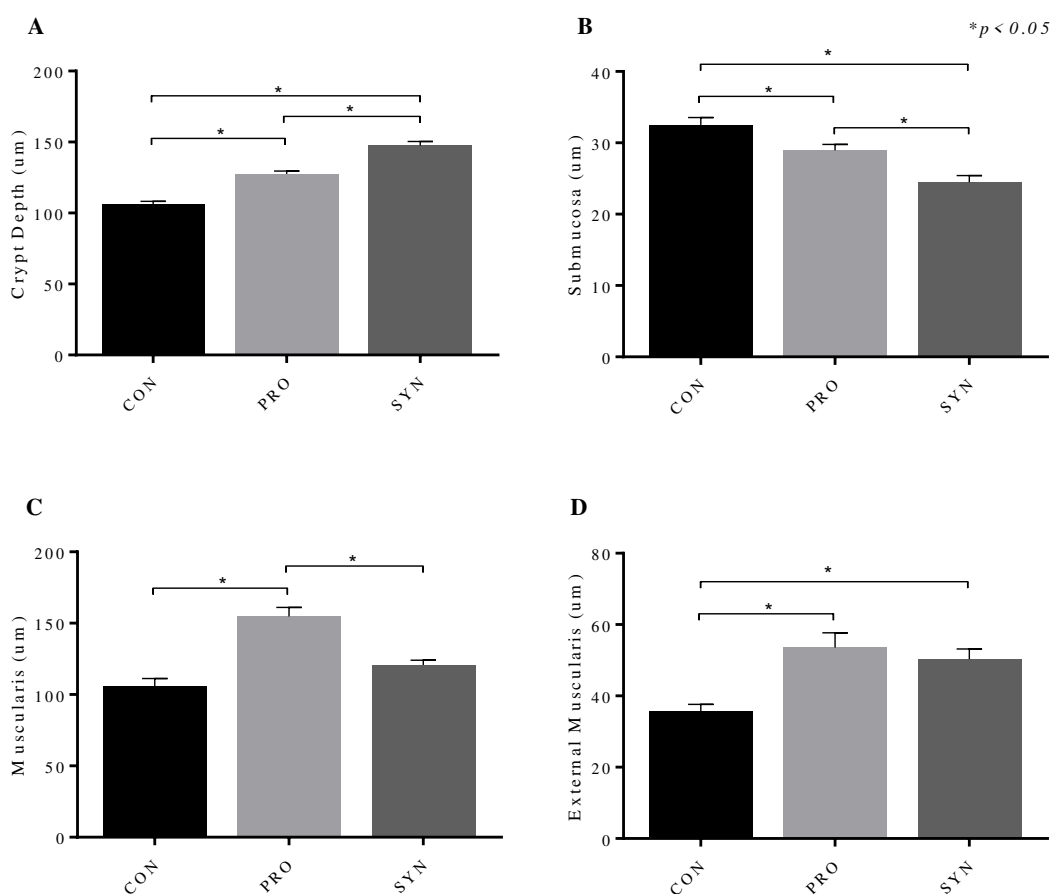


Figure 2. Effect of probiotic and synbiotic on intestinal morphometry in a colorectal carcinogenesis model. (a) Crypt depth, (b) submucosa layer, (c) muscularis layer, and (d) external muscularis layer. The data were expressed as mean \pm SD ($n = 7$ /group). Statistical difference between groups was analyzed by Anova test or Kruskal–Wallis test. (*) $p < 0.05$. CON, AIN-93 M diet; PRO, AIN-93 M diet and probiotic VSL#3; SYN, AIN-93 M diet with PBY and probiotic VSL#3

The total histopathological score, calculated from the sum of the individual scores of the (1) crypt damage, (2) severity of inflammation, and (3) injury depth, was approximately 1.3-fold ($p=0.000$) higher in the CON group compared to the others (Figure 3A). Similarly, when the parameters were evaluated alone, the CON group had a crypt damage score 2.4-fold higher than the PRO ($p=0.003$) and SYN ($p=0.000$) groups (Figure 3B).

Crypt damage, assessed by histopathological score, is a morphological alteration commonly observed during colorectal carcinogenesis. Mucosal damage occurs due to the genotoxicity of DMH and its active metabolites released into the colon (Genaro et al., 2019; Li et al., 2019). However, the use of probiotic and synbiotic can reduce the exposure of colon epithelial cells to genotoxic agents, as demonstrated in the present study.

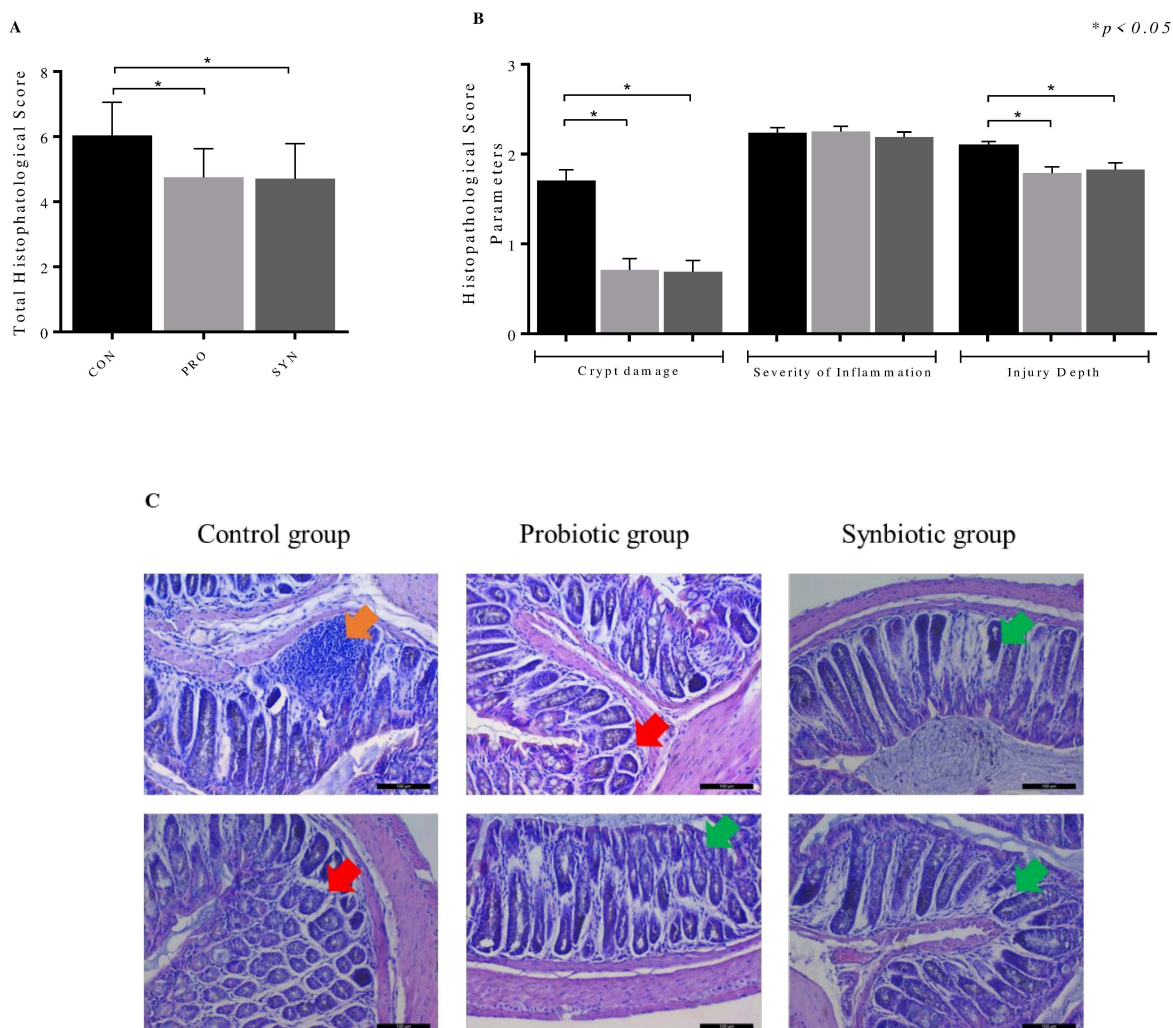


Figure 3. Effect of probiotic and synbiotic on histopathological score in a colorectal carcinogenesis model. (a) Total histopathological score, (b) histopathological score parameters, and (c) illustrative photomicrography of the colon of mice induced to carcinogenesis colorectal stained with hematoxylin-eosin (HE). Orange arrow: extensive area of inflammatory infiltrate (submucosa); red arrow: preserved colonic crypts and damaged crypt transition area; green arrow: preserved crypts and epithelium (scale bars, 100 μ m). The data were expressed as mean \pm SD (n = 7/group). Statistical difference between groups was analyzed by Anova test or Kruskal–Wallis test. (*) p < 0.05. CON, AIN-93 M diet; PRO, AIN-93 M diet and probiotic VSL#3; SYN, AIN-93 M diet with PBY and probiotic VSL#3

Local toxicity and DNA damage induced by DMH are accompanied by the inflammatory process, with increased production of pro-inflammatory cytokines. Tissue inflammation favors tumor development as it provides substrates for cell proliferation (Lenoir et al., 2016). However, it is important to highlight that the inflammatory process is fundamental for the elimination of tumor cells in the early stages of the disease, as in the development of ACF (O'Donnell, Teng & Smyth, 2019).

In the present study, we did not observe differences in the number of areas with inflammatory infiltrate between the groups, however, we previously demonstrated that the use of the synbiotic VSL#3+PBY was able to reduce TNF concentrations (1.4-fold, p=0.028) and increase interleukins 2 (1.5-fold, p=0.027) and 4 (1.5-fold, p=0.035), while the probiotic VSL#3 increased interleukin 4 levels (1.6-fold, p=0.044) (Cruz et al., 2020a). Furthermore, the CON group presented deeper infiltrate areas, reaching the submucosal and muscularis layers (Figure 3C).

Biochemical markers

Serum biomarkers were evaluated in order to verify alterations in liver and kidney functions. There were no differences between groups in serum levels of AST, ALT, alkaline phosphatase, GGT, urea, creatinine and albumin (Figure 4). The results were within the limits recommended for the animal model used.

Similar results were observed by Sivieri et al., (2008), in a study with animals induced to pre-neoplastic lesions and who received probiotic for 42 weeks. De Nadai Marcon et al., (2019) also did not observe differences between serum markers of liver

and renal function in mice induced to colorectal carcinogenesis and who received PBY for eight weeks. Traditionally, measurement of specific enzyme levels has served as a good indicator of tissue damage. The fact that there are no differences between the biomarkers evaluated may be the result of adaptations that have occurred due to stress conditions.

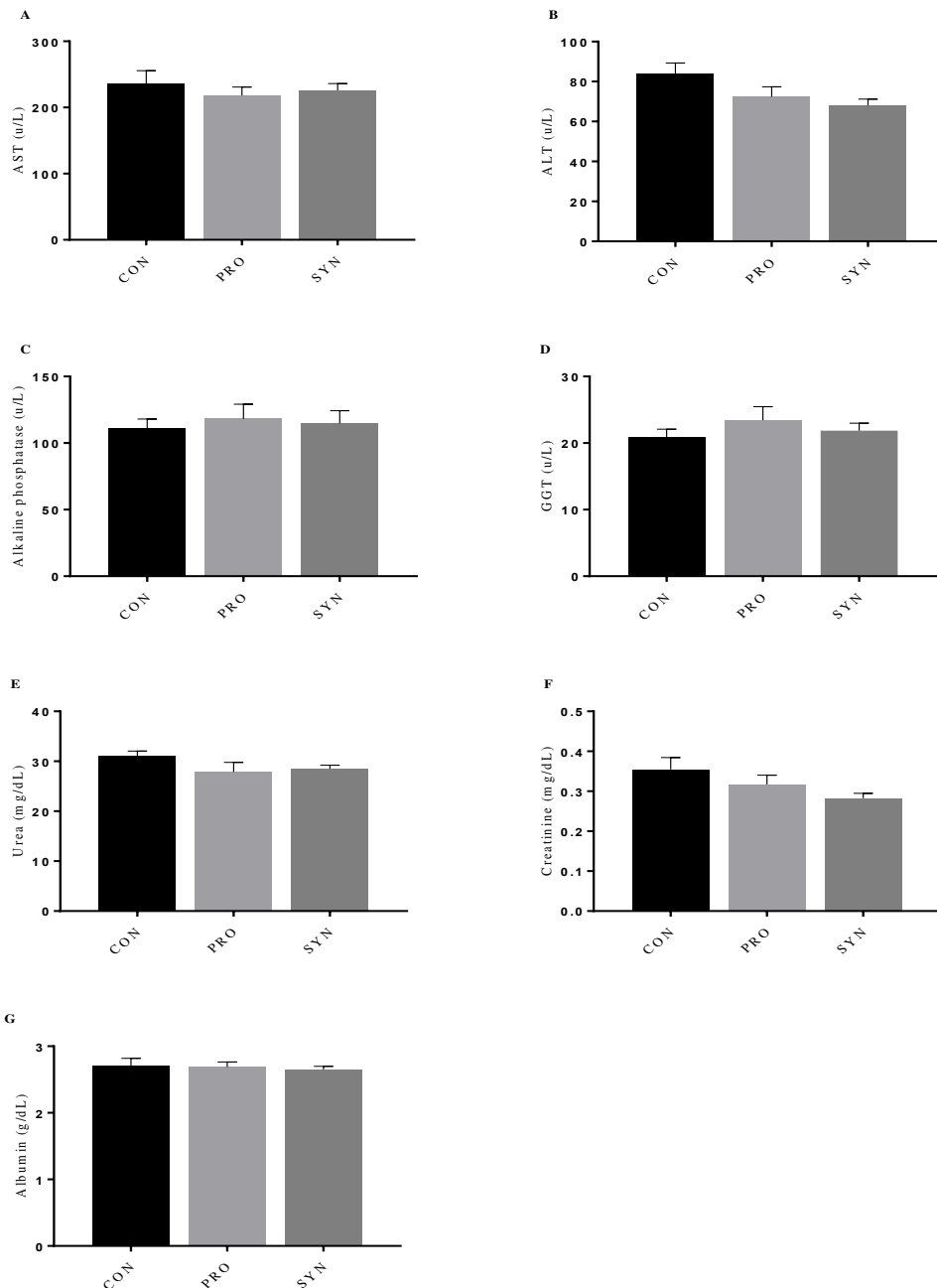


Figure 4. Effect of probiotic and synbiotic on biochemical markers in a colorectal carcinogenesis model. (a) aspartate aminotransferase, (b) alanine aminotransferase, (c) alkaline phosphatase, (d) gamma-glutamyl transferase, (e) area, (f) creatinine, and

(g) albumin. The data were expressed as mean \pm SD (n = 15/group). Statistical difference between groups was analyzed by Anova test or Kruskal–Wallis test

Intestinal permeability

The intestinal permeability was measured by the urinary excretion of lactulose and mannitol, two non-metabolizable sugars. Lactulose is absorbed via the paracellular route, while mannitol is absorbed via the transcellular route, through small aqueous pores, present in the intestinal epithelial cell membrane. Increased absorption of lactulose is indicative of increased permeability and evidences the occurrence of intestinal barrier dysfunction (Stewart, Pratt-Phillips & Gonzalez, 2017; Arrieta, Bistriz & Meddings, 2006).

Intestinal barrier dysfunction can increase the passage of antigens from the lumen to the intestinal mucosa and initiate an inflammatory process, increasing the risk of CRC (Molska & Regula, 2019; Mankertz & Schulzke, 2007). Thus, intestinal barrier is an important target in the prevention and treatment of intestinal diseases (Lee, 2015).

The percentage of urinary lactulose excretion was higher in the CON group compared to the PRO ($0.93\pm 0.62\%$ x $0.44\pm 0.05\%$, $p=0.048$) and SYN ($0.93\pm 0.62\%$ x $0.41\pm 0.12\%$, $p=0.043$) groups. The PRO and SYN groups have not presented differences from each other. Monosaccharide mannitol was not identified in any of the urine samples.

Probiotics and synbiotics have been proposed as promising interventions to reduce intestinal barrier dysfunction. Studies have shown a reduction in intestinal permeability after using probiotic or synbiotic (Russo et al., 2012; Gotteland, Cruchet & Verbeke, 2001). One of the mechanisms by which the consumption of probiotics and synbiotics could regulate the function of the intestinal barrier is by stimulating the expression of tight junction proteins and increasing mucus production by the goblet cells (Karczewski et al., 2010).

SCFA, produced from the fermentation of prebiotics, play a particularly important role in protecting the barrier of the intestinal mucosa. SCFAs activate 5'-adenosine monophosphate-activated protein kinase, which is a key agent in regulating energy metabolism in colonocytes, leading to the strengthening of intestinal epithelial junctions and, consequently, to a strong and healthy barrier. Inhibition of histone

deacetylase by butyrate increases mucus synthesis and mucosal thickness, as well as stimulates mucosal repair (Eslami et al., 2019; Molska & Regula, 2019). As previously demonstrated (Cruz et al., 2020a), the use of the synbiotic VSL#3+PBY significantly increased SCFA concentrations, which may explain the reduction in intestinal permeability.

Products of oxidation and antioxidant activity in hepatic and cecal tissues

Oxidative stress was evaluated in hepatic and cecal tissue, through the quantification of lipid and protein oxidation products, MDA and CP, respectively, and the evaluation of the activity of endogenous antioxidant enzymes (SOD, CAT and GST). The intestine and liver are constantly exposed to RF, whether they are produced endogenously (by intestinal bacteria) or by exogenous sources, such as the DMH used to induce pre-neoplastic lesions (Cruz et al., 2020b; Brenner, Paik & Schnabl, 2015). Thus, considering the close relationship between oxidative stress and tumor development, an antioxidant system capable of maintaining the redox balance is essential.

In hepatic tissue, the CON group presented MDA concentration 1.8-fold ($p=0.007$) and 1.5-fold ($p=0.035$) higher than in the PRO and SYN groups, respectively; for CP, the results are even more expressive: 2-fold ($p=0.008$) and 5.6-fold ($p=0.000$) higher (Table 2). The reduction in MDA and CP concentration corroborates the results obtained in the evaluation of the *in vitro* antioxidant activity of VSL#3 and PBY.

CAT enzyme activity increased 1.43-fold ($p=0.014$) in the SYN group. For the other enzymes, there were no differences between the groups. This enzyme is produced in large amounts in hepatic tissue, and composes one of the main defense systems against oxidative stress because it quickly converts H_2O_2 into H_2O and O_2 (Cheng et al., 2020); therefore, the increase in its activity indicates an increase in the endogenous antioxidant defense promoted by the synbiotic. In addition, some probiotic species, such as *Lactobacillus* present in the synbiotic formulation, are capable of producing CAT, which contributes to the increase of antioxidant response (Cruz et al., 2020b; Eslami et al., 2019).

In cecum, no significant differences were observed in oxidation products or enzyme activity for all groups. Some reasons support the differences observed between liver

and cecum. The activation of DMH in its active metabolite occurs predominantly in the liver, with the formation of a large amount of FR. Additionally, dysbiosis and increased intestinal permeability, will result in bacterial products in the portal blood, and the cells of the liver will be first to be exposed, thus, there is a great demand for the production of antioxidants in this organ specifically (Jackson et al., 2003).

Table 2 - Effect of probiotic and synbiotic on oxidation products and antioxidant enzymes activity in C57BL/6 mice.

	CON	PRO	SYN	<i>p</i>
MDA (<i>nmol/mg ptn</i>)				
Liver	0.232 ± 0.06 ^a	0.134 ± 0.06 ^b	0.154 ± 0.03 ^b	0.011 [#]
Cecum	0.973 ± 0.23	0.817 ± 0.12	1.022 ± 0.27	0.280 [*]
CP (<i>nmol/mL</i>)				
Liver	19.310 ± 7.02 ^a	9.693 ± 6.56 ^b	3.417 ± 1.49 ^b	0.000 [*]
Cecum	2.634 ± 1.19	2.262 ± 1.23	2.293 ± 0.74	0.584 [#]
SOD (<i>U/mg ptn</i>)				
Liver	19.903 ± 4.51	19.502 ± 1.60	21.519 ± 3.30	0.485 [*]
Cecum	38.440 ± 2.58	42.881 ± 4.73	37.787 ± 7.09	0.773 [*]
CAT (<i>U/mg ptn</i>)				
Liver	4.059 ± 1.34 ^a	4.405 ± 0.66 ^{a,b}	5.827 ± 1.06 ^b	0.014 [*]
Cecum	0.359 ± 0.18	0.298 ± 0.07	0.370 ± 0.06	0.474 [*]
GST (<i>nmol/min/mg ptn</i>)				
Liver	71.667 ± 5.30	73.097 ± 3.46	71.148 ± 5.01	0.726 [*]
Cecum	12.771 ± 1.23	13.526 ± 1.83	13.651 ± 2.90	0.701 [*]

MDA: malondialdehyde; CP: carbonylated protein; SOD: superoxide dismutase; CAT: catalase; GST: glutathione-S-transferase. The data were expressed as mean ± SD (n=8/group). Statistical difference between groups were analyzed by ANOVA^(*) test or Kruskal-Wallis test^(#), with p<0.05. Different letters in the same line indicate statistical difference. CON, AIN-93M diet; PRO, AIN-93M diet and probiotic VSL#3; SYN, AIN-93M diet with PBY and probiotic VSL#3.

The control of oxidative stress and the maintenance of the intestinal barrier are interconnected targets for the prevention of CRC. The use of probiotic and synbiotic contributes to a reduction in oxidative stress and inflammation, which in turn leads to increased expression of the tight junction protein, such as claudin-3 and occludin, thereby restoring barrier function (Molska & Regula, 2019; Cruz et al., 2020b).

Conclusion

The probiotic VSL#3 and the synbiotic VSL#3 + PBY showed antioxidant activity *in vitro* and *in vivo*, demonstrated by the significant reduction of markers of hepatic oxidative stress and increased activity of the enzyme catalase ($p < 0.005$). Through histopathological analysis, less damage was observed in the intestinal epithelium of animals that received probiotic or synbiotic, as well as the significant reduction ($p < 0.005$) in intestinal permeability, measured by the lower urinary excretion of lactulose. The crypt depth increased 1.2-fold and 1.4-fold with the use of probiotic and synbiotic, respectively, compared to the control. However, the synbiotic showed greater influence, since there was also a significant difference when compared to the group that received only the probiotic (1.1-fold; $p = 0.000$); this difference is justified by the trophic effect promoted by prebiotics. Reducing oxidative stress and permeability of the intestinal barrier are important ways to protect against CRC. Our findings suggest the promising use of probiotic and synbiotic as food ingredients for preventing CRC.

Acknowledgments

Our work was supported by the National Council of Technological and Scientific Development (CNPq), Coordination for the Improvement of Higher Education Personnel (CAPES), and Foundation for the Support to the Researches in Minas Gerais (Fapemig).

Author Contributions

B. Cruz: conception, methodology, formal analysis, investigation, data curation, writing (preparation, review and editing); L. de Sousa Moraes: methodology, formal analysis, investigation; L. De Nadai Marcon: methodology, formal analysis, investigation; K. Dias: formal analysis, investigation; L. Murad: conception, writing (review and editing); M. Sarandy: formal analysis, investigation; L. Conceição: methodology, resources; R. Gonçalves: methodology, resources; C. Ferreira: conception, methodology, resources, funding; M. Peluzio: conception, methodology, resources, writing (preparation, and review and editing), supervision, project administration, funding.

Conflicts of Interest

The authors declare no conflicts of interest.

References

Aebi, H. (1984). Catalase *in vitro*. *Methods in Enzymology*, 105, 121–126. [https://doi.org/10.1016/S0076-6879\(84\)05016-3](https://doi.org/10.1016/S0076-6879(84)05016-3)

AOAC International. Official Methods of Analysis. 16^a ed., 3^a rev. Gaithersburg: Published by AOAC International, 1997. v.2, cap. 32, p.1-43.

Arrieta, M. C., Bistriz, L., & Meddings, J. B. (2006). Alterations in intestinal permeability. *Gut*, 55(10), 1512–1520. <https://doi.org/10.1136/gut.2005.085373>

Arthur, J.C., Gharaibeh, R.Z., Uronis, J.M., Perez-Chanona, E., Sha, W., Tomkovich, S., Mühlbauer, M., Fodor, A.A., & Jobin, C. (2013) VSL#3 probiotic modifies mucosal microbial composition but does not reduce colitis-associated colorectal cancer. *Scientific Report* 8;3:2868. doi: 10.1038/srep02868

Bassaganya-Riera, J., Viladomiu, M., Pedragosa, M., De Simone, C., & Hontecillas, R. (2012). Immunoregulatory mechanisms underlying prevention of colitis-associated colorectal cancer by probiotic bacteria. *PloS one*, 7(4), e34676. <https://doi.org/10.1371/journal.pone.0034676>

Bird, R. P., & Good, C. K. (2000). The significance of aberrant crypt foci in understanding the pathogenesis of colon cancer. *Toxicology letters*, 112-113, 395–402. [https://doi.org/10.1016/s0378-4274\(99\)00261-1](https://doi.org/10.1016/s0378-4274(99)00261-1)

Brand-Williams, W., Cuvelier, M.E., & Berset, C. (1995) Use of a free radical method to evaluate antioxidant activity. *LWT-Food Science and Technology*, 28(1):25-30. [doi.org/10.1016/S0023-6438\(95\)80008-5](https://doi.org/10.1016/S0023-6438(95)80008-5)

Bray, F., Ferlay, J., Soerjomataram, I., Siegel, R. L., Torre, L. A., & Jemal, A. (2018). Global cancer statistics 2018: GLOBOCAN estimates of incidence and mortality worldwide for 36 cancers in 185 countries. *CA: a cancer journal for clinicians*, 68(6), 394–424. <https://doi.org/10.3322/caac.21492>

Brenner, D. A., Paik, Y. H., & Schnabl, B. (2015). Role of Gut Microbiota in Liver Disease. *Journal of clinical gastroenterology*, 49 Suppl 1(0 1), S25–S27. <https://doi.org/10.1097/MCG.0000000000000391>

Buege, J. A., & Aust, S. D. (1978). Microsomal lipid peroxidation. *Methods in Enzymology*. [https://doi.org/10.1016/S0076-6879\(78\)52032-6](https://doi.org/10.1016/S0076-6879(78)52032-6)

Carson, F. L., Martin, J. H., & Lynn, J. A. (1973). Formalin fixation for electron microscopy: a re-evaluation. *American journal of clinical pathology*, 59(3), 365–373. <https://doi.org/10.1093/ajcp/59.3.365>

Chang, J. H., Shim, Y. Y., Cha, S. K., Reaney, M., & Chee, K. M. (2012). Effect of *Lactobacillus acidophilus* KFR1342 on the development of chemically induced precancerous growths in the rat colon. *Journal of medical microbiology*, 61(Pt 3), 361–368. <https://doi.org/10.1099/jmm.0.035154-0>

Cheng, F. S., Pan, D., Chang, B., Jiang, M., & Sang, L. X. (2020). Probiotic mixture VSL#3: An overview of basic and clinical studies in chronic diseases. *World journal of clinical cases*, 8(8), 1361–1384. <https://doi.org/10.12998/wjcc.v8.i8.1361>

Corridoni, D., Pastorelli, L., Mattioli, B., Locovei, S., Ishikawa, D., Arseneau, K. O., Chieppa, M., Cominelli, F., & Pizarro, T. T. (2012). Probiotic bacteria regulate intestinal epithelial permeability in experimental ileitis by a TNF-dependent mechanism. *PloS one*, 7(7), e42067. <https://doi.org/10.1371/journal.pone.0042067>

Cruz, B., Sarandy, M. M., Messias, A. C., Gonçalves, R. V., Ferreira, C., & Peluzio, M. (2020b). Preclinical and clinical relevance of probiotics and synbiotics in colorectal carcinogenesis: a systematic review. *Nutrition reviews*, 78(8), 667–687. <https://doi.org/10.1093/nutrit/nuz087>

Cruz, B.C.S., da Silva Duarte, V., Giacomini, A., Corich, V., de Paula, S. O., da Silva Fialho, L., Guimarães, V. M., de Lucas Fortes Ferreira, C. L., & Gouveia Peluzio, M. (2020a). Synbiotic VSL#3 and yacon-based product modulate the intestinal microbiota and prevent the development of pre-neoplastic lesions in a colorectal carcinogenesis

model. *Applied microbiology and biotechnology*, 104(20), 8837–8857. <https://doi.org/10.1007/s00253-020-10863-x>

Dai, C., Zhao, D. H., & Jiang, M. (2012). VSL#3 probiotics regulate the intestinal epithelial barrier in vivo and in vitro via the p38 and ERK signaling pathways. *International journal of molecular medicine*, 29(2), 202–208. <https://doi.org/10.3892/ijmm.2011.839>

de Moura, N. A., Caetano, B. F., Sivieri, K., Urbano, L. H., Cabello, C., Rodrigues, M. A., & Barbisan, L. F. (2012). Protective effects of yacon (*Smallanthus sonchifolius*) intake on experimental colon carcinogenesis. *Food and chemical toxicology : an international journal published for the British Industrial Biological Research Association*, 50(8), 2902–2910. <https://doi.org/10.1016/j.fct.2012.05.006>

De Nadai Marcon, L., Moraes, L.F.S., Cruz, B.C.S., Teixeira, M.D.O., Gomides, A.F.F., Ferreira, C.L.L.F., Oliveira, L.L., Oliveira, L.L., & Peluzio, M.C.G. (2020). Yacon (*Smallanthus sonchifolius*)-based product increases fecal short-chain fatty acids concentration and up-regulates t-Bet expression in the colon of BALB/c mice during colorectal carcinogenesis. *Food Science and Nutrition*, 6(3), doi: 10.24966/FSN-1076/100069

De Nadai Marcon, L., Moraes, L.F.S., Cruz, B.C.S., Teixeira, M.D.O., Bruno, T.C.V., Ribeiro, I.E., Messias, A.C., Ferreira, C.L.L.F., Oliveira, L.L., & Peluzio, M.C.G. (2019). Yacon (*Smallanthus sonchifolius*)-based product increases fecal short-chain fatty acids and enhances regulatory T cells by downregulating ROR γ t in the colon of BALB/c mice. *J Funct Foods* 55:333–342

Dieleman, L. A., Ridwan, B. U., Tennyson, G. S., Beagley, K. W., Bucy, R. P., & Elson, C. O. (1994). Dextran sulfate sodium-induced colitis occurs in severe combined immunodeficient mice. *Gastroenterology*, 107(6), 1643–1652. [https://doi.org/10.1016/0016-5085\(94\)90803-6](https://doi.org/10.1016/0016-5085(94)90803-6)

Dieterich, S., Bieligk, U., Beulich, K., Hasenfuss, G., & Prestle, J. (2000). Gene expression of antioxidative enzymes in the human heart: Increased expression of

catalase in the end-stage failing heart. *Circulation*, 101, 33–39.
<https://doi.org/10.1161/01.cir.101.1.33>

Eslami, M., Yousefi, B., Kokhaei, P., Hemati, M., Nejad, Z. R., Arabkari, V., & Namdar, A. (2019). Importance of probiotics in the prevention and treatment of colorectal cancer. *Journal of cellular physiology*, 234(10), 17127–17143.
<https://doi.org/10.1002/jcp.28473>

Gagnière, J., Raisch, J., Veziat, J., Barnich, N., Bonnet, R., Buc, E., Bringer, M. A., Pezet, D., & Bonnet, M. (2016). Gut microbiota imbalance and colorectal cancer. *World journal of gastroenterology*, 22(2), 501–518. <https://doi.org/10.3748/wjg.v22.i2.501>

Genaro, S. C., Lima de Souza Reis, L. S., Reis, S. K., Rabelo Socca, E. A., & Fávoro, W. J. (2019). Probiotic supplementation attenuates the aggressiveness of chemically induced colorectal tumor in rats. *Life sciences*, 237, 116895.
<https://doi.org/10.1016/j.lfs.2019.116895>

Gibson, G. R., Hutkins, R., Sanders, M. E., Prescott, S. L., Reimer, R. A., Salminen, S. J., Scott, K., Stanton, C., Swanson, K. S., Cani, P. D., Verbeke, K., & Reid, G. (2017). Expert consensus document: The International Scientific Association for Probiotics and Prebiotics (ISAPP) consensus statement on the definition and scope of prebiotics. *Nature reviews. Gastroenterology & hepatology*, 14(8), 491–502.
<https://doi.org/10.1038/nrgastro.2017.75>

Gionchetti, P., Rizzello, F., Morselli, C., Poggioli, G., Tambasco, R., Calabrese, C., Brigidi, P., Vitali, B., Straforini, G., & Campieri, M. (2007). High-dose probiotics for the treatment of active pouchitis. *Diseases of the colon and rectum*, 50(12), 2075–2084.
<https://doi.org/10.1007/s10350-007-9068-4>

Gomides, A. F., de Paula, S. O., Gonçalves, R. V., de Oliveira, L. L., Ferreira, C. L., Comastri, D. S., & Peluzio, M. (2014). Prebiotics prevent the appearance of aberrant crypt foci (ACF) in the colon of BALB/c mice for increasing the gene expression of p16 protein. *Nutricion hospitalaria*, 30(4), 883–890.
<https://doi.org/10.3305/nh.2014.30.4.7672>

Gotteland, M., Cruchet, S., & Verbeke, S. (2001). Effect of *Lactobacillus* ingestion on the gastrointestinal mucosal barrier alterations induced by indometacin in humans. *Alimentary pharmacology & therapeutics*, 15(1), 11–17. <https://doi.org/10.1046/j.1365-2036.2001.00898.x>

Green, M., Arora, K., & Prakash, S. (2020). Microbial Medicine: Prebiotic and Probiotic Functional Foods to Target Obesity and Metabolic Syndrome. *International journal of molecular sciences*, 21(8), 2890. <https://doi.org/10.3390/ijms21082890>

Greenman, C., Stephens, P., Smith, R., Dalgliesh, G. L., Hunter, C., Bignell, G., Davies, H., Teague, J., Butler, A., Stevens, C., Edkins, S., O'Meara, S., Vastrik, I., Schmidt, E. E., Avis, T., Barthorpe, S., Bhamra, G., Buck, G., Choudhury, B., Clements, J., ... Stratton, M. R. (2007). Patterns of somatic mutation in human cancer genomes. *Nature*, 446(7132), 153–158. <https://doi.org/10.1038/nature05610>

Gusso, A. P., Mattanna, P., & Richards, N. (2015). Yacon: health benefits and technological applications. *Ciência Rural*, 45(5), 912-919. Epub December 16, 2014. <https://dx.doi.org/10.1590/0103-8478cr20140963>

Habig, W. H., & Jakoby, W. B. (1981). Glutathione-S-Transferase (rat and human). *Methods in Enzymology*, 77, 218–239.

Hill, C., Guarner, F., Reid, G., Gibson, G. R., Merenstein, D. J., Pot, B., Morelli, L., Canani, R. B., Flint, H. J., Salminen, S., Calder, P. C., & Sanders, M. E. (2014). Expert consensus document. The International Scientific Association for Probiotics and Prebiotics consensus statement on the scope and appropriate use of the term probiotic. *Nature reviews. Gastroenterology & hepatology*, 11(8), 506–514. <https://doi.org/10.1038/nrgastro.2014.66>

Jackson, P. E., O'Connor, P. J., Cooper, D. P., Margison, G. P., & Povey, A. C. (2003). Associations between tissue-specific DNA alkylation, DNA repair and cell proliferation in the colon and colon tumour yield in mice treated with 1,2-

dimethylhydrazine. *Carcinogenesis*, 24(3), 527–533.
<https://doi.org/10.1093/carcin/24.3.527>

Jahani-Sherafat, S., Alebouyeh, M., Moghim, S., Ahmadi Amoli, H., & Ghasemian-Safaei, H. (2018). Role of gut microbiota in the pathogenesis of colorectal cancer: a review article. *Gastroenterology and hepatology from bed to bench*, 11(2), 101–109.

Jin, W., Wang, H., Ji, Y., Hu, Q., Yan, W., Chen, G., & Yin, H. (2008). Increased intestinal inflammatory response and gut barrier dysfunction in Nrf2-deficient mice after traumatic brain injury. *Cytokine*, 44(1), 135–140.
<https://doi.org/10.1016/j.cyto.2008.07.005>

Karczewski, J., Troost, F. J., Konings, I., Dekker, J., Kleerebezem, M., Brummer, R. J., & Wells, J. M. (2010). Regulation of human epithelial tight junction proteins by *Lactobacillus plantarum in vivo* and protective effects on the epithelial barrier. *American journal of physiology. Gastrointestinal and liver physiology*, 298(6), G851–G859. <https://doi.org/10.1152/ajpgi.00327.2009>

Khajehei, F., Merkt, N., Claupein, W., & Graeff-Hoenninger, S. (2018). Yacon (*Smallanthus sonchifolius* Poepp. & Endl.) as a Novel Source of Health Promoting Compounds: Antioxidant Activity, Phytochemicals and Sugar Content in Flesh, Peel, and Whole Tubers of Seven Cultivars. *Molecules (Basel, Switzerland)*, 23(2), 278.
<https://doi.org/10.3390/molecules23020278>

Khare, S., Chaudhary, K., Bissonnette, M., & Carroll, R. (2009). Aberrant crypt foci in colon cancer epidemiology. *Methods in molecular biology (Clifton, N.J.)*, 472, 373–386. https://doi.org/10.1007/978-1-60327-492-0_17

Kich, D. M., Vincenzi, A., Majolo, F., Volken de Souza, C. F., & Goettert, M. I. (2016). Probiotic: effectiveness nutrition in cancer treatment and prevention. *Nutricion hospitalaria*, 33(6), 1430–1437. <https://doi.org/10.20960/nh.806>

Kim, H., Kim, J.S., Kim, Y., Jeong Y., Kim, J.E., Paek, N.S., Kang, C.H. (2020). Antioxidant and Probiotic Properties of Lactobacilli and Bifidobacteria of Human

Origins. *Biotechnol Bioproc E* 25, 421–430. <https://doi.org/10.1007/s12257-020-0147-x>

Lee S. H. (2015). Intestinal permeability regulation by tight junction: implication on inflammatory bowel diseases. *Intestinal research*, 13(1), 11–18. <https://doi.org/10.5217/ir.2015.13.1.11>

Lenoir, M., Del Carmen, S., Cortes-Perez, N. G., Lozano-Ojalvo, D., Muñoz-Provencio, D., Chain, F., Langella, P., de Moreno de LeBlanc, A., LeBlanc, J. G., & Bermúdez-Humarán, L. G. (2016). *Lactobacillus casei* BL23 regulates Treg and Th17 T-cell populations and reduces DMH-associated colorectal cancer. *Journal of gastroenterology*, 51(9), 862–873. <https://doi.org/10.1007/s00535-015-1158-9>

Leu, R.K.L., Hu, Y., Brown, I.L., Woodman, R.J., & Young, G.P. (2010). Synbiotic intervention of *Bifidobacterium lactis* and resistant starch protects against colorectal cancer development in rats. *Carcinogenesis*, 31, 246-251

Levine, R. L., Garland, D., Oliver, C. N., Amici, A., Climent, I., Lenz, A. G., ... Stadtman, E. R. (1990). Determination of carbonyl content in oxidatively modified proteins. *Methods in Enzymology*, 186, 464–478.

Li, S. C., Lin, H. P., Chang, J. S., & Shih, C. K. (2019). *Lactobacillus acidophilus*-fermented germinated brown rice suppresses preneoplastic lesions of the colon in rats. *Nutrients*, 11(11), 2718. <https://doi.org/10.3390/nu11112718>

Lowry, O. H., Rosebrough, N. J., Farr, A. L., & Randall, R. J. (1951). Protein measurement with folin phenol reagent. *The Journal of Biological Chemistry*, 193, 265–275. PMID: 14907713.

Lucas, C., Barnich, N., & Nguyen, H. (2017). Microbiota, Inflammation and Colorectal Cancer. *International journal of molecular sciences*, 18(6), 1310. <https://doi.org/10.3390/ijms18061310>

Mankertz, J., & Schulzke, J. D. (2007). Altered permeability in inflammatory bowel disease: pathophysiology and clinical implications. *Current opinion in gastroenterology*, 23(4), 379–383. <https://doi.org/10.1097/MOG.0b013e32816aa392>

Mau, J. L., Lin, H. C., & Chen, C. C. (2002). Antioxidant properties of several medicinal mushrooms. *Journal of Agricultural and Food Chemistry*, 50(21), 6072–6077. <https://doi.org/10.1021/jf0201273>

Mohania, D., Kansal, V., Sagwal, R., & Shah, D. (2013). Anticarcinogenic Effect of Probiotic Dahi and Piroxicam on DMH-induced Colorectal Carcinogenesis in Wistar Rats. *Cancer Therapy and Pharmacology*. <http://ivyunion.org/index.php/ajctp>

Molska, M., & Reguła, J. (2019). Potential Mechanisms of Probiotics Action in the Prevention and Treatment of Colorectal Cancer. *Nutrients*, 11(10), 2453. <https://doi.org/10.3390/nu11102453>

Newell, L. E., & Heddle, J. A. (2004). The potent colon carcinogen, 1,2-dimethylhydrazine induces mutations primarily in the colon. *Mutation research*, 564(1), 1–7. <https://doi.org/10.1016/j.mrgentox.2004.06.005>

O'Donnell, J. S., Teng, M., & Smyth, M. J. (2019). Cancer immunoediting and resistance to T cell-based immunotherapy. *Nature reviews. Clinical oncology*, 16(3), 151–167. <https://doi.org/10.1038/s41571-018-0142-8>

Oh, N. S., Joung, J. Y., Lee, J. Y., Kim, Y. J., Kim, Y., & Kim, S. H. (2020). A synbiotic combination of *Lactobacillus gasseri* 505 and *Cudrania tricuspidata* leaf extract prevents hepatic toxicity induced by colorectal cancer in mice. *Journal of dairy science*, 103(4), 2947–2955. <https://doi.org/10.3168/jds.2019-17411>

Pattananandecha, T., Sirilun, S., Duangjitcharoen, Y., Sivamaruthi, B. S., Suwannalert, P., Peerajan, S., & Chaiyasut, C. (2016). Hydrolysed inulin alleviates the azoxymethane-induced preneoplastic aberrant crypt foci by altering selected intestinal microbiota in Sprague-Dawley rats. *Pharmaceutical biology*, 54(9), 1596–1605. <https://doi.org/10.3109/13880209.2015.1110597>

Paula, H.A.A., Martins, J.F.L., Sartori, S.S.R., Castro, A.S.B., Abranches, M.V., Rafael, V.C., & Ferreira, C.L.L.F (2012) The yacon product PBY: which is the best dose to evaluate the functionality of this new source of prebiotic fructans? Functional Foods Forum Probiotics, Turku.

Rafter, J., Bennett, M., Caderni, G., Clune, Y., Hughes, R., Karlsson, P. C., Klinder, A., O'Riordan, M., O'Sullivan, G. C., Pool-Zobel, B., Rechkemmer, G., Roller, M., Rowland, I., Salvadori, M., Thijs, H., Van Loo, J., Watzl, B., & Collins, J. K. (2007). Dietary synbiotics reduce cancer risk factors in polypectomized and colon cancer patients. *The American Journal of Clinical Nutrition*, 85(2), 488–496. <https://doi.org/10.1093/ajcn/85.2.488>

Reagan-Shaw, S., Nihal, M., & Ahmad, N. (2008). Dose translation from animal to human studies revisited. *FASEB journal: official publication of the Federation of American Societies for Experimental Biology*, 22(3), 659–661. <https://doi.org/10.1096/fj.07-9574LSF>

Reeves, P. G., Nielsen, F. H., & Fahey, G. C. Jr (1993). AIN-93 purified diets for laboratory rodents: final report of the American Institute of Nutrition ad hoc writing committee on the reformulation of the AIN-76A rodent diet. *The Journal of nutrition*, 123(11), 1939–1951. <https://doi.org/10.1093/jn/123.11.1939>

Roberfroid M. (2007). Prebiotics: the concept revisited. *The Journal of nutrition*, 137 (3 Suppl 2), 830S–7S. <https://doi.org/10.1093/jn/137.3.830S>

Rodrigues, V.C. (2011). Formulação, índice glicêmico e aplicação alimentar de um produto à base de yacon (*Smallanthus sonchifolius*). Tesis, 89 p.

Russo, F., Linsalata, M., Clemente, C., Chiloiro, M., Orlando, A., Marconi, E., Chimienti, G., & Riezzo, G. (2012). Inulin-enriched pasta improves intestinal permeability and modifies the circulating levels of zonulin and glucagon-like peptide 2 in healthy young volunteers. *Nutrition research (New York, N.Y.)*, 32(12), 940–946. <https://doi.org/10.1016/j.nutres.2012.09.010>

Sant'Anna, M.S.L., Rodrigues, V.C., Araújo, T.F., Oliveira, T.T., Pelúzio, M.C.G., Ferreira, C.L.L. (2018). Yacon product (PBY) modulates intestinal constipation and protects the integrity of crypts in wistar rats. *Food Nutr Sci*, 9: 1391-1407

Sarao, L. K., & Arora, M. (2017). Probiotics, prebiotics, and microencapsulation: A review. *Critical reviews in food science and nutrition*, 57(2), 344–371. <https://doi.org/10.1080/10408398.2014.887055>

Schieber, M., & Chandel, N. S. (2014). ROS function in redox signaling and oxidative stress. *Current biology: CB*, 24(10), R453–R462. <https://doi.org/10.1016/j.cub.2014.03.034>

Shahidi, F., & Yeo, J. (2018). Bioactivities of Phenolics by Focusing on Suppression of Chronic Diseases: A Review. *International journal of molecular sciences*, 19(6), 1573. <https://doi.org/10.3390/ijms19061573>

Siegel, R. L., Miller, K. D., Goding Sauer, A., Fedewa, S. A., Butterly, L. F., Anderson, J. C., Cercek, A., Smith, R. A., & Jemal, A. (2020). Colorectal cancer statistics, 2020. *CA: a cancer journal for clinicians*, 70(3), 145–164. <https://doi.org/10.3322/caac.21601>

Sivieri, K., Spinardi-Barbisan, A.L.T., Barbisan, L.F., Bedani, R., Pauly, N.D., Carlos, I.Z., Benzatti, F., Vendramini, R.C. & Rossi, E.A. (2008) Probiotic *Enterococcus faecium* CRL 183 inhibit chemically induced colon cancer in male wistar rats. *Eur Food Res Technol* 228:231–237

Stewart, A. S., Pratt-Phillips, S., & Gonzalez, L. M. (2017). Alterations in Intestinal Permeability: The Role of the "Leaky Gut" in Health and Disease. *Journal of equine veterinary science*, 52, 10–22. <https://doi.org/10.1016/j.jevs.2017.02.009>

Uronis, J. M., Arthur, J. C., Keku, T., Fodor, A., Carroll, I. M., Cruz, M. L., Appleyard, C. B., & Jobin, C. (2011). Gut microbial diversity is reduced by the probiotic VSL#3 and

correlates with decreased TNBS-induced colitis. *Inflammatory bowel diseases*, 17(1), 289–297. <https://doi.org/10.1002/ibd.21366>

Verediano, T. A., Viana, M. L., das Graças Vaz Tostes, M., de Oliveira, D. S., de Carvalho Nunes, L., & Costa, N. M. (2020). Yacón (*Smallanthus sonchifolius*) prevented inflammation, oxidative stress, and intestinal alterations in an animal model of colorectal carcinogenesis. *Journal of the science of food and agriculture*, 100(15), 5442–5449. <https://doi.org/10.1002/jsfa.10595>

Wallin, B., Rosengren, B., Shetzer, H. G., & Cameja, G. (1993). Lipid oxidation and measurement of thiobarbituric acid reacting substances (TBARS) formation in a single microtitre plate: Its use for evaluation of antioxidants. *Analytical Biochemistry*, 208, 10–15. <https://doi.org/10.1006/abio.1993.1002>

Wang, Y., Wu, Y., Wang, Y., Xu, H., Mei, X., Yu, D., Wang, Y., & Li, W. (2017). Antioxidant properties of probiotic bacteria. *Nutrients*, 9(5), 521. <https://doi.org/10.3390/nu9050521>

Zhang, Y., Li, L., Guo, C., Mu, D., Feng, B., Zuo, X., & Li, Y. (2016). Effects of probiotic type, dose and treatment duration on irritable bowel syndrome diagnosed by Rome III criteria: a meta-analysis. *BMC gastroenterology*, 16(1), 62. <https://doi.org/10.1186/s12876-016-0470-z>

4.3 MANUSCRIPT 3

Manuscript submitted in **Food Research International** (Impact Factor: 6.475)

Synbiotic modulates intestinal microbiota metabolic pathways and inhibits DMH-induced colon tumorigenesis through c-myc and PCNA suppression.

Bruna Cristina dos Santos Cruz^a, Vinícius da Silva Duarte^b, Roberto Sousa Dias^c, Andressa Ladeira Bernardes^a, Sérgio Oliveira de Paula^c, Célia Lúcia de Luces Fortes Ferreira^d, Maria do Carmo Gouveia Peluzio^a

^aNutritional Biochemistry Laboratory, Department of Nutrition and Health, Universidade Federal de Viçosa – UFV, Viçosa, Minas Gerais, Brazil.

^bFaculty of Chemistry, Biotechnology and Food Science, Norwegian University of Life Sciences – NMBU, Norway.

^cImmunovirology Laboratory, Department of General Biology, Universidade Federal de Viçosa – UFV, Viçosa, Minas Gerais, Brazil.

^dInstitute of Biotechnology Applied to Agriculture & Livestock (Bioagro), Universidade Federal de Viçosa – UFV, Viçosa, Minas Gerais, Brazil.

Abstract

The use of probiotic and synbiotic is a promising strategy to modulate the intestinal microbiota, and thereby modify the risk of diseases. In this study, the effect of probiotic VSL#3, isolated or associated with a yacon-based product (PBY), on the functional metabolic pathways of the microbiota, in a colorectal carcinogenesis model, was evaluated. For this, mice induced to carcinogenesis were fed with standard diet AIN-93M (CON), diet AIN-93M and VSL#3 (PRO) or diet AIN-93M with yacon and VSL#3 (SYN). The SYN group showed a highly differentiated intestinal community based on the MetaCyc pathways. Of the 351 predicted functional pathways, 222 differed between groups. Most of them were enriched in the SYN group, namely: amino acid biosynthesis pathways, small molecule biosynthesis pathways (cofactors, prosthetic groups, electron carriers and vitamins) carbohydrate degradation pathways and fermentation pathways. In addition, the synbiotic was able to stimulate the anti-inflammatory immune response and reduce the gene expression of PCNA and c-myc. Thus, we conclude that the synbiotic impacted more significantly the metabolic functions of the microbiota compared to the isolated use of probiotic. We believe that the enrichment of these pathways can exert antiproliferative action, reducing colorectal carcinogenesis. The prediction of the functional activity of the microbiota is a promising tool for understanding the influence of the microbiome on tumor development.

Keywords: probiotic; prebiotic; colorectal cancer; gut microbiota; dysbiosis.

Abbreviations: CRC, colorectal cancer; PBY, yacon-based product; FOS, fructooligosaccharides; HPLC, high performance liquid chromatography; DMH, 1,2-dimethylhydrazine; BCFA, branched chain fatty acids; TNF, tumor necrosis factor; IFN, interferon.

Introduction

Colorectal cancer (CRC) is a global health problem, with more than 1.84 million new cases and 0.8 million deaths annually worldwide. Due to the population aging trend, the incidence rate is expected to increase by about 80% in the next decades (Perisetti, Goyal, Tharian, Inamdar & Mehta, 2021). The absence of a strong link between genetics and CRC points to the potential role of other variables as determinants of the disease, including lifestyle and environmental factors such as smoking, alcohol consumption, overweight, physical inactivity, high consumption of red and processed meats, and low consumption of dietary fiber and whole grains (Song, Chan & Sun, 2020; Thomas et al., 2019).

Notably, the gut microbiome (which includes microorganisms, their genomes, and the surrounding gut environment) has been implicated as a critical environmental factor in colorectal carcinogenesis. Microbiome studies -facilitated by next-generation sequencing platforms, 'omics' technologies, and advanced bioinformatics approaches- have made it possible to establish links between specific microorganisms, their functional activities, and the risk of CRC (Thomas et al., 2019).

Studies indicate that changes in the microbiome allow the initiation and promotion of CRC, directly affecting the host's immune response, the production of microbial metabolites, and the energy balance of cancer cells (Schmidt, Raes, & Bork, 2018; Marchesi et al., 2015). Differences in microbiota composition were observed between healthy and CRC individuals, as well as enrichment or depletion of specific bacteria in patients with CRC. There is evidence that these changes occur during the early stages of carcinogenesis and can be used to identify individuals at high risk for the disease (Song & Chan, 2016; Scott et al., 2019).

Furthermore, alterations in several metabolic pathways are being identified as key mediators in the regulation of microbiome-host interactions (Yang & Jobin, 2017). In a study by Yang et al. (2019), for example, differences were observed in the metabolic pathways and metabolite production in fecal samples from individuals with and without a diagnosis of CRC. Among healthy individuals, it was noted the enrichment of biosynthesis pathways of some sugars, sugar alcohols, amines, and organic acids (glycerol and octadecanoic, hexanedioic, benzenepropanoic, linoleic, and oleic acids). In individuals with CRC, there was a greater abundance of polyamines (cadaverine, 1,4-butanediamine), some amino acids, and urea (Yang et al., 2019).

Fortunately, the constitution and functionality of the microbiome can be modified by intrinsic and extrinsic factors, and it is likely that it adequately performs its functions as long as the homeostasis of the intestinal microbiota is maintained (Tu et al., 2020; Nicholson et al., 2012). The gut microbiome can therefore be modified as part of CRC preventive strategies.

In this sense, the search for compounds that can modify the microbiome and mitigate the development of CRC is being widely investigated. Probiotics are defined as *"live microorganisms that, when administered in adequate amounts, confer benefits to the health of the host"* (Hill et al., 2014). Its use is an attempt at targeted modulation of the intestinal microbiota, notably through the addition of specific probiotic strains. On the other hand, prebiotics, which are *"substrates that confer health benefits used selectively by host microorganisms"* (Gibson et al., 2017), are another strategy of targeted modulation of the microbiota, which aims to confer a selective advantage on resident microorganisms. Dietary intervention with synbiotics (which combine probiotic and prebiotic components) seems to be even more effective (Baştürk, Artan & Yılmaz, 2020; Sergeev, Aljutaily, Walton & Huarte, 2020).

In fact, we have previously demonstrated that the use of the synbiotic composed of the multispecies probiotic VSL#3 associated with the concentrated yacon-based product (PBY), but not the probiotic VSL#3 alone, was able to reduce the incidence of precursor lesions of CRC in mice induced with the chemical carcinogen 1,2-dimethylhydrazine (DMH) (Dos Santos Cruz et al., 2020). Complementary analyzes identified the following as potential mechanisms of action of this synbiotic: the change in the structure of the intestinal microbial community, the reduction of inflammation in the colon, the inhibition of the activity of the pro-carcinogenic enzyme β -glucuronidase, the increase in short-chain fatty acids, reduction of oxidative stress, and intestinal permeability (Dos Santos Cruz et al., 2020; Dos Santos Cruz et al., 2021).

Although there are studies that have established the relationship between specific microorganisms and CRC, the functional contribution of the intestinal microbial community to CRC has not yet been systematically characterized, as well as the production of microbial metabolites. In the present study, new insights into the host and its intestinal microbiota were investigated, predicting microbial metabolic pathways that may be associated with colorectal carcinogenesis. Thus, our objective was to evaluate the effects of the synbiotic VSL#3 + PBY and the probiotic VSL#3 on the modulation of metabolic pathways in the intestinal microbiota, the expression of genes

related to carcinogenesis, the pattern of the intestinal inflammatory response, and the concentrations of branched-chain fatty acids (BCFA) in an experimental model of colorectal carcinogenesis.

Material and Methods

Probiotic and synbiotic

The commercial probiotic VSL#3 (Sigma Tau Pharmaceuticals, Inc.; acquired in 2016, valid 04/2018, lot number 604094) was purchased lyophilized, in sachets containing 450 billion viable bacteria, and reconstituted in water, daily, before administration. This probiotic is composed of eight bacterial species: *Bifidobacterium breve*, *Bifidobacterium infantis*, *Bifidobacterium longum*, *Lactobacillus acidophilus*, *Lactobacillus bulgaricus*, *Lactobacillus casei*, *Lactobacillus plantarum*, and *Streptococcus thermophilus*. The dose of 2.25×10^9 CFU/day was chosen with the aim of improving intestinal health and ensuring a minimum count of 10^6 g⁻¹bacteria in the stool (Sarao & Arora, 2017).

The synbiotic was composed of the probiotic VSL#3 and the yacon-based product (PBY), source of the prebiotics fructooligosaccharides (FOS) and inulin (Patent: PI 1106621-0). The preparation of PBY involves crushing the yacon roots and concentrating the product in a boiler until it reaches 60° Brix (Paula et al., 2012). Previous studies have shown the benefits of using PBY when added to the diet to provide 6% FOS plus inulin (De Nadai Marcon et al., 2020; De Nadai Marcon et al., 2019; Paula et al., 2012), this being the dosage adopted in the present study. Considering that every 100g of PBY contains 23.6g of FOS and inulin, 25.4g of PBY was added for every 100g of standard rodent diet (AIN-93M) (Reeves, Nielsen, & Fahey, 1993). The carbohydrate, protein, and fiber contents were adjusted so that the experimental diets had a similar composition. Diets were prepared in pellet form and stored at -20°C.

Animals and experimental design

Male C57BL6/J mice, healthy, eight weeks old and initial body weight of approximately 22 g, were obtained from the Central Bioterium at the Biological

Sciences and Health Center at Federal University of Viçosa, Minas Gerais, Brazil. The animals were collectively allocated in polypropylene cages, and kept under controlled conditions, at a temperature of $22 \pm 2^\circ \text{C}$ and humidity of 60-70% with a 12 h light/dark cycle.

After a week of acclimatization, with free access to commercial diet (Purina®) and water, animals were divided into three different groups (n=15/group), to receive the following interventions for a period of 13 weeks:

1. Control group (CON): standard diet AIN-93M and 0.1 mL of water, via orogastric gavage;
2. Probiotic group (PRO): standard diet AIN-93M and 0.1 mL of probiotic VSL#3 (2.25×10^9 CFU/animal), via orogastric gavage;
3. Synbiotic group (SYN): modified AIN-93M diet, with PBY (6% FOS and inulin) and 0.1 mL of probiotic VSL#3 (2.25×10^9 CFU/animal), via orogastric gavage.

The experimental diets were offered *ad libitum*, and gavages administered in the morning, for five days a week (Arthur et al., 2013). In the third experimental week, the CRC precursor lesion induction protocol was started: all animals received intraperitoneal injection of the chemical carcinogen 1,2-dimethylhydrazine (DMH) (Sigma-Aldrich, Saint Louis, USA), 20 mg/kg, once a week, for eight consecutive weeks (Gomides et al., 2014; Newell & Heddle, 2004).

At the end of the experiment, the animals were anesthetized with 3% isoflurane and euthanized by cervical dislocation. The colon was resected and washed with buffered saline (pH 7.2). Part of the colon was stored in vials containing Trizol (Invitrogen™, Carlsbad, CA, USA) and the remaining tissue was immediately frozen at -80°C .

Feces collection

Feces samples from all animals were collected during the experimental period. To obtain samples, individual cages were previously cleaned and sanitized and a single mouse was kept there until a sufficient amount of feces was spontaneously expelled. Samples were kept at -80°C for further analysis. The samples collected in the last experimental week (13th week), were used to carrying out metagenomic sequencing and quantification of fecal fatty acids.

Bioinformatics processing and metagenoma functional prediction

The raw sequence data used in the present study were acquired from the amplification and sequencing of the V3-V5 hypervariable region of the 16S rRNA genes (Dos Santos Cruz et al., 2020). The genetic material was obtained by extracting bacterial metagenomic DNA present in fecal samples collected in the last experimental week.

Microbiota bioinformatics was carried-out with QIIME2 (version 2020.2) (Bolyen et al., 2019). Raw sequence data obtained across the C57BL6 mice stool samples belonging to the groups CON, PRO, and SYN were imported via the Casava1.8 single-end pipeline followed by denoising with DADA2 (Callahan et al., 2016) (via q2-dada2). Afterward, Amplicon Sequence Variants (ASVs) (read sequences and read counts) were used as inputs for the PICRUST2 (Phylogenetic Investigation of Communities by Reconstruction of Unobserved States) pipeline (Douglas et al., 2020). Briefly, ASVs were inserted and aligned into a reference tree composed of 20,000 full 16S rRNA genes from bacterial and archaeal genomes using, respectively, the tools HMMER (<http://www.hmmer.org>) and EPA-ng/ GAPPA (Barbera et al., 2019; Czech & Stamatakis, 2019).

Subsequently, the castor R package (Louca & Doebeli, 2018) was used to predict the missing gene families (Enzyme Commission numbers) for each ASV, as well as their respective copy number of 16S rRNA gene sequences, by using the output tree generated previously. Lastly, MinPath (Ye & Doak, 2009) was adopted to infer MetaCyc pathways based on EC number abundances.

Taxonomic drivers of functional changes in the gut microbiota

In order to identify the taxonomic group(s) responsible for the enrichment of certain metabolic pathways, the FishTaco (*Functional Shifts' Taxonomic Contributors*) analysis was carried-out as described by Manor & Borenstein (2017).

In short, the phylotypes with at least 0.01% relative abundance in at least one sample in the table of operational taxonomic units (OTUs), as well as the predicted metagenome (KEGG Orthology Group - KO) for each specimen from the PICRUST2 analysis were used as entries in the FishTaco software. The Multi_rate mode was run to evaluate the contribution of each taxon in functional categories of interest among

the groups. The output result was explored and visualized using ggplot2 (Wickham, 2016) in R package. The sequencing dataset for this study is available on the *Sequence Read Archive* (SRA) under BioProject accession number PRJNA625308.

Quantitative Real-Time Polymerase Chain Reaction (RT-qPCR)

Total RNA was extracted from colon tissue stored in Trizol (Invitrogen™, Carlsbad, CA, USA), according to manufacturer's instructions. Total RNA was quantified on a Multiskan™ GO spectrophotometer (Thermo Fisher Scientific; Waltham, MA, USA) and the purity was determined by the absorbance ratio 260/280 nm. After quantification, the mRNA samples were treated with DNase (DNase I; Promega, Madison, WI, USA), as described below: samples containing 2 µg of RNA were treated with 3 µL of DNase buffer and 4.5 µL of DNase. The final volume of 30 µL was completed with water. The samples were incubated at 37° C for 30 min, and at 70° C for 10 min. After incubation, they were placed on ice, for 5 min. Real-time PCR quantitative mRNA analyses were performed in an Illumina Eco Real-Time PCR system (Illumina, San Diego, CA, USA), using the GoTaq® 1-Step RT-qPCR System (Promega, Madison, WI, USA). 10 µL of the GoTaq® qPCR Master Mix, 0,4 µL of the Reverse Transcriptase, 0,4 µL of the sense primer, 0,4 µL of the antisense primer, sample (containing at least 100 ng of mRNA), and nuclease-free water were added to each reaction (20 µL final volume). The thermal cycles were used: 1 cycle reverse transcription (37° C, 15 min), and 1 cycle reverse transcriptase inactivation and GoTaq® DNA polymerase activation (95° C, 10 min), followed by 40 cycles of denaturation (95° C, 10 seconds), annealing (60° C, 30 seconds) and extension (72° C, 30 seconds). The analysis was performed by the $2^{-\Delta\Delta C_t}$ algorithm on the EcoStudy® software (Illumina), using GAPDH gene as an endogenous control. The sequences of murine primers used are described in Table 1.

Cytokine profile in colon

Pro- and anti-inflammatory cytokines were simultaneously determined by the Cytometric Bead Array (CBA) mouse Th1/Th2/Th17 Kit (BD Biosciences, San Jose, USA) in a BD FACSVerse Flow cytometry, as described below: colon samples (100 to 200 mg) were ground using a tissue homogenizer (T10 basic UltraTurrax, IKA®, Rio

de Janeiro, Brazil) in phosphate buffered saline (pH 7.2), centrifuged (10,000 g, for 10 min at 4° C) and the supernatant recovered. The beads were diluted with diluent solution and distributed in microtubes. 25 µL of the sample and 17 µL of the detector solution were added to each microtube, followed by incubation for 2 hours. Subsequently, 1 mL of the washing solution was added, followed by centrifugation (1,800 x g, for 5 min at 4° C), and despised part of the supernatant (approximately 800 µL). The remaining volume was used for reading on the flow cytometer. The standard curve was built from the most concentrated solution (top standard). The ratios IL-4/IFN, IL-4/IL-10, IFN/IL-10, IL-10/IL-6, and IL-10/TNF were assessed. The data was processed using the FCAP Array 3.0 (FCAP Array Software BD Biosciences, California, USA) and the results are expressed in pg/g of tissue.

Table 1. qRT-PCR murine primer sequences used in this study.

Gene	Sequence	References
c-myc	sense: 5'-TCGTGTACCTCGTCCGATTC-3'	Zeineldin et al., 2012
	antisense: 5'-GGAGGACAGCAGCGAGTC-3'	
P53	sense: 5'-GTATTTACCCTCAAGATCC-3'	Kiatpakdee et al., 2020
	antisense: 5'-TGGGCATCCTTTAACTCTA-3'	
PCNA	sense: 5'-TAAAGAAGAGGAGGCGGTAA-3'	Lin & Sun (2015)
	antisense: 5'-TAAGTGTCCCATGTCAGCAA-3'	
Caspase-3	sense: 5'-AGCAGCTTTGTGTGTGTGATTCTAA-3'	Mengying et al., 2017
	antisense: 5'-AGTTTCGGCTTTCCAGTCAGA-3'	
GAPDH	sense: 5'-AAGGTTCTCATCTCCGCTC-3'	Piranlioglu et al., 2019
	antisense: 5'-GTTCGAGATGATGGTGTGCT-3'	

PCNA: *proliferating cell nuclear antigen*; GAPDH: *glyceraldehyde-3-phosphate dehydrogenase*.

Fecal branched-chain fatty acids (BCFA) quantification

Isobutyric, valeric and isovaleric fatty acids were extracted from fecal samples collected in the last experimental week, and determined as described below (Smiricky-Tjardes, Grieshop, Flickinger, Bauer, and Fahey Jr, 2003): approximately 50 mg of feces were vortexed with deionized water (950 µL) and incubated in ice for 30 min, followed by homogenization in vortex every 5 min. Samples were centrifuged at 10,000 g, for 30 min at 4° C three times and the supernatant was collected and filtered through

a 0.45 µm membrane filter. The branched chain fatty acids (BCFA) were measured by high-performance liquid chromatography (HPLC) (Shimadzu®, Quito, Japan) using an Aminex HPX 87H column at 32°C, with acidified water (H₂SO₄, 0.005 M) as the eluent at a flow rate of 0.6 mL/min. The products were detected and quantified by an ultraviolet detector (SPD-20A VP) at 210 nm. Standard curves of isobutyric, isovaleric and valeric acid were constructed (Supelco®, Darmstadt, Germany). Results were expressed in µmol/g of feces.

Statistical analysis

To explore and compare the metabolic potential of intestinal microbial communities, the Statistical Analysis of Metagenomic Profile (STAMP) *software* was used. The functional profile was built on the Metabolic Pathway Database (MetaCyc) (Caspi et al., 2020). Kruskal-Wallis H test was adopted as a hypothesis test, followed by correction by *False discovery rate* (FDR). Compositional changes were compared using the Wilcoxon test, with correction by FDR. The remaining comparisons were carried out using the SPSS® v.20.0 *software*, using the ANOVA or Kruskal-Wallis tests and respective *posthoc* tests. The $\alpha < 0.05$ was adopted.

Results

Synbiotic modulates metabolic pathways of biosynthesis, degradation and fermentation of the intestinal microbiota

A scatter plot of the principal component analysis (PCA) using unstratified pathway abundances revealed that the SYN group significantly clustered separately from the CON and PRO groups (Fig. 1), indicating a high dissimilar intestinal community based on MetaCyc pathways.

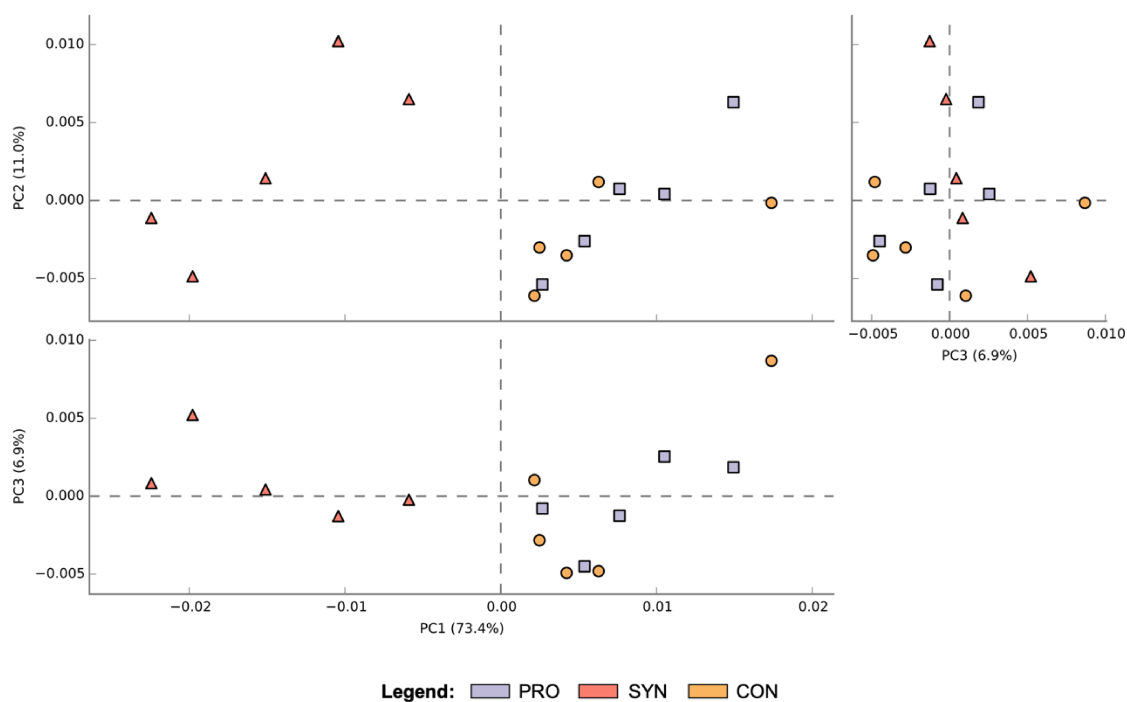


Figure 1 – Principal Component Analysis (PCA) based on the normalized abundance of predicted MetaCyc pathways across the different groups (CON, PRO and SYN).

To discriminate the potential functions of the gut bacterial community among the three groups, a Kruskal-Wallis H-test with Storey's FDR approach for multiple comparisons was used to the relative proportion of predicted MetaCyc pathways. From 351 predicted microbial pathways, 222 functional pathways differed significantly (Fig. 2), and the great majority (approximately 49.0%) were enriched in the SYN group when compared with CON e PRO groups (Supplementary Datasheet 1).

Taking into account only those MetaCyc pathways with an effect size greater than 0.5 (134 in total), the SYN group showed an enrichment specifically of the following microbial metabolic classes: i) amino acid biosynthesis (L-lysine, L-histidine, L-isoleucine, L-tryptophan, and L-valine); ii) biosynthetic pathways of small molecules such as cofactors (porphyrin compounds), prosthetic groups, electron carriers (quinol and quinone) and vitamins (vitamins B6 and K); iii) carbohydrate degradation related pathways (D-fructuronate, D-galacturonate, mannan and starch degradation); iv) fermentation to butanoate (superpathway of *Clostridium acetobutylicum* acidogenic fermentation and pyruvate fermentation to butanoate). In the groups CON e PRO, microbial metabolic pathways were predominantly related to nucleoside and nucleotide biosynthesis (pyrimidine nucleotide salvage, and purine/pyrimidine nucleotide *de novo* biosynthesis). Microbial biosynthetic pathways related to folate and the amino acids L-

tyrosine, L-serine, and L-phenylalanine were also enriched in these groups, however, in a very less extent manner.

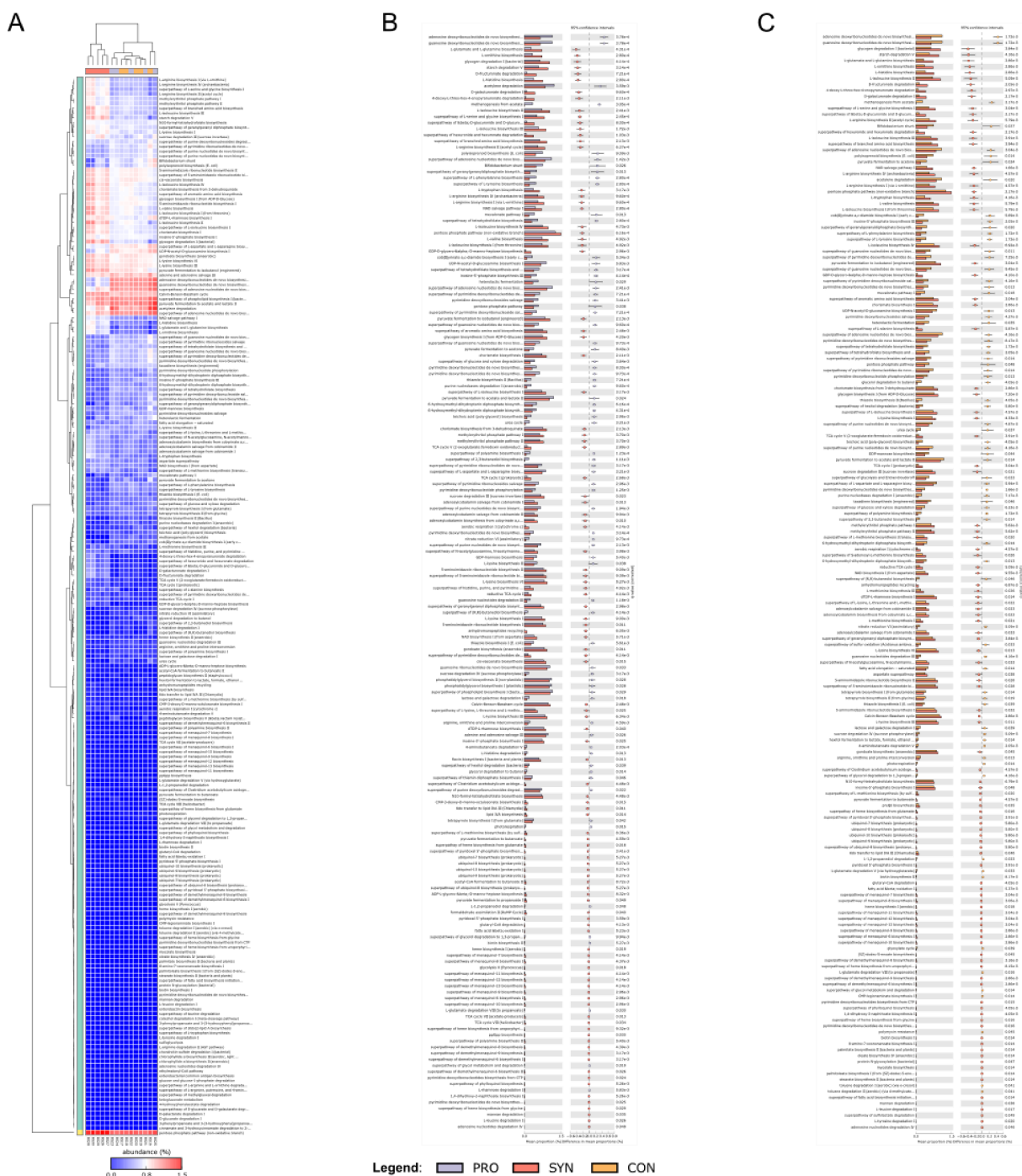


Figure 2 – Heatmap (A) of the predicted functional categories (MetaCyc pathways) obtained from fecal microbiota of C57BL/6 mice after the different interventions. Only statistically significant features were considered (222 metabolic pathways in total). Functional level extended error bar chart profile between the groups PRO and SYN (B), as well as CON vs SYN (C).

Additional investigation using FishTaco identified the enrichment of 32 KEGG pathways following the intervention with the synbiotic VSL#3 + PBY (Supplementary Datasheet 2). Taking into account only those KEGG classes in consonance with the predicted MetaCyc pathways, the taxonomic drivers of carbohydrate metabolism (ko00030, ko00040, ko00500, ko00630, and ko00660), amino acid metabolism (ko00260, ko00290, ko00300, ko00330, ko00340, and ko00400) and metabolism of cofactors and vitamins (ko00760 and ko00770) were mainly associated with members of the families *Lachnospiraceae*, *Coriobacteriaceae*, *Erysipelotrichaceae* and *Streptococcaceae* (Fig. 3A). There were no differentially abundant functions between CON e PRO. In fact, as reported in Fig. 3B, synbiotic administration favored the enrichment of various genera belonging to both families.

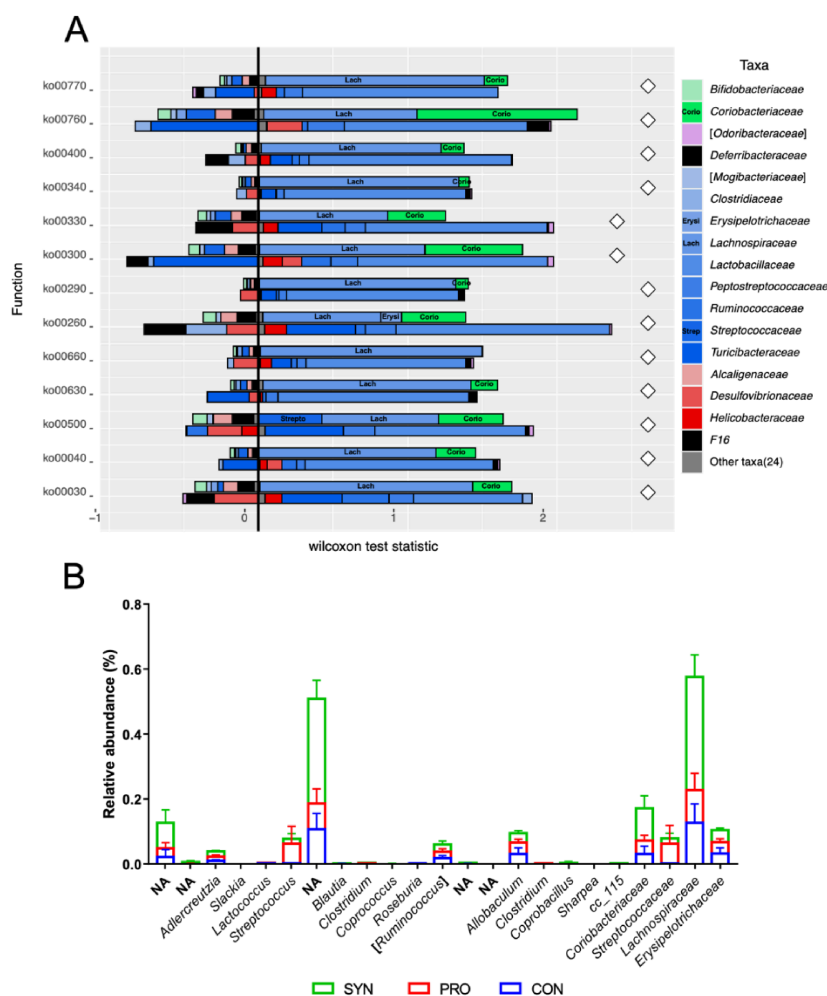


Figure 3 – Taxonomic contributors at the family level identified in fecal samples of C57BL6 mice determined by FishTaco (A). The bar on the top-right of Y axis represents SYN-associated families driving the enrichment in the functional module, whereas the

bar on the top-left of Y axis indicates SYN-associated families attenuating functional shift. The bar on the bottom-right of Y axis represents families depleted in the SYN group driving functional shift, whereas the bar on the bottom-left of Y axis shows families depleted in the SYN group attenuating functional shift. White diamonds represent family-based functional shift scores. (B) Overlapped stacked bar chart of SYN-associated families and genera driving the enrichment of selected KO pathways in fecal samples across the groups CON, PRO and SYN.

Synbiotic reduces the expression of c-myc and PCNA genes in the colon

PCR analysis showed the effect of interventions on the expression of important genes. The use of synbiotic VSL#3 + PBV, but not the probiotic alone, influenced the expression of genes associated with the colon carcinogenic process. We observed a down-regulation in the expression of c-myc ($p=0.024$) and PCNA ($p=0.028$) when compared to control group (Fig. 4A,C). The p53 and caspase-3 gene expression showed no statistical differences among the groups (Fig. 4B,D).

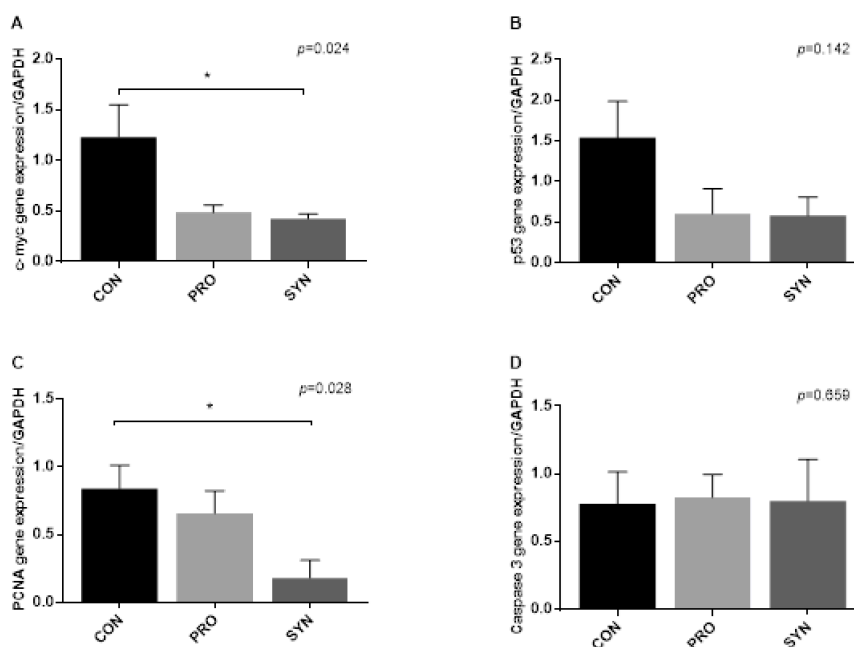


Figure 4. Effect of probiotic and synbiotic on gene expression in C57BL/J mice induced to colorectal tumorigenesis. (A) c-myc, (B) p53, (C) PCNA, and (D) caspase-3. Gene expression was calculated in relation to the constitutive GAPDH gene and presented as a relative variation of the control group. The data are expressed as mean \pm SD ($n=6$ or 7 /group). Statistical difference between groups were analyzed by ANOVA test or

Kruskal-Wallis test, (*) $p < 0.05$. CON, AIN-93M diet; PRO, AIN-93M diet and probiotic VSL#3; SYN, AIN-93M diet with PBY and probiotic VSL#3.

Synbiotic changes cytokine profile in colon tissue

The levels of seven cytokines (IL-2, IL-4, IL-6, IL-10, IL-17, TNF and IFN) were measured in colon tissue by flow cytometry and thereafter, the ratios IL-4/IFN, IL-4/IL-10, IFN/IL-10, IL-10/IL-6, and IL-10/TNF were assessed. The ratios IL-4/TNF, IL4-IL-10, IL-10/TNF significantly increased in the SYN group when compared to the CON group (Fig. 5A-B,E), while the ratio IFN/IL-10 decreased (Fig. 5C). IL-10/IL-6 ratio did not reveal any significant difference among the experimental groups (Fig. 5D).

Synbiotic and probiotic do not alter fecal concentrations of branched chain fatty acids (BCFA)

The BCFA profile, namely isobutyric, valeric, and isovaleric were evaluated in fecal samples collected at the end of the experimental period and the results are shown in Fig. 6. No significant differences were observed between the experimental groups.

Discussion

In a previous study, we demonstrated that the synbiotic VSL#3 + PBY modulated the composition and activity of the intestinal microbiota in an experimental model of colorectal carcinogenesis (Dos Santos Cruz et al., 2020). Here, we provide new *insights* between the host and its microbiome, predicting and investigating bacterial metabolic pathways that might be related to CRC.

In the present study, we found that intervention with VSL#3 + PBY enriched bacterial biosynthesis pathways of several different amino acids (L-lysine, L-serine, L-glycine, L-histidine, L-isoleucine, L-tryptophan, L-arginine, L-glutamate, L-glutamine, L-ornithine, and L-valine). It is described in the literature that healthy individuals present enrichment of the metabolism pathways of aspartate, alanine, glutamate, and methionine when compared to individuals with CRC (Yang et al., 2019).

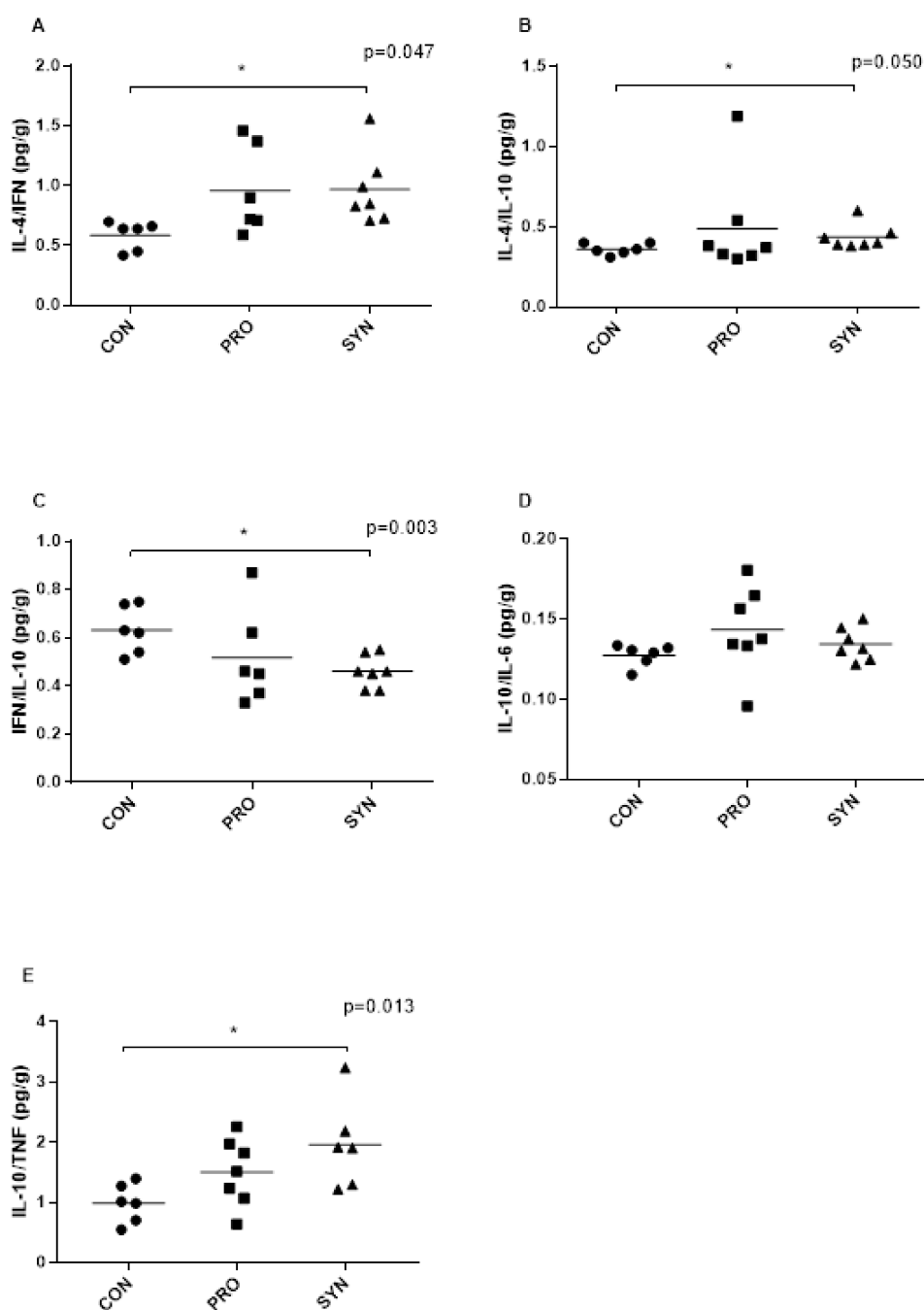


Figure 5. Effect of probiotic and synbiotic on cytokine profile in colon tissue in C57BL/J mice induced to colorectal tumorigenesis. (A) IL-4/IFN, (B) IL-4/IL-10, (C) IFN/IL-10, (D) IL-10/IL-6, and (E) IL-10/TNF. The data are expressed as mean \pm SD (n=6 or 7/group). Statistical difference between groups were analyzed by ANOVA test or Kruskal-Wallis test, (*) $p < 0.05$. CON, AIN-93M diet; PRO, AIN-93M diet and probiotic VSL#3; SYN, AIN-93M diet with PBY and probiotic VSL#3.

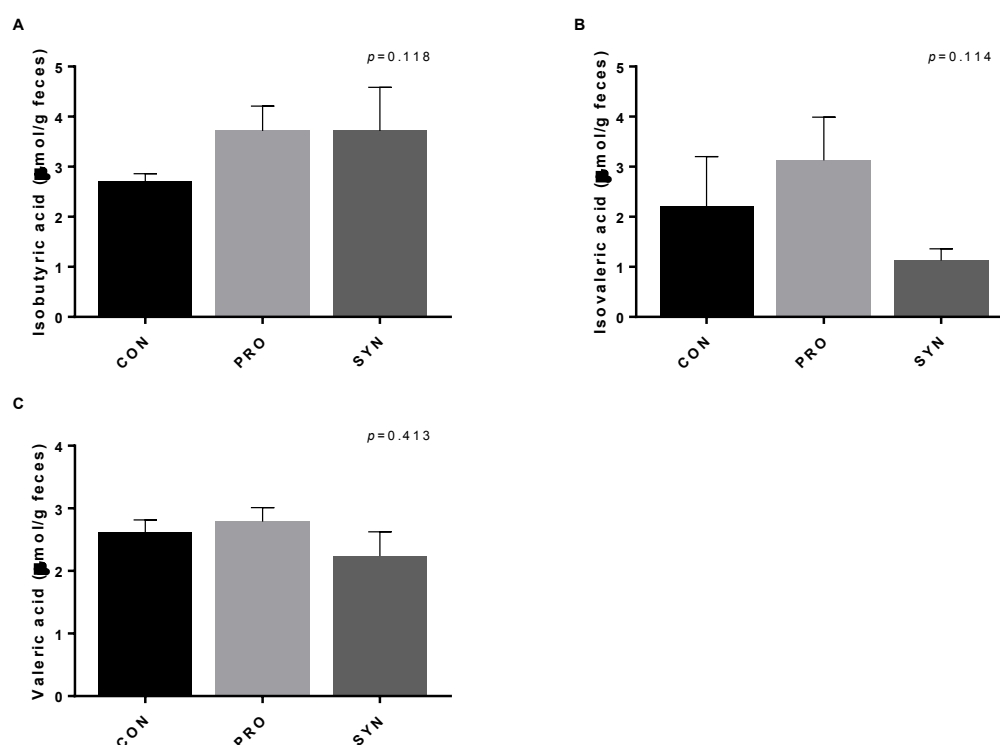


Figure 6. Effect of probiotic and synbiotic on fecal concentrations of branched chain fatty acids in C57BL/J mice induced to colorectal tumorigenesis. (A) isobutyric, (B) valeric, and (C) isovaleric. The data are expressed as mean \pm SD ($n=7$ /group). Statistical difference between groups were analyzed by ANOVA test or Kruskal-Wallis test, (*) $p < 0.05$. CON, AIN-93M diet; PRO, AIN-93M diet and probiotic VSL#3; SYN, AIN-93M diet with PBY and probiotic VSL#3.

It is noteworthy that the metabolic pathways related to the biosynthesis/metabolism of amino acids must be carefully investigated and, whenever possible, an evaluation of the concentrations of these metabolites must be conducted. Increased glutamate concentration, for example, regardless of glutamine concentrations, may indicate glutaminase hyperactivity in cancer cells, described as an important factor in tumor progression (Blachier, Boutry, Bos & Tomé, 2009).

Further investigation with FishTaco revealed that the families Lachnospiraceae, *Erysipelotrichaceae*, and *Coriobacteriaceae* were the main taxa responsible for the enrichment of the KEGG pathways related to the metabolism of the amino acids L-arginine, L-proline, and L-histidine, as well as to the biosynthesis of L-valine, L-leucine, L-isoleucine, L-lysine, L-phenylalanine, L-tyrosine and L-tryptophan. It is described in the literature that the CRC-associated microbiome has a high capacity to metabolize

amino acids through putrefaction, resulting in tumor-promoting compounds such as putrescines, cadaverine, and 1,4-butanediamine (Thomas et al., 2019; Yang et al., 2019).

In relation to branched-chain amino acids (BCAA), we observed an increase in the degradation pathway of the amino acid L-leucine. As reported by Dai & Zhu (2011), intestinal bacteria commonly contain a greater amount of BCAA compared to other amino acids, actively participating in host amino acid homeostasis (Thomas et al., 2019). Hydrocinnamic acid, which regulates BCAA breakdown, has already been identified as a potential protector against intestinal tumorigenesis (Anantharaju, Gowda, Vimalambike & Madhunapantula, 2016). Dietary fiber, present in prebiotics, can also alter the metabolism of microbial amino acids and their availability. Inulin ingestion, for example, was able to reduce BCAA degradation in an animal model (Neis, Dejong, & Rensen, 2015).

Overall, our findings suggest that an increased bacterial demand to synthesize different amino acids (with the exception of L-leucine) may be the result of the expanding gut microbiota in the large intestine (Gill et al., 2006), which could potentially reflect in the plasma levels of these amino acids. These findings deserve further investigation.

Microbial amino acids play a relevant role not only in the synthesis of bacterial cell components, but they can also be catabolized, generating, for example, bioactive molecules such as short-chain and branched-chain fatty acids (Lin, Liu, Piao, & Zhu, 2017). Bacteria belonging to the genus *Clostridium*, *Lactobacillus*, and *Streptococcus* are the main genera involved in amino acid fermentation (Wu et al., 2020). As previously reported by our group (Santos Cruz et al., 2020), these amino acid fermenting taxa were significantly enriched after using VSL#3 + PBV (*Clostridium*: 86 fold-change; *Lactobacillus*: 3 fold-change; *Streptococcus*: 24 fold-change) and were positively correlated with the production of short-chain fatty acid (SCFA).

The resident gut microbiota plays a significant role in the synthesis of several vitamins (B complex vitamins and vitamin K), contributing more than a quarter to the total *pool* of vitamins available in humans (Hill, 1997; Rowland et al., 2018). Among the MetaCyc pathways related to the biosynthesis of molecules that participate in enzymatic reactions (i.e., cofactors, prosthetic groups, electron carriers, and vitamins), we note in the SYN group a greater number of pathways associated with the production of different vitamins, such as vitamin B6 (pyridoxal 5'-phosphate biosynthesis and salvage), vitamin B12 (adenosylcobalamin biosynthesis from cobyrinate a,c-diamide I,

and adenosylcobalamin salvage from cobinamide II), vitamin K1 (superpathway of phyloquinol biosynthesis), and vitamin K2 (superpathways of menaquinol).

Menaquinones and ubiquinones are electron carriers that participate in the respiratory chain and in the energy generation process (Aussel et al., 2014). According to Allaway et al. (2020), the increased synthesis of specific menaquinones and ubiquinones may indicate the presence of specific taxa capable of adapting to microaerobic environments. In addition, menaquinones are considered to be an important class of growth factors for uncultured bacteria, such as members of the genera *Faecalibacterium*, *Bacteroides*, *Bilophila*, *Gordonibacter*, and *Sutterella* (Fenn et al., 2017). This fact is in agreement with our previous study, in which a reduction in the abundance of the genus *Sutterella* (27 times) was identified in the group that received only the probiotic VSL#3 (PRO), which possibly reflects the lower abundance of taxa involved in the production of quinones, the so-called “donor bacteria”.

The analysis using the FishTaco software also showed that the expansion of the taxa *Lachnospiraceae* and *Coriobacteriaceae* was associated with the enrichment of the biosynthesis pathways of pantothenate and CoA, and of the metabolism of nicotinate and nicotinamide. Vitamins have antineoplastic effects due to action on DNA metabolism (synthesis and methylation), anti-inflammatory and antioxidant activities, and suppression of cell proliferation (Dasari et al., 2017; Kiely et al., 2015; Zhang, Ma, Smith-Warner, Lee & Giovannucci, 2013).

Ogawa et al. (2007) investigated the antitumor properties of vitamin K in CRC through *in vitro* and *in vivo* assays. As the main outcome, the authors observed that vitamins K2, K3, and K5 induced apoptosis through activation of caspase-3. Kawakita et al. (2009) report that cell death varies in different colon cancer cell lines in response to vitamin K2 administration. In this study, we hypothesize that the enrichment of microbial biosynthetic pathways related to the production of vitamins and, consequently, the increase in the *pool* of vitamins in the intestine, may exert antiproliferative activity, targeting the proto-oncogene *c-myc* and PCNA, both genes down-regulated after the synbiotic intervention, but without activating caspase-3.

As expected, as carbohydrate degradation pathways (D-fructuronate degradation, D-galacturonate degradation I, starch degradation V and mannan degradation) and central metabolism (pentose phosphate pathway (non-oxidative branch), aerobic respiration I (cytochrome c), TCA cycle I (prokaryotic), TCA cycle V (2-oxoglutarate:ferredoxin oxidoreductase), and the fermentation pathway from

pyruvate to isobutanol (engineered) were enriched in the intestinal microbiota of mice that received VSL#3 + PBY. These findings suggest that animals that received the synbiotic are able to maintain carbohydrate metabolism even in a more reducing environment in intestine, compared to CON and PRO groups.

By adopting the FishTaco analysis, we were able to observe that the increase in the abundance of the families *Lachnospiraceae*, *Coriobacteriaceae* and *Streptococcaceae* was responsible for driving an increase in the following KEGG pathways linked to carbon metabolism: pentose phosphate pathway, pentose and glucuronate interconversions, metabolism starch and sucrose, glyoxylate and dicarboxylate metabolism and C5-branched dibasic acid metabolism.

Yacon is a tuberous root that has a high content of FOS and inulin which are minimally hydrolyzed by digestive enzymes in the small intestine, enabling these complex sugars to reach the large intestine without significant structural change (Russo, Valentão, Andrade, Fernandez, & Milella, 2015; Wang et al., 2020). After that prebiotic-degrading enzyme produced by specific bacterial taxa breakdown such as complex polysaccharides into smaller oligosaccharides or monosaccharides, those molecules reach the cytoplasm and serve as fermentable substrates for pyruvate formation, the main molecule involved in short-chain fatty acids (SCFA) production.

In terms of SCFA, two MetaCyc pathways were enriched, namely superpathway of *Clostridium acetobutylicum* acidogenic fermentation and pyruvate fermentation to butanoate, and associated with butanoate formation. This result is in agreement with what was previously demonstrated by Santos Cruz et al. (2020), who detected a greater amount of butyrate in fecal samples after the VSL#3 + PBY intervention that was positively correlated with greater abundances of the genera *Ruminococcus*, *Dorea*, *Coprococcus*, *Sutterella*, and *Coprobacillus*. Although further studies are needed to validate these microbial signatures, the identification of differentiated clusters between healthy and sick individuals, such as the greater enrichment of carbohydrate and fatty acid metabolism pathways in healthy individuals, and polyamines, drugs and other metabolites in sick individuals, reinforce the interrelationship between the microbiome and the CRC (Yang et al., 2019).

In the CON and PRO groups, we identified enrichment of MetaCyc pathways related to the metabolism of one carbon, and of biosynthesis and recovery of folate, biotin and purine, and pyrimidine. According to Allaway et al. (2020), the bacterial demand for these pathways is the result of greater needs for nucleotides used to

synthesize DNA and RNA molecules not available in the diet, which is essential for the growth of the microorganism. Interestingly, Lee et al. (2020) report that the intestinal microbiota is a relevant source of exogenous purines required by the intestinal mucosal barrier in different processes (e.g., energy production, proliferation, and innate immunity). Based on our results, we hypothesize that the synbiotic VSL#3 + PBY can positively modulate nucleotide biosynthesis in the intestinal bacterial community and therefore contribute to the barrier function of the intestinal mucosa (Cruz et al., 2021).

Uncontrolled cell proliferation and inhibition of apoptosis are common events of carcinogenesis. To elucidate the contribution of probiotic and synbiotic in gene regulation, the mRNA expression of markers associated with proliferation and apoptosis was evaluated. The synbiotic VSL#3 + PBY reduced the expression of c-myc and PCNA without, however, changing the expression of p53 and caspase 3, which suggests an action aimed at inhibiting cell proliferation. The c-myc oncogene is a critical downstream effector of cell proliferation, induced by the Wnt/ β -catenin pathway, and is overexpressed in 70%-80% of colon adenocarcinomas (Sipos, Firneisz, & Múzes, 2016). The reduction in c-myc expression is possibly associated with the synbiotic's antitumor activity.

PCNA is a nuclear protein that participates in DNA replication along with the reconstruction of double strands. It is considered a marker of cell cycle kinetics and proliferative activity. PCNA concentrations are correlated with tumor malignancy, invasion, and survival, and the ability of probiotics and synbiotics to suppress PCNA expression has been demonstrated in experimental studies (Cai, Li, Pan, Zhang, Wei, & Gao, 2017; Zhu, Zhu, Ge, Zhang, Jiang, Cui, & Ren, 2014; Le Leu, Hu, Brown, Woodman, & Young, 2010).

Although the predicted metabolic pathways were not directly related to the inflammatory process, the use of the synbiotic significantly increased the anti-inflammatory response in the colon. The regulation of inflammation is one of the mechanisms attributed to the protection provided by the synbiotic. In general, microorganisms and their metabolites interact with immune cells by binding to receptors, such as *Toll-like* and *NOD-like*. As a result, immune and intestinal cells secrete cytokines to regulate the innate and adaptive immune response, with an increase in the anti-inflammatory response (Igarashi et al., 2017).

The branched-chain fatty acids (BCFA) isobutyric, isovaleric, and valeric (also known as putrefactive acids) were evaluated in the present study; however, no

significant differences were observed between the experimental groups. Inulin supplementation was able to reduce the fecal concentrations of these fatty acids in experimental animals (Krupa-Kozak, Markiewicz, Lamparski, & Juśkiewicz, 2017); however, the relationship of these fatty acids with CRC specifically has not been clarified yet.

Conclusion

In general, it was possible to observe unique and differentiated metabolic signatures among animals that received the synbiotic VLS#3 + PBY. Although this exploratory study has limitations, such as the lack of determination of microbial metabolites, our findings demonstrated that the modulation of the intestinal microbiota confers particular characteristics in the enrichment of microbial metabolic pathways, which possibly contributes to a better response in the control of carcinogenesis and the inflammatory response of the host.

In this perspective, two approaches are essential for future studies: the identification of compounds capable of modifying the composition and activity of the intestinal microbiota and, therefore, preventing CRC, in addition to determining biomarkers that are sensitive enough to screen individuals with high risk to CRC, ensuring the reproducibility and predictive accuracy of microbial signatures.

Ethics statement

All experimental procedures were performed under the guidelines of the of the European Community (Directive 2010/63/EU), in compliance with the ethical principles for animal experimentation. The study protocol was approved by the Ethics Committee in Animal Experimentation of the Federal University of Viçosa (CEUA/UFV, protocol nº 08/2017. Date of approval: May 09, 2017).

CRedit authorship contribution statement

Bruna Cristina dos Santos Cruz: Conceptualization, Methodology, Formal analysis, Investigation, Writing - original draft. **Vinícius da Silva Duarte:** Investigation, Formal analysis, Writing - review & editing. **Roberto Sousa Dias:** Formal analysis, Writing - review & editing. **Andressa Ladeira Bernardes:** Formal analysis, Writing - review & editing. **Sérgio Oliveira de Paula:** Formal analysis, Investigation, Writing - original

draft. **Célia Lúcia de Luces Fortes Ferreira:** Conceptualization, Methodology. **Maria do Carmo Gouveia Peluzio:** Conceptualization, Methodology, Writing - review & editing.

Declaration of Competing Interest

The authors declare that they have no known competing financial interests or personal relationships that could have appeared to influence the work reported in this paper.

Acknowledgment

The authors would like to thank the funding agencies National Council of Technological and Scientific Development (CNPq), Coordination for the Improvement of Higher Education Personnel (CAPES), and Foundation for the Support to the Researches in Minas Gerais (Fapemig) for their financial support and fellowships.

References

Allaway, D., Haydock, R., Lonsdale, Z. N., Deusch, O. D., O'Flynn, C., & Hughes, K. R. (2020). Rapid Reconstitution of the Fecal Microbiome after Extended Diet-Induced Changes Indicates a Stable Gut Microbiome in Healthy Adult Dogs. *Applied and Environmental Microbiology*, 86(13). <https://doi.org/10.1128/AEM.00562-20>

Anantharaju, P. G., Gowda, P. C., Vimalambike, M. G., & Madhunapantula, S. V. (2016). An overview on the role of dietary phenolics for the treatment of cancers. *Nutrition journal*, 15(1), 99. <https://doi.org/10.1186/s12937-016-0217-2>

Arthur, J. C., Gharaibeh, R. Z., Uronis, J. M., Perez-Chanona, E., Sha, W., Tomkovich, S., Mühlbauer, M., Fodor, A. A., & Jobin, C. (2013). VSL#3 probiotic modifies mucosal microbial composition but does not reduce colitis-associated colorectal cancer. *Scientific reports*, 3, 2868. <https://doi.org/10.1038/srep02868>

Aussel, L., Pierrel, F., Loiseau, L., Lombard, M., Fontecave, M., & Barras, F. (2014). Biosynthesis and physiology of coenzyme Q in bacteria. *Biochimica et biophysica acta*, 1837(7), 1004–1011. <https://doi.org/10.1016/j.bbabi.2014.01.015>

Barbera, P., Kozlov, A. M., Czech, L., Morel, B., Darriba, D., Flouri, T., & Stamatakis, A. (2019). EPA-ng: Massively Parallel Evolutionary Placement of Genetic Sequences. *Systematic biology*, *68*(2), 365–369. <https://doi.org/10.1093/sysbio/syy054>

Baştürk, A., Artan, R., & Yılmaz, A. (2016). Efficacy of synbiotic, probiotic, and prebiotic treatments for irritable bowel syndrome in children: A randomized controlled trial. *The Turkish journal of gastroenterology: the official journal of Turkish Society of Gastroenterology*, *27*(5), 439–443. <https://doi.org/10.5152/tjg.2016.16301>

Blachier, F., Boutry, C., Bos, C., & Tomé, D. (2009). Metabolism and functions of L-glutamate in the epithelial cells of the small and large intestines. *The American journal of clinical nutrition*, *90*(3), 814S–821S. <https://doi.org/10.3945/ajcn.2009.27462S>

Bolyen, E., Rideout, J. R., Dillon, M. R., Bokulich, N. A., Abnet, C. C., Al-Ghalith, G. A., Alexander, H., Alm, E. J., Arumugam, M., Asnicar, F., Bai, Y., Bisanz, J. E., Bittinger, K., Brejnrod, A., Brislawn, C. J., Brown, C. T., Callahan, B. J., Caraballo-Rodríguez, A. M., Chase, J., Cope, E. K., ... Caporaso, J. G. (2019). Reproducible, interactive, scalable and extensible microbiome data science using QIIME 2. *Nature biotechnology*, *37*(8), 852–857. <https://doi.org/10.1038/s41587-019-0209-9>

Cai, F., Li, J., Pan, X., Zhang, C., Wei, D., & Gao, C. (2017). Increased Expression of PCNA-AS1 in Colorectal Cancer and its Clinical Association. *Clinical laboratory*, *63*(11), 1809–1814. <https://doi.org/10.7754/Clin.Lab.2017.170503>

Callahan, B. J., McMurdie, P. J., Rosen, M. J., Han, A. W., Johnson, A. J., & Holmes, S. P. (2016). DADA2: High-resolution sample inference from Illumina amplicon data. *Nature methods*, *13*(7), 581–583. <https://doi.org/10.1038/nmeth.3869>

Caspi, R., Billington, R., Keseler, I. M., Kothari, A., Krummenacker, M., Midford, P. E., Ong, W. K., Paley, S., Subhraveti, P., & Karp, P. D. (2020). The MetaCyc database of metabolic pathways and enzymes - a 2019 update. *Nucleic acids research*, *48*(D1), D445–D453. <https://doi.org/10.1093/nar/gkz862>

Cruz, B., de Sousa Moraes, L. F., De Nadai Marcon, L., Dias, K. A., Murad, L. B., Sarandy, M. M., Conceição, L., Gonçalves, R. V., Ferreira, C., & Peluzio, M. (2021). Evaluation of the efficacy of probiotic VSL#3 and synbiotic VSL#3 and yacon-based product in reducing oxidative stress and intestinal permeability in mice induced to colorectal carcinogenesis. *Journal of food science*, *86*(4), 1448–1462. <https://doi.org/10.1111/1750-3841.15690>

Czech, L., & Stamatakis, A. (2019). Scalable methods for analyzing and visualizing phylogenetic placement of metagenomic samples. *PloS one*, *14*(5), e0217050. <https://doi.org/10.1371/journal.pone.0217050>

Dai, Z. L., Wu, G., & Zhu, W. Y. (2011). Amino acid metabolism in intestinal bacteria: links between gut ecology and host health. *Frontiers in bioscience (Landmark edition)*, *16*, 1768–1786. <https://doi.org/10.2741/3820>

Dasari, S., Ali, S. M., Zheng, G., Chen, A., Dontaraju, V. S., Bosland, M. C., Kajdacsy-Balla, A., & Munirathinam, G. (2017). Vitamin K and its analogs: Potential avenues for prostate cancer management. *Oncotarget*, *8*(34), 57782–57799. <https://doi.org/10.18632/oncotarget.17997>

De Nadai Marcon, L., Moraes, L. F. S., Cruz, B. C. S., Teixeira, M. D. O., Bruno, T. C. V., Ribeiro, I. E., ... Peluzio, M. C. G. (2019). Yacon (*Smallanthus sonchifolius*)-based product increases fecal short-chain fatty acids and enhances regulatory T cells by downregulating ROR γ t in the colon of BALB/c mice. *Journal of Functional Foods*, *55*, 333–342

De Nadai Marcon, L., Moraes, L. F. S., Cruz, B. C. S., Teixeira, M. D. O., Gomides, A. F. F., ... Peluzio, M. C. G. (2020). Yacon (*Smallanthus sonchifolius*)-based product increases fecal short-chain fatty acids concentration and up-regulates t-Bet expression in the colon of BALB/c mice during colorectal carcinogenesis. *Food Science and Nutrition*, *6*, 1-12. <https://doi.org/10.24966/FSN-1076/100069>

Dos Santos Cruz, B. C., da Silva Duarte, V., Giacomini, A., Corich, V., de Paula, S. O.,

da Silva Fialho, L., Guimarães, V. M., de Lucas Fortes Ferreira, C. L., & Gouveia Peluzio, M. (2020). Synbiotic VSL#3 and yacon-based product modulate the intestinal microbiota and prevent the development of pre-neoplastic lesions in a colorectal carcinogenesis model. *Applied microbiology and biotechnology*, *104*(20), 8837–8857. <https://doi.org/10.1007/s00253-020-10863-x>

Douglas, G. M., Maffei, V. J., Zaneveld, J. R., Yurgel, S. N., Brown, J. R., Taylor, C. M., Huttenhower, C., & Langille, M. (2020). PICRUST2 for prediction of metagenome functions. *Nature biotechnology*, *38*(6), 685–688. <https://doi.org/10.1038/s41587-020-0548-6>

Fenn, K., Strandwitz, P., Stewart, E. J., Dimise, E., Rubin, S., Gurubacharya, S., Clardy, J., & Lewis, K. (2017). Quinones are growth factors for the human gut microbiota. *Microbiome*, *5* (1), 161. <https://doi.org/10.1186/s40168-017-0380-5>

Gibson, G. R., Hutkins, R., Sanders, M. E., Prescott, S. L., Reimer, R. A., Salminen, S. J., Scott, K., Stanton, C., Swanson, K. S., Cani, P. D., Verbeke, K., & Reid, G. (2017). Expert consensus document: The International Scientific Association for Probiotics and Prebiotics (ISAPP) consensus statement on the definition and scope of prebiotics. *Nature reviews. Gastroenterology & hepatology*, *14*(8), 491–502. <https://doi.org/10.1038/nrgastro.2017.75>

Gill, S. R., Pop, M., Deboy, R. T., Eckburg, P. B., Turnbaugh, P. J., Samuel, B. S., Gordon, J. I., Relman, D. A., Fraser-Liggett, C. M., & Nelson, K. E. (2006). Metagenomic analysis of the human distal gut microbiome. *Science (New York, N.Y.)*, *312*(5778), 1355–1359. <https://doi.org/10.1126/science.1124234>

Gomides, A. F., de Paula, S. O., Gonçalves, R. V., de Oliveira, L. L., Ferreira, C. L., Comastri, D. S., & Peluzio, M. (2014). Prebiotics prevent the appearance of aberrant crypt foci (ACF) in the colon of BALB/c mice for increasing the gene expression of p16 protein. *Nutricion hospitalaria*, *30*(4), 883–890. <https://doi.org/10.3305/nh.2014.30.4.7672>

Hill M. J. (1997). Intestinal flora and endogenous vitamin synthesis. *European journal*

of cancer prevention: the official journal of the European Cancer Prevention Organisation (ECP), 6 Suppl 1, S43–S45. <https://doi.org/10.1097/00008469-199703001-00009>

Hill, C., Guarner, F., Reid, G., Gibson, G. R., Merenstein, D. J., Pot, B., Morelli, L., Canani, R. B., Flint, H. J., Salminen, S., Calder, P. C., & Sanders, M. E. (2014). Expert consensus document. The International Scientific Association for Probiotics and Prebiotics consensus statement on the scope and appropriate use of the term probiotic. *Nature reviews. Gastroenterology & hepatology*, 11(8), 506–514. <https://doi.org/10.1038/nrgastro.2014.66>

Igarashi, M., Nakae, H., Matsuoka, T., Takahashi, S., Hisada, T., Tomita, J., & Koga, Y. (2017). Alteration in the gastric microbiota and its restoration by probiotics in patients with functional dyspepsia. *BMJ open gastroenterology*, 4(1), e000144. <https://doi.org/10.1136/bmjgast-2017-000144>

Kawakita, H., Tsuchida, A., Miyazawa, K., Naito, M., Shigoka, M., Kyo, B., Enomoto, M., Wada, T., Katsumata, K., Ohyashiki, K., Itoh, M., Tomoda, A., & Aoki, T. (2009). Growth inhibitory effects of vitamin K2 on colon cancer cell lines via different types of cell death including autophagy and apoptosis. *International journal of molecular medicine*, 23(6), 709–716. https://doi.org/10.3892/ijmm_00000184

Kiatpakdee, B., Sato, K., Otsuka, Y., Arashiki, N., Chen, Y., Tsumita, T., Otsu, W., Yamamoto, A., Kawata, R., Yamazaki, J., Sugimoto, Y., Takada, K., Mohandas, N., & Inaba, M. (2020). Cholesterol-binding protein TSPO2 coordinates maturation and proliferation of terminally differentiating erythroblasts. *The Journal of biological chemistry*, 295(23), 8048–8063. <https://doi.org/10.1074/jbc.RA119.011679>

Kiely, M., Hodgins, S. J., Merrigan, B. A., Tormey, S., Kiely, P. A., & O'Connor, E. M. (2015). Real-time cell analysis of the inhibitory effect of vitamin K2 on adhesion and proliferation of breast cancer cells. *Nutrition research (New York, N.Y.)*, 35(8), 736–743. <https://doi.org/10.1016/j.nutres.2015.05.014>

Krupa-Kozak, U., Markiewicz, L. H., Lamparski, G., & Juśkiewicz, J. (2017).

Administration of Inulin-Supplemented Gluten-Free Diet Modified Calcium Absorption and Caecal Microbiota in Rats in a Calcium-Dependent Manner. *Nutrients*, 9(7), 702. <https://doi.org/10.3390/nu9070702>

Le Leu, R. K., Hu, Y., Brown, I. L., Woodman, R. J., & Young, G. P. (2010). Synbiotic intervention of *Bifidobacterium lactis* and resistant starch protects against colorectal cancer development in rats. *Carcinogenesis*, 31(2), 246–251. <https://doi.org/10.1093/carcin/bgp197>

Lee, J. S., Wang, R. X., Goldberg, M. S., Clifford, G. P., Kao, D. J., & Colgan, S. P. (2020). Microbiota-Sourced Purines Support Wound Healing and Mucous Barrier Function. *IScience*. <https://doi.org/10.1016/j.isci.2020.101226>

Lin, R., Liu, W., Piao, M., & Zhu, H. (2017). A review of the relationship between the gut microbiota and amino acid metabolism. *Amino acids*, 49(12), 2083–2090. <https://doi.org/10.1007/s00726-017-2493-3>

Lin, Y., & Sun, Z. (2015). In vivo pancreatic β -cell-specific expression of antiaging gene *Klotho*: a novel approach for preserving β -cells in type 2 diabetes. *Diabetes*, 64(4), 1444–1458. <https://doi.org/10.2337/db14-0632>

Louca, S., & Doebeli, M. (2018). Efficient comparative phylogenetics on large trees. *Bioinformatics (Oxford, England)*, 34(6), 1053–1055. <https://doi.org/10.1093/bioinformatics/btx701>

Manor, O., & Borenstein, E. (2017). Systematic Characterization and Analysis of the Taxonomic Drivers of Functional Shifts in the Human Microbiome. *Cell host & microbe*, 21(2), 254–267. <https://doi.org/10.1016/j.chom.2016.12.014>

Mengying, Z., Yiyue, X., Tong, P., Yue, H., Limpanont, Y., Ping, H., Okanurak, K., Yanqi, W., Dekumyoy, P., Hongli, Z., Watthanakulpanich, D., Zhongdao, W., Zhi, W., & Zhiyue, L. (2017). Apoptosis and necroptosis of mouse hippocampal and parenchymal astrocytes, microglia and neurons caused by *Angiostrongylus cantonensis* infection. *Parasites & vectors*, 10(1), 611. <https://doi.org/10.1186/s13071->

017-2565-y

Marchesi, J. R., Adams, D. H., Fava, F., Hermes, G. D., Hirschfield, G. M., Hold, G., Quraishi, M. N., Kinross, J., Smidt, H., Tuohy, K. M., Thomas, L. V., Zoetendal, E. G., & Hart, A. (2016). The gut microbiota and host health: a new clinical frontier. *Gut*, *65*(2), 330–339. <https://doi.org/10.1136/gutjnl-2015-309990>

Neis, E. P., Dejong, C. H., & Rensen, S. S. (2015). The role of microbial amino acid metabolism in host metabolism. *Nutrients*, *7*(4), 2930–2946. <https://doi.org/10.3390/nu7042930>

Newell, L. E., & Heddle, J. A. (2004). The potent colon carcinogen, 1,2-dimethylhydrazine induces mutations primarily in the colon. *Mutation research*, *564*(1), 1–7. <https://doi.org/10.1016/j.mrgentox.2004.06.005>

Nicholson, J. K., Holmes, E., Kinross, J., Burcelin, R., Gibson, G., Jia, W., & Pettersson, S. (2012). Host-gut microbiota metabolic interactions. *Science (New York, N.Y.)*, *336*(6086), 1262–1267. <https://doi.org/10.1126/science.1223813>

Ogawa, M., Nakai, S., Deguchi, A., Nonomura, T., Masaki, T., Uchida, N., Yoshiji, H., & Kuriyama, S. (2007). Vitamins K2, K3 and K5 exert antitumor effects on established colorectal cancer in mice by inducing apoptotic death of tumor cells. *International journal of oncology*, *31*(2), 323–331

Paula, H. A. A., Martins, J. F. L., Sartori, S. S. R., Castro, A. S. B., Abranches, M. V., Rafael, V. C., & Ferreira, C. L. L. F. (2012). *The yacon product PBY: Which is the best dose to evaluate the functionality of this new source of prebiotic fructans?* Finland: Functional Foods Forum Probiotics. Turku.

Perisetti, A., Goyal, H., Tharian, B., Inamdar, S., & Mehta, J. L. (2021). Aspirin for prevention of colorectal cancer in the elderly: friend or foe?. *Annals of gastroenterology*, *34*(1), 1–11. <https://doi.org/10.20524/aog.2020.0556>

Piranlioglu, R., Lee, E., Ouzounova, M., Bollag, R. J., Vinyard, A. H., Arbab, A. S.,

Marasco, D., Guzel, M., Cowell, J. K., Thangaraju, M., Chadli, A., Hassan, K. A., Wicha, M. S., Celis, E., & Korkaya, H. (2019). Primary tumor-induced immunity eradicates disseminated tumor cells in syngeneic mouse model. *Nature communications*, *10*(1), 1430. <https://doi.org/10.1038/s41467-019-09015-1>

Reeves, P. G., Nielsen, F. H., & Fahey, G. C., Jr (1993). AIN-93 purified diets for laboratory rodents: final report of the American Institute of Nutrition ad hoc writing committee on the reformulation of the AIN-76A rodent diet. *The Journal of nutrition*, *123*(11), 1939–1951. <https://doi.org/10.1093/jn/123.11.1939>

Rowland, I., Gibson, G., Heinken, A., Scott, K., Swann, J., Thiele, I., & Tuohy, K. (2018). Gut microbiota functions: metabolism of nutrients and other food components. *European journal of nutrition*, *57*(1), 1–24. <https://doi.org/10.1007/s00394-017-1445-8>

Russo, D., Valentão, P., Andrade, P. B., Fernandez, E. C., & Milella, L. (2015). Evaluation of antioxidant, antidiabetic and anticholinesterase activities of smallanthus sonchifolius landraces and correlation with their phytochemical profiles. *International Journal of Molecular Sciences*. <https://doi.org/10.3390/ijms160817696>

Sarao, L. K., & Arora, M. (2017). Probiotics, prebiotics, and microencapsulation: A review. *Critical reviews in food science and nutrition*, *57*(2), 344–371. <https://doi.org/10.1080/10408398.2014.887055>

Schmidt, T., Raes, J., & Bork, P. (2018). The Human Gut Microbiome: From Association to Modulation. *Cell*, *172*(6), 1198–1215. <https://doi.org/10.1016/j.cell.2018.02.044>

Scott, A. J., Alexander, J. L., Merrifield, C. A., Cunningham, D., Jobin, C., Brown, R., Alverdy, J., O'Keefe, S. J., Gaskins, H. R., Teare, J., Yu, J., Hughes, D. J., Verstraelen, H., Burton, J., O'Toole, P. W., Rosenberg, D. W., Marchesi, J. R., & Kinross, J. M. (2019). International Cancer Microbiome Consortium consensus statement on the role of the human microbiome in carcinogenesis. *Gut*, *68*(9), 1624–1632. <https://doi.org/10.1136/gutjnl-2019-318556>

Sergeev, I. N., Aljutaily, T., Walton, G., & Huarte, E. (2020). Effects of Synbiotic Supplement on Human Gut Microbiota, Body Composition and Weight Loss in Obesity. *Nutrients*, 12(1), 222. <https://doi.org/10.3390/nu12010222>

Sipos, F., Firneisz, G., & Múzes, G. (2016). Therapeutic aspects of c-MYC signaling in inflammatory and cancerous colonic diseases. *World journal of gastroenterology*, 22(35), 7938–7950. <https://doi.org/10.3748/wjg.v22.i35.7938>

Smiricky-Tjardes, M. R., Grieshop, C. M., Flickinger, E. A., Bauer, L. L., & Fahey, G. C., Jr (2003). Dietary galactooligosaccharides affect ileal and total-tract nutrient digestibility, ileal and fecal bacterial concentrations, and ileal fermentative characteristics of growing pigs. *Journal of animal science*, 81(10), 2535–2545. <https://doi.org/10.2527/2003.81102535x>

Song, M., & Chan, A. T. (2019). Environmental Factors, Gut Microbiota, and Colorectal Cancer Prevention. *Clinical gastroenterology and hepatology: the official clinical practice journal of the American Gastroenterological Association*, 17(2), 275–289. <https://doi.org/10.1016/j.cgh.2018.07.012>

Thomas, A. M., Manghi, P., Asnicar, F., Pasolli, E., Armanini, F., Zolfo, M., Beghini, F., Manara, S., Karcher, N., Pozzi, C., Gandini, S., Serrano, D., Tarallo, S., Francavilla, A., Gallo, G., Trompetto, M., Ferrero, G., Mizutani, S., Shiroma, H., Shiba, S., ... Segata, N. (2019). Metagenomic analysis of colorectal cancer datasets identifies cross-cohort microbial diagnostic signatures and a link with choline degradation. *Nature medicine*, 25(4), 667–678. <https://doi.org/10.1038/s41591-019-0405-7>

Tu, P., Chi, L., Bodnar, W., Zhang, Z., Gao, B., Bian, X., Stewart, J., Fry, R., & Lu, K. (2020). Gut Microbiome Toxicity: Connecting the Environment and Gut Microbiome-Associated Diseases. *Toxics*, 8(1), 19. <https://doi.org/10.3390/toxics8010019>

Wang, S., Xiao, Y., Tian, F., Zhao, J., Zhang, H., Zhai, Q., & Chen, W. (2020). Rational use of prebiotics for gut microbiota alterations: Specific bacterial phylotypes and

related mechanisms. *Journal of Functional Foods*.
<https://doi.org/10.1016/j.jff.2020.103838>

Wickham, H. (2016). ggplot2: Elegant Graphics for Data Analysis. In *Journal of the Royal Statistical Society: Series A (Statistics in Society)*.

Wu, W., Zhang, L., Xia, B., Tang, S., Liu, L., Xie, J., & Zhang, H. (2020). Bioregional Alterations in Gut Microbiome Contribute to the Plasma Metabolomic Changes in Pigs Fed with Inulin. *Microorganisms*, 8(1), 111.
<https://doi.org/10.3390/microorganisms8010111>

Yang, Y., & Jobin, C. (2017). Novel insights into microbiome in colitis and colorectal cancer. *Current opinion in gastroenterology*, 33(6), 422–427.
<https://doi.org/10.1097/MOG.0000000000000399>

Yang, Y., Misra, B. B., Liang, L., Bi, D., Weng, W., Wu, W., Igarashi, S., Qin, H., Goel, A., Li, X., & Ma, Y. (2019). Integrated microbiome and metabolome analysis reveals a novel interplay between commensal bacteria and metabolites in colorectal cancer. *Theranostics*, 9(14), 4101–4114. <https://doi.org/10.7150/thno.35186>

Ye, Y., & Doak, T. G. (2009). A parsimony approach to biological pathway reconstruction/inference for genomes and metagenomes. *PLoS computational biology*, 5(8), e1000465. <https://doi.org/10.1371/journal.pcbi.1000465>

Zeineldin, M., Cunningham, J., McGuinness, W., Alltizer, P., Cowley, B., Blanchat, B., Xu, W., Pinson, D., & Neufeld, K. L. (2012). A knock-in mouse model reveals roles for nuclear Apc in cell proliferation, Wnt signal inhibition and tumor suppression. *Oncogene*, 31(19), 2423–2437. <https://doi.org/10.1038/onc.2011.434>

Zhang, X. H., Ma, J., Smith-Warner, S. A., Lee, J. E., & Giovannucci, E. (2013). Vitamin B6 and colorectal cancer: Current evidence and future directions. *World Journal of Gastroenterology*. <https://doi.org/10.3748/wjg.v19.i7.1005>

Zhu, J., Zhu, C., Ge, S., Zhang, M., Jiang, L., Cui, J., & Ren, F. (2014). Lactobacillus

salivarius Ren prevent the early colorectal carcinogenesis in 1, 2-dimethylhydrazine-induced rat model. *Journal of applied microbiology*, 117(1), 208–216.
<https://doi.org/10.1111/jam.12499>

SUPPLEMENTARY MATERIAL

Supplementary Datasheet 1 – Predicted microbial pathways (cont.).

Pathway	Description	BS16	BS17	BS18	BS19	BS20	BS21	BS22	BS23	BS24	BS25	BS26	BS27	BS28	BS29	BS30
1CMET2-PWY	N10-formyl-tetrahydrofolate biosynthesis	20039,01	20719,5	25784,94	20634,94	24669,28	16559,09	24445,19	23035,58	15939,04	20840,71	21843,21	30081,03	31174,04	19381,82	26917,07
3-HYDROXYPHENYLACETATE-DEGRADATION-PWY	4-hydroxyphenylacetate degradation	0,6795	0	1,3647	5,1304	8,8151	2,5181	6,4292	0	0,8394	4,9628	0	3,7766	0	0	0
AEROBACTINSYN-PWY	aerobactin biosynthesis	0	0	0	0	0	0	0	0	0	0	0	0	0	0	0
ALL-CHORISMATE-PWY	superpathway of chorismate metabolism	4,1361	0	196,1579	29,9298	214,0022	71,3088	138,1469	0	24,9212	331,8674	0	130,4345	0	0	0
ANAEROFUCAT-PWY	homolactic fermentation	28513,55	29707,79	34769,93	30551,76	35439,19	24147,93	34663,01	32522,62	22690,47	30415,96	31064,87	37358,21	27534,86	27037,8	27035,61
ANAGLYCOLYSIS-PWY	glycolysis III (from glucose)	31361	30741,74	36702,91	32846,37	37670,57	25394,63	35978,87	35843,68	25045,64	35049,69	32838,02	42655,53	41324,86	29303,63	36239,57
ARG-POLYAMINE-SYN	superpathway of arginine and polyamine biosynthesis	1908,891	2580,487	7241,946	1681,494	3952,788	2321,269	5222,954	2776,061	2500,558	1585,751	2295,523	4329,98	5692,087	1846,693	4062,959
ARGDEG-PWY	superpathway of L-arginine, putrescine, and 4-aminobutanoate degradation	0,9332	0	1,8664	6,9955	12,5893	4,1981	10,7219	0	1,3997	5,4337	0	6,7744	0	0	0
ARGORNPROST-PWY	arginine, ornithine and proline interconversion	5058,81	5751,857	6601,057	5581,29	8325,574	5029,238	8066,149	6872,84	5210,78	6391,985	5029,875	3301,277	5769,406	3965,516	4159,284
ARGSYN-PWY	L-arginine biosynthesis I (via L-ornithine)	10376,68	18355,09	22213,68	17494,51	21969,67	14511,19	20809	16907,46	13460,33	13356,3	21374,29	32748,37	33927,16	18180,09	30796,57
ARGSYNSUB-PWY	L-arginine biosynthesis II (acetyl cycle)	9320,602	18971,1	22186,73	18078,01	22284,07	14904,25	20624	16220,79	13282,25	13090,33	22328,72	34050,8	35107,87	19063,86	32016,71
ARO-PWY	chorismate biosynthesis I	18037,38	22095,04	26821,3	19781,56	25296,98	17217,8	26921,09	23083,26	16843,13	18632,81	24858,82	36492,66	38536,89	20770,69	33585,7
ASPASN-PWY	superpathway of L-aspartate and L-asparagine biosynthesis	25984,6	24677,41	29992,68	23976,13	31519,54	19622,51	29835,79	29147,84	19415,99	26697,76	20837,48	27866,13	30375,79	19515,01	24318,97
AST-PWY	L-arginine degradation II (AST pathway)	0,4	0	0,8	3	5,4	1,8	4,6	0	0,6	2,33	0	2,7	0	0	0
BIOTIN-BIOSYNTHESIS-PWY	biotin biosynthesis I	5,579	0	11,1687	40,6808	113,5019	24,8487	135,585	13,8783	377,4739	302,4663	190,2685	354,4226	202,9876	60,3582	406,0272
BRANCHED-CHAIN-AA-SYN-PWY	superpathway of branched amino acid biosynthesis	15949,19	20232,75	26307,55	18761,1	23004,29	15828,84	23608,66	20647,79	14896,59	14884,8	24280,12	36403,68	40890,26	20284,41	35343,64
CALVIN-PWY	Calvin-Benson-Bassham cycle	25721,69	30013,02	34415,44	29456,56	34912,37	23331,3	34832,74	30220,47	21606,5	27820,41	31031,73	42672,1	41723,43	26573,18	37499,68
CATECHOL-ORTHO-CLEAVAGE-PWY	catechol degradation to β-ketoacid	0	0	7	0	11	0	0	0	0	35,3571	0	0	0	0	0
CENTFERM-PWY	pyruvate fermentation to butanoate	13,2924	149,3627	757,7363	210,6885	265,9156	181,8664	236,6316	142,6555	142,8502	429,4843	788,8524	2106,313	2724,41	1914,364	1568,836
COA-PWY	coenzyme A biosynthesis I	26616,97	26295,83	30720,39	27328,33	31904,93	21648,71	30554,89	29950,81	20997,13	29367,96	26729,22	35064,57	32903,19	23599,46	29449,75
COBALSYN-PWY	adenosylcobalamin salvage from cobinamide I	11781,95	12935,89	17696,33	10316,48	16737,12	9463,666	16880,65	13272,81	8057,033	10807,39	13450,78	20433,44	26451,3	11933,11	20590,09
CODH-PWY	reductive acetyl coenzyme A pathway	316,0457	774,1819	908,1218	403,7729	694,7973	627,0148	588,8812	411,1077	722,028	373,5477	142,6047	1430,44	1024,561	594,839	1628,025
COLANSYN-PWY	colanic acid building blocks biosynthesis	2750,03	8190,014	8760,287	7328,431	7999,718	5737,822	6972,531	3915,517	3652,211	3998,084	4353,629	6468,749	8535,175	4861,14	7395,907
COMPLETE-ARO-PWY	superpathway of aromatic amino acid biosynthesis	18748,92	22848,51	27764,71	20428,43	26130,05	17774,18	27691,96	23858,34	17355,22	19126,35	25454,14	37674,39	39962,95	21330,68	34717,72
DAPLISINESYN-PWY	L-lysine biosynthesis I	20349,36	19173,65	23932,36	18963,33	23183,38	16613,6	25269,65	23877,54	17362,55	18821,99	22239,17	34094,8	35959,79	19113,8	30765,69
DENITRIFICATION-PWY	nitrate reduction I (denitrification)	0	0	0	0	0	0	0	0	0	0	0	0	0	0	0
DENOVOPURINEZ-PWY	superpathway of purine nucleotides de novo biosynthesis II	21539,44	19173,16	24458,04	21022,44	23878,64	17049,66	21759,43	22969,79	15768,47	18673,18	14005,24	23590,15	23675,92	14408,63	17454,07
DHGLUCONATE-PYR-CAT-PWY	glucose degradation (oxidative)	0	0	0	0	0	0	0	0	0	0	0	0	0	0	0
DTDPRHAMSYN-PWY	dTDP-L-rhamnose biosynthesis I	23268,35	21843,15	26284,14	22127,19	24517,5	17798,49	25775,52	26378,62	17475,84	25469,2	25565,07	34015,53	34563,27	22986,16	29671,3
ECASYN-PWY	enterobacterial common antigen biosynthesis	0,8565	0	1,7134	6,3844	11,5331	3,8481	9,8254	0	1,2849	4,9706	0	5,7708	0	0	0
ENTBACSYN-PWY	enterobactin biosynthesis	2,1323	0	41,3801	15,9386	86,6005	9,5839	24,4559	0	3,1977	151,04	0	14,3813	0	0	0
FAO-PWY	fatty acid β-oxidation I	5,6978	85,7525	432,9327	119,3137	152,0151	90,6422	120,3177	83,9504	77,6491	241,4693	402,3837	1200,553	1351,933	1089,111	851,4255
FASYN-ELONG-PWY	fatty acid elongation -- saturated	12547,41	14811,24	17618,73	16508,42	19573,79	12561,24	14615,7	12502,34	9500,946	12016,22	9503,552	18224,5	16845,81	10531,49	17052,59
FASYN-INITIAL-PWY	superpathway of fatty acid biosynthesis initiation (E. coli)	1,9999	0	3,9997	14,9947	41,9673	8,9978	50,4547	4,9995	162,2143	151,0566	77,3589	138,7043	74,9192	22,4862	159,5697
FERMENTATION-PWY	mixed acid fermentation	13363,09	14519,13	14123,67	17676,04	15869,99	13071,57	14890,47	20142,53	15623,85	19353,14	19635,33	18578,54	13811,72	16465,74	14079,36
FOLSYN-PWY	superpathway of tetrahydrofolate biosynthesis and salvage	15251,54	17138,23	20150,77	15044,82	20830,17	14635,42	20939	20058,22	14957,57	15462,24	9187,268	14768,8	17467,65	9296,051	14882,07
FUC-RHAMCAT-PWY	superpathway of fucose and rhamnose degradation	169,834	703,0454	666,0103	321,0192	506,5211	250,3098	930,888	599,6304	279,0927	721,8884	290,0089	594,3657	431,4507	447,5145	369,8994
FUCCAT-PWY	fucose degradation	140,2199	838,8059	1116,735	347,7025	479,9825	156,8806	1350,997	924,8445	360,7978	1147,088	567,9802	700,7642	606,2644	739,0071	396,129
GALACT-GLUCUROCAT-PWY	superpathway of hexuronide and hexuronate degradation	710,0564	4330,049	5060,493	3232,622	5237,552	2387,83	4048,565	1979,247	971,0525	2693,43	8998,534	15560,07	17791,6	7060,731	15581,68
GALACTARDEG-PWY	D-galactarate degradation I	0,7992	0	1,5993	5,9876	10,7711	3,5952	9,1802	0	1,1988	16,531	0	5,39	0	0	0
GALACTUROCAT-PWY	D-galacturonate degradation I	816,9229	5167,814	6118,719	3794,604	6407,385	2883,65	4741,108	2160,544	1162,429	2806,46	10809,12	17934,49	20639,73	8193,609	18137,94
GALLATE-DEGRADATION-I-PWY	gallate degradation II	0	0	0	0	0	0	0	0	0	0	0	0	0	0	0
GALLATE-DEGRADATION-II-PWY	gallate degradation I	0	0	0	0	0	0	0	0	0	0	0	0	0	0	0
GLCMANNANAUT-PWY	superpathway of N-acetylglucosamine, N-acetylmannosamine and N-acetylneuraminic acid degradation	8677,506	13860,33	15267,04	14031,21	19624,47	10434,2	16692,14	11462,01	8307,95	12251,46	15396,02	21090,38	23616,99	12467,75	20199
GLUCARDEG-PWY	D-glucarate degradation I	0,7992	0	1,5993	5,9876	10,7711	3,5952	9,1802	0	1,1988	22,4221	0	5,39	0	0	0
GLUCARGALACTSUPER-PWY	superpathway of D-glucarate and D-galactarate degradation	0,7992	0	1,5993	5,9876	10,7711	3,5952	9,1802	0	1,1988	16,531	0	5,39	0	0	0
GLUCONEO-PWY	gluconeogenesis I	11801,35	22828,4	24516,84	24839,45	28282,89	19518,15	23289,53	15934,53	12069,64	14610,47	17904,69	30163,34	27042,53	16235,66	25802,93
GLUCOSE1PMETAB-PWY	glucose and glucose-1-phosphate degradation	0,8	0	1,6	5,9994	10,7984	3,5997	9,1988	0	1,2	4,6597	0	5,3997	0	0	0
GLUCUROCAT-PWY	superpathway of β-D-glucuronide and D-glucuronate degradation	927,8512	5219,96	6303,461	4028,77	6440,595	3041,074	5187,794	2544,683	1344,848	3470,773	9696,628	16837,45	19270,97	8150,556	16736,22

Supplementary Datasheet 1 – Predicted microbial pathways (cont.).

GLUTORN-PWY	L-ornithine biosynthesis	3967,501	12872,79	14635,32	11920,43	14484,66	9592,929	13024,61	9114,742	8320,264	7268,603	19694,46	29390,65	30336,81	15670,41	28457,3
GLYCOCAT-PWY	glycogen degradation I (bacterial)	9467,617	20998,33	23703,87	21129,9	24111,41	16345,46	23245,08	20131,45	16436,05	14512,14	30141,75	40393,74	41515,55	22961,83	39478,15
GLYCOGENSYNTH-PWY	glycogen biosynthesis I (from ADP-D-Glucose)	18665,26	22855,61	28663,36	22473,14	28852,4	18492,66	28475,83	23347,99	17127,96	18111,25	25187,88	36959,32	40391,38	20966,54	35029,76
GLYCOL-GLYOXDEG-PWY	superpathway of glycol metabolism and degradation	101,1298	531,6256	745,9337	804,2926	452,7099	639,6985	633,8939	237,7761	125,2624	404,7124	19,5693	150,0828	32,897	17,796	133,5529
GLYCOLYSIS	glycolysis I (from glucose 6-phosphate)	29356,9	31005,97	36502,05	31235,24	36992,27	24934,34	36385,69	33583,97	23398,27	31397,51	31658,2	39777,4	31175,75	27630,53	29723,82
GLYCOLYSIS-E-D	superpathway of glycolysis and Entner-Doudoroff	9590,079	17500,91	18654,48	19803,43	22103,92	15267,11	17474,11	12829,82	9526,453	11970,97	12210,03	17512,14	15104,68	11946,12	12316,18
GLYCOLYSIS-TCA-GLYOX-BYPASS	superpathway of glycolysis, pyruvate dehydrogenase, TCA, and glyoxylate bypass	1580,401	3615,786	3175,316	2221,855	2688,305	1347,704	2267,936	1474,848	1646,073	1323,608	1287,176	2500,241	1741,815	2085,948	3549,16
GLYOXYLATE-BYPASS	glyoxylate cycle	651,1606	1586,684	1875,428	1317,314	2053,244	1332,408	1724,693	962,6695	789,8239	645,7347	438,6319	796,8049	498,8828	738,716	1904,398
GOLPDLCAT-PWY	superpathway of glycerol degradation to 1,3-propanediol	2021,784	1406,945	1897,943	2826,374	3168,938	1549,37	1164,799	1067,012	711,5869	1034,786	398,0281	1134,523	493,7978	275,9448	520,5036
HCAMHPDEG-PWY	3-phenylpropanoate and 3-(3-hydroxyphenyl)propanoate degradation to 2-oxopent-4-enoate	0,4364	0	9,2599	3,2727	18,9337	1,9636	5,0182	0	0,6545	35,6154	0	2,9455	0	0	0
HEME-BIOSYNTHESIS-II	heme biosynthesis I (aerobic)	95,4466	623,7382	537,351	287,3225	331,3003	520,9237	194,0598	182,2869	506,8332	208,7954	468,8383	1369,918	1715,592	1333,512	751,4133
HEMESYN2-PWY	heme biosynthesis II (anaerobic)	3516,194	5159,731	5191,798	5163,048	6375,273	4226,986	3435,612	4067,786	3899,48	2377,03	3330,892	7332,89	8067,345	4305,38	6088,108
HEXITOLDEGSUPER-PWY	superpathway of hexitol degradation (bacteria)	6817,614	6327,492	9021,674	11330,64	12957,92	6860,244	6750,911	5625,01	4122,049	4360,144	3490,088	8147,099	3036,513	3300,299	5023,7
HISDEG-PWY	L-histidine degradation I	7769,75	2659,83	6734,716	2180,25	2436,405	1912,493	4436,65	5946,42	2799,112	3517,627	818,317	1729,073	4576,137	1554,266	2160,233
HISTSYN-PWY	L-histidine biosynthesis	5154,12	13735,88	16250,02	12986,49	15086,25	10312,36	14758,44	10996,7	9849,278	8352,144	20750,3	30553,75	31215,4	16574,92	29306,31
HOMOSER-METSYN-PWY	L-methionine biosynthesis I	3236,859	6435,639	5664,763	8330,177	6835,29	6708,601	6683,121	7849,128	7437,268	3093,961	10188,15	11322,61	8513,754	6863,544	12891,46
HOSERMETANA-PWY	L-methionine biosynthesis III	3252,894	6823,069	5960,125	8814,744	7216,304	7282,394	7156,985	8272,844	8197,724	3166,07	11176,99	12183,22	8261,138	7338,666	14190,27
ILEUSYN-PWY	L-isoleucine biosynthesis I (from threonine)	17212,1	22646,38	28906,83	20305,54	26234,37	18011,73	27498,78	23755,18	17269,37	17245,43	25439,48	37686,99	42929,09	21122,78	37178,53
KDO-NAGLIPASYN-PWY	superpathway of (Kdo)2-lipid A biosynthesis	3,1937	0	6,3904	23,7936	42,7076	14,3157	36,402	0	4,7885	18,3421	0	21,5294	0	0	0
KETOGLUCONMET-PWY	ketoglucuronate metabolism	0,6	0	1,4745	5,7568	9,1145	3,4782	8,1525	0	1,1143	4,4305	0	4,7831	0	0	0
LACTOSECAT-PWY	lactose and galactose degradation I	4735,547	4616,873	4963,251	7013,552	7261,267	4269,323	7248,235	6680,476	5681,858	5151,789	5655,673	4352,099	1370,916	3624,802	1919,816
LEU-DEG2-PWY	L-leucine degradation I	0	0	11,5264	0	6,7506	0	11,2491	4,6001	9,4434	25,6853	57,1928	93,8957	28,0453	12,9033	98,0517
LIPASYN-PWY	phospholipases	0	0	0	0	0	0	0	0	0	0	0	0	0	0	0
LPSSYN-PWY	superpathway of lipopolysaccharide biosynthesis	0	0	0	0	0	0	0	0	0	9,2527	0	3,9611	0	0	0
MET-SAM-PWY	superpathway of S-adenosyl-L-methionine biosynthesis	4841,666	9250,455	8260,277	11871,13	10010,45	9560,648	9702,058	11333,53	10576,8	4700,14	13754,42	15578,7	11975,66	9586,418	16920,69
METH-ACETATE-PWY	methanogenesis from acetate	6535,313	8694,717	10369,72	6724,937	13733,35	8127,131	14023,29	10337,97	8005,073	8260,967	0	300,7112	341,1031	639,6577	86,7283
METHGLYUT-PWY	superpathway of methylglyoxal degradation	0,665	0	1,9762	7,2183	11,4807	4,3657	10,7014	0	1,4558	5,6867	0	6,6294	0	0	0
METHYLGALLATE-DEGRADATION-PWY	methylgallate degradation	0	0	0	0	0	0	0	0	0	0	0	0	0	0	0
NAD-BIOSYNTHESIS-II	NAD salvage pathway II	165,2965	1062,124	816,1425	600,2625	1222,668	719,4371	2041,635	860,2455	509,3254	1636,446	2204,191	268,4988	2539,337	1712,507	303,9299
NAGLIPASYN-PWY	lipid IVA biosynthesis	1507,253	3162,4	3918,001	2657,512	3508,08	2345,896	3119,777	1579,04	1718,792	1028,303	2320,112	6049,689	5267,141	2533,25	5450,27
NONMEVIPP-PWY	methylerythritol phosphate pathway I	15842,88	20183,31	24989,49	18122,98	23331,99	15113,71	24814,94	19307,85	14164,06	15866,55	21166,51	31717,23	33396,77	17862,46	29325,02
NONOXIPENT-PWY	pentose phosphate pathway (non-oxidative branch)	34158,17	37415,81	44545,47	36549,67	45291,18	29361,63	44494,66	40171,83	28420,78	37117,71	44451,05	60680,54	57067,54	37238,42	52406,05
OANTIGEN-PWY	O-antigen building blocks biosynthesis (E. coli)	24039,54	22570,52	26813,34	23693,9	26246,61	18789,2	26140,47	27127,57	18813,63	26034,06	23548,74	29338,27	26141,66	20984,73	23444,69
ORNARGDEG-PWY	superpathway of L-arginine and L-ornithine degradation	0,9332	0	1,8664	6,9955	12,5893	4,1981	10,7219	0	1,3997	5,4337	0	6,7744	0	0	0
ORNDEG-PWY	superpathway of ornithine degradation	0,8	0	1,5998	5,9981	10,7937	3,5989	9,1931	0	1,1999	4,6591	0	9,3905	0	0	0
P101-PWY	ectoine biosynthesis	0	0	11,6651	0	18,3295	0	0	0	0	46,524	0	0	0	0	0
P105-PWY	TCA cycle IV (2-oxoglutarate decarboxylase)	50,0029	0	115,3025	429,2798	273,1045	26,7646	154,7887	238,1919	82,3319	510,1376	287,2048	515,3349	133,1179	103,1776	504,8465
P108-PWY	pyruvate fermentation to propanoate I	1169,505	2306,376	5008,02	1550,783	2610,333	1603,96	3348,552	1810,632	2110,985	1432,176	2143,971	4649,208	5196,193	1749,95	4626,232
P122-PWY	heterolactic fermentation	17208,9	14165,42	15471,91	17671,78	19070,95	12724,98	13970,25	18262,09	12875,26	21548,15	14254,01	13424,76	7852,77	13419,32	6040,187
P124-PWY	Bifidobacterium shunt	22529,83	19647,95	23004,28	23530,59	26579,35	17043,38	20259,86	24522,11	17301,9	26707,54	19300,55	18900,68	11350,51	17614,44	9108,164
P125-PWY	superpathway of (R,R)-butanediol biosynthesis	8939,37	2570,036	5835,526	2377,37	1416,7	1875,766	4219,921	6908,33	2965,98	4277,981	40,4602	115,0877	2542,497	1237,195	34,3774
P161-PWY	acetylene degradation	36123,21	28665,53	36149,91	32467,55	35489,98	26179,92	36742,25	42038,25	27698,29	39396,18	27583,88	31819,62	31338,01	24697,05	25782,04
P162-PWY	L-glutamate degradation V (via hydroxyglutarate)	455,4405	1183,222	2349,025	1131,533	2667,683	864,1258	1068,951	638,7154	586,8065	451,3134	449,2815	959,168	1187,823	457,7469	463,2734
P163-PWY	L-lysine fermentation to acetate and butanoate	501,0013	811,1449	1752,82	414,0567	1256,391	500,0819	1271,391	787,0102	782,4587	388,2436	545,9888	1001,119	1825,523	492,8032	1422,328
P164-PWY	purine nucleobases degradation I (anaerobic)	4794,663	8133,111	9038,954	5439,906	12232,51	6011,488	12590,18	8461,877	5901,743	8026,15	3482,071	3218,287	5703,736	3123,768	2757,173
P221-PWY	octane oxidation	0	0	13,9919	0	21,9771	0	0	0	0	53,7311	0	0	0	0	0
P23-PWY	reductive TCA cycle I	3153,688	4825,516	8666,53	4009,188	5834,225	4200,656	6819,07	4454,96	5011,055	3006,687	7434,967	14156,46	9245,245	6812,098	11240,38
P281-PWY	3-phenylpropanoate degradation	0	0	0	0	0	0	0	0	0	9,7864	0	0	0	12,6964	
P341-PWY	glycolysis V (Pyrococcus)	139,5784	541,7191	744,2676	570,1324	1097,756	359,3357	749,0499	353,9618	163,083	376,0996	589,8827	984,1274	1868,674	586,5206	1511,444
P381-PWY	adenosylcobalamin biosynthesis II (late cobalt incorporation)	0	0	67,4728	0	105,5704	0	0	0	0	249,1544	0	19,3345	0	0	0

Supplementary Datasheet 1 – Predicted microbial pathways (cont.).

PWY-6277	superpathway of 5-aminoimidazole ribonucleotide biosynthesis	20287,88	24447,99	29393,25	24336,13	30551,22	19807,85	28675,07	24319,21	17936,79	19989,57	24206,07	37361,44	38360,29	20681,26	33568,81
PWY-6282	palmitoleate biosynthesis I (from (5Z)-dodec-5-enoate)	2,3998	0	4,7995	17,992	50,3497	10,7964	60,5248	5,9991	194,2933	181,0427	92,7848	166,3458	89,8704	26,9789	191,337
PWY-6317	galactose degradation I (Leioir pathway)	27510,02	25141,13	29915,59	27020,49	30407,26	20799,32	29512,29	30819,72	21286,48	30534,25	27265,52	33439,19	31941,02	23536,83	27753,42
PWY-6353	purine nucleotides degradation II (aerobic)	2010,008	5654,11	9714,895	5412,512	8574,409	3505,093	6423,565	3980,975	2748,893	3170,327	3498,672	5521,657	6459,291	3260,162	4244,06
PWY-6383	mono-trans, poly-cis decaprenyl phosphate biosynthesis	0	0	13,9938	61,8967	21,9877	0	0	23,985	0	53,9315	0	0	0	0	0
PWY-6385	peptidoglycan biosynthesis III (mycobacteria)	28632,55	28261,2	33505,88	29782,03	34832,75	23513,3	32759,43	32661,37	23187,93	31527,6	29093,18	37784,22	35629,47	25566,31	31609,79
PWY-6386	UDP-N-acetylmuramoyl-pentapeptide biosynthesis II (lysine-containing)	28328,45	28053,77	33424,9	29530,09	34522,19	23279,29	32586,13	32389,94	23030,89	30925,45	29253	38362,34	36441,23	25583,92	32434,4
PWY-6387	UDP-N-acetylmuramoyl-pentapeptide biosynthesis I (meso-diaminopimelate containing)	29163,7	28738,69	34041,66	30389,13	35452,61	23899,61	33248,43	33240,57	23608,08	32079,42	29606,97	38468,58	36119,73	26022,3	32108,18
PWY-6396	superpathway of 2,3-butanediol biosynthesis	7949,768	3928,366	5586,501	4245,363	2968,926	3324,696	4607,366	7523,423	4182,883	6023,187	105,5278	294,251	2053,198	2023,603	88,271
PWY-6397	mycolyl-arabinogalactan-peptidoglycan complex biosynthesis	0	0	7,6363	0	12,1844	0	0	0	0	29,7154	0	0	0	0	0
PWY-6467	Kdo transfer to lipid IVA III (Chlamydia)	1473,4	3104,83	3703,3	2611	3395,82	2254,13	2972,27	1523,17	1687,43	1016,83	2310,92	5997,45	5178,17	2537,25	5370,92
PWY-6470	peptidoglycan biosynthesis V (β-lactam resistance)	103,2404	48,5705	554,3288	313,0855	979,2505	5365,03	593,506	8179,097	6853,163	210,2463	1814,216	291,9099	4465,702	136,7288	2033,021
PWY-6471	peptidoglycan biosynthesis IV (Enterococcus faecium)	22835,49	21659,75	24141,45	24903,04	27316,36	18484,17	23180,04	26526,77	19198,38	27232,94	23962,04	25772	15558,05	20895,18	18705,13
PWY-6478	GDP-D-glycero- α -D-manno-heptose biosynthesis	537,0221	2792,528	2954,29	2484,153	3245,058	1729,857	2619,424	962,1227	496,946	1741,349	6397,558	12289,63	13398,84	4505,602	12692,73
PWY-6507	4-deoxy-L-threo-hex-4-enopyranuronate degradation	608,6708	3842,868	4736,824	2371,315	4737,675	2036,066	3696,216	1487,967	791,6668	2224,03	9577,642	17226,38	18858,44	6866,192	17739,92
PWY-6519	8-amino-7-oxononanoate biosynthesis I	4,3866	0	8,7799	32,0401	89,606	19,5542	107,3293	10,9202	307,5617	246,1827	152,2601	283,1262	160,5722	47,6258	324,5087
PWY-6545	pyrimidine deoxyribonucleotides de novo biosynthesis III	10642,92	11056,38	13846,68	10900,69	13577,37	10088,32	12868,32	12030,61	8796,097	9437,986	6275,686	11214,87	9846,185	6310,758	7772,157
PWY-6562	norspermidine biosynthesis	0	0	0	0	0	0	0	0	0	7,0538	0	0	0	0	0
PWY-6572	chondroitin sulfate degradation I (bacterial)	0	0	0	0	0	0	0	0	0	0	0	4,2837	0	3,4268	0
PWY-6588	pyruvate fermentation to acetone	18982	10101,69	19795,36	8745,393	10974,59	6305,997	13590,01	16720,26	8468,087	11021,01	3364,763	5361,298	13336,32	5310,567	7138,862
PWY-6590	superpathway of Clostridium acetobutylicum acidogenic fermentation	17,0882	191,7804	968,406	270,4055	341,2279	233,361	303,6541	183,205	183,3653	550,3214	1006,749	2664,781	3426,969	2412,763	1988,027
PWY-6608	guanosine nucleotides degradation III	4497,969	6743,531	8129,509	4803,255	8894,302	5011,964	10057,74	7118,434	4840,277	6177,619	3208,987	3769,061	5764,947	2999,001	3026,792
PWY-6609	adenine and adenosine salvage III	29339,74	26168,91	34499,6	28010,01	32283,4	22318,5	34251,78	32793,85	22374,12	24975,74	26830,51	35103,87	35239,51	21793,68	30583,46
PWY-6612	superpathway of tetrahydrofolate biosynthesis	13277,74	15079,01	17500,17	12692,8	18202,33	13029,12	18555,08	18076,86	13596,89	13483,77	7032,225	11533,94	14085,8	7306,701	11923,38
PWY-6628	superpathway of L-phenylalanine biosynthesis	10968,54	13304,05	15321,79	10857,73	17830,06	11226,33	18792,81	15010,32	11489,97	11727,92	3526,568	9686,411	8974,924	5624,029	8281,013
PWY-6629	superpathway of L-tryptophan biosynthesis	4,7983	0	9,5962	35,924	64,6026	21,5689	55,0617	0	7,196	27,9076	0	32,3693	0	0	0
PWY-6630	superpathway of L-tyrosine biosynthesis	10309,15	13308,47	15114,82	10892,47	17962,13	11263,22	18598,26	14676,93	11410,91	11741,91	3529,205	9695,289	8951,988	5625,043	8273,588
PWY-6641	superpathway of sulfolactate degradation	0	0	39,3035	32,0389	0	0	155,6062	0	29,6108	0	22,5404	163,6424	37,1327	21,5405	92,9821
PWY-6690	cinnamate and 3-hydroxycinnamate degradation to 2-oxopent-4-enoate	0,4364	0	9,2599	3,2727	18,9337	1,9636	5,0182	0	0,6545	35,6154	0	2,9455	0	0	0
PWY-6700	queuosine biosynthesis	2333,227	5537,949	5841,917	5139,946	6547,796	5659,644	6257,656	4787,747	4299,038	2320,604	3439,269	7441,112	9046,573	5235,079	7894,366
PWY-6703	preQ0 biosynthesis	1702,465	3646,28	4934,216	4117,283	4862,747	4661,624	4546,926	3954,073	3777,079	1917,496	3151,612	6416,528	7565,485	4375,482	6562,619
PWY-6708	ubiquinol-8 biosynthesis (prokaryotic)	0,9998	0	105,8604	7,4934	68,0281	78,6378	83,1919	4,9944	28,8097	199,6133	545,525	1628,047	1878,551	1436,567	900,5407
PWY-6728	methylaspartate cycle	0	0	0	0	0	0	0	0	0	0	0	0	0	36,8343	0
PWY-6737	starch degradation V	7877,422	19558,07	21453,64	19822,33	22475,34	15168,31	21071,31	18202,16	15397,19	13082,44	28950,96	38357,34	38528,87	21900,89	35897,93
PWY-6749	CMP-legionaminatate biosynthesis I	42,6257	359,5383	527,4242	396,4784	669,6575	507,3956	839,5685	186,7641	51,2789	76,5601	12,3372	11,9979	106,4872	17,9932	29,3251
PWY-6876	isopropanol biosynthesis	0	0	0	0	0	0	0	0	0	0	0	0	0	0	0
PWY-6891	thiazole biosynthesis II (Bacillus)	4614,463	8674,543	8912,592	7036,454	11932,69	7776,399	11217,27	7531,65	5990,853	6528,722	2394,422	3456,917	4262,277	1818,598	4940,598
PWY-6892	thiazole biosynthesis I (E. coli)	6690,811	11664,28	12679,85	9611,941	15496,38	9733,574	15596,93	10930,59	8817,004	9415,751	6669,142	9182,903	13070,03	8215,906	8581,463
PWY-6895	superpathway of thiamin diphosphate biosynthesis II	3533,69	6783,764	9752,457	5890,631	7747,286	5373,012	7913,397	4213,114	4081,059	3253,254	4651,801	8347,253	8867,84	3959,933	9073,648
PWY-6897	thiamin salvage II	16418,59	16984,62	21989,91	14519,32	21060,93	13849,84	21199,72	18703,17	12103,19	16276,29	15351,32	24742,97	28465,55	14915,43	22282,78
PWY-6901	superpathway of glucose and xylose degradation	11951,29	10695,02	11801,9	11157,09	13534,26	9838,53	10822,85	14213,97	10717,69	13999,52	8027,736	10710,01	7433,873	8059,001	5697,654
PWY-6969	TCA cycle V (2-oxoglutarate:ferredoxin oxidoreductase)	2344,941	3422,349	7495,397	2619,157	4243,247	2984,452	5534,361	3414,961	3990,748	2205,036	6434,799	14347,7	12473,58	5648,795	10124,27
PWY-7003	glycerol degradation to butanol	6284,273	4318,162	6714,65	8692,19	9969,21	4546,78	3752,276	3263,14	2159,439	3051,358	1208,579	3442,882	3188,792	836,2702	2105,715
PWY-7007	methyl ketone biosynthesis	0	0	13,7807	49,3773	20,5233	0	0	20,9274	0	48,7011	0	0	0	0	0
PWY-7013	L-1,2-propanediol degradation	127,8351	985,8273	2321,463	1390,588	2137,603	1479,57	2669,527	773,2295	326,7781	432,4328	129,8007	316,9081	413,9016	53,9591	792,9515
PWY-7031	protein N-glycosylation (bacterial)	0	0	86,0319	0	0	9,1119	38,6874	30,9389	155,0049	18,222	31,6364	389,0754	233,2408	0	171,7194
PWY-7090	UDP-2,3-diacetamido-2,3-dideoxy- α -D-mannuronate biosynthesis	296,8679	917,5006	1129,535	532,8205	880,5474	558,6074	938,0706	436,3557	445,1227	316,2347	620,0181	772,4622	1328,273	589,0115	1041,178
PWY-7094	fatty acid salvage	5,0277	0	168,6733	0	143,9263	0	31,3008	18,6591	25,1305	255,029	104,2376	177,4896	52,9205	41,1747	196,0288
PWY-7111	pyruvate fermentation to isobutanol (engineered)	19233,67	26112,51	32299,75	23478,51	30385,42	20929,08	31084,01	27546,42	20206,97	20758,86	29223,63	41262,78	43804,59	24314,3	38308,24
PWY-7159	chlorophyllide a biosynthesis III (aerobic, light independent)	0	0	0	0	0	0	0	0	0	0	0	0	12,9305	0	15,9831

Supplementary Datasheet 1 – Predicted microbial pathways (cont.).

PWY-7184	pyrimidine deoxyribonucleotides de novo biosynthesis I	19000,21	12830,06	17279,01	14876,03	15390,66	12046,18	14238,65	17691,59	11334,82	13701,44	7760,036	13598,55	13031,03	8750,049	9113,93
PWY-7187	pyrimidine deoxyribonucleotides de novo biosynthesis II	21167,93	16783,18	21459,34	19023,37	20279,05	15021,82	18886,71	21856,16	14605,22	18658,24	12585,62	19051,21	17215,44	12969,78	13683,83
PWY-7196	superpathway of pyrimidine ribonucleosides salvage	21311,31	16214,68	21663,52	17940,43	19359,55	14441,91	17962,46	20932,5	13259,82	16976,77	10924,91	19363,1	20106,68	11901,86	13815,38
PWY-7197	pyrimidine deoxyribonucleotide phosphorylation	17270,38	12113,05	16382,89	14097,46	14573,03	11386,31	13393,67	16299,54	10416,53	12684,43	7679,11	14001,69	13341,82	8560,439	9429,184
PWY-7198	pyrimidine deoxyribonucleotides de novo biosynthesis IV	0	76,6762	55,8723	80,1961	0	80,1223	235,2484	24,4763	45,3737	0	185,8975	616,3041	204,1061	347,1653	176,0386
PWY-7199	pyrimidine deoxyribonucleosides salvage	16015,73	16053,75	20552,32	14469,48	19319,46	12634,61	19817,68	19013,53	12402,55	16313,53	11914,36	13901,92	13418,77	11366,76	8549,371
PWY-7200	superpathway of pyrimidine deoxyribonucleoside salvage	17509,6	13514,44	17919,33	14649,19	16434,49	12080,3	15545,9	17834,16	11492,73	14544,5	8877,998	13093,28	12223,41	9487,8	8037,002
PWY-7208	superpathway of pyrimidine nucleobases salvage	33978,44	32998,33	39138,98	35819,79	39449,88	27323,82	36711,13	38109,08	26556,88	37841,72	36321,61	45564,66	42352,94	31958,41	37561
PWY-7210	pyrimidine deoxyribonucleotides biosynthesis from CTP	0	109,2102	79,6932	114,2599	0	114,0972	333,306	34,9423	64,6896	0	262,0485	860,9345	289,3548	485,5736	248,9682
PWY-7211	superpathway of pyrimidine deoxyribonucleotides de novo biosynthesis	3950,701	7072,658	10659,72	4239,655	5403,055	3545,388	6837,162	4207,733	4140,594	3304,915	5091,676	11764,2	11438,53	7274,25	9586,84
PWY-7219	adenosine ribonucleotides de novo biosynthesis	31769,25	31739,53	37750,24	32834,01	38902,36	26183,53	36943,63	36328,42	25691,12	34902,91	32479,94	42587,08	41167,8	28587,36	36018,06
PWY-7220	adenosine deoxyribonucleotides de novo biosynthesis II	31622,39	31934,02	37711,03	32287,61	39585,68	26592,8	37787,48	36880,17	25374,88	34949,09	18499,31	25918,36	25219,88	20559,95	17773,2
PWY-7221	guanosine ribonucleotides de novo biosynthesis	29090,3	28679,7	33701,32	30304,01	35518,93	24302,82	32926,74	33824,27	24293,05	32533,84	29066,23	37026,28	34918,22	25734,9	30532,16
PWY-7222	guanosine deoxyribonucleotides de novo biosynthesis II	31622,39	31934,02	37711,03	32287,61	39585,68	26592,8	37787,48	36880,17	25374,88	34949,09	18499,31	25918,36	25219,88	20559,95	17773,2
PWY-7228	superpathway of guanosine nucleotides de novo biosynthesis I	21708,99	15699,18	20699,87	17880,15	18914,35	14560,29	17388,55	20963,63	13613,21	16648,39	9902,399	17423,22	17200,51	11010,75	11923,63
PWY-7229	superpathway of adenosine nucleotides de novo biosynthesis I	32691,5	31901,09	38111,76	32787,19	39361,78	26593,85	37586,13	37230,47	26052,99	35289,37	27479,65	36958,59	36027,59	26202,85	29006,91
PWY-7234	inosine-5'-phosphate biosynthesis III	13925,97	13188,36	15063,42	16764,91	19372,58	13293,71	14563,61	15747,4	12112,34	13490,9	8381,34	12816,73	9188,271	7767,127	7434,215
PWY-7237	myo-, chiro- and scillo-inositol degradation	48,6465	207,6951	630	172,2486	322,5931	67,5132	323	190	138	135,7705	159,6653	102,1045	113,6089	105,7283	122,5484
PWY-7242	D-fructuronate degradation	925,2583	5691,052	7050,059	4229,482	7167,467	3226,154	5826,737	2602,946	1407,977	3661,833	11892,09	19984,64	22530,44	9428,839	20055,02
PWY-7254	TCA cycle VII (acetate-producers)	896,3783	2237,085	1537,216	1054,214	1214,625	552,656	1010,287	674,7366	836,6693	686,0361	752,4849	1799,559	1671,907	1310,912	1752,047
PWY-7255	ergothioneine biosynthesis I (bacteria)	0	0	10,6416	0	17,3516	0	0	43,0839	0	0	0	0	0	0	0
PWY-7315	dTDP-N-acetylthomosamine biosynthesis	491,2195	3531,495	2269,718	2639,821	2704,009	1241,801	2076,545	1271,663	1119,418	1981,902	1517,948	1961,628	3338,506	1569,038	2281,985
PWY-7323	superpathway of GDP-mannose-derived O-antigen building blocks biosynthesis	2256,606	6616,757	7372,113	5890,096	6397,814	4717,829	5613,257	3158,918	3150,351	3204,276	3798,318	6662,652	7790,913	4121,683	6429,547
PWY-7328	superpathway of UDP-glucose-derived O-antigen building blocks biosynthesis	2195,654	7229,943	6522,848	7211,42	7688,228	5268,126	6045,416	3529,424	3475,809	4002,921	3171,323	6002,702	7252,23	3784,824	6409,554
PWY-7332	superpathway of UDP-N-acetylglucosamine-derived O-antigen building blocks biosynthesis	790,8559	3253,786	6161,009	2783,077	4103,831	3977,947	4569,428	2090,17	1230,703	1624,681	4358,525	3758,576	5235,247	2196,68	4346,545
PWY-7371	1,4-dihydroxy-6-naphthoate biosynthesis II	1011,14	3069,181	3129,246	2750,794	3119,748	2409,789	2503,647	1194,478	1245,115	1066,027	1315,276	2750,762	2915,661	1240,738	3509,449
PWY-7373	superpathway of demethylmenaquinol-6 biosynthesis II	692,5284	1935,929	1344,616	1047,365	1170,063	536,4733	986,3404	543,909	680,7792	525,5999	629,5038	1473,132	1376,889	847,5632	1606,324
PWY-7374	1,4-dihydroxy-6-naphthoate biosynthesis I	816,7904	2577,421	2855,62	2571,51	2880,583	2323,916	2302,317	1087,651	1094,832	945,2805	1123,87	2264,569	2425,163	816,7773	3163,507
PWY-7376	cob(II)yrinate a,c-diamide biosynthesis II (late cobalt incorporation)	0	0	39,9669	0	62,7323	0	0	0	0	149,1364	0	11,4566	0	0	0
PWY-7377	cob(II)yrinate a,c-diamide biosynthesis I (early cobalt insertion)	10931,63	9479,41	13450,26	7420,561	11668,1	7253,19	13426,2	11487,87	6578,911	8984,851	831,3551	2069,536	10403,83	4462,572	705,8759
PWY-7392	taxadiene biosynthesis (engineered)	16917,94	18277,76	21165,85	18810,53	22442,98	15116,26	20330,43	19862,42	14193,48	17661,66	17564,97	20132,26	13067,06	15692,2	12739,34
PWY-7400	L-arginine biosynthesis IV (archaeobacteria)	10203,45	18190,78	22028,42	17328,14	21768,44	14369,81	20621,74	16727,17	13338,03	13199,98	21265,2	32582,44	33765,1	18066,26	30657,49
PWY-7431	aromatic biogenic amine degradation (bacteria)	0	4,6661	29,9825	1,7142	53,2729	0	10,6647	5,9993	0	71,8708	0	44,5945	33,3083	1,9998	23,9772
PWY-7446	sulfoglycolysis	0,4	0	0,8	3	5,4	1,8	4,6	0	0,6	2,33	0	2,7	0	0	0
PWY-7456	mannan degradation	0	23,3871	0	0	13,3349	0	8,9453	0	11,8304	0	135,0695	134,7614	17,3392	5,7085	132,6422
PWY-7527	L-methionine salvage cycle III	5,9907	0	0	0	7,3677	0	0	0	0	4,8899	0	0	0	0	0
PWY-7539	6-hydroxymethyl-dihydropterin diphosphate biosynthesis III (Chlamydia)	15764,92	14164,32	16985,63	11014,33	15326,49	10928,8	17359,11	17803,24	11959,92	14487,61	8519,794	13720,8	15357,71	9552,548	10274,38
PWY-7560	methylerythritol phosphate pathway II	15842,88	20183,31	24989,49	18122,98	23331,99	15113,71	24814,94	19307,85	14164,06	15866,55	21166,51	31717,23	33396,77	17862,46	29325,02
PWY-7616	methanol oxidation to carbon dioxide	0	0	0	46,4872	0	0	0	0	0	0	0	0	0	0	0
PWY-7663	gondatoe biosynthesis (anaerobic)	22162,02	25397,4	31777,05	24961,53	31464,94	20253,46	30588,79	25654,97	18141,46	21521,99	24982,95	38158,48	38671,91	21423,26	34407,28
PWY-7664	oleate biosynthesis IV (anaerobic)	2,7998	0	7,3776	23,6771	71,1317	16,7638	83,8153	9,3258	294,9377	210,9229	137,691	200,4965	137,4796	36,7781	275,3779
PWY-841	superpathway of purine nucleotides de novo biosynthesis I	21351,59	18757,01	24048,68	20370,49	22847,87	16608,39	21303,75	22615,49	15409,48	18217,03	13560,5	22895,28	22887,7	13983,12	16851,79
PWY-922	mevalonate pathway I	13442,85	9635,103	9804,05	12926,18	13095,85	9370,487	8987,652	14293,71	9582,947	17045,74	8566,711	6617,168	2467,67	8505,888	2057,137
PWY0-1061	superpathway of L-alanine biosynthesis	1695,603	2155,604	1378,23	5381,892	1132,588	4407,207	4076,281	8348,619	8585,136	2916,592	10845,58	10164,01	5535,636	6661,43	10394,21
PWY0-1241	ADP-L-glycero-β-D-manno-heptose biosynthesis	1022,929	2863,463	2702,107	1993,456	2225,884	1803,755	2203,234	1023,212	1343,618	1187,68	1789,951	3627,279	4040,411	2256,976	3292,973

Supplementary Datasheet 1 – Predicted microbial pathways (cont.).

PWYO-1261	anhidromuropeptides recycling	5,5991	0	11,1968	41,9405	117,2154	25,174	147,8136	27,9789	147,4989	254,616	1252,381	5689,476	4438,562	2897,282	6421,816
PWYO-1277	3-phenylpropanoate and 3-(3-hydroxyphenyl)propanoate degradation	0,833	0	22,6604	6,2491	44,2554	3,7522	9,5763	0	1,2497	83,0292	0	5,6254	0	0	0
PWYO-1296	purine ribonucleosides degradation	21100,16	19471,65	24091,65	19212,63	23912,61	16294,93	25026,77	23351,82	15269,22	18758,67	17610,26	25822,89	29355,69	15327,42	23681,12
PWYO-1297	superpathway of purine deoxyribonucleosides degradation	21621,74	18961,31	23589,24	19005,53	23396,33	15923,55	24438,12	23949,16	15665,47	19701,83	17752,43	25037,24	28048,53	15495,5	22620,25
PWYO-1298	superpathway of pyrimidine deoxyribonucleosides degradation	17528,37	17412,36	21592,67	15933,77	21264,75	13872,73	22037,09	19673,32	12836,49	16285,65	15336,73	22540,47	26436,46	13752,67	20401,66
PWYO-1319	CDP-diacylglycerol biosynthesis II	34367,56	33308,14	39792,67	34124,44	40196,4	27085,93	39026,53	38702,99	26791,72	36874,03	33889,47	44721,04	43556,73	30094,48	38304,09
PWYO-1338	polymyxin resistance	85,8058	601,4418	399,4363	246,8751	288,3248	360,923	206,101	128,4085	375,4499	148,2001	44,3375	306,0871	166,7581	0	174,6236
PWYO-1415	superpathway of heme biosynthesis from uroporphyrinogen-III	1,1949	82,856	222,2163	8,9035	70,609	169,0302	100,1713	53,9185	67,3909	94,2792	139,3034	952,3799	728,7209	543,3908	867,5507
PWYO-1479	tRNA processing	1341,364	3890,529	4510,742	4922,554	5070,094	4299,784	4018,913	3075,052	2769,545	1919,358	2562,48	4730,14	5318,914	2894,109	5922,531
PWYO-1533	methylphosphonate degradation I	0,7111	0	1,4221	5,3297	9,5956	3,1991	8,1749	0	1,0666	23,5388	3,5506	11,3539	9,7257	0	0
PWYO-1586	peptidoglycan maturation (meso-diaminopimelate containing)	23852,38	25185,76	27299,3	28068,92	31388,48	20893,23	25551,1	30163,09	21655,57	31735,48	27834,32	27264,4	19891,3	24601,23	19423,41
PWYO-162	superpathway of pyrimidine ribonucleotides de novo biosynthesis	23892,15	19384,75	24820,1	21573,38	23135,39	17235,39	21345,34	24294,58	16113,35	20377,59	14051,39	24207,91	24051,02	14861,62	17439,16
PWYO-166	superpathway of pyrimidine deoxyribonucleotides de novo biosynthesis (E. coli)	21951,4	16831,8	21678,42	19107,32	20393,56	15183,31	19055,93	22321,29	14879,97	18852,17	12000,16	18144,17	16375,88	12568,02	12804,08
PWYO-321	phenylacetate degradation I (aerobic)	0	0	0	0	0	0	0	0	0	0	0	0	0	0	0
PWYO-41	allantoin degradation IV (anaerobic)	0,7967	0	1,5976	5,9583	10,7218	3,5745	11,0464	0	1,7826	6,7406	0	12,3428	0	7,9327	0
PWYO-42	2-methylcitrate cycle I	0,4999	0	9,7235	41,759	20,348	2,2475	5,7353	14,8333	0,7498	45,0446	0	3,7733	6,7161	0	7,484
PWYO-781	aspartate superpathway	7046,791	12744,75	12885,21	14084,55	14590,22	11566,1	14216,08	13741,87	10592,45	7773,447	15444,32	20084,08	16700,6	12034,6	16229,94
PWYO-845	superpathway of pyridoxal 5'-phosphate biosynthesis and salvage	1,2918	114,0608	344,4684	9,672	149,9625	247,7206	129,1513	63,721	115,0997	294,856	746,8196	2017,258	2502,735	1181,065	1241,476
PWYO-862	(5Z)-dodec-5-enoate biosynthesis	2,3998	11,0069	134,0228	32,9717	166,6112	2105,007	164,2056	3277,222	2889,467	181,005	652,4299	191,4475	1832,249	63,8641	801,3514
PWY1G-0	mycothiol biosynthesis	0	0	7	32,5897	12,6042	0	0	14,9318	0	28,877	0	0	0	0	0
PWY490-3	nitrate reduction VI (assimilatory)	3696,194	5144,277	5526,955	3869,136	8398,753	4706,037	8548,892	5854,235	4590,866	4537,707	1641,992	2016,66	2561,817	1983,897	2472,781
PWY4F5-7	phosphatidylglycerol biosynthesis I (plastidic)	31747,91	31094,88	36738,5	31911,83	37911,65	25534,47	36429,47	36223,39	25481,76	34491,72	30971,1	39965,33	38501,81	27169,24	33439,13
PWY4F5-8	phosphatidylglycerol biosynthesis II (non-plastidic)	31747,91	31094,88	36738,5	31911,83	37911,65	25534,47	36429,47	36223,39	25481,76	34491,72	30971,1	39965,33	38501,81	27169,24	33439,13
PWYG-321	mycolate biosynthesis	2,9084	0	5,8169	21,7855	60,9423	13,0839	73,232	7,271	234,8622	217,2708	112,1361	200,7766	108,8117	32,6508	231,0218
PYRIDNUCSAL-PWY	NAD salvage pathway I	13486,74	14249,29	17400,93	13750,92	13798,55	9859,408	17047,44	15716,65	10915,99	12415,6	20221,27	27590,62	28974,45	16285,13	26041,64
PYRIDNUCSYN-PWY	NAD biosynthesis I (from aspartate)	7480,735	12701,36	15257,36	11652,09	15513,08	9888,338	16689,9	11416,32	9416,487	9912,659	15452,21	20933,18	18243,86	12633,22	19078,26
PYRIDOXSYN-PWY	pyridoxal 5'-phosphate biosynthesis I	1,0278	89,6384	270,1718	7,6865	117,7128	190,6502	101,8569	50,2072	89,9666	216,423	535,4335	1443,109	1740,704	660,6119	940,8336
REDTICYC	TCA cycle VIII (helicobacter)	1113,538	2966,588	2033,79	1329,791	1487,027	660,321	1212,333	808,2331	997,9086	1347,868	898,881	2124,676	1975,799	1579,419	2090,882
RHAMCAT-PWY	L-rhamnose degradation I	267,3993	703,5705	1129,417	411,3695	604,6752	438,4762	934,7856	688,4295	396,8435	478,1438	281,5311	582,5867	330,3441	309,7956	434,8912
RIBOSYN2-PWY	flavin biosynthesis I (bacteria and plants)	18985,11	17896,97	22943,86	15887,28	21129,75	13868,6	21707,83	19742,72	12907,01	17242,24	17405,15	27638,73	27959,38	16158,08	23922,84
RUMP-PWY	formaldehyde oxidation I	485,8372	1470,218	1250,74	1805,399	2487,264	1247,656	2007,424	1285,092	1223,878	962,3036	1467,275	1877,901	2901,742	1726,092	1953,728
SALVADEHYPOX-PWY	adenosine nucleotides degradation II	1045,681	3709,361	7332,7	3842,066	6490,519	2107,948	3888,674	2248,177	1563,64	1792,539	2417,366	4057,263	4361,006	2213,952	2992,569
SER-GLYSYN-PWY	superpathway of L-serine and glycine biosynthesis I	9925,8	16726,59	20134,74	17493,57	21517,82	13306,91	17880,27	15394,9	11955,27	13692,62	22677,74	32893,5	34087,36	19162,7	30190,49
SO4ASSIM-PWY	sulfate reduction I (assimilatory)	692,161	1949,659	2155,564	2168,126	2934,38	1948,726	2084,008	1011,129	935,8868	724,3935	1284,726	2309,45	3421,193	1789,889	2894,893
SULFATE-CYS-PWY	superpathway of sulfate assimilation and cysteine biosynthesis	1381,941	3755,349	4210,83	4050,615	5504,742	3631,917	3984,745	2064,458	1889,398	1468,611	2579,623	4566,423	6553,533	3440,034	5586,474
TCA	TCA cycle I (prokaryotic)	2192,083	3412,814	6685,555	2744,036	4197,838	3099,872	5141,651	3377,046	3982,793	2153,802	6252,876	13779,45	11853,86	5526,623	9585,221
TCA-GLYOX-BYPASS	superpathway of glyoxylate bypass and TCA	840,575	1951,499	1687,477	1159,335	1406,549	696,0278	1187,155	769,409	878,1559	689,8921	669,5602	1316,083	900,7347	1115,26	1901,079
TEICHOICACID-PWY	teichoic acid (poly-glycerol) biosynthesis	9314,26	7057,133	6921,951	9336,165	10089,21	7049,399	6346,814	9830,719	6717,163	10088,3	4076,45	5482,89	2790,027	4397,602	2522,985
THISYN-PWY	superpathway of thiamin diphosphate biosynthesis I	6302,544	10416,83	11314,72	8606,738	13876,59	9269,95	13342,79	9367,297	7028,586	8004,384	6142,025	11943,94	12223,66	5828,427	10748,72
THREOCAT-PWY	superpathway of L-threonine metabolism	0	0	4,9154	18,5221	28,0782	0	0	0	0	14,4924	0	1,846	0	0	0
THRESYN-PWY	superpathway of L-threonine biosynthesis	21969,06	24594,24	30316,17	24053,74	30796,11	20038,08	30170,66	26518,72	19197,85	22029,89	23635,59	34528,08	36008,93	20367,66	31131,5
TRNA-CHARGING-PWY	tRNA charging	25866,89	27075,42	32574,51	28257,03	32775,67	21990,48	31377,22	30129,76	27563,19	28870,72	37276,53	35618,91	25043,2	31834,58	
TRPSYN-PWY	L-tryptophan biosynthesis	7159,183	13231,46	16371,89	10829,98	13051,97	9799,071	13587,39	11742,39	7693,505	9155,506	15159,81	24233,33	29920,99	13359,83	22959,65
TYRFUMCAT-PWY	L-tyrosine degradation I	0	0	9,9937	0	15,7047	0	7,4979	2,4997	6,2475	49,6861	24,6949	41,574	11,2277	8,7295	44,6214
UBISYN-PWY	superpathway of ubiquinol-8 biosynthesis (prokaryotic)	0,9597	0	101,6066	7,1934	65,2848	75,463	79,818	4,7943	27,6472	190,9025	520,0641	1547,313	1802,227	1370,158	865,5522
UDPNAAGSYN-PWY	UDP-N-acetyl-D-glucosamine biosynthesis I	26270,52	24641,72	28867,19	26517,26	30284,78	20947,86	28334,6	29536,27	21278,91	28057,23	22392,69	27376,42	22472,25	20314,31	20311
VALSYN-PWY	L-valine biosynthesis	17212,1	22646,38	28906,83	20305,54	26234,37	18011,73	27498,78	23755,18	17269,37	17245,43	25439,48	37686,99	42929,09	21122,78	37178,53

Supplementary Datasheet 2 – KEGG pathways.

KO	Name	Class	meanCases	meanControls	StatValue	pval	singLogP	FDR
ko00030	Pentose phosphate pathway	Metabolism; Carbohydrate metabolism	20,47320112	17,28070316	2,611164839	0,009023439	2,044627922	0,02863961
ko00040	Pentose and glucuronate interconversions	Metabolism; Carbohydrate metabolism	8,439489175	5,65657322	2,611164839	0,009023439	2,044627922	0,02863961
ko00260	Glycine, serine and threonine metabolism	Metabolism; Amino acid metabolism	19,37688656	17,1125471	2,611164839	0,009023439	2,044627922	0,02863961
ko00281	Geraniol degradation	Metabolism; Metabolism of terpenoids and polyketides	0,081864962	0,032957279	2,402271652	0,016293604	1,787982853	0,043252111
ko00290	Valine, leucine and isoleucine biosynthesis	Metabolism; Amino acid metabolism	9,601464895	5,825957294	2,611164839	0,009023439	2,044627922	0,02863961
ko00300	Lysine biosynthesis	Metabolism; Amino acid metabolism	14,88798302	13,07596316	2,402271652	0,016293604	1,787982853	0,043252111
ko00330	Arginine and proline metabolism	Metabolism; Amino acid metabolism	18,69452611	15,41830291	2,402271652	0,016293604	1,787982853	0,043252111
ko00340	Histidine metabolism	Metabolism; Amino acid metabolism	8,686988666	5,444199057	2,611164839	0,009023439	2,044627922	0,02863961
ko00361	Chlorocyclohexane and chlorobenzene degradation	Metabolism; Xenobiotics biodegradation and metabolism	0,339426725	0,152557429	2,402271652	0,016293604	1,787982853	0,043252111
ko00363	Bisphenol degradation	Metabolism; Xenobiotics biodegradation and metabolism	1,279465405	0,826630262	2,611164839	0,009023439	2,044627922	0,02863961
ko00400	Phenylalanine, tyrosine and tryptophan biosynthesis	Metabolism; Amino acid metabolism	16,29411741	11,22370179	2,611164839	0,009023439	2,044627922	0,02863961
ko00460	Cyanoamino acid metabolism	Metabolism; Metabolism of other amino acids	3,919632807	3,469307846	2,402271652	0,016293604	1,787982853	0,043252111
ko00500	Starch and sucrose metabolism	Metabolism; Carbohydrate metabolism	19,38105666	16,97828801	2,611164839	0,009023439	2,044627922	0,02863961
ko00521	Streptomycin biosynthesis	Metabolism; Biosynthesis of other secondary metabolites	7,14323401	5,711469589	2,611164839	0,009023439	2,044627922	0,02863961
ko00523	Polyketide sugar unit biosynthesis	Metabolism; Metabolism of terpenoids and polyketides	3,896708481	3,205839646	2,611164839	0,009023439	2,044627922	0,02863961
ko00591	Linoleic acid metabolism	Metabolism; Lipid metabolism	1,299793717	0,851240643	2,611164839	0,009023439	2,044627922	0,02863961
ko00603	Glycosphingolipid biosynthesis - globo and isoglobo series	Metabolism; Glycan biosynthesis and metabolism	1,304558851	0,908015529	2,611164839	0,009023439	2,044627922	0,02863961
ko00630	Glyoxylate and dicarboxylate metabolism	Metabolism; Carbohydrate metabolism	12,70691093	9,465707847	2,611164839	0,009023439	2,044627922	0,02863961
ko00660	C5-Branched dibasic acid metabolism	Metabolism; Carbohydrate metabolism	4,791747252	3,020658159	2,611164839	0,009023439	2,044627922	0,02863961
ko00710	Carbon fixation in photosynthetic organisms	Metabolism; Energy metabolism	14,17961573	12,39750789	2,611164839	0,009023439	2,044627922	0,02863961
ko00760	Nicotinate and nicotinamide metabolism	Metabolism; Metabolism of cofactors and vitamins	8,445284144	7,733825995	2,611164839	0,009023439	2,044627922	0,02863961
ko00770	Pantothenate and CoA biosynthesis	Metabolism; Metabolism of cofactors and vitamins	11,90235528	9,6523556	2,611164839	0,009023439	2,044627922	0,02863961
ko00906	Carotenoid biosynthesis	Metabolism; Metabolism of terpenoids and polyketides	0,0044412	0,00186874	2,611164839	0,009023439	2,044627922	0,02863961
ko00940	Phenylpropanoid biosynthesis	Metabolism; Biosynthesis of other secondary metabolites	1,253982661	0,634538994	2,611164839	0,009023439	2,044627922	0,02863961
ko01040	Biosynthesis of unsaturated fatty acids	Metabolism; Lipid metabolism	2,408337566	1,938382657	2,611164839	0,009023439	2,044627922	0,02863961
ko02010	Environmental Information Processing; Membrane transport	Environmental Information Processing; Membrane transport	62,77205204	54,93537699	2,611164839	0,009023439	2,044627922	0,02863961
ko03018	RNA degradation	Genetic Information Processing; Folding, sorting and degradation	9,96780239	9,670231553	2,402271652	0,016293604	1,787982853	0,043252111
ko03060	Protein export	Genetic Information Processing; Folding, sorting and degradation	14,24742037	13,38278144	2,611164839	0,009023439	2,044627922	0,02863961
ko03070	Environmental Information Processing; Membrane transport	Environmental Information Processing; Membrane transport	12,22122072	11,55739935	2,611164839	0,009023439	2,044627922	0,02863961
ko03450	Non-homologous end-joining	Genetic Information Processing; Replication and repair	0,026862125	0,006498793	2,611164839	0,009023439	2,044627922	0,02863961
ko04146	Peroxisome	Cellular Processes; Transport and catabolism	2,236696023	1,786355761	2,611164839	0,009023439	2,044627922	0,02863961
ko05204	Chemical carcinogenesis	Human Diseases; Cancer: overview	0,025873376	0,001386045	2,611164839	0,009023439	2,044627922	0,02863961

4.4 Manuscript 4

Manuscript published in **Food Research International** (Impact Factor: 6.475)
(Attachment 3)

Use of the synbiotic VSL#3 and yacon-based concentrate attenuates intestinal damage and reduces the abundance of Candidatus Saccharimonas in a colitis-associated carcinogenesis model.

Bruna Cristina dos Santos Cruz^a, Lisiane Lopes da Conceição^a, Tiago Antônio de Oliveira Mendes^b, Célia Lúcia de Lucas Fortes Ferreira^b, Reggiani Vilela Gonçalves^d, Maria do Carmo Gouveia Peluzio^a

^aNutritional Biochemistry Laboratory, Department of Nutrition and Health, Universidade Federal de Viçosa – UFV, Viçosa, Minas Gerais, Brazil.

^bDepartment of Biochemistry and Molecular Biology, Universidade Federal de Viçosa – UFV, Viçosa, Minas Gerais, Brazil.

^cInstitute of Biotechnology Applied to Agriculture & Livestock (Bioagro), Universidade Federal de Viçosa – UFV, Viçosa, Minas Gerais, Brazil.

^dDepartment of Animal Biology, Universidade Federal de Viçosa – UFV, Viçosa, Minas Gerais, Brazil.

Received 6 April 2020/Received in revised form 22 July 2020

Accepted 9 September 2020/Available online 25 September 2020

<https://doi.org/10.1016/j.foodres.2020.109721>

Abstract

Individuals with inflammatory bowel disease are at high risk of developing colitis-associated cancer; thus, strategies to inhibit disease progression should be investigated. The study aimed to explore the role of the synbiotic (probiotic VSL#3[®] and yacon-based concentrate) in a colitis-associated carcinogenesis model. IL-10^{-/-} mice were induced to carcinogenesis with 1,2-dimethylhydrazine and divided into two experimental groups: control and synbiotic. Manifestations of colitis, colon histology, expression of antioxidant enzymes, production of organic acids and intestinal microbiota were evaluated. The use of the synbiotic showed benefits, such as the preservation of intestinal architecture, increased expression of antioxidant enzymes and the concentration of organic acids, especially butyrate. It was also observed different microbial community profiles between the groups during the study. Together, these factors contributed to mitigate the manifestations of colitis and improve intestinal integrity, suggesting the potential benefit of the synbiotic in intestinal diseases.

Keywords: synbiotic; colitis; colorectal cancer; inflammatory bowel disease; gut microbiota; dysbiosis.

Introduction

Individuals with inflammatory bowel disease (IBD), which includes ulcerative colitis (UC) and Crohn's disease (CD), are at higher risk of developing colorectal cancer (CRC) (Zheng et al., 2016). Colitis-associated carcinogenesis (CAC) is the main complication of IBD in humans (Wang et al., 2019; Richard et al., 2018) and is directly related to chronic inflammation (Potack; Itzkowitz, 2008). The risk for developing CRC is particularly relevant in patients with long-standing IBD involving at least 1/3 of the colon, and starts approximately 7 years after diagnosis, increasing linearly thereafter (Clarke; Feuerstein, 2019; Zhou et al., 2019). For the UC, the cumulative risk of CRC is 2% at 10 years, 8% at 20 years and 18% at 30 years. The overall prevalence of CRC is shown to be 3.7% in patients with UC and 5.4% in patients with pancolitis (Eaden et al., 2001).

Although the mechanisms of association between IBD and carcinogenesis are not completely understood, it is believed that the malignant process is enhanced by the time, extent and severity of tissue inflammation (Herszenyi et al., 2015). Chronic inflammation is responsible for the increase of a variety of pro-inflammatory cytokines, such as tumor necrosis factor (TNF), interleukin 1 β and interleukin 6, which stimulate cell proliferation and inhibit apoptosis, contributing to carcinogenesis (De Almeida et al., 2019; Francescone et al., 2016; Grivennikov, 2013). On the other hand, interleukin 10 (IL-10) is a critical immunosuppressive cytokine, associated with CAC inhibition (Mantovani et al., 2008; Uronis et al., 2009).

In particular, the presence of dysbiosis in individuals with IBD is among the possible factors that explain the association between intestinal inflammation and the potential risk of cancer (Kostic et al., 2013; Rubinstein et al., 2013; Arthur et al., 2012). It is estimated that the colon hosts 70% of the human microbiome, being the most colonized site of the gastrointestinal tract (Sekirov et al., 2010). It is also the most prone place for the development of cancer, with a 12-fold higher incidence compared to the small intestine (Gagniere et al., 2016). Thus, a plausible hypothesis is that colonization by pathogenic microorganisms or the imbalance in the microbiota metabolic activity promotes a more inflammatory microenvironment, favorable to tumor development (Wong et al., 2017; Tanaka, 2012).

Knowing specific microbial signatures and their relationship with the origin and progression of CAC is useful for generating tools for screening and discovering specific

bacterial genera for therapeutic purposes (Villéger et al., 2018). Recent studies have demonstrated changes in the microbiota associated with IBD and CRC (Guo et al., 2020; Kim et al., 2020). However, little is known about the structure and function of the microbiota in the progression of CAC so far.

To understand the pathogenesis of CAC, experimental models of drug-induced colitis are used, such as dextran sulfate sodium (DSS) and trinitrobenzene sulfonic acid (TNBS) or even genetically modified animals, such as interleukin-10-knockout mice (IL-10^{-/-}) (Rothemich; Arthur, 2019). These animals have defects in immune regulation and spontaneously develop chronic enterocolitis (Hale et al., 2010; Mizoguchi et al., 2002). When exposed to chemical carcinogens, inflammation-dependent colorectal mutagenesis and tumorigenesis occurs, driven by the composition of the intestinal microbiota (Rothemich; Arthur, 2019).

In this context, the use of probiotics, prebiotics and, or synbiotics has gained support in the scientific community (Lynch; Pedersen, 2016; Schmidt et al. 2018; Montalban-Arques; Scharl, 2019). In a recent systematic review, the protective effect of probiotics and synbiotics on colorectal carcinogenesis and on the progression of colitis-associated cancer was demonstrated by different mechanisms, such as modulation of the intestinal microbiota and immune response, reduction of inflammation, biosynthesis of compounds with antitumor activity and improvement in the antioxidant system (Cruz et al., 2020).

The probiotic VSL#3[®] has a high bacterial concentration, and has been proved significantly effective in the treatment of inflammatory bowel diseases, in clinical and experimental studies (Babiloni et al., 2003; Mimura et al., 2004; Kim et al., 2003). Rats with colitis who received VSL#3[®] had lower macroscopic and microscopic damage in the colon, reduction of macrophage infiltration, reduction of serum cytokine levels, and restoration of colonic transcript levels for anti-inflammatory, and barrier proteins (Whang et al., 2019; Isidro et al., 2017; Kumar et al., 2017). However, the effects of probiotic VSL#3[®] in models of colitis-associated colorectal carcinogenesis are controversial (Talero et al., 2015; Appleyard et al., 2011; Arthur et al., 2013).

Yacon (*Smallanthus sonchifolius*) is a tuberous root rich in phenolic compounds and considered a prebiotic food due to its high soluble fibers contents (Russo et al., 2015). The yacon-based product (PBY) is a concentrate rich in fructooligosaccharides (FOS) and inulin. The evaluation of the effects of PBY on colitis-associated carcinogenesis is unprecedented, however, in colorectal carcinogenesis model, the

use of PBY intensified fecal short-chain fatty acid (SCFA) production, increased the number of regulatory T cells, and downregulated the expression of ROR γ t transcription factor in the colon, improving anti-inflammatory immune responses (De Nadai Marcon et al., 2019).

The yacon powder decrease IFN- γ levels and improve the healing of intestinal mucosa by increasing the number of goblet cells in TNBS-induced colitis model (Umizah et al., 2020). In colorectal carcinogenesis induced with DMH, the animals that received yacon powder had a percentage reduction of aberrant crypt foci (preneoplastic lesions) in more than 40%, lower intestinal permeability, higher concentrations of SCFA and increase in the depth and number of colonic crypts (Grancieri et al., 2017).

The concomitant administration of the probiotic VSL#3[®] and the prebiotic PBY is an unprecedented synbiotic formulation. Previous studies that used synbiotics in CRC or colitis obtained additional results when compared to the use of probiotic and prebiotic alone (Moura, 2012; Sheng et al., 2020). In these studies, the efficacy of synbiotics was explained by the additive combination of the direct anti-inflammatory effects of the probiotic and prebiotic components and their ability to fortify colonic epithelial barrier integrity. Our hypothesis is that the prophylactic administration of the synbiotic could be able to modulate the composition and metabolism of the intestinal microbiota and, consequently, reduce the manifestations of CAC.

Thus, the present study aimed to evaluate the effects of the synbiotic, composed of the probiotic VSL#3[®] and the concentrated product based on yacon (PBY), in the manifestations of CAC, in the oxidative stress, in the intestinal microbiota composition and in the production of short-chain fatty acids (SCFA) an experimental model of colitis-associated carcinogenesis.

Material and Methods

Synbiotic

The probiotic VSL#3[®] (Sigma Tau Pharmaceuticals, Inc.; acquired in 2016, valid 04/2018, lot number 604094) was selected based on studies that demonstrated its benefits in the treatment of IBD (Chen et al., 2019; Isidro et al., 2017; Liu, Yu, & Zou, 2019). This is a mixture of eight bacterial species, including *Bifidobacterium breve*,

Bifidobacterium infantis, *Bifidobacterium longum*, *Lactobacillus acidophilus*, *Lactobacillus bulgaricus*, *Lactobacillus casei*, *Lactobacillus planatarum*, and *Streptococcus thermophilus*. The probiotic was obtained lyophilized, in sachets containing 450 billion viable bacteria. Reconstitution was performed daily in distilled water immediately before administration.

The description of PBY processing has been safeguarded due to the requirements of the patent application (PI 1106621-0). In order to define the diet composition containing PBY, it was necessary to determine its centesimal composition. Therefore, the concentrations of total carbohydrates, sugars, proteins, lipids, total fiber, ash and moisture (AOAC, 1997), and the concentrations of FOS and inulin by high performance liquid chromatography (HPLC) were analyzed. PBY was added to the diet in sufficient quantity to provide 6% FOS and inulin (Paula et al., 2012).

The control and PBY diets were based on the AIN-93M diet as recommended by the American Institute of Nutrition (Reeves et al., 1993), and they had the contents of carbohydrates, proteins and fibers adjusted so that both had similar composition. The diets were prepared in the form of pellets and stored at -20°C.

Animals and experimental design

Interleukin-10-knockout mice (IL-10^{-/-}), male, with eight weeks of age and body weight of approximately 25 g, from the Central Bioterium of the Federal University of Alfenas (UNIFAL), Minas Gerais, Brazil, were used. The IL-10^{-/-} mice were generated from the C57BL/6J background. Under conventional housing conditions, they develop chronic colitis at six weeks of age (Sturlan et al., 2001).

The animals were housed collectively in polypropylene boxes covered with metal gratings, in a controlled temperature environment (22 ± 2°C) and a 12-hour light/dark cycle. After a week of acclimatization with free access to the commercial diet and water, the animals were randomly divided into two experimental groups: control group (KOCON, n = 8), AIN-93M diet and gavage with distilled water, and synbiotic group (KOSYN, n = 7), AIN-93M diet with PBY (6% FOS and inulin) and gavage with probiotic VSL#3®.

The animals in the KOSYN group received the probiotic in a volume of 0.1 mL by orogastric gavage in the morning, five days a week (Arthur et al., 2012). The KOCON group received gavage with distilled water in the same volume. The amount

of probiotic administered was adjusted to ensure a daily supply of 2.25×10^9 CFU, based on an approximate intake of 10^9 CFU/day for a 70 kg adult (Dai et al., 2013; Zavisic et al., 2012). Diets and water were provided *ad libitum* for 13 weeks (Figure 1).

In the 3rd experimental week, the protocol for inducing precursor lesions of the CRC was started and all animals received an intraperitoneal injection (0.1 mL) of the drug 1,2-dimethylhydrazine (DMH) (Sigma-Aldrich®), at a dose of 20 mg/kg of body weight, once a week, for eight consecutive weeks (Gomides et al., 2015). DMH was prepared in 0.9% saline, with 1 mM EDTA and 10 mM sodium citrate, pH 8 (Newell; Heddle, 2004).

At the end of 13 weeks, the animals were anesthetized with isoflurane 3% (Isoflorine®, Cristalia), followed by total exsanguination by the retro orbital sinus. After dissection, the tissues were washed with phosphate-buffered solution, weighed in a semi-analytical balance, placed in a container with liquid nitrogen and stored at -80°C until the time of analysis.

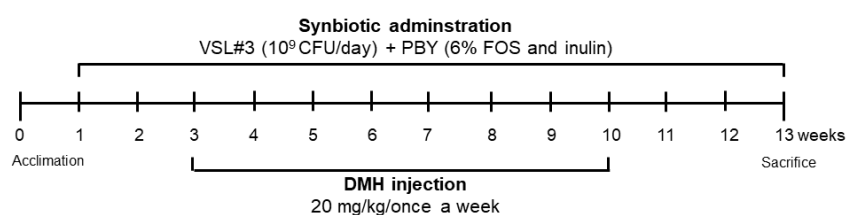


Figure 1. Experimental timeline for colitis-associated colorectal carcinogenesis model with synbiotic administration. Carcinogenesis was initiated with eight injections of DMH (20 mg/kg), once a week. The VSL#3® was administered via gavage (10^9 CFU/day) and the PBW added to the standard diet throughout the experiment. After thirteen weeks, IL-10-deficient mice were sacrificed and tissues and feces were harvested.

Body weight and dietary intake

To evaluate the weight loss or gain of the animals, individual body weight was recorded weekly using a digital weighing scale. Dietary intake was measured daily and was calculated by the difference in the amount of diet offered (g) and the remaining amount in the day after. This quantification was done during all experimental period using a digital weighing scale. The coefficient of food efficiency (CFE) was calculated by the equation: $\text{CFE} = \text{weight gain (g)} / \text{total dietary intake (g)}$.

Analysis of serum biomarkers

The blood was centrifuged at $1190 \times g$ for 10 minutes at 4°C . The serum markers albumin, creatinine, and urea were assessed by specific colorimetric assays following manufacturer's recommendations (Bioclin[®], Brazil) using a clinical chemistry analyzer BS-200 (Mindray[®]).

Assessment of colitis symptoms and disease activity index

The disease activity index (DAI) was evaluated from the first application of DMH (third experimental week). Mice were monitored weekly for body weight loss, compared to baseline weight (score 0-4), fecal consistency (score 0-4) and blood in stool (score 0-4). The DAI score was assessed as the combined score of the above three criteria (Hamamoto et al., 1999).

Colonic tissue processing, morphometry and histopathological score

After washing, fragments of the colon were fixed with Carson's formalin for 24 hours (Carson, 1973) and then transferred to a 70% ethanol solution. Subsequently, they were dehydrated in an increasing gradient of ethanol, diaphanized in xylol and included in paraffin. Cross sections of $5 \mu\text{m}$ thick were obtained on a rotary microtome for the preparation of slides.

The slides were stained with hematoxylin-eosin (HE) and the images were obtained directly from the light microscope (Leica Microsystems[®], Inc.) to assess intestinal morphometry and histopathological score. Intestinal morphometry was performed using the Image Pro Plus 4.5 software in which the crypt depth, thickness of the submucosa, muscular and external muscular layers were measured. The crypt length measure was taken after the identification of the base and the apex of the crypt. Only the straight aspect crypts were included in this assessment. It was prepared slides of seven animals per group, each one with ten non-consecutive cuts. It was taken about 20 photos of each slide.

The histopathological score was calculated by adding the combined score of three criteria: damage to the colonic crypt (score 0: none; 1: basal 1/3; 2: basal 2/3; 3: only surface epithelium intact; 4: complete loss of crypt and epithelium), presence of

inflammatory infiltrate (score 0: none; 1: slight; 2: moderate; 3: severe) and infiltration depth (score 0: none; 1: mucosal; 2: mucosal and submucosal; 3: transmural) (Dieleam et al., 1994). The assessment was carried out by two examiners, independently.

Determination of oxidation products and hepatic enzyme expression

The liver samples were weighed (150 mg) and properly homogenized in cold potassium phosphate buffer (1.5 mL, pH 7.4) using an Ultra-Turrax homogenizer (IKA T10 basic). The homogenate was centrifuged at $10,000 \times g$ for 10 minutes at $4^\circ C$. The supernatant was then pipetted into eppendorf tubes and used for hepatic enzyme analysis, catalase (Dieterich et al., 2000), superoxide dismutase (Buege et al., 1978; Aebi et al., 1984) and glutathione-S-transferase (Habig et al., 1981); and for oxidation biomarkers assessment, malondyaldeide (Wallin et al., 1993) and carbonyls protein (Levine et al., 1990). The results were normalized by total protein concentration of supernatant (Lowry et al., 1951).

16S rRNA gene sequencing

The feces were collected on the first (t0) and last (t1) experimental week. To obtain those samples, individual cages were previously cleaned and sanitized and mice kept there until a sufficient amount of feces have been spontaneously expelled. Samples were kept at $-80^\circ C$ until processing. The DNA extraction was performed as previously described (Zhang et al., 2006). The concentration and integrity of bacterial DNA were assessed using Qubit and agarose gel electrophoresis 1.8%, respectively. The DNA sequencing for microbial analysis was performed by Macrogen (Seoul, Korea). The V3-V4 hypervariable region of the 16S rRNA gene was initially amplified using the primers Bakt_341F (CCTACGGGNGGCWGCAG) and Bakt_805R (GACTACHVGGGTATCTAATCC). The PCR products were sequencing in MiSeq plataform (Illumina, USA).

Microbial bioinformatics analysis

The raw data (fastq format) were filtered to remove low quality reads with Phred Quality score smaller than 30 using the program Trimmomatic v0.36 (Bolger et al.,

2014). The high quality reads were inputted in DADA2 package version 1.8 (Callahan et al., 2016) implemented in R platform version 3.6.1. Chimeric sequences were identified and deleted. The representative OTU sequences were taxonomically classified using the Silva 16S rRNA Database release 138 (Quast et al., 2013).

To estimate the diversity of the microbial community of the sample, we calculated the within-sample alpha-diversity using the Shannon and Simpson index, and Chao-1 for richness assessment using the phyloseq package (McMurdie et al., 2012). Beta-diversity was estimated by computing Jaccard distance and visualized by multidimensional scaling (MDS) plot using R platform. Bacterial abundance profiles were calculated at taxonomic levels from phylum to species in percent abundance and compared using a paired Student's t-test or Wilcoxon test for dependent samples and Student's t-test or Mann-Whitney test for independent samples (IBM SPSS Statistics 20).

Fecal short chain-fatty acids quantification

Mice fecal samples were obtained at the end of the experimental period for SCFA assessment. The concentration of acetate, propionate, butyrate and total SCFA were evaluated by high-performance liquid chromatography (HPLC) according to the method described by Smiricky-Tjardes et al., (2003), with some modifications. Approximately 50 mg of frozen feces, which was previously weighed and thoroughly vortexed with deionized water (950 μ L) was used. While being incubated on ice for 30 min, the samples were homogenized every 5 min for 2 min. The samples were centrifuged (10,000 \times g, 30 min, 4 °C) three times and the supernatants were collected. The final supernatant from each sample was filtered through a 0.45 μ m membrane and transferred to vials. SCFA were measured by high performance liquid chromatography - HPLC (Shimadzu®) using an Aminex HPX 87H column (300 \times 7,8 mm, Bio-rad®, Rio de Janeiro, Brazil) at 32 °C with acidified water (0.005M H₂SO₄) as eluent at a flow rate of 0.6 mL/minute. The products were detected and quantified by an ultraviolet detector (model SPD-20A VP) at 210 nm. Standard curves of acetic, propionic and butyric acids (Supelco®) were constructed. Results are expressed in μ mol/g feces.

Statistical analyses

Data were analyzed using Software Social Package Statistical Science for Windows-SPSS (20 version, IBM® SPSS, Chicago, USA). The means were evaluated by the Shapiro-Wilk normality test and the groups with a normal distribution were tested using the unpaired Student's t-test. The samples that did not follow a normal distribution were tested by the Mann-Whitney test. $p < 0.05$ was considered to be statistically significant and the data are expressed as the mean \pm standard deviation (SD). The graphics were built using Graphpad Prism (version 7.0).

Results

The composition of the experimental diets was described in Table 1. Considering that 100 g of PBV contains 23.6 g of FOS and inulin, to meet the dose of 6%, 25.4 g of PBV was added for each 100 g of diet.

Synbiotic reduces dietary intake and body weight without change the CFE

Dietary intake was lower in the KOSYN group at the 5th, 6th and 11th experimental weeks (Figure 2A). Consequently, a reduction in the average body weight was observed in this group (Figure 2B). Only at the 7th week, the ingestion of the KOSYN group increased without, however, promoting weight gain. We point out that at the 3rd experimental week, when the carcinogenesis induction protocol with DMH was started, the lowest mean food intake was observed in both groups. There was no significant difference on the CFE (Figure 2C).

Table 1. Composition of AIN-93M diet for control and synbiotic diet.

Ingredients (g 100g ⁻¹)	Control Diet	Synbiotic Diet
Cornstarch	33.20	28.55
Casein	16.50	16.40
Dextrinized starch	15.50	15.50
Sucrose	10.00	5.20
Soybean oil	4.00	4.00
Microfine cellulose	6.40	0.00
PBY*	0.00	25.40
Mineral mix	3.50	3.50
Vitamin mix	1.00	1.00
L-Cystine	0.18	0.18
Choline bitartrate	0.25	0.25
Energy density (kcal/g)	3.37	3.19

*Centesimal composition and digestible content of carbohydrate. inulin and FOS on PBY (100g of product): fructose: 9.4g; glucose: 6.45g; sucrose: 3.05g; FOS: 17.65g; inulin: 5.95; total carbohydrate: 42.49g; fibers: 1.64g; humidity: 37.20g; ashes: 1.55g; lipids: 0.04g; protein: 2.51g.

The weight of the liver ($1.17 \text{ g} \pm 0.03 \times 1.21 \text{ g} \pm 0.03$; $p=0.531$), the weight of the colon ($0.22 \text{ g} \pm 0.01 \times 0.25 \text{ g} \pm 0.01$; $p=0.059$) and the length of the colon ($6.42 \text{ cm} \pm 0.19 \times 6.07 \text{ cm} \pm 0.22$; $p=0.261$) did not differ between the KOCON and KOSYN groups. On the other hand, the animals that received the synbiotic showed an increase in the weight of the cecum ($0.26 \text{ g} \pm 0.02 \times 0.44 \text{ g} \pm 0.03$; $p=0.000$).

Synbiotic does not alter the biomarkers of liver function and albumin

Serum biomarkers were evaluated in order to verify alterations in kidney function, and albumin production. No change was observed between the groups KOCON and KOSYN in relation to serum levels of urea ($31.90\text{mg} \pm 1.43 \times 40.47\text{mg} \pm 1.17$; $p=0.460$), creatinine ($0.31\text{mg} \pm 0.01 \times 0.30\text{mg} \pm 0.01$; $p=0.673$), and albumin ($2.37\text{g} \pm 0.14 \times 2.58\text{g} \pm 0.04$; $p=0.168$).

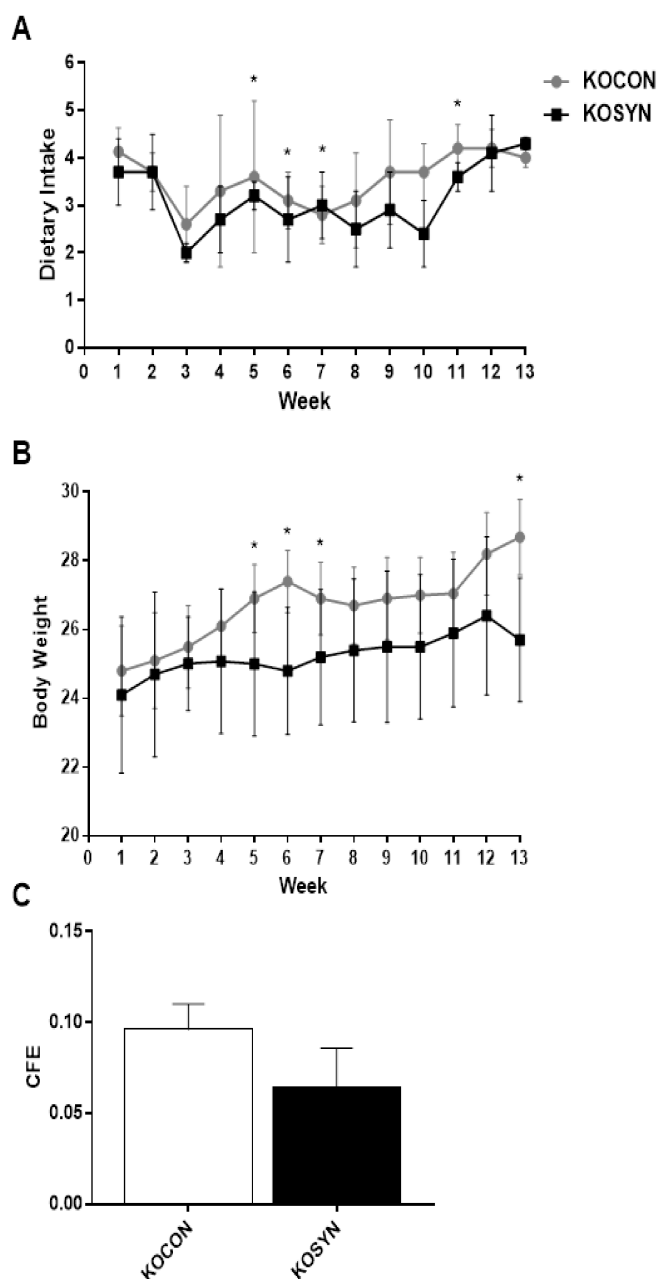


Figure 2. Effect of synbiotic on (A) dietary intake, (B) body weight and (C) food efficiency (CFE) in colitis-associated carcinogenesis model. *p-value lesser than 0.05 using Student's t-test between control (KOCON) and synbiotic-treated group (KOSYN).

Synbiotic attenuates the manifestations of colitis in CAC model

The experimental groups showed significant differences in the symptomatic parameters of colitis (% of weight loss, stool consistency and presence of visible blood in the stool) only in the seventh experimental week (Figure 3). The mortality rate was

20% in the KOCON group and 10% in the KOSYN group. Two animals in the KOSYN group showed rectal prolapse and were excluded.

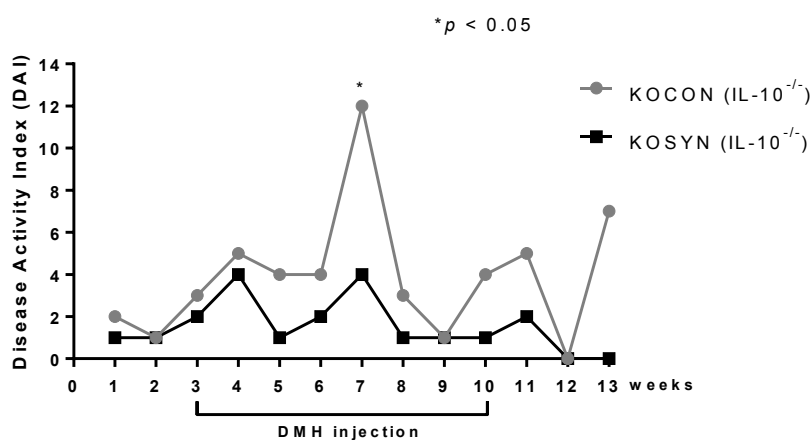


Figure 3. Effect of synbiotic on disease activity index (DAI) in colitis-associated carcinogenesis model. *p-value lesser than 0.05 using Student's t-test between control (KOCON) and synbiotic-treated group (KOSYN).

Synbiotic alters colonic morphometry and improves histopathological score

The use of the synbiotic caused changes in layers thickness that make up the colonic tissue. An increase was observed in the crypts depth and in the thickness of the external muscular layer (Figure 4A and D), which, besides the trophic effect of the synbiotic, demonstrates the possible benefit regarding the integrity of the intestinal barrier. Measurements of the colon layers are shown in Figure 4E.

The total histopathological score, calculated based on the cumulative scores of the crypts damage parameters, the presence of inflammatory infiltrate and the infiltration depth, was significantly higher in the KOCON group (Figure 5A). Similarly, when the aforementioned parameters were evaluated in isolation, a higher score was also observed in the KOCON group (Figure 5B), with emphasis on the presence of damaged crypts and infiltration of immune cells involving the submucosa and the muscular layer (Figure 5C).

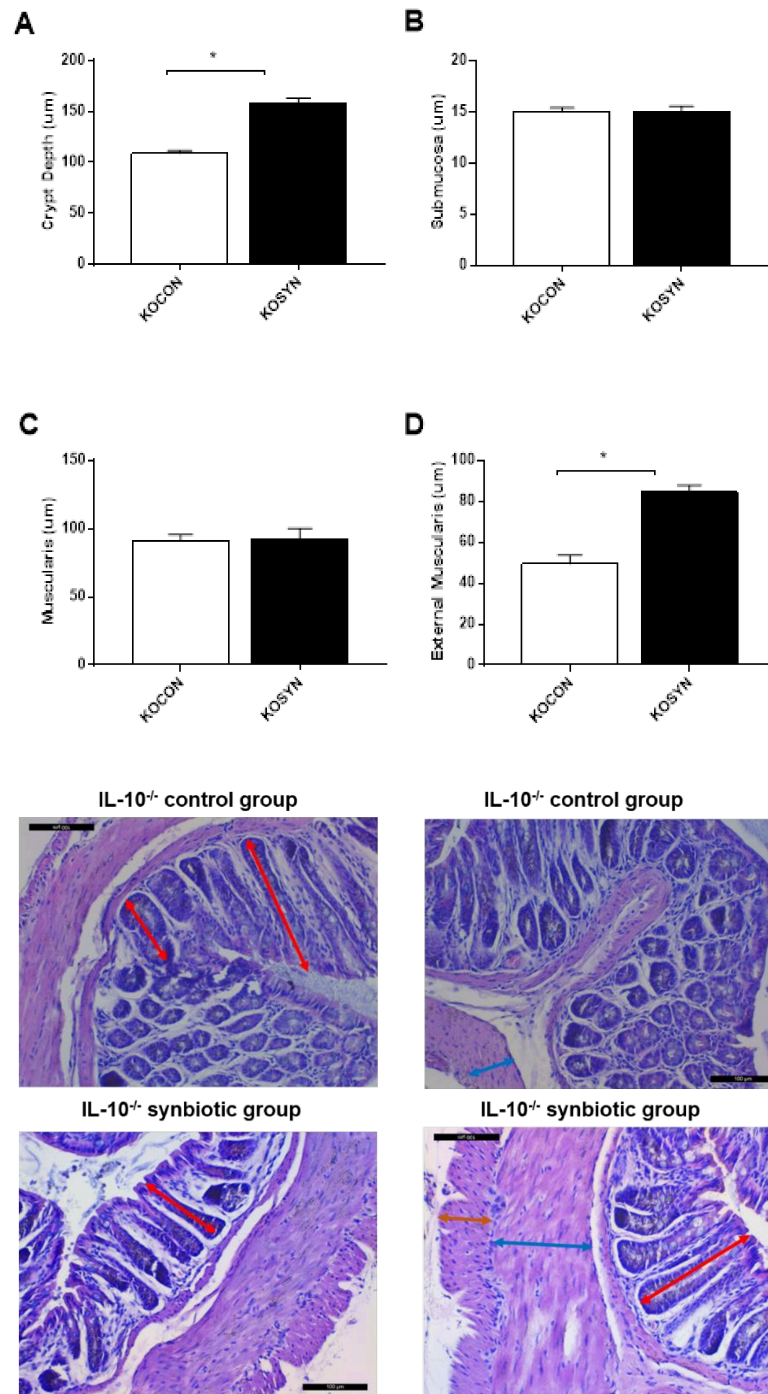


Figure 4. Effect of synbiotic on intestinal morphometry in colitis-associated carcinogenesis model. (A) crypt depth, (B) submucosa, (C) muscularis, (D) external muscularis, and (E) illustrative photomicrography of the intestinal morphometry. Red arrow: measure of crypt depth; blue arrow: muscularis layer; orange arrow: external muscularis layer (scale bars, 100 μm). *p-value lesser than 0.05 using Student's t-test between control (KOCON) and synbiotic-treated group (KOSYN).

Synbiotic positively modulates hepatic antioxidants enzymes expression

The effects of supplementation with the synbiotic on biomarkers of oxidative stress were evaluated by measuring the products of lipid and protein oxidation, malondialdehyde (MDA) and carbonyls protein (CP), respectively. The enzymes involved in the endogenous antioxidant defense system (SOD, CAT, and GST) were measured. The concentrations of the MDA and CP were not altered with the use of the synbiotic (Figure 6A,B). However, according to our results, increased liver expression of SOD and CAT was observed, when compared to the KOCON (Figure 6C,D). GST enzyme expression has not been altered (Figure 6E).

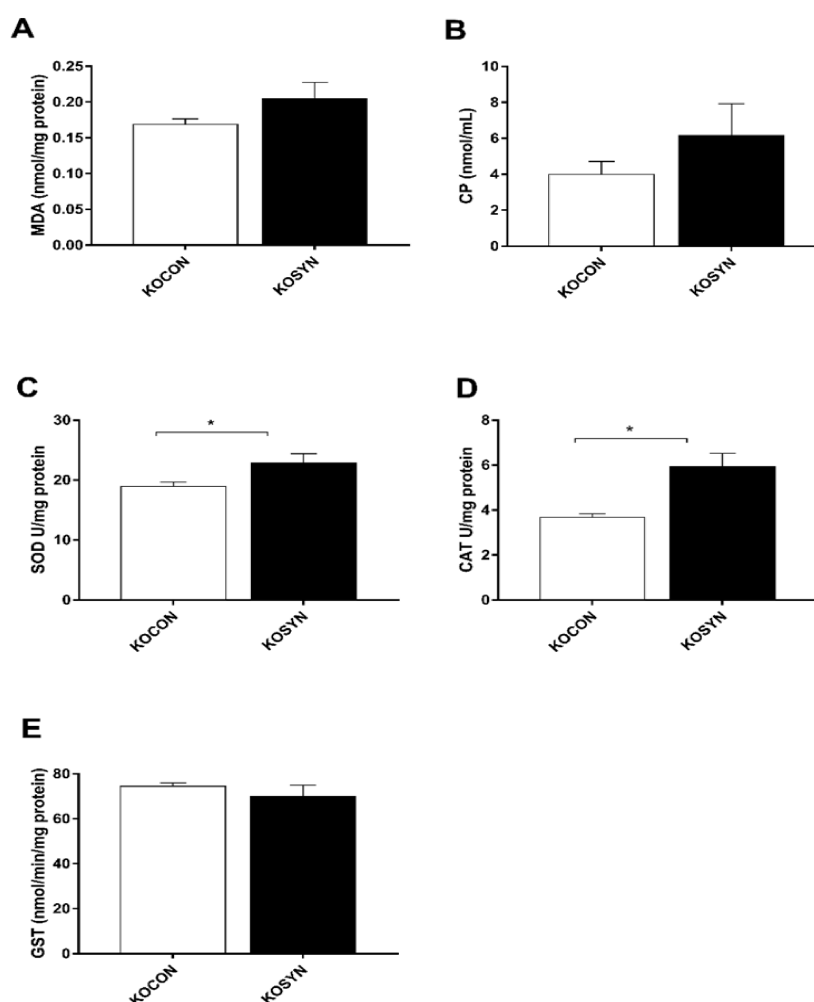


Figure 6. Effect of synbiotic on liver concentrations of (A) MDA, malondialdehyde and (B) CP, carbonylated protein, and on antioxidants enzymes expression (C) SOD, superoxide dismutase, (D) CAT, catalase, and (E) GST, glutathione-S-transferase in colitis-associated carcinogenesis model. *p- value lesser than 0.05 using Student's t-test between control (KOCON) and synbiotic-treated group (KOSYN).

Bioinformatics analysis and microbiota profiling

Conducting a deep amplicon sequencing of the V4-V6 hypervariable regions of the 16S rRNA gene, a total of 222,228 to 328,252 sequences with a length of 100 to 301 bp were obtained. After the removal of low quality and chimeric sequences, a total of 161,035 to 237,864 high-quality sequences, with an average of 188,280 sequences for each sample that were assigned to 2,415 OTUs ($\geq 97\%$ similarity). The number of OTU per sample ranged from 124 to 306.

The global fecal bacterial community structures of animals fed with synbiotic before and after colon carcinogenesis induction with DMH were assessed by the multidimensional scaling (MDS). As depicted (Figure 7A), scatter plot of the MDS revealed that KOSYN groups did not clustering separated from KOCON group.

Alpha diversities were compared among the groups by Shannon and Simpson indices, whereas Chao 1 index was used to evaluate bacterial richness. There was no statistically significant difference in terms of bacterial diversity among the groups before or after synbiotic use (Figure 7B,C). With regards to the bacterial richness, also there was no significant difference among the groups (Figure 7D).

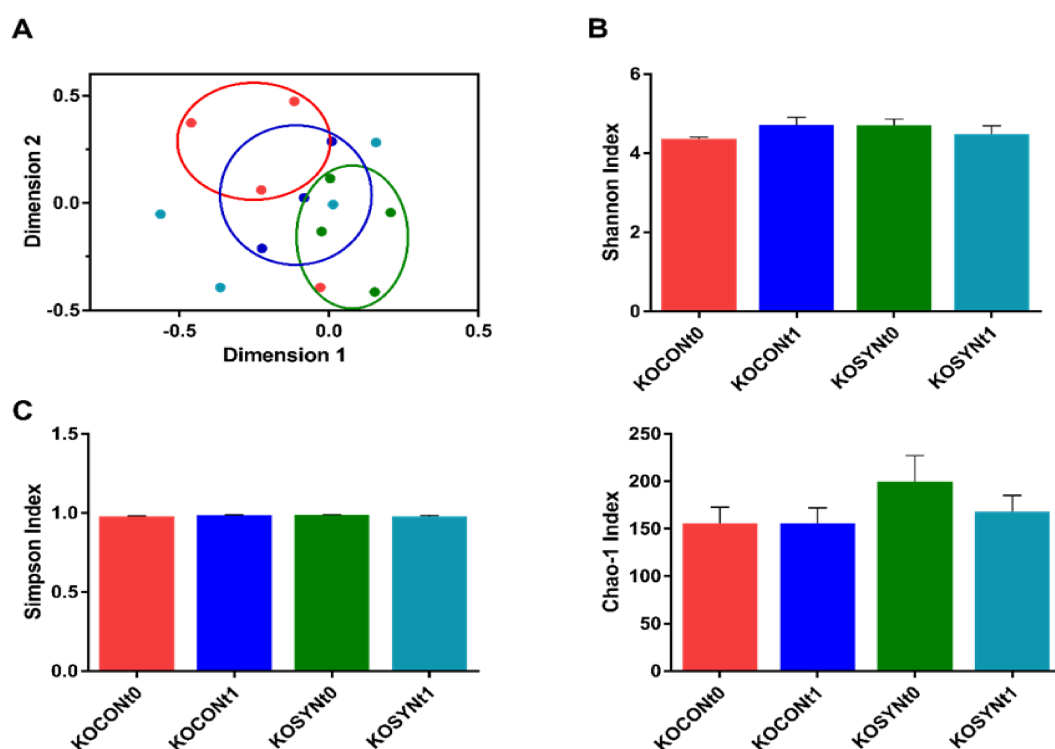


Figure 7. Microbiome characterization before (t_0) and after (t_1) using the synbiotic in colitis-associated carcinogenesis model. (A) Multidimensional scaling (MDS), (B)

Shannon Index, (C) Simpson Index, and (D) Chao-1 Index. Red and blue colors represent the control group before and after treatment, respectively. Green and cyan colors represent the synbiotic group before and after the treatment.

The relative distributions of bacteria at the phylum, family and genus level identified by 16S rRNA gene amplicon sequencing are depicted in Figure 8. The most prevalent bacterial phyla among all groups were Patescibacteria (68.2%), Proteobacteria (14.2%), Firmicutes (11.0%), Actinobacteria (4.8%), and Bacteroidetes (1.5%).

In the intra-group comparison ($t_0 \times t_1$), a reduction in the phylum Patescibacteria in the KOSYN group (1.2-fold) and an increase in the KOCON group (1.3-fold) were observed. Similarly, the phylum Firmicutes decreased in the KOSYN group (1.6-fold) and increased in the KOCON group (2.1-fold). On the other hand, there was an increase in Proteobacteria after the synbiotic use (2.7-fold) and a reduction in the control group (3.8-fold). The use of the synbiotic also resulted in a reduction in the relative abundance of the phylum Bacteroidetes for both groups (KOSYN = 2.0-fold; KONCON = 1.9-fold) and a concomitant increase in Actinobacteria (KOSYN = 2.9-fold; KONCON = 0.1-fold).

At the family level, 10 bacterial taxa were identified in total with 4 families accounted for more than 90% of the relative abundance in all groups. Among them, the family Saccharimonadaceae was the most abundant between all groups and in both times ($t_0 \times t_1$). Regarding microbial changes at the family level before and after the intervention ($t_0 \times t_1$), there was a Saccharimonadaceae reduction in the KOSYN group (1.2-fold) and an increase in the KOCON group (1.3-fold), following the same profile of the corresponding phylum (phylum Patescibacteria). Two families of the phylum Proteobacteria were identified: Desulfovibrionaceae and Legionellaceae. In both families, an increase in relative abundance in the KOSYN group (2.7-fold and 0.5-fold, respectively) and a reduction in the KOCON group (3.9-fold and 1.7-fold) were identified after intervention. The Ruminococcaceae, Lachnospiraceae and Erysipelotrichaceae families, belonging to the phylum Firmicutes, presented different profiles of changes compared to time zero. There was a Ruminococcaceae reduction in the KOSYN group (3.3-fold) and an increase in the KOCON group (6.6-fold); a Lachnospiraceae reduction in both groups (KOSYN = 2.9-fold; KONCON = 1.3-fold);

and an Erysipelotrichaceae increase in the KOSYN group (2.7-fold) and reduction in the KOCON group (3.9-fold).

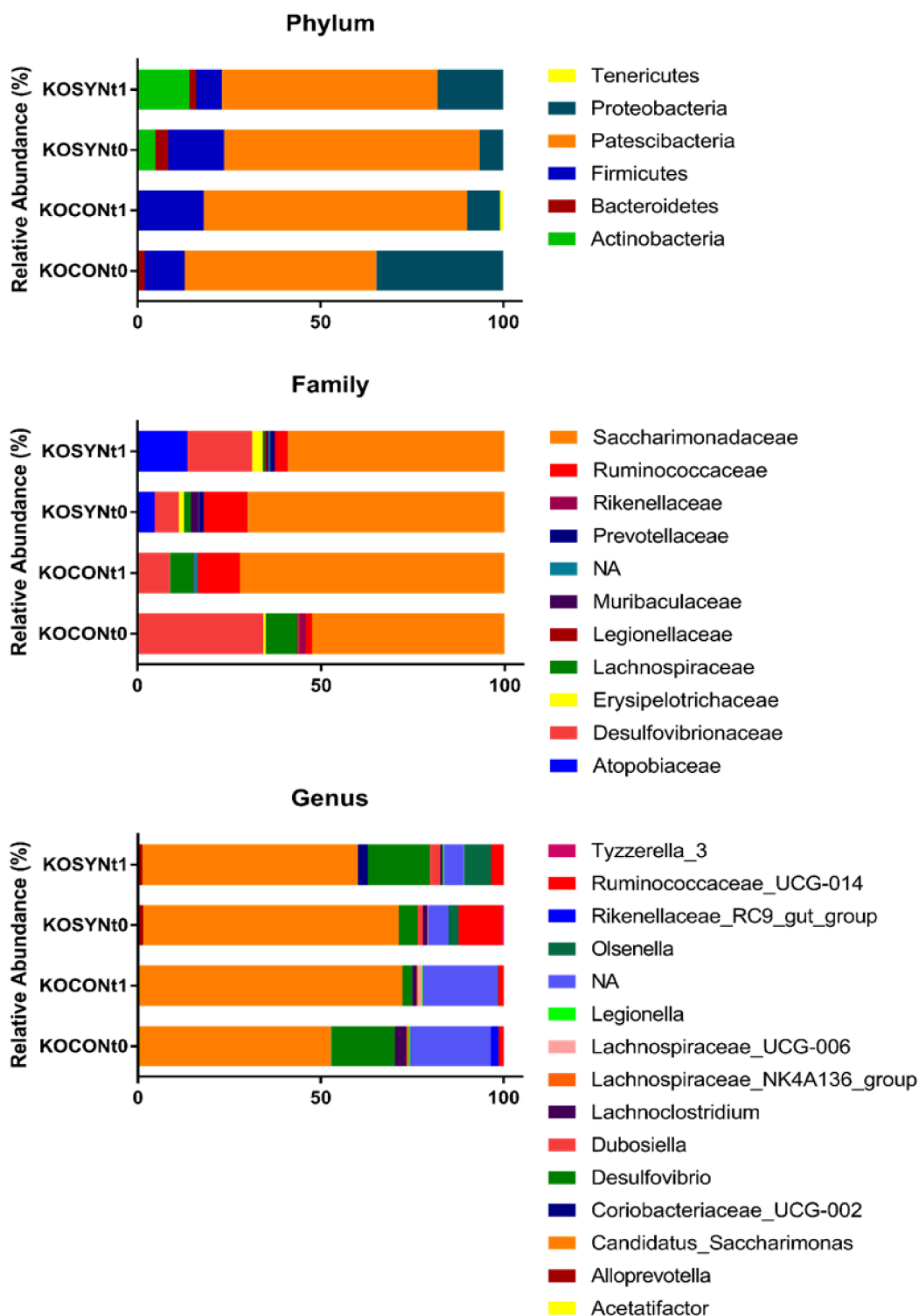


Figure 8. Relative abundance (%) of Phylum, Family and Genus levels before (t_0) and after (t_1) use the synbiotic in colitis-associated carcinogenesis model.

In total, 14 bacterial taxa were assigned to the genus level. After defining the most abundant genera (relative abundance higher than 4%), 4 OTUs accounted 93.1% of the total sequences of groups. *Candidatus Saccharimonas* was the most abundant genus in all groups. The intra-group ($t_0 \times t_1$) comparison revealed a less abundance of *Candidatus Saccharimonas* (1.2-fold; $p=0.002$), *Ruminococcaceae_UCG-014* (3.5-fold; $p<0.0001$), *Aloprevotella* (1.1-fold), *Lachnospiraceae_UCG-006* (0.2-fold), and *Tyzzarella_3* (0.4-fold) in KOSYN. In contrast, there was an increase of *Coriobacteriaceae_UCG-002* (2.6-fold), *Dubosiella* (1.9-fold), *Legionella* (0.4-fold), and *Olsenella* (2.7-fold).

In KOCON t_1 group, a decrease in the relative abundance of *Desulfovibrio* (6.2-fold; $p=0.003$), *Lacnospiraceae_UCG-006* (3-fold; $p=0.043$), *Acetatifactor* (1.4-fold), *Lachnospiraceae_NK4A136-group* (2.2-fold), *Legionella* (1.7-fold), and *Rikenellaceae_RC9-group* (1.9-fold) was observed. There was an increase of *Candidatus Saccharimonas* (1.4-fold), *Lachnospiraceae_UCG-006* (27.9-fold) and *Olsenella* (0.2-fold).

The comparison between groups after intervention (t_1) revealed a significant difference ($p<0.0001$) in abundance of *Desulfovibrio* genus between KOSYN (17%) and KOCON (3%) groups.

Synbiotic increases the fecal short-chain fatty acids

Intestinal bacteria activity was evaluated by fecal SCFA concentration. The KOSYN group presented higher levels of acetic ($p=0.010$), propionic ($p=0.013$), butyric ($p=0.001$), and total fatty acids ($p=0.009$) compared to the KOCON group (Table 2).

Table 2. Effect of synbiotic on the production of faecal short-chain fatty acids in colitis-associated colorectal cancer model.

SCFA ($\mu\text{mol/g feces}$)	KOCON	KOSYN	p
Acetic acid	137.6 \pm 52.4	561.2 \pm 180.1	0.010*
Propionic acid	2.2 \pm 2.2	9.9 \pm 5.93	0.013*
Butyric acid	6.3 \pm 2.8	12.6 \pm 2.3	0.001*
Total SCFA	146.2 \pm 56.2	583.7 \pm 179.0	0.009*

SCFA: short-chain fatty acids. Data are expressed as the mean \pm SD (n=8/group). Statistical difference between groups were analyzed by *Student's t-test* with $p < 0.05$. KOCON. control diet; KOSYN. synbiotic diet.

Discussion

Chronic intestinal inflammation that occurs in IBD induces increased mucosal permeability and persistent damage throughout the gastrointestinal tract, playing an important role in the development of CRC (McConnell & Yang, 2009). The manipulation of the intestinal microbiota with probiotics and prebiotics use has been shown to be effective in the regulation of intestinal homeostasis, by suppressing the growth of pathogenic bacteria and the production of beneficial metabolites (Israel, 2000).

The present study evaluated the influence of the synbiotic VSL#3[®] + PBV in a CAC model. In general, the use of the synbiotic showed benefits, such as the attenuation of CAC manifestations in the seventh experimental week, improvement of the histopathological score and intestinal morphometry, increased expression of antioxidant enzymes and concentration of SCFA, and alteration in the general composition of the intestinal microbiota.

This is a prevention study, therefore, the synbiotic was administered prophylactically, 3 weeks before the induction of preneoplastic lesions. The pre-treatment period is variable in the literature, and studies were found that started the intervention 1 week before or even months before the induction of injury. It is expected that the prophylactic use of synbiotic is able to modulate the intestinal microenvironment, altering the responses of the host to inflammatory and carcinogenic stimuli. Modulation of the composition and metabolism of the intestinal microbiota, with consequent improvement of the innate immune system and intestinal barrier function, is the key mechanism of synbiotic action (Appleyard, 2011; Bassaganya-Riera, Viladomiu, Pedragosa, De Simone, & Hontecillas, 2012; Chung et al., 2017; Fong, Li, & Yu, 2020; Leu, Hu, Brown, Woodman, & Young, 2010).

Studies using the CAC model show contradictory results in relation to the weight gain in animals, in which some authors identify weight gain in groups that receive synbiotic (Kumar, Singh, & Sinha, 2010; Urbanska, Bhatena, Cherif, & Prakash, 2012) and others find no difference (Chang, Shim, Cha, Reaney, & Chee, 2012; Leu

et al., 2010). In our study, a lower average body weight was observed in the KOSYN group in some weeks, possibly due to the lower intake of the PBY diet, which, being rich in soluble fibers, promotes greater satiety. A similar result was observed in the study by De Nadai Marcon et al. (2019), in which mice fed a diet supplemented with PBY (6% FOS + inulin) had lower food intake. In addition, it is known that SCFA (identified in higher concentrations in the KOSYN group), can influence satiety mechanisms through the production of leptin (Xiong, 2004). However, it is worth mentioning that there was no significant difference in the coefficient of feeding efficiency (CFE) final average between the groups.

The synbiotic administration significantly reduced the DAI score only at the 7th experimental week, even though the mean values of the score have remained lower in almost every period evaluated. It is worth mentioning that the presence of visible blood in the stool was identified exclusively in the KOCON group (data not shown). In a similar study, Shinde et al. (2020) found that the synbiotic administration was able to reduce the DAI over the entire experimental period, which, however, was considerably lower than in our study (14 days). The short period of exposure to the drug that induces intestinal inflammation may explain, at least partially, the differences observed.

Histopathological evaluation also showed a beneficial result with the use of synbiotic. Greater preservation of the intestinal crypts architecture was observed, with limited damage to the epithelial surface, compared to the KOCON group. In addition, the areas of inflammatory infiltrate were more extensive in the control group, as well as the infiltration depth, which reached areas of the submucosa and mucosa. The benefits of using the probiotic VSL#3[®] alone in reducing chronic inflammation scores had already been demonstrated in IL-10^{-/-} mice induced to colorectal carcinogenesis and inflammatory diseases such as colitis and ileitis (Fitzpatrick, 2007; López-Posadas, 2011; Pagnini, 2010; Reiff, 2009; Soo, 2008).

Similarly, the effect of isolated dietary supplementation of PBY (6% FOS and inulin) in the treatment of precursor lesions of CRC in mice has been previously assessed (De Nadai Marcon et al., 2019). The authors observed an increase in regulatory T cells and downregulation in the transcription factor ROR γ t expression in the colon of the animals, suggesting the potential of PBY in improving the anti-inflammatory and immune response.

One of the possible mechanisms attributed to the synbiotic in the control of CAC is the ability to stimulate the endogenous antioxidant defenses, that can mitigate the

damage caused by the chemical carcinogen and the effects of intestinal inflammation on the liver.

The biotransformation of DMH into its active metabolite occurs predominantly in the liver, with formation of a large amount of free radicals occurs, involved in the genesis and progression of intestinal diseases (Jackson, O'Connor, Cooper, Margison, & Povey, 2003). Additionally, dysbiosis and increased intestinal permeability will result in bacterial products in the portal blood, and the cells of the liver will be first to be exposed. Liver cells have receptors, such as TLR 4, in which the presumed ligand is a bacterial product. The LPS produced by gram negative bacteria, for example, is a ligand for TLR4 associated with liver injury (Brenner, Paik, & Schnabl, 2015). Thus, the determination of the antioxidant enzyme expression aimed to assess whether the changes in the gut microenvironment triggered by the synbiotic could minimize the oxidative stress induced by DMH/intestinal inflammation on the liver.

The antioxidant potential of probiotics has been reported for decades (Lin & Yen, 1999) and is attributed to its ability to eliminate and inhibit the formation of free radicals in the intestine, chelate metal ions, inhibit the autoxidation of ascorbate (Azcárate-Peril, Sikes, & Bruno-Bárcena, 2011), and induce the transcription of genes involved in the synthesis of glutathione by the intestinal mucosa (Lutgendorff, 2009) and in pancreatic cells (Lutgendorff, 2008).

In addition, yacon has in its composition flavonoids and phenolic compounds that protect biomolecules against damage caused by free radicals (Simonovska, Vovk, Andresek, Valentová, & Ulrichová, 2003). Protein and lipid oxidation products were identified in both groups, which was expected since they were IL-10^{-/-} mice that received injections with the DMH carcinogen. Although the concentrations of these products did not differ between groups, there was an increase in the expression of the antioxidant enzymes SOD and CAT in the KOSYN group.

Although the indexes of richness and diversity have not changed significantly with the use of the synbiotic, the relative abundance of some microorganisms at the end of the intervention (*t1*) differed significantly from the initial profile (*t0*) (intra-group analysis). Studies have indicated that perturbed gut microbiota, for example, reduced microbial diversity is associated with several diseases including gastrointestinal disorders (Gong, Gong, Wang, Yu, & Dong, 2016; Mosca, Leclerc, & Hugot, 2016). Changes in the indexes of richness and diversity with the use of probiotics and

synbiotics may not be observed, although there are variations in the abundance of bacterial species (Jacouton, Chain, Sokol, Langella, & Bermúdez-Humarán, 2017).

Significant differences were observed for *Candidatus Saccharimonas* (KOSYN t_0 × KOSYN t_1), *Desulfovibrio* (KOCON t_0 × KOCON t_1 and KOCON t_1 × KOSYN t_1), *Lacchnoclostridium* (KOCON t_0 × KOCON t_1) and Ruminococcaceae (KOCON t_0 × KOCON t_1 and KOSYN t_0 × KOSYN t_1) after the intervention. Therefore, it is likely that the results obtained cannot be attributed solely to changes in the composition of the intestinal microbiota.

Furthermore, we highlight that the microbiota of the experimental model used was characterized by a restricted biodiversity, with a limited number of bacterial genera representing the total microbial community. This finding has been consistently demonstrated in cases of cancer in experimental models and in humans, and in IBD patients (Richard et al., 2018; Saraggi et al., 2017; Sartor & Wu, 2017).

The evidence on the microbiota profile in IBD is limited, especially when associated with carcinogenesis. Some studies have shown a reduction in the phylum Firmicutes (*Roseburia* and Ruminococcaceae) and in the *Fusobacterium* genus; an increase in classes of the phylum Proteobacteria, such as Gammaproteobacteria and Deltaproteobacteria; and an increase of the Enterobacteriaceae family, of the genus *Sphingomonas*, and of the species *Ruminococcus gnavus* (Morgan, 2012; Richard et al., 2018).

Candidatus Saccharimonas was the main genus identified in our study, in both groups (KOCON t_0 = 52.4%, KOCON t_1 = 72.0%, KOSYN t_0 = 69.9%, KOSYN t_1 = 58.9%). There is little data in the literature concerning this genus, and its genome was sequenced relatively recently (Abrams, 2012; Albertsen et al., 2013). This microorganism belongs to the superphylum Patescibacteria, formerly known as TM7. It is an important member of the oral microbiome (Bor, Bedree, Shi, McLean, & He, 2019), and is also found throughout the gastrointestinal tract, skin and genital tract (Dewhirst, 2010; Fredricks, Fiedler, & Marrazzo, 2005; Grice & Segre, 2011).

Although incipient, human and animal studies have indicated that oral microbiota can translocate into the intestine and alter its microbiota and possibly the immune defense (Olsen & Yamazaki, 2019). Association of oral microbiota with the CRC was previously demonstrated (Flemer, Warren, & Barrett, 2018). Several OTUs were shared between oral swabs and stool samples of patients with CRC, amongst them *Parvimonas micra*, *Peptostreptococcus stomatitis* and *Fusobacterium*

nucleatum, a species commonly enriched in tumor tissues (Sun et al., 2019). We speculate whether the oral translocation of *Candidatus Saccharimonas* could contribute to the high abundance of this genus in the intestinal microbiota and for intestinal inflammation.

The expansion of the *Candidatus Saccharimonas* has been associated with inflammatory disease such as gingivitis and other periodontal dysfunctions (Camelo-Castillo, 2015). Apparently, can also play a role in other clinical conditions, having an increase identified, for example, in a study of obesity induced by high-fat diet (Lin, An, Hao, Wang, & Tang, 2016).

The relationship between *Candidatus Saccharimonas*, IBD, CRC or CAC has not been established previously, however, it is a microorganism globally distributed and often associated with inflammatory mucosal diseases in humans. Its ability to suppress the production of TNF in macrophages has been demonstrated, suggesting a potential capacity for immune suppression (He et al., 2015). We emphasize that the use of the synbiotic reduced the abundance of *Candidatus Saccharimonas* by 1.2- fold, while in the KOCON group there was an increase of 1.4-fold. It is speculated whether *Candidatus Saccharimonas* could directly influence the inflammatory response in the initiation and progression of CAC or have its growth favored by the presence of an inflammatory condition.

SCFA produced in the colon are active metabolites that act to reduce inflammatory mediators and increase the function of the intestinal barrier (Fernández et al., 2016). These are important indicators of dysbiosis in IBD and CRC, since the depletion of SCFA-producing bacteria in these situations is common (Levy, Thaiss, & Elinav, 2016). Low concentrations of SCFA, especially butyrate, have been shown to have a direct effect on intestinal homeostasis, resulting in intestinal barrier defects and in aberrant immune response activation (Geier, Butler, & Howarth, 2006; van der Beek, Dejong, Troost, Masclee, & Lenaerts, 2017).

The most abundant SCFA in the colon are acetate, propionate and butyrate, produced by the intestinal microbiota through the fermentation of non-digestible fibers, with butyrate being the preferred energy source for colonocytes (Koh, De Vadder, Kovatcheva-Datchary, & Backhed, 2016). In this study, it was observed that the synergistic administration of the probiotic VSL#3® and the prebiotic PBY was able to increase the production of SCFA. These results possibly mediated beneficial trophic effects on CAC, resulting in improved colon morphometry, integrity of the barrier with

increased intestinal crypts depth, increased cecum weight and attenuation of CAC manifestations. Similar results were observed in the study by Shinde et al. (2020), with the use of the synbiotic composed of the prebiotic based on resistant starch and the probiotic *Bacillus coagulans* MTCC 5856 in an IBD model.

The increase in the acetate and propionate metabolites, observed with the synbiotic supplementation, also benefits the integrity of the intestinal barrier through modulation of the immune response and binding to G protein-coupled receptors, such as GPR43 and GPR109A (Tedelind, Westberg, Kjerrulf, & Vidal, 2007). Thus, the joint offer of fermentable substrates, such as FOS and inulin, which directly or indirectly influence the production of SCFA and probiotic bacteria, can be an advantageous strategy in the progression of CAC.

In the present study, genera producing SCFA were identified, such as *Dubosiella*, *Ruminococcaceae_UCG-014* (ordem Clostridia) and *Lachnospirillum* (Gutiérrez & Garrido, 2019; Li et al., 2020; Takahashi et al., 2016), that can justify the increase in SCFA in the synbiotic group. Some genus of *Ruminococcaceae* can consume hydrogen to produce acetate, which is subsequently used by other bacteria to produce butyrate (Wang, Hua, et al., 2019; Wang, Li, et al., 2019). Moreover, the prebiotics are being researched to stimulate beneficial bacterial species, such as butyrate producers. Of particular interest are prebiotics that cause a bifidogenic and butyrogenic effect, such as inulin-type fructans (Riviere, Gagnon, Weckx, Roy, & DeVuyst, 2015). The increase in SCFA after administration of the yacon-based product (PBY), rich in fructooligosaccharides and inulin, has been previously demonstrated (De Nadai Marcon et al., 2019).

Conclusion

The synbiotic combination of VSL#3[®] and PBY showed potential benefits in the CAC model. Although we have identified changes in the microbial community associated with the use of the synbiotic, the causal relationship between these changes and the attenuation of CAC manifestations cannot be directly established at this time. The predominance of the *Candidatus Saccharimonas* genus, previously related to inflammatory mucosal diseases, may be a key component of CAC that needs to be further investigated. The use of the synbiotic reduced the abundance of the *Candidatus Saccharimonas* genus in the treated group when compared to the control

one. It is speculated whether *Candidatus Saccharimonas* could directly influence the inflammatory response in the initiation and progression of CAC. The increase in the antioxidant enzymes expression and the concentration of SCFA in the synbiotic group may also partially explain our findings. Together, these changes contributed especially to the trophism and improvement of the intestinal mucosa integrity.

Ethics statement

All experimental protocols were approved by the Ethics Committee in Animal Experimentation of the Federal University of Viçosa (nº 08/ 2017, date of approval: May 09, 2017), under the guidelines of the of the European Community (Directive 2010/63/EU).

CRedit authorship contribution statement

Bruna Cristina dos Santos Cruz: Conceptualization, Methodology, Formal analysis, Investigation, Writing - original draft. Lisiane Lopes da Conceição: Investigation, Formal analysis, Writing - review & editing. Tiago Antônio de Oliveira Mendes: Methodology, Formal analysis, Writing - review & editing. Célia Lúcia de Lucas Fortes Ferreira: Conceptualization, Methodology. Reggiani Vilela Gonçalves: Conceptualization, Methodology, Formal analysis. Maria do Carmo Gouveia Peluzio: . : Conceptualization, Methodology, Writing - review & editing.

Declaration of Competing Interest

The authors declare that they have no known competing financial interests or personal relationships that could have appeared to influence the work reported in this paper.

Acknowledgements

The authors would like to thank the funding agencies National Council of Technological and Scientific Development (CNPq), Coordination for the Improvement of Higher Education Personnel (CAPES), and Foundation for the Support to the Researches in Minas Gerais (Fapemig) for their financial support and fellowships.

References

Abrams, M., et al. (2012). Genomic characteristics of an environmental microbial community harboring a novel human uncultivated TM7 bacterium associated with oral diseases. *Open Access Scientific Reports*, 1.

Aebi H. (1984). Catalase *in vitro*. *Methods in Enzymology*, 105, 121-126. doi.org/10.1016/S0076-6879(84)05016-3.

Albertsen, M., Hugenholtz, P., Skarszewski, A., Nielsen, K.L., Tyson, G.W., Nielsen, P.H. (2013). Genome sequences of rare, uncultured bacteria obtained by differential coverage binning of multiple metagenomes. *Nat Biotechnol*, 31, 533-538.

Appleyard, T.R., et al. Pretreatment with the probiotic VSL#3 delays transition from inflammation to dysplasia in a rat model of colitis-associated cancer. (2011). *Am J Physiol Gastrointest Liver Physiol*. 301: G1004-G1013. doi: 10.1152/ajpgi.00167.2011.

Arthur, J.C. et al. (2012). Intestinal inflammation targets cancer-inducing activity of the microbiota. *Science* 338, 120-123.

Arthur, J.C. et al. (2013). VSL#3 probiotic modifies mucosal microbial composition but does not reduce colitis-associated colorectal cancer. *Scientific Reports*. 3:2868. doi: 10.1038.

Association of Official Analytical Chemists. (1997). *Official Methods of Analysis* (16th ed.). Gaithersburg.

Azcárate-Peril, M. A, et al. (2011). The intestinal microbiota, gastrointestinal environment and colorectal cancer: a putative role for probiotics in prevention of colorectal cancer. *Am J Physiol Gastrointest Liver Physiol*, 301, G401-G424.

Bassaganya-Riera, J., Viladomiu, M., Pedragosa, M., De Simone, C., Hontecillas, R. (2012). Immunoregulatory mechanisms underlying prevention of colitis-associated

colorectal cancer by probiotic bacteria. *PloS one*, 7(4), e34676. <https://doi.org/10.1371/journal.pone.0034676>

Bibiloni, R., Fedorak, R.N., Tannock, G.W., et al. (2005). VSL#3 probiotic-mixture induces remission in patients with active ulcerative colitis. *Am J Gastroenterol*. 100:1539-46.

Bolger, A.M., Lohse, M., Usadel, B. (2014). Trimmomatic: a flexible trimmer for Illumina sequence data. *Bioinformatics*, 30, 2114-2120. doi: 10.1093/bioinformatics/btu170.

Bor, B., Bedree, J.K., Shi, W., McLean, J.S. & He, X. (2019). Saccharibacteria (TM7) in the human oral microbiome. *Journal of Dental Research*. 1-10. <https://doi.org/10.1177/00220345198316>.

Brenner, D.A., Paik, Y.H., & Schnabl, B. (2015). Role of gut microbiota in liver disease. *J Clin Gastroenterol*. 49(1): S25-S27.

Buege, J. A., & Aust, S. D. (1978). Microsomal Lipid Peroxidation. *Methods in Enzymology*. [https://doi.org/10.1016/S0076-6879\(78\)52032-6](https://doi.org/10.1016/S0076-6879(78)52032-6)

Callahan, B.J., McMurdie, P.J., Rosen, M.J., Han, A.W., Johnson, A.J.A., Holmes, S.P. (2016). DADA2: High resolution sample inference from Illumina amplicon data. *Nat Methods*, 13, 581–583. doi: 10.1038/nmeth.3869.

Camelo-Castillo, A.J. et al. (2015). Subgingival microbiota in health compared to periodontitis and the influence of smoking. *Front Microbiol*, 6, 1-12.

Carson, F. L. et al. (1973). Formalin fixation for electron microscopy: a re-evaluation. *American Journal of Clinical Pathology*, 59, 365-73.

Chang, J.H., Shim, Y.Y., Cha, S.K., Reaney, M.J.T., Chee, K.M. (2012). Effect of *Lactobacillus acidophilus* KFRI342 on the development of chemically induced precancerous growths in the rat colon. *J Med Microbiol*, 61, 361-368.

Chen, X., Fu, Y., Wang, L., Qian, W., Zheng, F., & Hou, X. (2019). *Bifidobacterium longum* and VSL#3[®] amelioration of TNBS-induced colitis associated with reduced HMGB1 and epithelial barrier impairment. *Dev Comp Immunol*, 92, 77-86. doi: 10.1016/j.dci.2018.09.006.

Chung, E.J., Do, E.J., Kim, S.Y., Cho, E.A., Kim, D.H., Pak, S., Hwang, S.W., Lee, H.J., Byeon, J.S., Ye, B.D., Yang, D.H., Park, S.H., Yang, S.K., Kim, J.H., Myung, S.J. (2017). Combination of metformin and VSL#3 additively suppresses western-style diet induced colon cancer in mice. *European journal of pharmacology*, 794, 1–7. <https://doi.org/10.1016/j.ejphar.2016.11.012>

Clarke, W.T., Feuerstein, J.D. (2019). Colorectal cancer surveillance in inflammatory bowel disease: Practice guidelines and recent developments. *World J Gastroenterol*. 25(30):4148-4157. doi:10.3748/wjg.v25.i30.4148.

Cruz, B. C. S., Sarandy, M. M., Messias, A. C., Gonçalves, R. V, Ferreira, C. L. L. F., & Peluzio, M. C. G. (2020). Preclinical and clinical relevance of probiotics and synbiotics in colorectal carcinogenesis: a systematic review. *Nutrition Reviews*. <https://doi.org/10.1093/nutrit/nuz087>.

Dai, C., Zheng, C.Q., Meng, F., Zhou, Z., Sang, L., & Jiang, M. (2013). VSL#3 probiotics exerts the anti-inflammatory activity via PI3k/Akt and NF-κB pathway in rat model of DSS-induced colitis. *Molecular and Cellular Biology*, 374, 1-11. doi: 10.1007/s11010-012-1488-3.

De Almeida, C. V., De Camargo, M. R., Russo, E., & Amedei, A. (2019). Role of diet and gut microbiota on Colorectal cancer immunomodulation. *World Journal of Gastroenterology*. <https://doi.org/10.3748/wjg.v25.i2.151>.

De Nadai Marcon, L., Moraes, L.F.S., Cruz, B.C.S., Teixeira, M.D.O., Bruno, T.C.V., Ribeiro, I.E., Messias, A.C., Ferreira, C.L.L.F., Oliveira, L.L., & Peluzio, M.C.G. (2019). Yacon (*Smallanthus sonchifolius*)-based product increases fecal short-chain fatty acids and enhances regulatory T cells by downregulating RORγt in the colon of BALB/c mice. *Journal of Functional Foods*, 55, 333-342.

- Dewhirst FE, et al. (2010). The human oral microbiome. *J Bacteriol*, *192*, 5002-5017.
- Dieleam, L.A., Ridwan, B.U., Tennyson, G.S., Beagley, K.W., Bucy, R.P., & Elson, C.O. (1994). Dextran sulfate sodium-induced colitis occurs in severe combined immunodeficient mice. *Gastroenterology*, *107*, 1643-1652. doi: 10.1016/0016-5085(94)90803-6.
- Dieterich, S., Bieligk, U., Beulich, K., Hasenfuss, G., & Prestle, J. (2000). Gene expression of antioxidative enzymes in the human heart: increased expression of catalase in the end-stage failing heart. *Circulation*, *101*, 33-39. doi: 10.1161/01.cir.101.1.33.
- Eaden, J.A., Abrams, K.R., Mayberry, J.F. (2001). The true risk of colorectal cancer in ulcerative colitis: a meta-analysis. *Gastroenterology*; *48*:526–535.
- Fernández, J., Redondo-Blanco, S., Gutierrez-del-Rio, I., Miguélez, E.M., Villar, C.J., Lombo, F. (2016). Colon microbiota fermentation of dietary prebiotics towards short-chain fatty acids and their roles as anti-inflammatory and antitumour agents: a review. *J Funct Foods*, *25*, 511-522.
- Fitzpatrick LR, et al. (2007). Effects of the probiotic formulation VSL#3 on colitis in weanling rats. *J Pediatr Gastroenterol Nutr*, *44*, 561-570.
- Flemer, B., Warren. R.D, Barrett, M.P., et al. (2018). The oral microbiota in colorectal cancer is distinctive and predictive. *Gut*; *67*(8):1454–1463.
- Fong, W., Li, Q., Yu, J. (2020). Gut microbiota modulation: a novel strategy for prevention and treatment of colorectal cancer. *Oncogene* *39*, 4925–4943. <https://doi.org/10.1038/s41388-020-1341-1>
- Francescone, R. et al. (2016). Cytokines, IBD, and colitis-associated cancer, *Inflamm. Bowel Dis.* *21*, 409-418. doi: 10.1097/MIB.0000000000000236.

Fredricks, D.N., Fiedler, T.L., & Marrazzo, J.M. (2005). Molecular identification of bacteria associated with bacterial vaginosis. *N Engl J Med*, *353*, 1899-1911.

Gagniere, J. et al. (2016). Gut microbiota imbalance and colorectal cancer. *World J. Gastroenterol.* *22*, 501-518.

Geier, M.S., Butler, R.N., Howarth, G.S. (2006). Probiotics, prebiotics and synbiotics: a role in chemoprevention for colorectal cancer? *Cancer Biol Ther*, *5*, 1265-1269.

Gomides, A.F., Gonçalves, R.V., de Paula, S.O., Ferreira, C.L., Comastri, D.S., & Peluzio, M.C.G. (2015). Defatted flaxseed meal prevents the appearance of aberrant crypt foci in the colon of mice increasing the gene expression of p53. *Nutr Hosp*, *31*, 1675-1681. doi: 10.3305/nh.2015.31.4.8279.

Gong, D., Gong, X., Wang, L., Yu, X., & Dong, Q. (2016). Involvement of reduced microbial diversity in inflammatory bowel disease. *Gastroenterology Research and Practice*. 1-7. <https://doi.org/10.1155/2016/6951091>.

Grancieri, M., Costa, N. M. B., Vaz Tostes, M. D. G., de Oliveira, D. S., Nunes, L. D. C., Marcon, L. D. N., et al. (2017). Yacon flour (*Smallanthus sonchifolius*) attenuates intestinal morbidity in rats with colon cancer. *Journal of Functional Foods*. *37*. <https://doi.org/10.1016/j.jff.2017.08.039>.

Grice, E.A., & Segre, J.A. (2011). The skin microbiome. *Nat Rev Microbiol*, *9*, 244-253.

Grivennikov, S. I. (2013). Inflammation and colorectal cancer: colitis-associated neoplasia. *Semin. Immunopathol*, *35*, 229-244. doi: 10.1007/s00281-012-0352 -6.

Guo, X.Y., Liu, X.J., & Hao, J.Y. (2020). Gut Microbiota in Ulcerative Colitis: Insights on Pathogenesis and Treatment. *J Dig Dis*. doi: 10.1111/1751-2980.12849.

Gutiérrez N., & Garrido, D. (2019). Species deletions from microbiome consortia reveal key metabolic interactions between gut microbes. *mSystems*. *4*(4): e00185-19.

Habig, W.H., & Jakoby, W.B. (1981). Glutathione-S-Transferase (rat and human). *Methods in Enzymology*, 77, 218-239.

Hale, L.P. et al. (2010). Dietary supplementation with fresh pineapple juice decreases inflammation and colonic neoplasia in IL-10-deficient mice with colitis. *Inflamm. Bowel Dis.*, 16, 2012-2021.

Hamamoto, N., Maemura, K., Hirata, I., Murano, M., Sasaki, S., & Katsu, K. (1999). Inhibition of dextran sulphate sodium (DSS)-induced colitis in mice by intracolonicly administered antibodies against adhesion molecules (endothelial leucocyte adhesion molecule-1 (elam-1) or intercellular adhesion molecule-1 (icam-1). *Clin. Exp. Immunol.*, 117, 462-468.

He, X., McLean, J.S., Edlund, A., Yooseph, S., Hall, A.P., Liu, S.Y., Dorrestein, P.C., Esquenazi, E., Hunter, R.C., Cheng, G., Nelson, K.E., Lux, R., & Shia, W. (2015). Cultivation of a human-associated TM7 phylotype reveals a reduced genome and epibiotic parasitic lifestyle. *PNAS*, 112. doi/10.1073/pnas.1419038112.

Herszenyi, L., et al. (2015). Colorectal cancer in patients with inflammatory bowel disease: the true impact of the risk, *Dig. Dis.*, 33, 52-57.

Isidro, R.A., Lopez, A., Cruz, M.L., Gonzalez Torres, M.I., Chompre, G., Isidro, A.A., & Appleyard, C.B. (2017). The probiotic VSL#3 modulates colonic macrophages, inflammation, and microflora in acute trinitrobenzene sulfonic acid colitis. *J Histochem Cytochem*, 65, 445-461. doi: 10.1369/0022155417718542.

Israel, A. (2000). The IKK complex: an integrator of all signals that activate NFkappaB? *Trends Cell Biol*, 10, 129-133.

Jackson, P.E., O'Connor, P.J., Cooper, D.P., Margison, G.P., Povey, A.C. (2003). Associations between tissue-specific DNA alkylation, DNA repair and cell proliferation in the colon and colon tumour yield in mice treated with 1,2-dimethylhydrazine. *Carcinogenesis*, 24, 527-533.

Jacouton, E., Chain, F., Sokol, H., Langella, P., & Bermúdez-Humarán, L. G. (2017). Probiotic strain *Lactobacillus casei* BL23 prevents colitis-associated colorectal cancer. *Front Immunol.* 8: 1553.

Kim, H.J., Camilleri, M., McKinzie, S., et al. (2003). A randomized controlled trial of a probiotic, VSL#3, on gut transit and symptoms in diarrhea-predominant irritable bowel syndrome. *Aliment Pharmacol Ther.* 17:895-904.

Kim, M., Vogtmann, E., Ahlquist, D.A., Devens, M.E., Kisiel, J.B., Taylor, W.R., White, B.A., Hale, V.L., Sung, J., Chia, N., Sinha, R., & Chen, J. (2020). Fecal metabolomic signatures in colorectal adenoma patients are associated with gut microbiota and early events of colorectal cancer pathogenesis. *mBio*, 18. doi: 10.1128/mBio.03186-19.

Koh, A., De Vadder, F., Kovatcheva-Datchary, P., Bäckhed F. (2016). From dietary fiber to host physiology: short-chain fatty acids as key bacterial metabolites. *Cell*, 165, 1332-1345. doi. org/10.1016/j.cell.2016.05.041.

Kostic, A.D. et al. (2013) *Fusobacterium nucleatum* potentiates intestinal tumorigenesis and modulates the tumor-immune microenvironment. *Cell Host Microbe* 14, 207-215

Kumar, A., Singh, N.K., Sinha, P.R. (2010). Inhibition of 1,2-dimethylhydrazine induced colon genotoxicity in rats by the administration of probiotic curd. *Mol Biol Rep*, 37, 1373-1376.

Kumar, M., Kisson-Singh, V., Coria, A.L., Moreau, F., & Chadee, K. (2017). Probiotic mixture VSL#3 reduces colonic inflammation and improves intestinal barrier function in muc2 mucin-deficient mice. *Am J Physiol Gastrointest Liver Physiol.* 1;312(1):G34-G45. doi: 10.1152/ajpgi.00298.2016.

Leu, R.K.L., Hu, Y., Brown, I.L., Woodman, R.J., Young, G.P. (2010). Synbiotic intervention of *Bifidobacterium lactis* and resistant starch protects against colorectal cancer development in rats. *Carcinogenesis*, 31 246-251.

Levine, R.L. et al. (1990). Determination of carbonyl content in oxidatively modified proteins. *Methods in Enzymology*, 186, 464-478.

Levy, M., Thaiss, C.A., Elinav, E. (2016). Metabolites: messengers between the microbiota and the immune system. *Genes Dev*, 30, 1589-1597.

Li, L.L., Wang, Y.T., Zhu, L.M., Liu, Z.Y., Ye, C.Q. & Qin, S. (2020). Inulin with different degrees of polymerization protects against diet-induced endotoxemia and inflammation in association with gut microbiota regulation in mice. *Scientific Reports*. 10(978).

Lin, M.Y., & Yen, C.L. (1999). Antioxidative ability of lactic acid bacteria. *J Agric Food Chem*, 47, 1460-1466.

Lin, H., An, Y., Hao, F., Wang, Y., & Tang, H. (2016). Correlations of fecal metabonomic and microbiomic changes induced by high-fat diet in the pre-obesity state. *Scientific Reports*, 6, doi: 10.1038/srep21618.

Liu, X.J., Yu, R., & Zou, K.F. Probiotic mixture VSL#3 alleviates dextran sulfate sodium-induced colitis in mice by downregulating t follicular helper cells. (2019). *Curr Med Sci*, 39, 371-378. doi: 10.1007/s11596-019-2045-z.

López-Posadas R et al. (2011). Tissue-nonspecific alkaline phosphatase is activated in enterocytes by oxidative stress via changes in glycosylation. *Inflamm Bowel Dis*, 17, 543-556.

Lowry, O. H. et al. (1951). Protein measurement with folin phenol reagent. *The Journal of Biological Chemistry*, 193, 265-275. PMID: 14907713.

Lutgendorff, F., et al. (2008). Probiotics enhance pancreatic glutathione biosynthesis and reduce oxidative stress in experimental acute pancreatitis. *American Journal of Physiology - Gastrointestinal and Liver Physiology*, 295, G1111-G1121.

Lutgendorff, F., et al. (2009). Probiotics prevent intestinal barrier dysfunction in acute pancreatitis in rats via induction of ileal mucosal glutathione biosynthesis. *PLoS One*, 4, 4512-4524.

Lynch, S.V., & Pedersen, O. (2016). The human intestinal microbiome in health and disease. *N. Engl. J. Med*, 375, 2369-2379.

Mantovani, A., Allavena, P., Sica, A., & Balkwill, F. (2008). Cancer-related inflammation. *Nature*, 454, 436-444. doi: 10.1038/nature07205.

McConnell, B.B., & Yang, V.W. (2009). The Role of Inflammation in the Pathogenesis of Colorectal Cancer. *Curr Colorectal Cancer Rep*, 5, 69-74.

McMurdie, P.J., & Holmes, S. (2012). Phyloseq: a bioconductor package for handling and analysis of high-throughput phylogenetic sequence data. *Pac Symp Biocomput*, 235-246.

Mimura, T., Rizzello, F., Helwig, U., et al. (2004). Once daily high dose probiotic therapy (VSL#3) for maintaining remission in recurrent or refractory pouchitis. *Gut*. 53:108-14.

Mizoguchi, A., Mizoguchi, E., Takedatsu, H., Blumberg, R.S., Bhan, A.K. (2002). Chronic intestinal inflammatory condition generates IL-10-producing regulatory B cell subset characterized by CD1d upregulation. *Immunity*, 16, 219-230

Montalban-Arques, A., & Scharl, M. (2019). Intestinal microbiota and colorectal carcinoma: implications for pathogenesis, diagnosis, and therapy. *EBioMedicine*. <https://doi.org/10.1016/j.ebiom.2019.09.050>.

Morgan, X.C. et al. (2012). Dysfunction of the intestinal microbiome in inflammatory bowel disease and treatment. *Genome Biol*, 13, R79. doi: 10.1186/gb-2012-13-9-r79.

Mosca, A., Leclerc, M., & Hugot, J. P. (2016). Gut microbiota diversity and human diseases: Should we reintroduce key predators in our ecosystem? *Frontiers in Microbiology*, 7, 455. <https://doi.org/10.3389/fmicb.2016.00455>.

Moura, N.A. (2012). Protective effects of yacon (*Smallanthus sonchifolius*) intake on experimental colon carcinogenesis. *Food and Chemical Toxicology*, 50:2902-10.

Newell, L. E., & Heddle, J. A. (2004). The potent colon carcinogen, 1,2-dimethylhydrazine induces mutations primarily in the colon. *Mutation Research Genetic Toxicology and Environmental Mutagenesis*. <https://doi.org/10.1016/j.mrgentox.2004.06.005>

Olsen, I., Yamazaki, K. (2019). Can oral bacteria affect the microbiome of the gut?. *Journal of oral microbiology*, 11(1), 1586422. <https://doi.org/10.1080/20002297.2019.1586422>.

Pagnini, C., et al. (2010). Probiotics promote gut health through stimulation of epithelial innate immunity. *Proc Natl Acad Sci USA*, 107, 454-459.

Paula, H.A.A., Martins, J.F.L., Sartori, S.S.R., Castro, A.S.B., Abranches, M.V., Rafael, V.C., & Ferreira, C. L. L. F. (2012). The yacon product PBY: Which is the best dose to evaluate the functionality of this new source of prebiotic fructans? Functional Foods Forum Probiotics. Turku. Finland.

Potack, J., & Itzkowitz, S. H. (2008). Colorectal cancer in inflammatory bowel disease. *Gut Liver* 2, 61-73. doi: 10.5009/gnl.2008.2.2.61.

Quast, C., Pruesse, E., Yilmaz, P., Gerken, J., Schweer, T., Yarza, P., Peplies, J., & Frank Oliver Glöckner. (2013). The SILVA ribosomal RNA gene database project: improved data processing and web-based tools. *Nucleic Acids Res*, 41, D590-D596. doi: 10.1093/nar/gks1219.

Reeves, P.G., Nielsen, F.H., & Fahey, G.C. (1993). AIN-93 purified diets for laboratory rodents: final report of the American Institute of Nutrition *ad hoc* writing Committee on the reformulation of the AIN-76A rodent diet. *The Journal of Nutrition*, 1939-1951.

Reiff, C. et al. (2009). Balancing inflammatory, lipid, and xenobiotic signaling pathways by VSL#3, a biotherapeutic agent, in the treatment of inflammatory bowel disease. *Inflamm Bowel Dis*, 15, 17213-6.

Richard, M.L., Liguori, G., Lamas, B., Brandi, G., da Costa, G., Hoffmann, T.W., Pierluigi Di Simone, M., Calabrese, C., Poggioli, G., Langella, P., Campieri, M., & Sokol, H. (2018). Mucosa-associated microbiota dysbiosis in colitis associated cancer. *Gut Microbes* 9, 131-142. doi: 10.1080/19490976.2017.1379637.

Rivière, A., Gagnon, M., Weckx, S., Roy, D., & DeVuyst, L. (2015). Mutual cross-feeding interactions between *Bifidobacterium longum* NCC2705 and *Eubacterium rectale* ATCC33656 explain the bifidogenic and butyrogenic effects of arabinoxylan-oligosaccharides. *Appl. Environ. Microbiol.* 81, 7767-81. doi:10.1128/AEM.02089-15.

Rothemich, A., & Arthur, J.C. (2019). The Azoxymethane/Il10^{-/-} Model of Colitis-Associated Cancer (CAC). *Methods Mol Biol*, 1960, 215-225. doi: 10.1007/978-1-4939-9167-9_19.

Rubinstein, M.R. et al. (2013). *Fusobacterium nucleatum* promotes colorectal carcinogenesis by modulating E-cadherin/ β -catenin signaling via its FadA adhesin. *Cell Host Microbe* 14, 195-206.

Russo, D., Valentão, P., Andrade, P. B., Fernandez, E. C., & Milella, L. (2015). Evaluation of antioxidant, antidiabetic and anticholinesterase activities of *Smallanthus sonchifolius* landraces and correlation with their phytochemical profiles. *International Journal of Molecular Sciences*. 16(8), 17696-718. <https://doi.org/10.3390/ijms160817696>.

Saraggi, D., Fassan, M., Mescoli, C., Scarpa, M., Valeri, N., Michielan, A., D'Inca, R., Rugge, M. (2017). The molecular landscape of colitis-associated carcinogenesis. *Digestive and Liver Disease*, 49, 326-330. <http://dx.doi.org/10.1016/j.dld.2016.12.011>.

Sartor, R.B., Wu, G.D. (2017). Roles for intestinal bacteria, viruses, and fungi in pathogenesis of inflammatory bowel diseases and therapeutic approaches. *Gastroenterology*. 152(2):327-39 e4. <https://doi.org/10.1053/j.gastro.2016.10.012>

Schmidt, T.S.B., Raes, J., & Bork, P. (2018). The human gut microbiome: from association to modulation. *Cell*, 172, 1198-1215.

Sekirov, I. et al. (2010). Gut microbiota in health and disease. *Physiol. Rev.* 90, 859-904.

Sheng, K., He, S., Sun, M., Zhang, G., Kong, X., Wang, J., Wang, Y., (2020). Synbiotic supplementation containing *Bifidobacterium infantis* and xylooligosaccharides alleviates dextran sulfate sodium-induced ulcerative colitis. *Food & function*, 11(5), 3964–3974. <https://doi.org/10.1039/d0fo00518e>

Shinde, T., Perera, A.P., Vemuri, R., Gondalia, S.V., Beale, D.J., Karpe, A.V., Shastri, S., Basheer, W., Southam, B., Eri, R., Stanley, R. (2020). Synbiotic supplementation with prebiotic green banana resistant starch and probiotic *Bacillus coagulans* spores ameliorates gut inflammation in mouse model of inflammatory bowel diseases. *European Journal of Nutrition*. <https://doi.org/10.1007/s00394-020-02200-9>.

Simonovska, B., et al. (2003). Investigation of phenolic acids in yacon (*Smallanthus sonchifolius*) leaves and tubers. *J Chromatogr A*, 1016, 89-98.

Smiricky-Tjardes, M.R. et al. (2003). Dietary galactooligosaccharides affect ileal and total tract nutrient digestibility, ileal and fecal bacterial concentrations, and ileal fermentative characteristics of growing pigs. *Journal of Animal Science*, 81, 2535-2545. doi: 10.2527/2003.81102535x.

Soo, I., et al. (2008). VSL#3 probiotic upregulates intestinal mucosal alkaline sphingomyelinase and reduces inflammation. *Can J Gastroenterol*, 22, 237-242.

Sturlan, S., Oberhuber, G., Beinhauer, B.G., Tichy, B. Kappel, S., Wang, J., & Rogy, M.A. (2001). Interleukin-10-deficient mice and inflammatory bowel disease associated cancer development. *Carcinogenesis*, 22, 665-671.

Sun, C.H., Li, B.B., Wang, B., Zhao, J., Zhang, X.Y., Li, T.T., Li, W.B., Tang, D., Qiu, M. J., Wang, X.C., Zhu, C.M., Qian, Z.R. (2019). The role of *Fusobacterium nucleatum* in colorectal cancer: from carcinogenesis to clinical management. *Chronic diseases and translational medicine*, 5(3), 178–187. <https://doi.org/10.1016/j.cdtm.2019.09.001>

Takahashi, K., Nishida, A., Fujimoto, T., Fujii, M., Shioya, M., Imaeda, H. et al. (2016). Reduced abundance of butyrate-producing bacteria species in the fecal microbial community in Crohn's Disease. *Digestion*. 93:59-65. doi: 10.1159/000441768.

Talero, E., Bolivar, S., Ávila-Román, J., Alcaide, A., Fiorucci, S., & Motilva, V. (2015). Inhibition of chronic ulcerative colitis-associated adenocarcinoma development in mice by VSL#3. *Inflamm Bowel Dis*. 21:1027-37.

Tanaka T. et al. (2012). Animal models of carcinogenesis in inflamed colorectum: potential use in chemoprevention study, *Curr. Drug Targets* 13, 1689-1697.

Tedelind, S., Westberg, F., Kjerrulf, M., Vidal, A. (2007). Anti-inflammatory properties of the short-chain fatty acids acetate and propionate: a study with relevance to inflammatory bowel disease. *World J Gastroenterol*, 13, 2826.

Umizah, L.P., Wasityastuti, W., Widasari, D.Y., & Setyo, P. (2020). Effects of yacon on colonic IFN- γ and goblet cells of 2,4,6-trinitrobenzene sulfonic acid-induced colitis mouse model. *Iran Biomed J*. doi: 10.29252/ibj.24.5.276.

Urbanska, A.M., Bhatena, J., Cherif, S., Prakash, S., Orally delivered microencapsulated probiotic formulation favorably impacts polyp formation in APC (Min/+) model of intestinal carcinogenesis. (2012). *Artif Cells Nanomed Biotechnol*, 1-11.

Uronis, J. M., Muhlbauer, M., Herfarth, H. H., Rubinas, T. C., Jones, G. S., and Jobin, C. (2009). Modulation of the intestinal microbiota alters colitis-associated colorectal cancer susceptibility. *PLoS ONE*, *4*, doi: 10.1371/journal.pone.0006026.

van der Beek, C.M., Dejong, C.H., Troost, F.J., Masclee, A.A., Lenaerts, K. (2017). Role of short-chain fatty acids in colonic inflammation, carcinogenesis, and mucosal protection and healing. *Nutr Ver*, *75*, 286-305. doi.org/10.1093/nutrit/nuw067.

Villéger, R., Lopès, A., Veziat, J., Gagnière, J., Barnich, N., Billard, E., & Bonnet, M. (2018). Microbial markers in colorectal cancer detection and/or prognosis. *World Journal of Gastroenterology*, *24*, 2327–2347. <https://doi.org/10.3748/wjg.v24.i22.2327>.

Wallin, B., Rosengren, B., Shetzer, H.G., & Cameja, G. (1993). Lipid oxidation and measurement of thiobarbituric acid reacting substances (TBARS) formation in a single microtitre plate: its use for evaluation of antioxidants. *Analytical Biochemistry*, *208*, 10-15. doi: 10.1006/abio.1993.1002.

Wang, H., Li, S., Li, H., Du, F., Guan, J., & Wu, Y., (2019). Mechanism of Probiotic VSL#3 Inhibiting NF- κ B and TNF- α on Colitis through TLR4-NF- κ B Signal Pathway. *Iran J Public Health*. *48*(7): 1292–1300.

Wang, Z., Hua, W., Li, C., Chang, H., Liu, R., Ni, Y., Sun, H., Li, Y., Wang, X., Hou, M., Liu, Y., Xu, Z., & Ji, M. (2019). Protective role of fecal microbiota transplantation on colitis and colitis-associated colon cancer in mice is associated with treg cells. *Front Microbiol*, *10*. doi: 10.3389/fmicb.2019.02498.

Wong, S.H. et al. (2017). Quantitation of faecal *Fusobacterium* improves faecal immunochemical test in detecting advanced colorectal neoplasia. *Gut*, *66*, 1441-1448.

Xiong, Y. et al. (2004). Short-chain fatty acids stimulate leptin production in adipocytes through the G protein-coupled receptor GPR41. *Proc Natl Acad Sci USA*, *101*, 1045-1050.

Zavasic, G., Petricevic, S., Radulovic, Z., Begovic, J., Golic, N., Topisirovic, L., & Strahinic, I. (2012). Probiotic features of two oral *Lactobacillus* isolates. *Brazilian Journal of Microbiology*, *43*, 418-428. doi: 10.1590/S1517-838220120001000050.

Zhang, B.W., Li, M., Ma, L.C., Wei, F.W. (2006). A widely applicable protocol for DNA isolation from fecal samples. *Biochemical Genetics*, *44*. doi: 10.1007/s10528-006-9050-1.

Zheng, H.H., & Jiang X.L. (2016). Increased risk of colorectal neoplasia in patients with primary sclerosing cholangitis and inflammatory bowel disease: a meta-analysis of 16 observational studies. *Eur. J. Gastroenterol. Hepatol.* *28*, 383-390. doi: 10.1097/MEG.0000000000000576.

Zhou, Q., Shen, Z. F., Wu, B. S., Xu, C. B., He, Z. Q., Chen, T., Shang, H. T., Xie, C. F., Huang, S. Y., Chen, Y. G., Chen, H. B., & Han, S. T. (2019). Risk of Colorectal Cancer in Ulcerative Colitis Patients: A Systematic Review and Meta-Analysis. *Gastroenterology research and practice*, 5363261. <https://doi.org/10.1155/2019/5363261>.

4.5 MANUSCRIPT 5

Manuscript in submission process (British Journal of Nutrition - Impact Factor: 3.718)

Modulation of metabolic pathways in the intestinal microbiota and on the expression of genes related to tumorigenesis in a colitis-associated carcinogenesis model, using synbiotic VSL#3 and yacon-based product (PBY).

Bruna Cristina dos Santos Cruz^a, Vinícius da Silva Duarte^b, Roberto Sousa Dias^c, Valéria Monteze Guimarães^d, Célia Lúcia de Luces Fortes Ferreira^e, Maria do Carmo Gouveia Peluzio^a

^aNutritional Biochemistry Laboratory, Department of Nutrition and Health, Universidade Federal de Viçosa – UFV, Viçosa, Minas Gerais, Brazil.

^bFaculty of Chemistry, Biotechnology and Food Science, Norwegian University of Life Sciences – NMBU, Norway.

^cImmunovirology Laboratory, Department of General Biology, Universidade Federal de Viçosa – UFV, Viçosa, Minas Gerais, Brazil.

^dBiochemical Analysis Laboratory, Department of Biochemistry and Molecular Biology, Universidade Federal de Viçosa – UFV, Viçosa, Minas Gerais, Brazil.

^eInstitute of Biotechnology Applied to Agriculture & Livestock (Bioagro), Universidade Federal de Viçosa – UFV, Viçosa, Minas Gerais, Brazil.

Abstract

Previously, a synbiotic combination of probiotic VSL#3 and yacon based product (PBY), showed an effect in the preservation of intestinal architecture, increased expression of antioxidant enzymes, improved intestinal integrity and changes in the intestinal microbiota in a colitis-associated carcinogenesis model (CAC). In this study, we investigate the effects of the synbiotic VSL#3 and PBY on the intestinal inflammatory response, expression of genes associated with colorectal carcinogenesis, β -glucuronidase enzyme activity, functional metabolic pathways of the microbiota, and production of fecal fatty acids. For this, IL-10^{-/-} mice were divided into three experimental groups: negative control (KONEG), without cancer induction and standard diet; positive control (KOCON), with induction of cancer and standard diet, and synbiotic group (KOSYN), with cancer induction and diet enriched with PBY and probiotic VSL#3. Lower expression of p53 and c-myc in the KONEG and KOSYN groups compared to KOCON was observed. Similarly, IL-17 levels were also lower in these groups. There was also an increase in IL-4 in the KOSYN group compared to KONEG, and an increase in TNF in the KOCON group compared to KONEG. The principal component analysis revealed a poorly differentiated intestinal community based on MetaCyc pathways. These findings support the similarity in predicted metabolic pathways between groups. There was also a reduction in the activity of the β -glucuronidase enzyme and an increase in short-chain fatty acids in the KOSYN group. Thus, it is suggested that the synbiotic could be a novel potential health-protective natural agent against CAC.

Keywords: synbiotic, gut microbiota, colitis, colorectal cancer, inflammatory bowel disease.

Introduction

Inflammatory bowel disease (IBD), which includes Crohn's Disease (CD), ulcerative colitis (UC) and indeterminate colitis, are complex disorders associated with an unregulated immune response. Inflammation is triggered by response T (Th) 1 and Th17, with consequent secretion of pro-inflammatory cytokines. The inflammatory response can also be mediated by Th2, leading to activation of B cells and natural killer T cells (Sairenji, Collins, & Evans, 2017; Flynn, & Eisenstein, 2019).

The chronic intestinal inflammatory process is a predisposing factor for the onset of complications associated with IBD, such as colitis-associated cancer (CAC). CAC accounts for approximately 5% of colorectal cancer (CRC) cases, and the estimated risk of individuals with IBD developing CAC increases by 0.5% to 1% per year after 8 to 10 years of diagnosis (Tan, Huang, Chen & Zhi, 2020; Askling et al., 2001).

Although the incidence of IBD and, consequently, its complications have increased, the causal factors have not yet been fully elucidated. It is believed that the interaction between genetic factors, luminal factors (related to the intestinal microbiota, its antigens and metabolic products), factors related to the intestinal barrier (including aspects related to innate immunity and intestinal permeability), and factors related to immunoregulation (acquired immunity), contribute to the development of intestinal inflammation (Kelsen, Russo, & Sullivan, 2019; Chou et al., 2020).

The participation of the intestinal microbiota in the pathogenesis of these diseases has gained prominence, since studies have shown changes in the structure and activity of the intestinal microbiota in sick individuals (Imhann et al, 2018; Blander et al., 2017). In general, gut microbiota exhibits general decreases in taxonomic diversity relative, along with Phylum-level decreases in Firmicutes and increases in Proteobacteria. Proportions of the *Clostridia* family are altered: the *Roseburia* and *Faecalibacterium* genera of the *Lachnospiraceae* and *Ruminococcaceae* families are decreasing, since *Ruminococcus gnavus* increases (Sokol & Seksik, 2010; Jacobs et al., 2016).

It is possible that bacterial metabolites are involved in signaling and modulating the intestinal immune response (Dorrestein et al, 2014), and could be considered targets in the prevention of IBD and CAC. Short chain fatty acids (SCFA), for example, are produced by gut bacteria when they break down dietary fiber. SCFA, especially

butyrate, can affect host cells by modulating histone deacetylase inhibitory activity, gene expression, cell proliferation, and immune response, regulating Treg cell production and enhancing antibacterial activity of macrophages (Kim, Kim, Park, & Kwak, 2014; Fernando, Saxena, Reyes & McKay, 2016). Although scarce in the literature, some studies have identified differences in the production of fecal metabolites in individuals with intestinal diseases (Lee Gal et al., 2011; Jacobs et al., 2016).

We demonstrated previously, in a colitis-associated carcinogenesis model, that the microbiota of the experimental model is characterized by a restricted biodiversity, with a limited number of bacterial genera. A high abundance of *Candidatus Saccharimonas*, a genus still little associated with the genesis of intestinal diseases, was observed. However, the use of a synbiotic, which combined probiotic bacterial species with a highly fermentable fiber source, was able to cause some changes in the structure of the microbiota, which possibly contributed to attenuate the manifestations of colitis and improve intestinal integrity in this model (Cruz, Conceição, Mendes, Ferreira, Gonçalves & Peluzio, 2020).

In this sense, we hypothesize that the use of synbiotic, targeting the modulation of the intestinal microbiota, is able to improve intestinal inflammation, regulate the expression of genes associated with carcinogenesis, and modify microbial activity, altering metabolic pathways, enzymatic activity and production of metabolites. Due to the limited data in the literature about the influence of microbiota on the progression of CAC and its clinical relevance, our objective was to investigate the effects of the synbiotic on the intestinal inflammatory response, on the expression of genes associated with colorectal carcinogenesis, on the β -glucuronidase enzyme activity, in the functional metabolic pathways of the microbiota, and in the production of fecal fatty acids.

Material and Methods

Synbiotic

The synbiotic was composed of the yacon-based product (PBY) associated with the multispecies probiotic VSL#3. The PBY is a concentrated product prepared from fresh yacon (*Smallanthus sonchifolius*) root, and is a source of the prebiotics fructooligosaccharides (FOS) and inulin. PBY was produced as described by Paula et

al., (2012) (Patent: PI 1106621-0). The centesimal composition of PBY was determined according to the AOAC methodology; FOS and inulin contents were determined by high performance liquid chromatography (HPLC) (Table 1). Probiotic VSL#3 (Sigma Tau Pharmaceuticals, Inc.; acquired in 2016, valid 04/2018, lot number 604094) is composed of the following bacterial species: *Bifidobacterium breve*, *Bifidobacterium infantis*, *Bifidobacterium longum*, *Lactobacillus acidophilus*, *Lactobacillus bulgaricus*, *Lactobacillus casei*, *Lactobacillus plantarum* and *Streptococcus thermophilus*.

Table 1. Centesimal composition and oligofructanos content of the yacon-based product (PBY).

Components	g/100g
Carbohydrates	38.16
Fructose	9.4
Glucose	6.45
Sucrose	3.05
<i>Fructooligosaccharide (FOS)</i>	17.65
<i>Inulin</i>	5.95
Fiber	1.64
Protein	2.51
Fat	0.04
Moisture	37.2
Ashes	1.55

The experimental diets were elaborated according to the recommendations of Reeves, Nielsen & Fahey (1993), and adapted to include the synbiotic formulation. PBY was added to the diet to provide 6% FOS and inulin (De Nadai Marcon et al., 2020; De Nadai Marcon et al., 2019; Paula et al., 2012).

Animals and experimental design

Twenty-one interleukin-10-knockout mice (IL-10^{-/-}), male, from the Central Bioterium of the Federal University of Alfenas (UNIFAL), Minas Gerais, Brazil, were used. The IL-10^{-/-} mice were generated from the C57BL/6J background. Under conventional housing conditions, they develop chronic colitis at six weeks of age

(Sturlan et al., 2001). The animals were collectively allocated in polypropylene cages, kept under controlled conditions, at a temperature of $22 \pm 2^\circ \text{C}$ and humidity of 60% - 70%, with a 12-hour light/dark cycle.

After a one-week acclimation period in the experimental animal house, receiving a standard pellet commercial diet (Purina®), the eight-week-old animals with an average weight of 25g were distributed into three experimental groups: (1) negative control group (KONEG; n = 6), (2) control group (KOCON; n = 8), and synbiotic group (KOSYN; n = 7).

Experimental diets were offered for a period of 13 weeks. From the third experimental week on, the colorectal carcinogenesis induction protocol was started. The animals (except the negative control group) received a weekly intraperitoneal injection with the carcinogen 1,2 dimethylhydrazine (20 mg/kg) (Sigma-Aldrich, Saint Louis, USA), totaling eight applications (Gomides et al., 2014; Newell & Heddle, 2004).

The animals in the negative control group (KONEG) received standard rodent diet (AIN93-M), water (0.1 mL) via orogastric gavage, and were not induced to colorectal carcinogenesis. The control group (KOCON) received AIN93-M diet, water (0.1 mL) via orogastric gavage, and were induced to colorectal carcinogenesis with DMH. The animals in the synbiotic group (KOSYN) received modified AIN93-M diet, with addition of PBV (6% FOS and inulin) and probiotic VSL#3, via orogastric gavage (0.1 mL; 2.25×10^9 CFU/ day) and were induced to colorectal carcinogenesis with DMH.

The animals were weighed weekly and food intake assessed daily. In addition, feces collected in the first (t_0) and last (t_1) experimental week were used to determine SCFA, and to assess the activity of the β -glucuronidase enzyme (t_1) and fecal pH (t_1). To obtain the samples, the animals were kept individually, in sanitized cages, until they expelled a sufficient amount of feces. Samples were transferred to microtubes and stored at -80°C .

At the end of 13 experimental weeks, the animals were anesthetized with isoflurane 3% (Isoflurine®, Cristalia, Itapira, Brazil), followed by total exsanguination by the retro orbital sinus. After dissection, the tissues were washed with cold 0.1 M phosphate-buffered saline (PBS, pH 7.2) and weighed in a semi-analytical balance. The colon tissue was divided into two parts, one being stored at -80°C (as well as the spleen) and the other stored in Trizol (Invitrogen™, Carlsbad, CA, USA) for further analysis.

All experimental protocols were approved by the Ethics Committee in Animal Experimentation of the Federal University of Viçosa (n° 08/ 2017, date of approval: May 09, 2017), under the guidelines of the of the European Community (Directive 2010/63/EU).

Quantitative real-time polymerase chain reaction (RT-qPCR)

The expression of genes related to carcinogenesis, p53, c-myc, PCNA, and caspase 3 was evaluated in the colon using the quantitative real-time polymerase chain reaction (RT-qPCR). Total RNA was extracted and quantified on a Multiskan™ GO spectrophotometer (Thermo Fisher Scientifics; Waltham, MA, USA). The RNA samples were treated with DNase (DNase I; Promega, Madison, WI, USA), as described below: samples containing 2 µg of RNA were treated with 3 µL of DNase buffer and 4.5 µL of DNase. For this, the samples were incubated at 37° C for 30 min, and at 70° C for 10 min. After incubation, they were placed on ice, for 5 min. Real-time PCR quantitative mRNA analyses were performed in an Illumina Eco Real-Time PCR system (Illumina, San Diego, CA, USA), using the GoTaq® 1-Step RT-qPCR System (Promega, Madison, WI, USA), according to the manufacturer's instructions. The analysis conditions were: one cycle reverse transcription (37° C, 15 min), and one cycle reverse transcriptase inactivation and GoTaq® DNA polymerase activation (95° C, 10 min), followed by 40 cycles of denaturation (95° C, 10 seconds), annealing (60° C, 30 seconds) and extension (72° C, 30 seconds). The results were analyzed by the $2^{-\Delta\Delta C_t}$ algorithm on the EcoStudy® software (Illumina), using GAPDH gene as an endogenous control. The following sequences of murine primers were used: c-myc – sense: 5'-TCGTGTACCTCGTCCGATTC-3', antisense: 5'-GGAGGACAGCAGCGAGTC-3' (Zeineldin et al., 2012); p53 – sense: 5'-GTATTTACCCCTCAAGATCC-3', antisense: 5'-TGGGCATCCTTTAACTCTA-3' (Kiatpakdee et al., 2020); PCNA – sense: 5'-TAAAGAAGAGGAGGCGGTAA-3', antisense: 5'-TAAGTGTCCCATGTCAGCAA-3' (Lin & Sun, 2015); caspase 3 – sense: 5'-AGCAGCTTTGTGTGTGATTCTAA-3', antisense: 5'-AGTTTCGGCTTTCCAGTCAGA-3' (Mengying et al., 2017); GAPDH – sense: 5'-AAGTTTCTCATCTCCGCTC-3', antisense: 5'-GTTTCGAGATGATGGTGTGCT-3' (Piranlioglu et al., 2019).

Cytokine profile in colon and spleen

Pro- and anti-inflammatory cytokines profile (IL-2, IL-4, IL-6, IL-17, TNF and IFN) was evaluated in the colon and spleen using the Cytometric Bead Array (CBA) mouse Th1/Th2/Th17 Kit (BD Biosciences, San Jose, USA) in a BD FACSVerse Flow cytometry, as described below: colon and spleen samples (approximately 100 mg) were crushed using a tissue homogenizer (T10 basic UltraTurrax, IKA®, Rio de Janeiro, Brazil) in PBS, pH 7.2, centrifuged (10,000 g, for 10 min at 4° C), and the supernatant was used in the determination of cytokines. The beads were diluted with diluent solution and distributed in microtubes. 25 µL of the supernatant and 17 µL of the detector solution were added to each microtube, followed by incubation for 2 hours. Subsequently, 500 µL of the washing solution was added, followed by centrifugation (1,800 x g, for 5 min at 4° C), and despised part of the supernatant (approximately 450 µL). The remaining volume was used for reading on the flow cytometer. The data was processed using the FCAP Array 3.0 (FCAP Array Software BD Biosciences, California, USA) and the results are expressed in pg/mL.

Bioinformatics processing and metagenoma functional prediction

The raw sequence data used in the present study were acquired from the amplification and sequencing of the V3-V4 hypervariable region of the 16S rRNA genes (Cruz, Conceição, Mendes, Ferreira, Gonçalves & Peluzio, 2020). The genetic material was obtained by extracting bacterial metagenomic DNA present in fecal samples collected in the last experimental week.

Microbiota bioinformatics was carried-out with QIIME2 (version 2020.2) (Bolyen et al., 2019). Raw sequence data obtained from the IL-10^{-/-} mice feces samples belonging to the groups KONEG, KOCON, and KOSYN were imported via the Casava1.8 single-end pipeline followed by denoising with DADA2 (Callahan et al., 2016) (via q2-dada2). Afterward, Amplicon Sequence Variants (ASVs) (read sequences and read counts) were used as inputs for the PICRUST2 (Phylogenetic Investigation of Communities by Reconstruction of Unobserved States) pipeline (Douglas et al., 2020). Briefly, ASVs were inserted and aligned into a reference tree composed of 20,000 full 16S rRNA genes from bacterial and archaeal genomes using,

respectively, the tools HMMER (<http://www.hmmmer.org>) and EPA-ng/ GAPPA (Barbera et al., 2019; Czech & Stamatakis, 2019).

Subsequently, the *castor* R package (Louca & Doebeli, 2018) was used to predict the missing gene families (Enzyme Commission numbers) for each ASV, as well as their respective copy number of 16S rRNA gene sequences, by using the output tree generated previously. Lastly, MinPath (Ye & Doak, 2009) was adopted to infer MetaCyc pathways based on EC number abundances.

Evaluation of β -glucuronidase activity

The activity of the bacterial enzyme β -glucuronidase was evaluated in feces samples collected in the last week experimental, according to de Moreno de LeBlanc and Perdigon (2005), with the modifications described below. For the preparation of enzymatic extract, feces samples were homogenized in distilled water (1:30), for 1 min, on ice. Then, samples were sonicated (Branson 1210 Ultrasonic, Marshall Scientific LLC, Hampton, USA), on ice, by 3 bursts of 2 min each (1-min interval between each burst) and then centrifuged (10,000 *g*, for 15 min at 4° C). The supernatant was used for determination of enzyme activity. All enzymatic assays were carried out in phosphate buffer (200 mM, pH 6.5) at 37° C in triplicate, and the mean values calculated. Relative standard deviations of measurements were below 5%. The enzymatic reaction contained 65 μ L buffer, 25 μ L *p*-nitrophenyl β -D-glucuronide 4 mM (*p*NPG, Sigma-Aldrich, Saint Louis, USA), and 10 μ L enzymatic extract. The samples were incubated at 37°C for 3 h. Absorbance was measured at 410 nm and the amount of *p*-nitrophenol released assessed by a standard curve. One enzyme activity unit (U) was defined as the amount of enzyme which released a micromole of the *p*-nitrophenol/h under assay conditions.

Fecal fatty acids quantification

Fatty acids (acetic, propionic, butyric, isobutyric, isovaleric and valeric acids) were quantified in feces samples collected in the first (*t0*) and last (*t1*) experimental week. For this, approximately 50 mg of feces were vortexed with deionized water (950 μ L) and incubated in ice for 30 min, followed by homogenization in vortex every 5 min. Samples were centrifuged at 10,000 *g*, for 30 min at 4° C three times and the

supernatant was collected and filtered through a 0.45 μm membrane filter (Smiricky-Tjardes, Grieshop, Flickinger, Bauer, and Fahey Jr, 2003). The fatty acids were measured by high-performance liquid chromatography (HPLC) (Shimadzu[®], Quito, Japan) using an Aminex HPX 87H column at 32°C, with acidified water (H_2SO_4 , 0.005 M) as the eluent at a flow rate of 0.6 mL/min. The products were detected and quantified by an ultraviolet detector (SPD-20A VP) at 210 nm. Standard curves of acetic, propionic, butyric, isobutyric, isovaleric and valeric acids were constructed (Supelco[®], Darmstadt, Germany), and results were expressed in $\mu\text{mol/g}$ feces.

Fecal pH

To determine fecal pH, feces samples collected in the last experimental week were homogenized in distilled water (1:10) until complete dissolution, using a homogenizer (T10 basic UltraTurrax, IKA[®], Rio de Janeiro, Brazil). The pH was measured with calibrated digital pH meter (Ultra Basic UB-10[®], Hexis, Jundiaí, Brazil) in temperature-controlled environment after adequate time for pH stabilization (Bedani et al. 2011).

Statistical analysis

Statistical processing and analysis were performed using the Statistical Package for the Social Sciences 20.0 (SPSS Software IBM, Chicago, USA), and graphs were constructed using GraphPad Prism 7 (GraphPad Software LLC, La Jolla, CA). Variables were checked for distribution with the Shapiro Wilk test. The comparison between experimental groups (KONEG, KOCON, KOSYN) was assessed by one-way analysis of variance ANOVA or Kruskal-Wallis test, followed by their respective *post hoc*. Paired t-test or Wilcoxon test was used to evaluate the concentration of fatty acids after and before synbiotic administration ($t_0 \times t_1$). Correlations between continuous variables were determined by Pearson's (parametric data) or Spearman (non-parametric data) correlation. Differences were considered significant at $\alpha < 0.05$. Results were expressed as mean \pm standard deviation (SD).

Results

Food intake and body weight

Food intake was verified daily throughout the experimental period. Although fluctuations in consumption were observed at some times, the total mean intake did not differ between the groups (Figure 1A). On the other hand, despite the animals started the experimental period with homogeneous body weight, at the end of the experiment a higher mean weight was noted among the animals in the KONEG group compared to the others (Figure 1B); weight was also significantly higher in the KOCON group compared to the KOSYN group, indicating that there was interference of synbiotic consumption in weight gain.

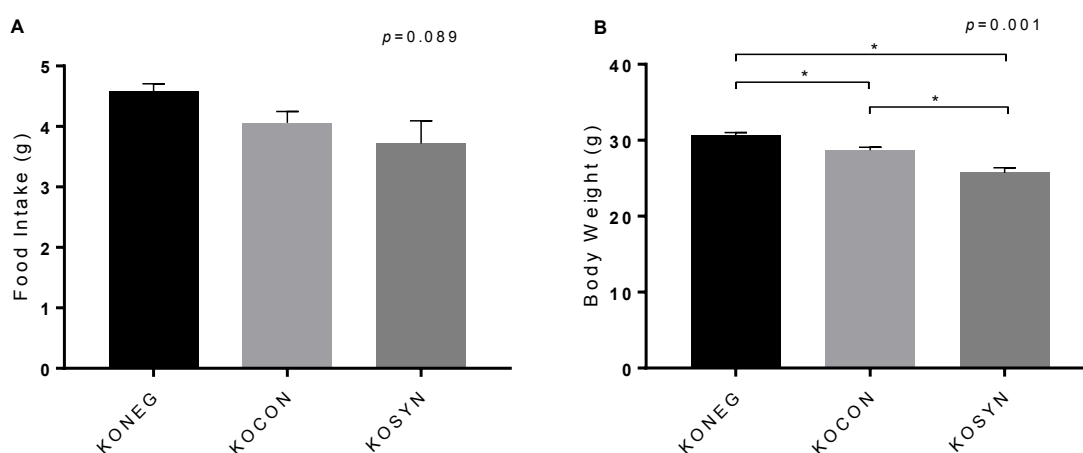


Figure 1. Effect of synbiotic VSL#3 + PBV on (A) food intake, and (B) body weight in colitis-associated carcinogenesis model. The data were expressed as mean \pm SD. Statistical differences between groups were analyzed by ANOVA test, (*) $p < 0.05$. KONEG, AIN-93M diet, without induction with DMH; KOCON, AIN-93M diet, induced with DMH; KOSYN, AIN-93M diet with PBV and probiotic VSL#3, induced with DMH.

RT-qPCR

Uncontrolled proliferation and inhibition of apoptosis are considered common events during colon carcinogenesis. To elucidate apoptosis regulation in the tumorigenesis of colon tissue using synbiotic VSL#3 and PBV, changes in mRNA expressions were monitored. The expression of p53 was significantly lower in the KONEG (5.7 fold-change) and KOSYN (4.2 fold-change) groups compared to the KOCON group ($p=0.008$) (Figure 2A). Similarly, c-myc expression was also lower in

these groups (KONEG: 7.4 fold-change; KOSYN: 1.8 fold-change; $p=0.000$) (Figure 2B).

Although synbiotic did not significantly influence PCNA and caspase 3 expression, it was observed that PCNA expression was 3.8 fold-change and 2.9 fold-change lower in KONEG and KOSYN groups, respectively, compared to KOCON (Figure 2C), and caspase 3 expression increased by 4.3 fold-change and 2.0 fold-change in the KOSYN group compared to the KONEG and KOCON groups, respectively (Figure 2D).

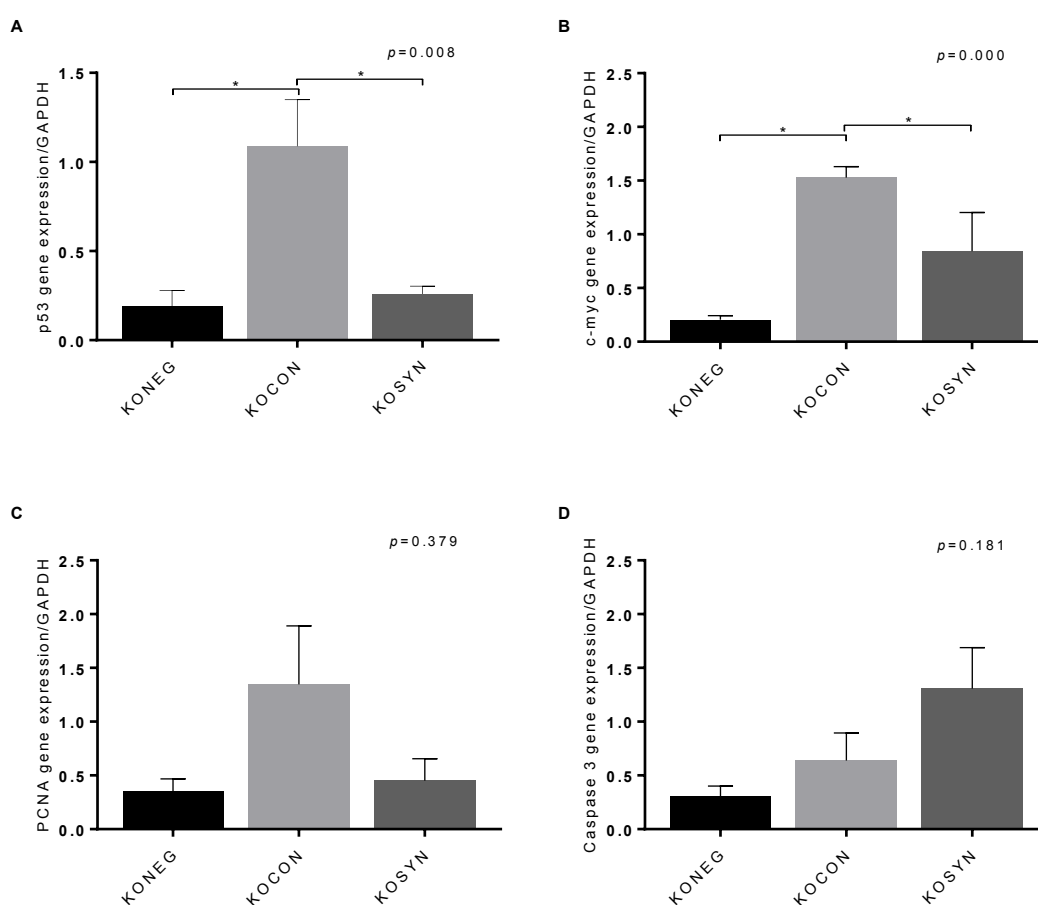


Figure 2. Effect of synbiotic VSL#3 + PBV on gene expression in colitis-associated carcinogenesis model. (A) p53, (B) c-myc, (C) PCNA, and (D) caspase-3. Gene expression was calculated in relation to the constitutive GAPDH gene and presented as a relative variation of the control group. The data are expressed as mean \pm SD. Statistical difference between groups were analyzed by *ANOVA test* or *Kruskal-Wallis test*, (*) $p < 0.05$. KONEG, AIN-93M diet, without induction with DMH; KOCON, AIN-93M diet, induced with DMH; KOSYN, AIN-93M diet with PBV and probiotic VSL#3, induced with DMH.

Cytokine profile

Comparison of Th1 (IL-2, TNF), Th2 (IL-4, IL-6) and Th17 (IL-17) levels in the colon is shown in Figure 3. Increased IL-4 concentrations were observed in the KOSYN group compared to KONEG (Figure 3B). IL-17 levels were higher in the KOCON group when compared to the other groups (Figure 3D), and increased TNF in the KOCON group compared to the KONEG (Figure 3E). No difference was observed in the cytokine profile in the spleen (data not shown).

Metabolic pathways of the intestinal microbiota

A scatter plot of the principal component analysis (PCA) using unstratified pathway abundances revealed that the experimental groups did not significantly clustered separately (Figure 4), indicating a poorly differentiated intestinal community based on metacyc pathways.

To discriminate the potential functions of the gut bacterial community among the three groups, a ANOVA test with Tukey-Kramer approach for multiple comparisons was used to the relative proportion of predicted MetaCyc pathways. From 381 predicted microbial pathways, only 12 functional pathways differed significantly (Figure 5), and the great majority (91.6%) were enriched in the KOCON group when compared with KONEG e KOSYN groups (Supplementary datasheet 1).

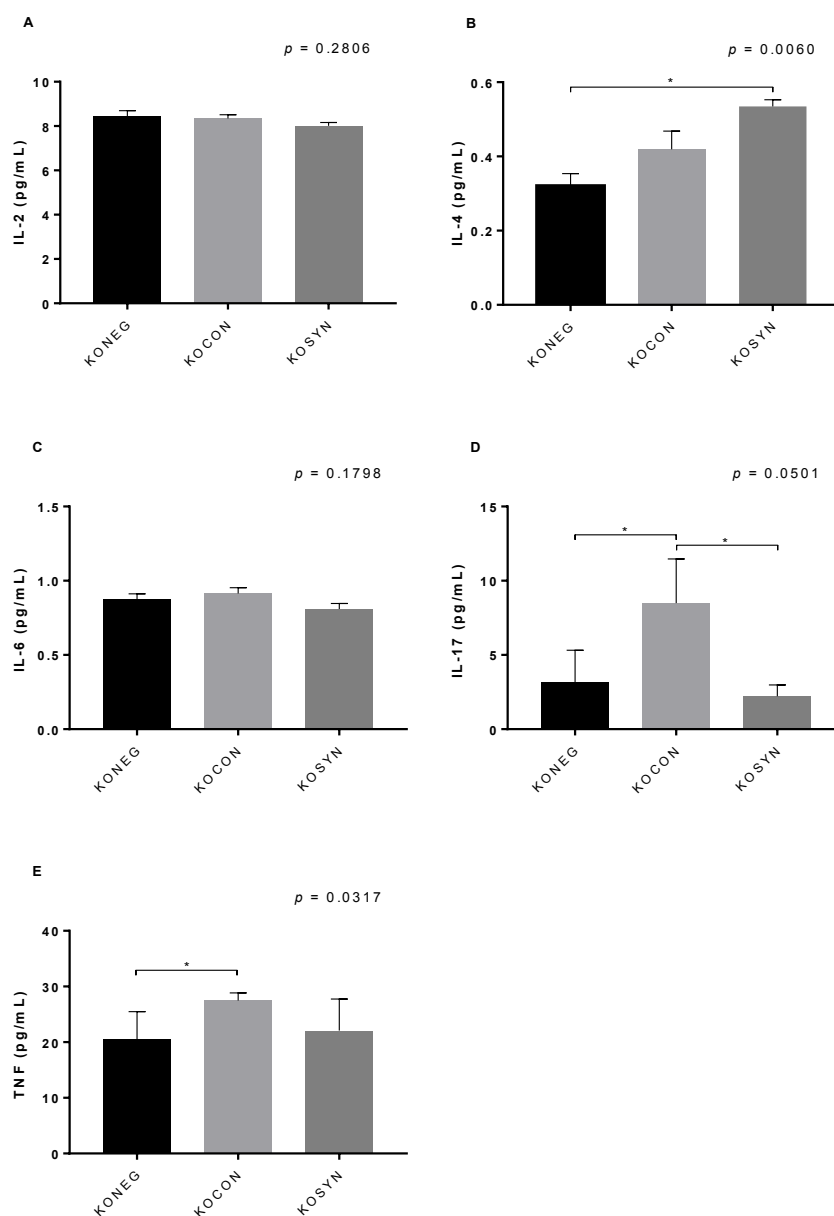


Figure 3. Effect of synbiotic VSL#3 + PBY on cytokine profile in colon tissue in colitis-associated carcinogenesis model. (A) IL-2, (B) IL-4, (C) IL-6, (D) IL-17, and (E) TNF. The data are expressed as mean \pm SD. Statistical difference between groups were analyzed by *ANOVA test* or *Kruskal-Wallis test*, (*) $p < 0.05$. KONEG, AIN-93M diet, without induction with DMH; KOCON, AIN-93M diet, induced with DMH; KOSYN, AIN-93M diet with PBY and probiotic VSL#3, induced with DMH.

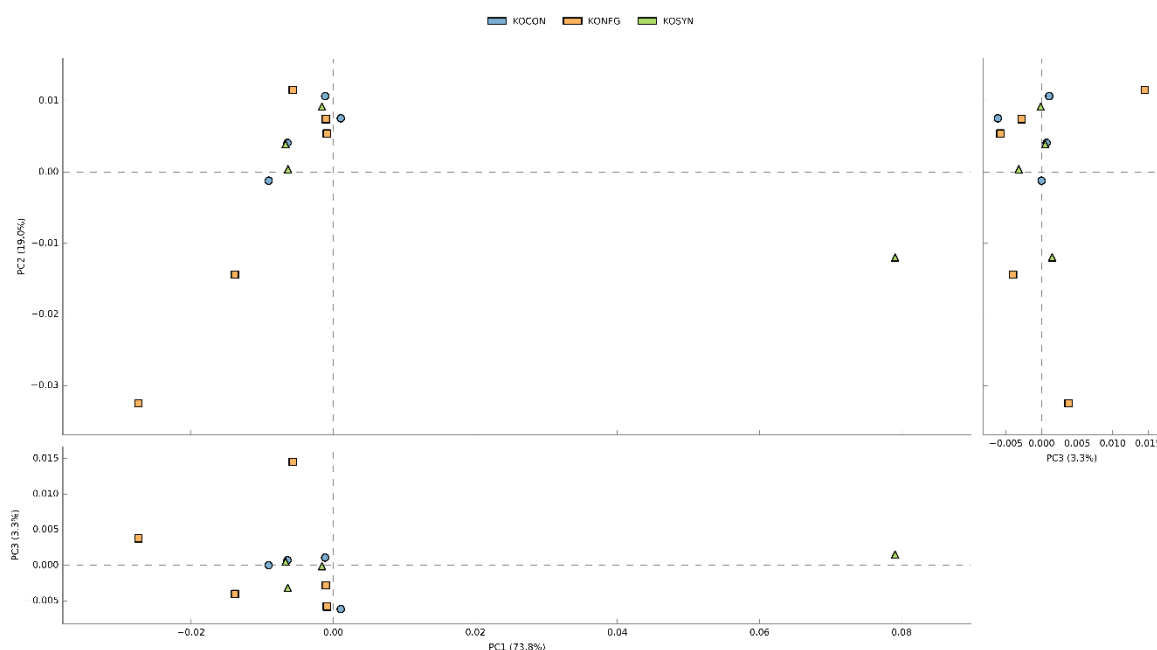


Figure 4. Principal Component Analysis (PCA) based on the normalized abundance of predicted MetaCyc pathways across the different groups (KONEG, KOCON, and KOSYN).

Taking into account only those MetaCyc pathways with an effect size greater than 0.5, those that differed significantly between the groups were: chitin derivatives degradation; D-galactarate degradation I; L-glutamate degradation V (via hydroxyglutarate); L-glutamate degradation VIII; L-lysine fermentation to acetate and butanoate; superpathway of methylglyoxal degradation; myo-, chiro- and scillo-inositol degradation; nylon-6 oligomer degradation; superpathway of glycerol degradation to 1,3-propanediol; superpathway methylglyoxal; superpathway of UDP-N-acetylglucosamine-derived O-antigen building blocks biosynthesis; superpathway of D-glucarate and D-galactarate degradation; superpathway ornithine. The KOSYN group exhibited an enrichment specifically only in the D-galactarate degradation I pathway.

β -glucuronidase enzyme activity

Animals in the KOCON group displayed a significant increase in β -glucuronidase enzyme activity when compared to the others (Figure 6). The activity of the KOSYN group did not differ from the KONEG group.

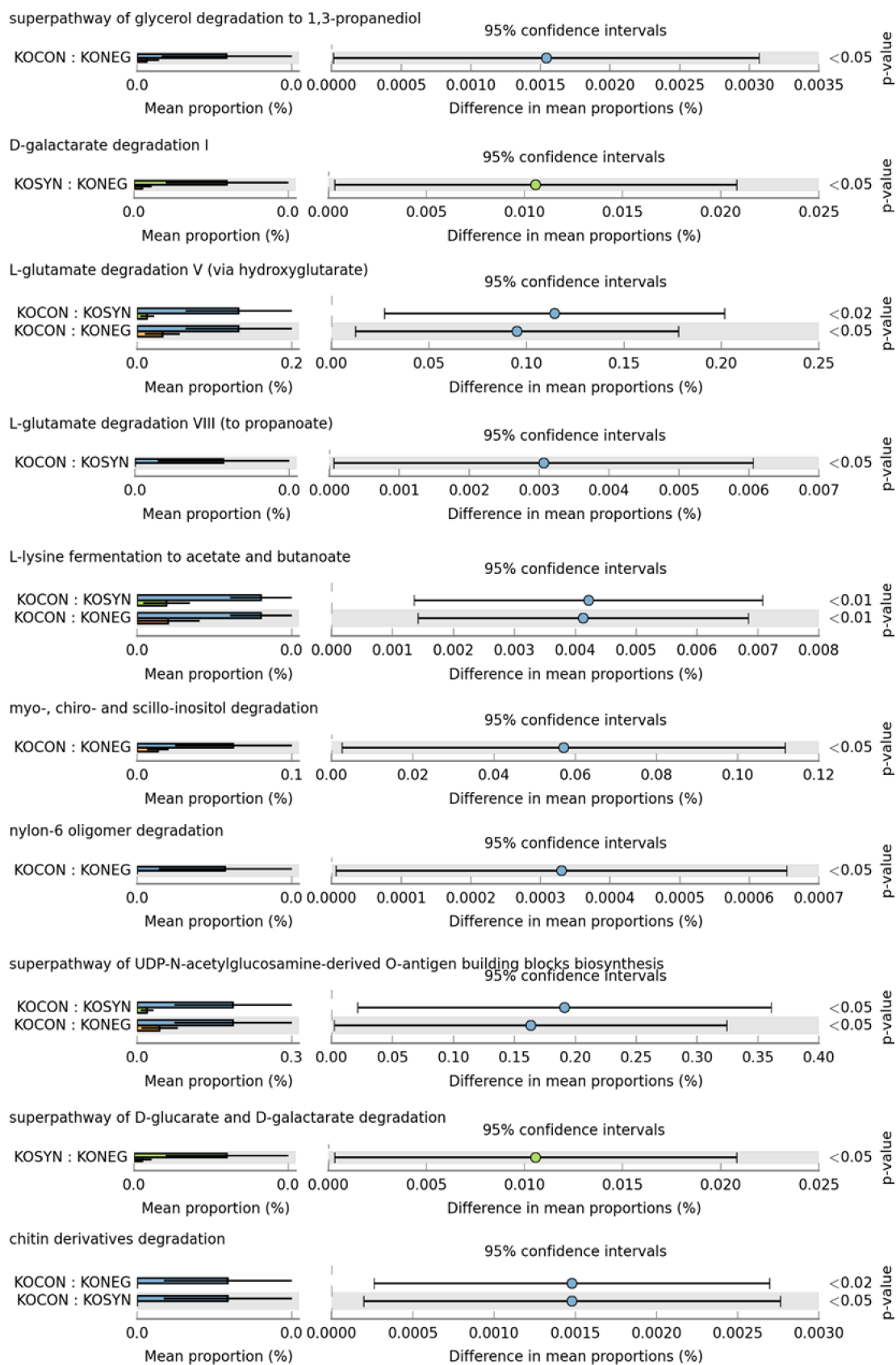


Figure 5. Predicted functional categories (MetaCyc pathways) obtained from the fecal microbiota of IL-10^{-/-} mice after intervention. Only statistically significant features were

considered (10 metabolic pathways in total, with significant *post hoc*). Functional level extended error bar chart profile between the groups KONEG, KOCON and KOSYN.

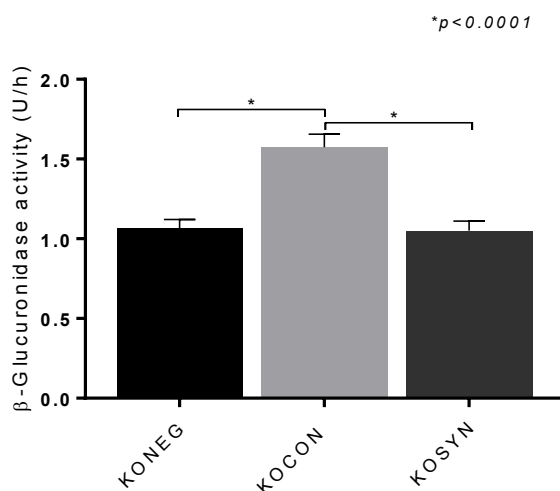


Figure 6. Effect of synbiotic VSL#3 + PBV on β -glucuronidase activity in colitis-associated carcinogenesis model. The data were expressed as mean \pm SD. Statistical differences between groups were analyzed by ANOVA test, (*) $p < 0.05$. KONEG, AIN-93M diet, without induction with DMH; KOCON, AIN-93M diet, induced with DMH; KOSYN, AIN-93M diet with PBV and probiotic VSL#3, induced with DMH.

Fecal concentration of short-chain fatty acids and branched-chain fatty acids

Fecal fatty acids were quantified at the beginning (t0) and at the end (t1) of the experimental period. The final concentrations (t1) of acetic, propionic, butyric and isobutyric acids were significantly higher in the KOSYN group compared to the others (Figures 7A-D), and there was a reduction in valeric acid concentrations in the KOCON and KOSYN groups compared to KONEG (Figure 7F). For isovaleric acid, no differences were observed between groups (differences not shown in the figure). On the other hand, the intragroup comparison (t0 x t1) showed a reduction in isobutyric acid in the KOCON group, and in isovaleric and valeric acids in the KOSYN group.

Fecal pH

Corroborating previous results, the use of synbiotic significantly reduced fecal pH (Figure 8). Similarly, the KONEG group had lower fecal pH compared to the

KOCON group. Fecal pH was inversely correlated to concentrations of acetic acid ($r = -0.593$, $p = 0.015$), butyric acid ($r = -0.634$, $p = 0.008$) and total SCFA ($r = -0.581$, $p = 0.009$), and directly correlated to isovaleric acid ($r = 0.439$) and valeric acid ($r = 0.465$) (non-significant correlation, $p > 0.05$)

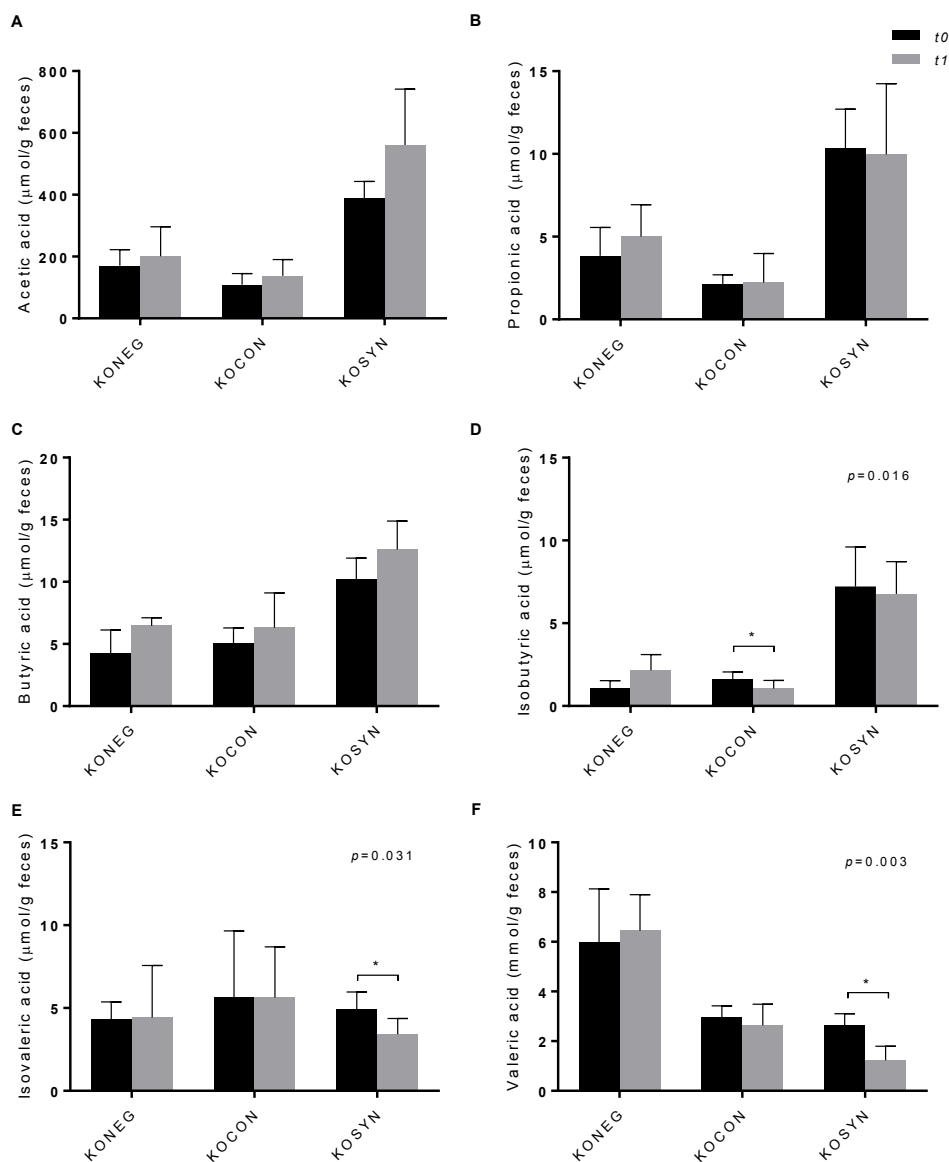


Figure 7. Effect of synbiotic VSL#3 + PBV on fecal concentrations of fatty acids after (t_0) and before (t_1) intervention in colitis-associated carcinogenesis model. The data were expressed as mean \pm SD. Statistical differences between groups were analyzed by *paired t-test* or *Wilcoxon test*, (*) $p < 0.05$. KONEG, AIN-93M diet, without induction with DMH; KOCON, AIN-93M diet, induced with DMH; KOSYN, AIN-93M diet with PBV and probiotic VSL#3, induced with DMH.

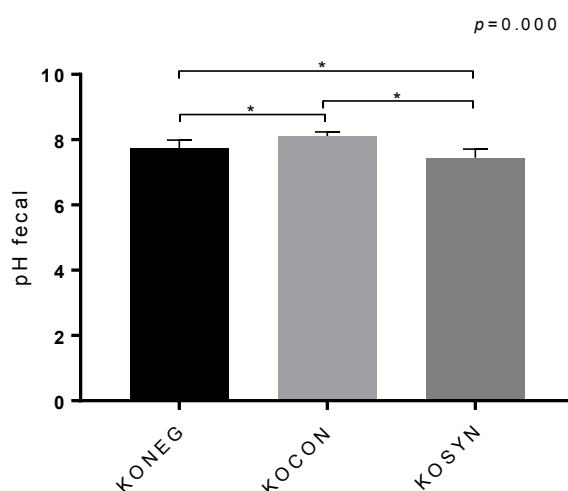


Figure 8. Effect of synbiotic VSL#3 + PBV on fecal pH in colitis-associated carcinogenesis model. Data were expressed as mean \pm SD. Statistical differences between groups were analyzed by ANOVA test, (*) $p < 0.05$. KONEG, AIN-93M diet, without induction with DMH; KOCON, AIN-93M diet, induced with DMH; KOSYN, AIN-93M diet with PBV and probiotic VSL#3, induced with DMH.

Discussion

The genesis of IBD and CRC is associated with genetic disorders, aberrant immune response, chronic inflammation, oxidative stress, and intestinal dysbiosis. These conditions are also observed in CAC models, and seem to be essential in the evolution of the disease (Keshavarzian et al., 2003; Carroll et al., 2007). To reduce the progression of IBD, studies have suggested the prophylactic use of probiotics, prebiotics and synbiotics, aiming to reduce oxidative stress, attenuate the intestinal inflammatory response, produce anti-carcinogenic metabolites, and improve intestinal barrier function. These effects are attributed to quantitative and qualitative changes in the intestinal microbiota (Genaro et al., 2019).

To substantiate this, a report showed that superoxide dismutase (SOD) overexpression in *Lactobacillus gasseri* revealed an anti-inflammatory effect on, and recovery of, colonic tissue in an interleukin-10 (IL-10)-deficient mouse model of colitis, alleviating IBD symptoms (Carroll et al., 2007). The combination of resistant starch and *Bifidobacterium animalis* subsp. *lactis* showed a protective effect in an azoxymethane (AOM)-induced rodent model of CRC (Le Leu et al., 2010). A recent report suggests

that proper modulation of gut microbiota, by ingesting specific probiotics, may help prevent tumor formation (Genaro et al., 2019).

Thus, the multispecies probiotic VSL#3 and the yacon-based product (PBY), a natural source of prebiotics, were chosen to compose a new synbiotic formulation. In a previously published report, we demonstrate that the synbiotic VSL#3 + PBY caused some changes in the structure of the microbiota, which possibly contributed to attenuate the manifestations of colitis, improve intestinal integrity, and reduce oxidative stress (Cruz, Conceição, Mendes, Ferreira, Gonçalves & Peluzio, 2020). In the present study, we investigate the effects of the synbiotic on the intestinal inflammatory response, on the expression of genes associated with colorectal carcinogenesis, on the β -glucuronidase enzyme activity, in the functional metabolic pathways of the microbiota, and in the production of short-chain fatty acids, and branched-chain fatty acids.

As noted in Fig 1. we conclude that both the use of the chemical carcinogen DMH and the synbiotic impacted on the body homeostasis of the animals. At the end of the experimental period, although food intake did not differ significantly, the KOCON and KOSYN groups had lower mean body weight compared to KONEG. Weight loss is one of the characteristics inherent to the CAC model, which is one of the parameters used to assess disease activity (disease activity index) (Han et al., 2020).

The lower body weight in the KOSYN group, besides being influenced by the drug DMH, is justified by lower food intake in the 5th, 6th, 7th and 11th week (data not shown). PBY is rich in soluble fiber, which gives the synbiotic greater satiety (Li, Li, & Xu, 2021). Furthermore, the fermentation of FOS and inulin leads to the production of SCFA, which also increase satiety by influencing leptin production (Xiong, 2004). A similar result was demonstrated by De Nadai Marcon et al., (2019), in mice fed with PBY for eight weeks.

DMH is a chemical carcinogen widely used to induce colon tumors in rodents in a dose-dependent manner (Rosenberg et al., 2009). DMH undergoes metabolic activation in the liver by cytochrome (CYP)2E1, and is converted into highly reactive intermediates such as azoxymethane, methylsoxymethanol acetate and methyldiazonium and methyl ions. These metabolites are transported by bile or the bloodstream to the colon, where they can alkylate the bases of DNA, triggering carcinogenesis (Perše and Cerar, 2011).

Apoptosis is a programmed cell death event caused by cell changes, such as blebbing, morphological change, cell shrinkage, chromatin condensation, apoptotic DNA fragmentation, and mRNA decay. While cancer cells avoid the apoptosis for carcinogenesis, apoptosis may be a process for suppression and even death of cancer cells (Lowe & Lin, 2000). The tumor suppressor protein p53 plays an important role in triggering apoptosis by up-regulating the pro-apoptotic Bcl2-associated X protein (Bax). This Bax protein induces opening of the mitochondrial voltage-dependent anion channel, indicating the induction of mitochondrial outer membrane permeability. This induced permeability helps release cytochrome C and other pro-apoptotic proteins, as well as activating caspases (Miyashita, & Reed, 1995). In this study, DMH treatment of IL-10^{-/-} mice (KOCON) induced p53, however, no difference was observed in caspase 3 expression.

Despite the essential role of p53 in inducing apoptosis, high levels of p53 (suggestive of mutated p53) are seen in the inflamed colonic tissue of colitis patients, even before neoplastic lesions have formed (Dibra, Mishra & Li, 2014). A mechanistic link between mutant p53 and sustained inflammation was identified: different tumor cell lines that harbored mutant p53 were prone to sustained nuclear factor-(NF-κB) activation (inflammatory pathway) even in the presence of low levels of tumor necrosis factor (TNF). In addition, was demonstrated that in mice, one copy of mutant p53 promoted colitis and IBD-mediated carcinogenesis by sustaining NF-κB activation (Cooks et al., 2013).

Although mutations in p53 were not investigated in the present study, our results suggest that the overexpression of p53 in the KOCON group may be associated with intestinal inflammation, characteristic of the experimental model used. We emphasize that other markers of apoptotic pathways such as p21, Bax, and Bcl-2 should be investigated.

C-myc expression was significantly lower in the KOSYN group compared to KOCON. C-myc is an overexpressed oncoprotein in a wide variety of malignancies, and its aberrant amplification leads to tumor aggression. The overactivation of c-myc has been implicated in aberrant cell cycle progression, genomic instability, malignant transformation, immortalization and eventual migration and metastasis, via regulation of the numerous target genes (Kress, Sabò & Amati, 2015; Beroukhim et al., 2010). As mentioned earlier for p53, non-resolving inflammation has been recognized as a major driver of many human disorders including cancer, being that pro-inflammatory

cytokines can induce the expression of oncogenes such as c-myc (Zhong, Lee, & Surh, 2018).

In the present study, the use of the synbiotic VSL#3 and PBY proved to be able to reduce the expression of the c-myc oncogene. Its suppression is indicated as a potential target in the control of colitis-induced tumorigenesis (Parang et al, 2017). Although the exact mechanisms that lead to downregulation of c-myc by synbiotic are not fully understood, it is believed that two factors may contribute to this finding: the reduction of intestinal inflammation and the regulation of cellular signaling pathways, such as the Wnt/ β -catenin pathway (Zhong, Lee, & Surh, 2018; Dibra, Mishra & Li, 2014).

We observed higher IL-17 levels in the KOCON group compared to the others; in addition, TNF levels were higher in the KOCON group compared to KONEG, which demonstrates the role of carcinogenesis induction in the increase in intestinal inflammation. Up-regulation of IL-17 has reported in colorectal tumors. The differentiation of Th17 cells may occur in the presence of different combinations of the cytokines TGF- β , IL-6, IL-1 β and/or IL-23, while its maintenance requires IL-23 and/or IL-1 β (Grivennikov et al., 2012; Chung et al.; 2009). Although we have not attempted to elucidate the molecular mechanisms that mediate the inhibitory role of synbiotic in the regulation of IL-17 in our study, we believe that this result requires further investigation.

Also regarding the control of cell proliferation, numerous reports showed the aberrant activation of the Wnt/ β -catenin signaling pathway in cases of CRC (Zhong et al., 2021; Yu et al., 2017; Matly et al., 2021). The constitutive activation of this pathway culminates in the overexpression of genes that induce cell proliferation, such as c-myc, survivin, cyclin D1, among others (Dibra, Mishra & Li, 2014). Butyric acid is appointed as a potential histone deacetylase (iHDAC) inhibitor, altering the expression of target genes, suppressing the aberrant activation of the pathway (Zhou et al., 2018; Bach Knudsen et al., 2018). In the present study, it was observed that animals that received synbiotic showed increased concentrations of SCFA (acetate, propionate and butyrate) at the end of the experimental period. Similar results were observed by Oh et al., (2020), after administration of the synbiotic *Lactobacillus gasseri* 505 and *Cudrania tricuspidata* leaf in a colitis-associated colorectal cancer model.

In the intra-group comparison, a reduction in BCFA (valeric and isovaleric), also known as putrefactive fatty acids, was observed in the KOSYN group. Although the

role of these fatty acids has not been fully elucidated, their increase has been associated with conditions where an increase in inflammation is observed (Krupa-Kozak et al., 2017).

The microbiota plays a key role in intestinal health and is currently considered a target to reduce the risk of developing intestinal diseases. In a previous report, we demonstrated that the use of the synbiotic VSL#3 and PBY caused some changes in the composition of the microbiota, such as reduction of the abundance of genera *Candidatus Saccharimonas*, *Ruminococcaceae_UCG-014*, *Aloprevotella*, *Lachnospiraceae_UCG-006*, and *Tyzzarella_3*, and an increase of *Coriobacteriaceae_UCG-002*, *Dubosiella*, *Legionella*, and *Olsenella* (Cruz, Conceição, Mendes, Ferreira, Gonçalves & Peluzio, 2020). In the present study, we sought to know the functional metabolic pathways of the microbiota that could be related to the development of colitis-associated carcinogenesis. Although a significant number of pathways were predicted, only 12 differed significantly between groups (one enriched in the KOSYN group; the other pathways were enriched in the KOCON group).

Data on the influence of synbiotics on the microbiota metabolic pathways in a CAC model are scarce in the literature. Our results showed differences in the pathways of carbohydrate and amino acid metabolism in the KOCON group, possibly associated with tumorigenesis. It is noteworthy that the intestinal microbiota of IL-10^{-/-} mice is still poorly explored, with identification of few taxa, which limits the identification of metabolic pathways. Future research should seek to elucidate the role of these pathways in CAC progression.

Enrichment of specific metabolic pathways is directly related to the activity of the intestinal microbiota, as activity of bacterial-derived enzymes that are involved in xenobiotic metabolism, which in turn may alter the toxicity of carcinogenic chemicals in the intestine. In particular, gut microbial β -glucuronidase is a major modulator of ingested xenobiotics found in certain gut microbial strains in the phyla Actinobacteria, Bacteroidetes, Firmicutes, Proteobacteria, and Verrucomicrobia (Pollet et al., 2017). Most chemicals are metabolized through hepatic glucuronidation, the major phase II reaction constituting 40 to 75% or more of xenobiotic metabolism (Panebianco, Andriulli & Paziienza, 2018). During this process, active or toxic chemicals are conjugated with glucuronic acid to become relatively stable and inactive, before they are eliminated from the body through urinary excretion. However, some glucuronides that enter the intestine via the bile duct are hydrolyzed by gut microbial β -glucuronidase

to be converted back to the active metabolites (Takasuna et al., 1996). In the present study, we demonstrated that the activity of the β -glucuronidase enzyme was higher in the KOCON group compared to the other groups, and these results are possibly associated with alterations in the intestinal microbiota.

In conclusion, the synbiotic combination of VSL#3 and PBY showed potential benefits in the CAC model. Regulation of expression of genes related to carcinogenesis, control of intestinal inflammation, production of anticarcinogenic compounds such as SFCA, and reduction in the activity of bacterial-derived enzymes are potential targets for future investigations.

References

Askling, J., Dickman, P. W., Karlén, P., Broström, O., Lapidus, A., Löfberg, R., & Ekbom, A. (2001). Family history as a risk factor for colorectal cancer in inflammatory bowel disease. *Gastroenterology*, *120*(6), 1356–1362. <https://doi.org/10.1053/gast.2001.24052>

Bach Knudsen, K. E., Lærke, H. N., Hedemann, M. S., Nielsen, T. S., Ingerslev, A. K., Gundelund Nielsen, D. S., Theil, P. K., Purup, S., Hald, S., Schioldan, A. G., Marco, M. L., Gregersen, S., & Hermansen, K. (2018). Impact of Diet-Modulated Butyrate Production on Intestinal Barrier Function and Inflammation. *Nutrients*, *10*(10), 1499. <https://doi.org/10.3390/nu10101499>

Barbera, P., Kozlov, A. M., Czech, L., Morel, B., Darriba, D., Flouri, T., & Stamatakis, A. (2019). EPA-ng: Massively Parallel Evolutionary Placement of Genetic Sequences. *Systematic biology*, *68*(2), 365–369. <https://doi.org/10.1093/sysbio/syy054>

Bedani R, Pauly-Silveira ND, Cano VSP, Valentini SR, Valdez GF, Rossi EA (2011) Effect of ingestion of soy yogurt on intestinal parameters of rats fed on a beef-based animal diet. *Braz J Microbiol* *42*(3):1238–1247. <https://doi.org/10.1590/S1517-83822011000300050>

Beroukhim, R., Mermel, C., Porter, D. *et al.* (2010). The landscape of somatic copy-number alteration across human cancers. *Nature* 463, 899–905. <https://doi.org/10.1038/nature08822>

Blander, J. M., Longman, R. S., Iliev, I. D., Sonnenberg, G. F., & Artis, D. (2017). Regulation of inflammation by microbiota interactions with the host. *Nature immunology*, 18(8), 851–860. <https://doi.org/10.1038/ni.3780>

Bolyen, E., Rideout, J. R., Dillon, M. R., Bokulich, N. A., Abnet, C. C., Al-Ghalith, G. A., Alexander, H., Alm, E. J., Arumugam, M., Asnicar, F., Bai, Y., Bisanz, J. E., Bittinger, K., Brejnrod, A., Brislawn, C. J., Brown, C. T., Callahan, B. J., Caraballo-Rodríguez, A. M., Chase, J., Cope, E. K., ... Caporaso, J. G. (2019). Reproducible, interactive, scalable and extensible microbiome data science using QIIME 2. *Nature biotechnology*, 37(8), 852–857. <https://doi.org/10.1038/s41587-019-0209-9>

Callahan, B. J., McMurdie, P. J., Rosen, M. J., Han, A. W., Johnson, A. J., & Holmes, S. P. (2016). DADA2: High-resolution sample inference from Illumina amplicon data. *Nature methods*, 13(7), 581–583. <https://doi.org/10.1038/nmeth.3869>

Carroll, I. M., Andrus, J. M., Bruno-Bárcena, J. M., Klaenhammer, T. R., Hassan, H. M., & Threadgill, D. S. (2007). Anti-inflammatory properties of *Lactobacillus gasseri* expressing manganese superoxide dismutase using the interleukin 10-deficient mouse model of colitis. *American journal of physiology. Gastrointestinal and liver physiology*, 293(4), G729–G738. <https://doi.org/10.1152/ajpgi.00132.2007>

Chou, Y. C., Ho, P. Y., Chen, W. J., Wu, S. H., & Pan, M. H. (2020). *Lactobacillus fermentum* V3 ameliorates colitis-associated tumorigenesis by modulating the gut microbiome. *American journal of cancer research*, 10(4), 1170–1181.

Chung, Y., Chang, S. H., Martinez, G. J., Yang, X. O., Nurieva, R., Kang, H. S., Ma, L., Watowich, S. S., Jetten, A. M., Tian, Q., & Dong, C. (2009). Critical regulation of early Th17 cell differentiation by interleukin-1 signaling. *Immunity*, 30(4), 576–587. <https://doi.org/10.1016/j.immuni.2009.02.007>

Cooks, T., Pateras, I. S., Tarcic, O., Solomon, H., Schetter, A. J., Wilder, S., Lozano, G., Pikarsky, E., Forshew, T., Rosenfeld, N., Harpaz, N., Itzkowitz, S., Harris, C. C., Rotter, V., Gorgoulis, V. G., & Oren, M. (2013). Mutant p53 prolongs NF- κ B activation and promotes chronic inflammation and inflammation-associated colorectal cancer. *Cancer cell*, 23(5), 634–646. <https://doi.org/10.1016/j.ccr.2013.03.022>

Cruz, B., Conceição, L., Mendes, T., Ferreira, C., Gonçalves, R. V., & Peluzio, M. (2020). Use of the synbiotic VSL#3 and yacon-based concentrate attenuates intestinal damage and reduces the abundance of *Candidatus Saccharimonas* in a colitis-associated carcinogenesis model. *Food research international (Ottawa, Ont.)*, 137, 109721. <https://doi.org/10.1016/j.foodres.2020.109721>

Czech, L., & Stamatakis, A. (2019). Scalable methods for analyzing and visualizing phylogenetic placement of metagenomic samples. *PloS one*, 14(5), e0217050. <https://doi.org/10.1371/journal.pone.0217050>

de Moreno de LeBlanc, A., & Perdigón, G. (2005). Reduction of beta-glucuronidase and nitroreductase activity by yoghurt in a murine colon cancer model. *Biocell: official journal of the Sociedades Latinoamericanas de Microscopia Electronica ... et. al*, 29(1), 15–24.

De Nadai Marcon, L., Moraes, L. F. S., Cruz, B. C. S., Teixeira, M. D. O., Bruno, T. C. V., Ribeiro, I. E., ... Peluzio, M. C. G. (2019). Yacon (*Smallanthus sonchifolius*)-based product increases fecal short-chain fatty acids and enhances regulatory T cells by downregulating ROR γ t in the colon of BALB/c mice. *Journal of Functional Foods*, 55, 333–342

De Nadai Marcon, L., Moraes, L. F. S., Cruz, B. C. S., Teixeira, M. D. O., Gomides, A. F. F., ... Peluzio, M. C. G. (2020). Yacon (*Smallanthus sonchifolius*)-based product increases fecal short-chain fatty acids concentration and up-regulates t-Bet expression in the colon of BALB/c mice during colorectal carcinogenesis. *Food Science and Nutrition*, 6, 1-12. <https://doi.org/10.24966/FSN-1076/100069>

Dibra, D., Mishra, L., & Li, S. (2014). Molecular mechanisms of oncogene-induced inflammation and inflammation-sustained oncogene activation in gastrointestinal tumors: an under-appreciated symbiotic relationship. *Biochimica et biophysica acta*, *1846*(1), 152–160. <https://doi.org/10.1016/j.bbcan.2014.05.001>

Dorrestein, P. C., Mazmanian, S. K., & Knight, R. (2014). Finding the missing links among metabolites, microbes, and the host. *Immunity*, *40*(6), 824–832. <https://doi.org/10.1016/j.immuni.2014.05.015>

Douglas, G. M., Maffei, V. J., Zaneveld, J. R., Yurgel, S. N., Brown, J. R., Taylor, C. M., Huttenhower, C., & Langille, M. (2020). PICRUST2 for prediction of metagenome functions. *Nature biotechnology*, *38*(6), 685–688. <https://doi.org/10.1038/s41587-020-0548-6>

Fernando, M. R., Saxena, A., Reyes, J. L., & McKay, D. M. (2016). Butyrate enhances antibacterial effects while suppressing other features of alternative activation in IL-4-induced macrophages. *American journal of physiology. Gastrointestinal and liver physiology*, *310*(10), G822–G831. <https://doi.org/10.1152/ajpgi.00440.2015>

Flynn, S., & Eisenstein, S. (2019). Inflammatory Bowel Disease Presentation and Diagnosis. *The Surgical clinics of North America*, *99*(6), 1051–1062. <https://doi.org/10.1016/j.suc.2019.08.001>

Genaro, S. C., Lima de Souza Reis, L. S., Reis, S. K., Rabelo Socca, E. A., & Fávaro, W. J. (2019). Probiotic supplementation attenuates the aggressiveness of chemically induced colorectal tumor in rats. *Life sciences*, *237*, 116895. <https://doi.org/10.1016/j.lfs.2019.116895>

Gomides, A. F., de Paula, S. O., Gonçalves, R. V., de Oliveira, L. L., Ferreira, C. L., Comastri, D. S., & Peluzio, M. (2014). Prebiotics prevent the appearance of aberrant crypt foci (ACF) in the colon of BALB/c mice for increasing the gene expression of p16 protein. *Nutricion hospitalaria*, *30*(4), 883–890. <https://doi.org/10.3305/nh.2014.30.4.7672>

Grivennikov, S. I., Wang, K., Mucida, D., Stewart, C. A., Schnabl, B., Jauch, D., Taniguchi, K., Yu, G. Y., Osterreicher, C. H., Hung, K. E., Datz, C., Feng, Y., Fearon, E. R., Oukka, M., Tessarollo, L., Coppola, V., Yarovinsky, F., Cheroutre, H., Eckmann, L., Trinchieri, G., ... Karin, M. (2012). Adenoma-linked barrier defects and microbial products drive IL-23/IL-17-mediated tumour growth. *Nature*, *491*(7423), 254–258. <https://doi.org/10.1038/nature11465>

Han, Y. M., A Kang, E., Min Park, J., Young Oh, J., Yoon Lee, D., Hye Choi, S., & Baik Hahm, K. (2020). Dietary intake of fermented kimchi prevented colitis-associated cancer. *Journal of clinical biochemistry and nutrition*, *67*(3), 263–273. <https://doi.org/10.3164/jcbrn.20-77>

Imhann, F., Vich Vila, A., Bonder, M. J., Fu, J., Gevers, D., Visschedijk, M. C., Spekhorst, L. M., Alberts, R., Franke, L., van Dullemen, H. M., Ter Steege, R., Huttenhower, C., Dijkstra, G., Xavier, R. J., Festen, E., Wijmenga, C., Zhernakova, A., & Weersma, R. K. (2018). Interplay of host genetics and gut microbiota underlying the onset and clinical presentation of inflammatory bowel disease. *Gut*, *67*(1), 108–119. <https://doi.org/10.1136/gutjnl-2016-312135>

Jacobs, J. P., Goudarzi, M., Singh, N., Tong, M., McHardy, I. H., Ruegger, P., Asadourian, M., Moon, B. H., Ayson, A., Borneman, J., McGovern, D. P., Fornace, A. J., Jr, Braun, J., & Dubinsky, M. (2016). A Disease-Associated Microbial and Metabolomics State in Relatives of Pediatric Inflammatory Bowel Disease Patients. *Cellular and molecular gastroenterology and hepatology*, *2*(6), 750–766. <https://doi.org/10.1016/j.jcmgh.2016.06.004>

Kelsen, J. R., Russo, P., & Sullivan, K. E. (2019). Early-Onset Inflammatory Bowel Disease. *Immunology and allergy clinics of North America*, *39*(1), 63–79. <https://doi.org/10.1016/j.iac.2018.08.008>

Keshavarzian, A., Banan, A., Farhadi, A., Komanduri, S., Mutlu, E., Zhang, Y., & Fields, J. Z. (2003). Increases in free radicals and cytoskeletal protein oxidation and nitration in the colon of patients with inflammatory bowel disease. *Gut*, *52*(5), 720–728. <https://doi.org/10.1136/gut.52.5.720>

Kiatpakdee, B., Sato, K., Otsuka, Y., Arashiki, N., Chen, Y., Tsumita, T., Otsu, W., Yamamoto, A., Kawata, R., Yamazaki, J., Sugimoto, Y., Takada, K., Mohandas, N., & Inaba, M. (2020). Cholesterol-binding protein TSPO2 coordinates maturation and proliferation of terminally differentiating erythroblasts. *The Journal of biological chemistry*, *295*(23), 8048–8063. <https://doi.org/10.1074/jbc.RA119.011679>

Kim, S., Kim, J. H., Park, B. O., & Kwak, Y. S. (2014). Perspectives on the therapeutic potential of short-chain fatty acid receptors. *BMB reports*, *47*(3), 173–178. <https://doi.org/10.5483/bmbrep.2014.47.3.272>

Kress, T., Sabò, A. & Amati, B. (2015). MYC: connecting selective transcriptional control to global RNA production. *Nat Rev Cancer* *15*, 593–607. <https://doi.org/10.1038/nrc3984>

Krupa-Kozak, U., Markiewicz, L. H., Lamparski, G., & Juśkiewicz, J. (2017). Administration of Inulin-Supplemented Gluten-Free Diet Modified Calcium Absorption and Caecal Microbiota in Rats in a Calcium-Dependent Manner. *Nutrients*, *9*(7), 702. <https://doi.org/10.3390/nu9070702>

Le Gall, G., Noor, S. O., Ridgway, K., Scovell, L., Jamieson, C., Johnson, I. T., Colquhoun, I. J., Kemsley, E. K., & Narbad, A. (2011). Metabolomics of fecal extracts detects altered metabolic activity of gut microbiota in ulcerative colitis and irritable bowel syndrome. *Journal of proteome research*, *10*(9), 4208–4218. <https://doi.org/10.1021/pr2003598>

Le Leu, R. K., Hu, Y., Brown, I. L., Woodman, R. J., & Young, G. P. (2010). Synbiotic intervention of *Bifidobacterium lactis* and resistant starch protects against colorectal cancer development in rats. *Carcinogenesis*, *31*(2), 246–251. <https://doi.org/10.1093/carcin/bgp197>

Li, L., Li, P., & Xu, L. (2021). Assessing the effects of inulin-type fructan intake on body weight, blood glucose, and lipid profile: A systematic review and meta-analysis of

randomized controlled trials. *Food science & nutrition*, 9(8), 4598–4616. <https://doi.org/10.1002/fsn3.2403>

Lin, Y., & Sun, Z. (2015). In vivo pancreatic β -cell-specific expression of antiaging gene Klotho: a novel approach for preserving β -cells in type 2 diabetes. *Diabetes*, 64(4), 1444–1458. <https://doi.org/10.2337/db14-0632>

Louca, S., & Doebeli, M. (2018). Efficient comparative phylogenetics on large trees. *Bioinformatics* (Oxford, England), 34(6), 1053–1055. <https://doi.org/10.1093/bioinformatics/btx701>

Lowe, S. W., & Lin, A. W. (2000). Apoptosis in cancer. *Carcinogenesis*, 21(3), 485–495. <https://doi.org/10.1093/carcin/21.3.485>

Matly, A., Quinn, J. A., McMillan, D. C., Park, J. H., & Edwards, J. (2021). The relationship between β -catenin and patient survival in colorectal cancer systematic review and meta-analysis. *Critical reviews in oncology/hematology*, 163, 103337. <https://doi.org/10.1016/j.critrevonc.2021.103337>

Mengying, Z., Yiyue, X., Tong, P., Yue, H., Limpanont, Y., Ping, H., Okanurak, K., Yanqi, W., Dekumyoy, P., Hongli, Z., Watthanakulpanich, D., Zhongdao, W., Zhi, W., & Zhiyue, L. (2017). Apoptosis and necroptosis of mouse hippocampal and parenchymal astrocytes, microglia and neurons caused by *Angiostrongylus cantonensis* infection. *Parasites & vectors*, 10(1), 611. <https://doi.org/10.1186/s13071-017-2565-y>

Miyashita, T., & Reed, J. C. (1995). Tumor suppressor p53 is a direct transcriptional activator of the human bax gene. *Cell*, 80(2), 293–299. [https://doi.org/10.1016/0092-8674\(95\)90412-3](https://doi.org/10.1016/0092-8674(95)90412-3)

Newell, L. E., & Heddle, J. A. (2004). The potent colon carcinogen, 1,2-dimethylhydrazine induces mutations primarily in the colon. *Mutation research*, 564(1), 1–7. <https://doi.org/10.1016/j.mrgentox.2004.06.005>

Oh, N. S., Lee, J. Y., Kim, Y. T., Kim, S. H., & Lee, J. H. (2020). Cancer-protective effect of a synbiotic combination between *Lactobacillus gasseri* 505 and a *Cudrania tricuspidata* leaf extract on colitis-associated colorectal cancer. *Gut microbes*, 12(1), 1785803. <https://doi.org/10.1080/19490976.2020.1785803>

Panebianco, C., Andriulli, A., & Paziienza, V. (2018). Pharmacomicrobiomics: exploiting the drug-microbiota interactions in anticancer therapies. *Microbiome*, 6(1), 92. <https://doi.org/10.1186/s40168-018-0483-7>

Parang, B., Kaz, A. M., Barrett, C. W., Short, S. P., Ning, W., Keating, C. E., Mittal, M. K., Naik, R. D., Washington, M. K., Revetta, F. L., Smith, J. J., Chen, X., Wilson, K. T., Brand, T., Bader, D. M., Tansey, W. P., Chen, R., Brentnall, T. A., Grady, W. M., & Williams, C. S. (2017). BVES regulates c-Myc stability via PP2A and suppresses colitis-induced tumourigenesis. *Gut*, 66(5), 852–862. <https://doi.org/10.1136/gutjnl-2015-310255>

Paula, H. A. A., Martins, J. F. L., Sartori, S. S. R., Castro, A. S. B., Abranches, M. V., Rafael, V. C., & Ferreira, C. L. L. F. (2012). *The yacon product PBY: Which is the best dose to evaluate the functionality of this new source of prebiotic fructans?* Finland: Functional Foods Forum Probiotics. Turku.

Perše, M., Cerar, A., 2011. Morphological and molecular alterations in 1,2 dimethylhydrazine and azoxymethane induced colon carcinogenesis in rats. *J. Biomed. Biotechnol.* 2011. <https://doi.org/10.1155/2011/473964>

Piranlioglu, R., Lee, E., Ouzounova, M., Bollag, R. J., Vinyard, A. H., Arbab, A. S., Marasco, D., Guzel, M., Cowell, J. K., Thangaraju, M., Chadli, A., Hassan, K. A., Wicha, M. S., Celis, E., & Korkaya, H. (2019). Primary tumor-induced immunity eradicates disseminated tumor cells in syngeneic mouse model. *Nature communications*, 10(1), 1430. <https://doi.org/10.1038/s41467-019-09015-1>

Pollet, R. M., D'Agostino, E. H., Walton, W. G., Xu, Y., Little, M. S., Biernat, K. A., Pellock, S. J., Patterson, L. M., Creekmore, B. C., Isenberg, H. N., Bahethi, R. R., Bhatt, A. P., Liu, J., Gharaibeh, R. Z., & Redinbo, M. R. (2017). An Atlas of β -

Glucuronidases in the Human Intestinal Microbiome. *Structure (London, England: 1993)*, 25(7), 967–977.e5. <https://doi.org/10.1016/j.str.2017.05.003>

Reeves, P. G., Nielsen, F. H., & Fahey, G. C., Jr (1993). AIN-93 purified diets for laboratory rodents: final report of the American Institute of Nutrition ad hoc writing committee on the reformulation of the AIN-76A rodent diet. *The Journal of nutrition*, 123(11), 1939–1951. <https://doi.org/10.1093/jn/123.11.1939>

Rosenberg, D.W., Giardina, C., Tanaka, T., 2009. Mouse models for the study of colon carcinogenesis. *Carcinogenesis* 30, 183–196. <https://doi.org/10.1093/carcin/bgn267>.

Sairenji, T., Collins, K. L., & Evans, D. V. (2017). An Update on Inflammatory Bowel Disease. *Primary care*, 44(4), 673–692. <https://doi.org/10.1016/j.pop.2017.07.010>

Smiricky-Tjardes, M. R., Grieshop, C. M., Flickinger, E. A., Bauer, L. L., & Fahey, G. C., Jr (2003). Dietary galactooligosaccharides affect ileal and total-tract nutrient digestibility, ileal and fecal bacterial concentrations, and ileal fermentative characteristics of growing pigs. *Journal of animal science*, 81(10), 2535–2545. <https://doi.org/10.2527/2003.81102535x>

Sokol, H., & Seksik, P. (2010). The intestinal microbiota in inflammatory bowel diseases: time to connect with the host. *Current opinion in gastroenterology*, 26(4), 327–331. <https://doi.org/10.1097/MOG.0b013e328339536b>

Sturlan, S., Oberhuber, G., Beinhauer, B. G., Tichy, B., Kappel, S., Wang, J., & Rogy, M. A. (2001). Interleukin-10-deficient mice and inflammatory bowel disease associated cancer development. *Carcinogenesis*, 22, 665–671.

Takasuna, K., Hagiwara, T., Hirohashi, M., Kato, M., Nomura, M., Nagai, E., Yokoi, T., & Kamataki, T. (1996). Involvement of beta-glucuronidase in intestinal microflora in the intestinal toxicity of the antitumor camptothecin derivative irinotecan hydrochloride (CPT-11) in rats. *Cancer research*, 56(16), 3752–3757

Tan, G., Huang, C., Chen, J., & Zhi, F. (2020). HMGB1 released from GSDME-mediated pyroptotic epithelial cells participates in the tumorigenesis of colitis-associated colorectal cancer through the ERK1/2 pathway. *Journal of hematology & oncology*, *13*(1), 149. <https://doi.org/10.1186/s13045-020-00985-0>

Xiong, Y., Miyamoto, N., Shibata, K., Valasek, M. A., Motoike, T., Kedzierski, R. M., & Yanagisawa, M. (2004). Short-chain fatty acids stimulate leptin production in adipocytes through the G protein-coupled receptor GPR41. *Proceedings of the National academy of Sciences of the United States of America*, *101*, 1045–1050

Ye, Y., & Doak, T. G. (2009). A parsimony approach to biological pathway reconstruction/inference for genomes and metagenomes. *PLoS computational biology*, *5*(8), e1000465. <https://doi.org/10.1371/journal.pcbi.1000465>

Yu, B., Ye, X., Du, Q., Zhu, B., Zhai, Q., & Li, X. X. (2017). The Long Non-Coding RNA CRNDE Promotes Colorectal Carcinoma Progression by Competitively Binding miR-217 with TCF7L2 and Enhancing the Wnt/ β -Catenin Signaling Pathway. *Cellular physiology and biochemistry : international journal of experimental cellular physiology, biochemistry, and pharmacology*, *41*(6), 2489–2502. <https://doi.org/10.1159/000475941>

Zeineldin, M., Cunningham, J., McGuinness, W., Alltizer, P., Cowley, B., Blanchat, B., Xu, W., Pinson, D., & Neufeld, K. L. (2012). A knock-in mouse model reveals roles for nuclear Apc in cell proliferation, Wnt signal inhibition and tumor suppression. *Oncogene*, *31*(19), 2423–2437. <https://doi.org/10.1038/onc.2011.434>

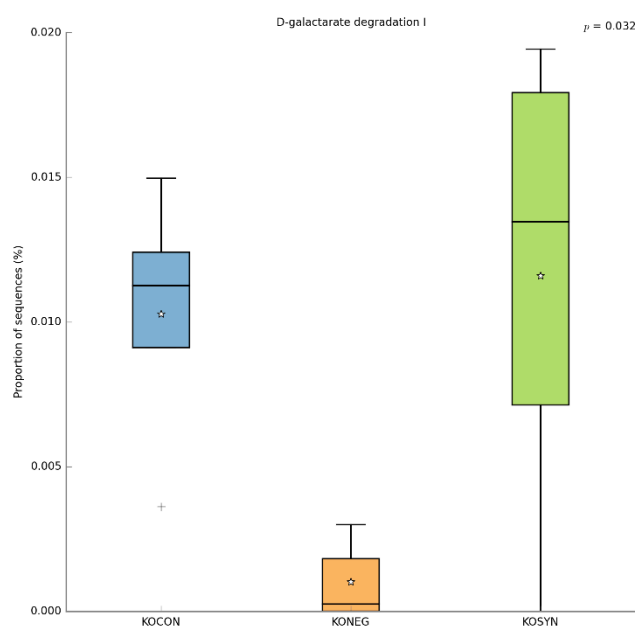
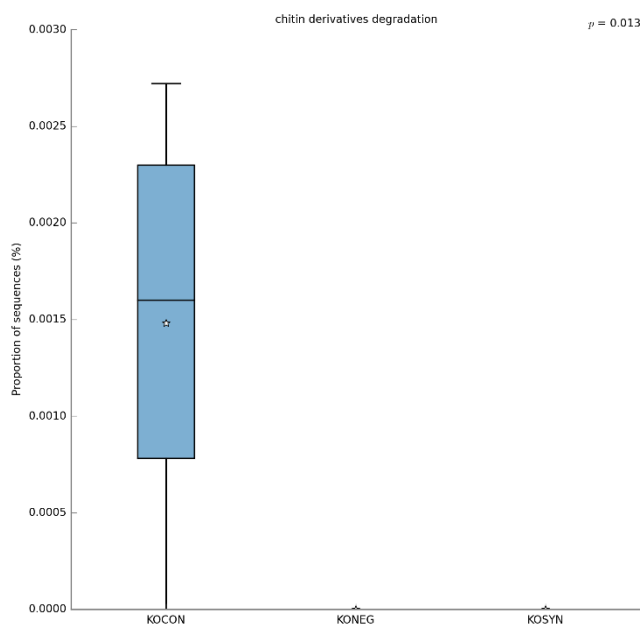
Zhong, X., Lee, H. N., & Surh, Y. J. (2018). RvD1 inhibits TNF α -induced c-Myc expression in normal intestinal epithelial cells and destabilizes hyper-expressed c-Myc in colon cancer cells. *Biochemical and biophysical research communications*, *496*(2), 316–323. <https://doi.org/10.1016/j.bbrc.2017.12.171>

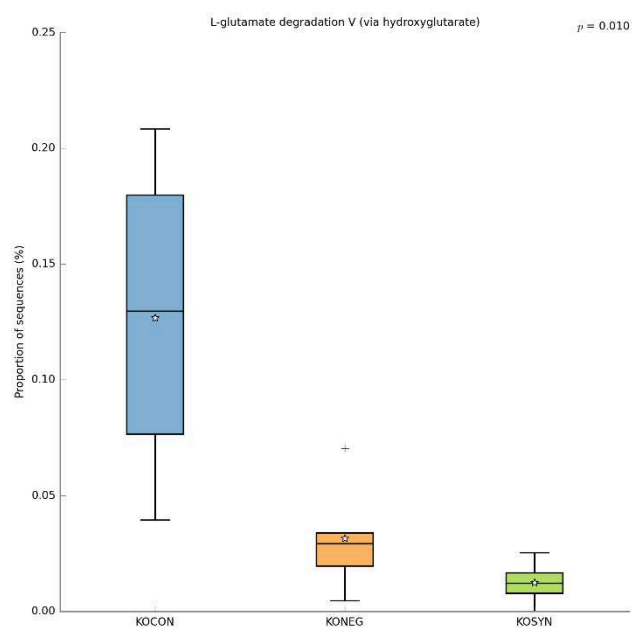
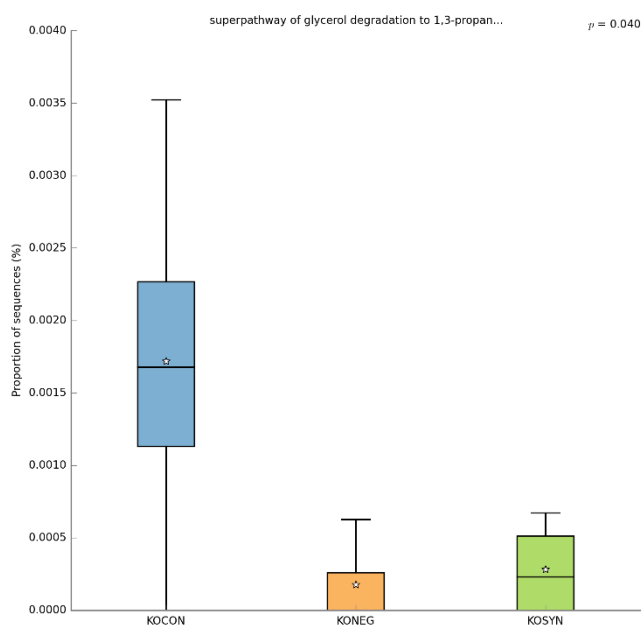
Zhong, Z. A., Michalski, M. N., Stevens, P. D., Sall, E. A., & Williams, B. O. (2021). Regulation of Wnt receptor activity: Implications for therapeutic development in colon cancer. *The Journal of biological chemistry*, *296*, 100782. <https://doi.org/10.1016/j.jbc.2021.100782>

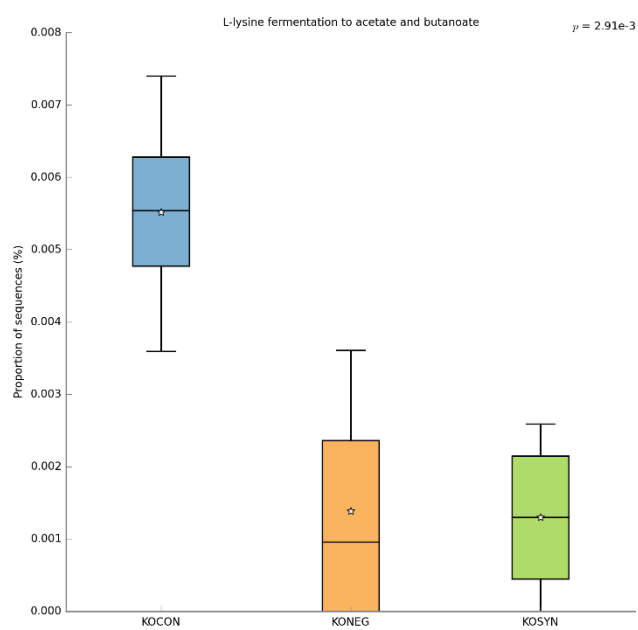
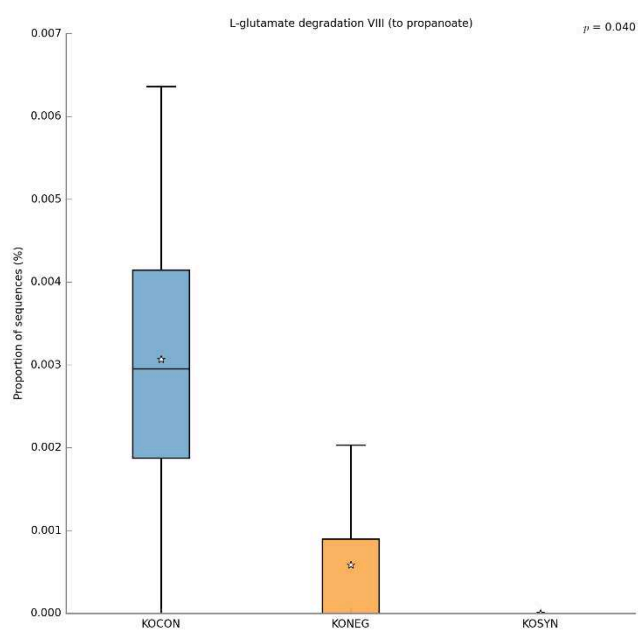
Zhou, L., Zhang, M., Wang, Y., Dorfman, R. G., Liu, H., Yu, T., Chen, X., Tang, D., Xu, L., Yin, Y., Pan, Y., Zhou, Q., Zhou, Y., & Yu, C. (2018). Faecalibacterium prausnitzii Produces Butyrate to Maintain Th17/Treg Balance and to Ameliorate Colorectal Colitis by Inhibiting Histone Deacetylase 1. *Inflammatory bowel diseases*, 24(9), 1926–1940. <https://doi.org/10.1093/ibd/izy182>

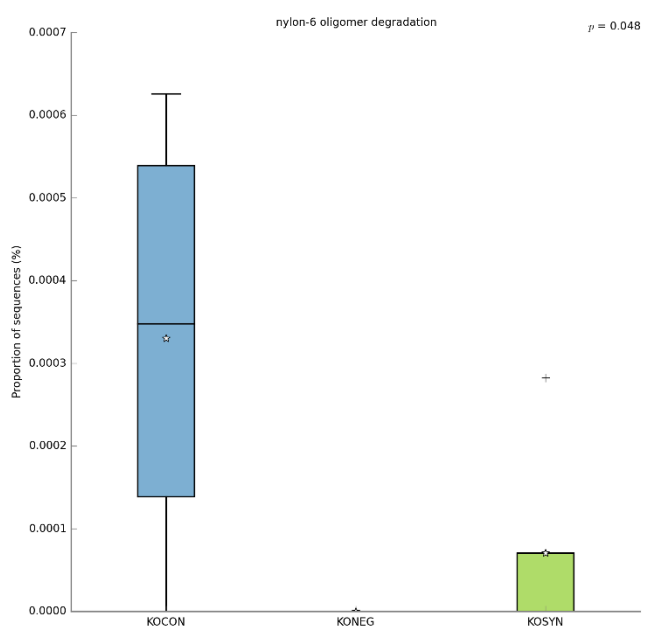
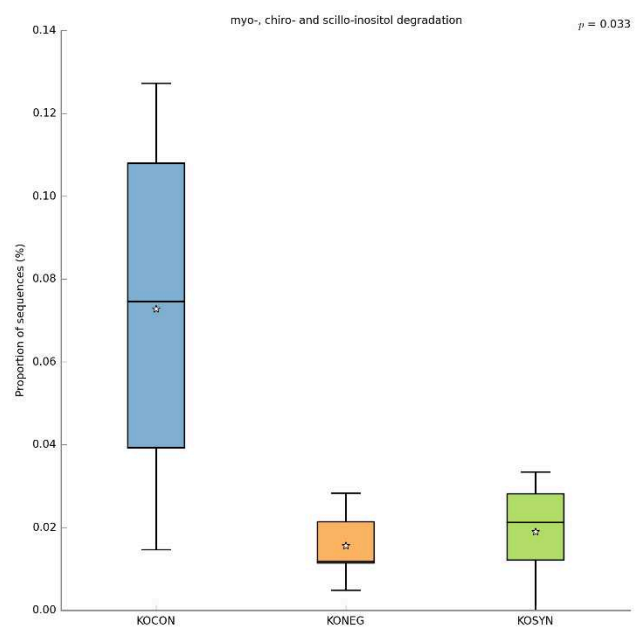
SUPPLEMENTARY MATERIAL

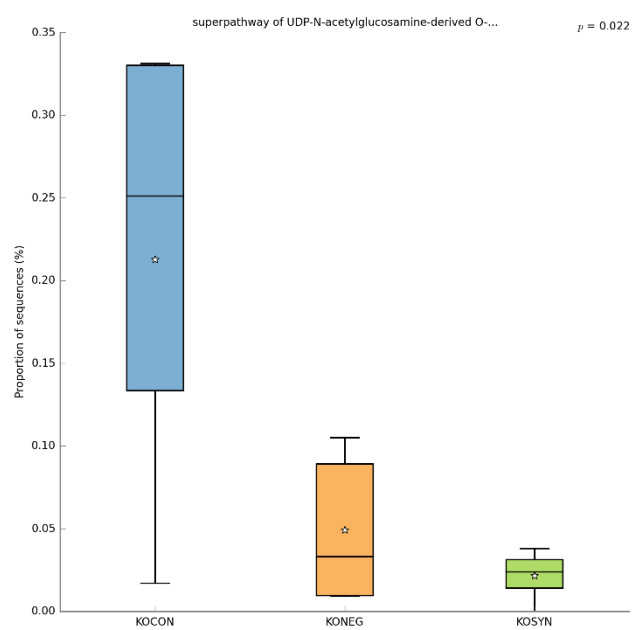
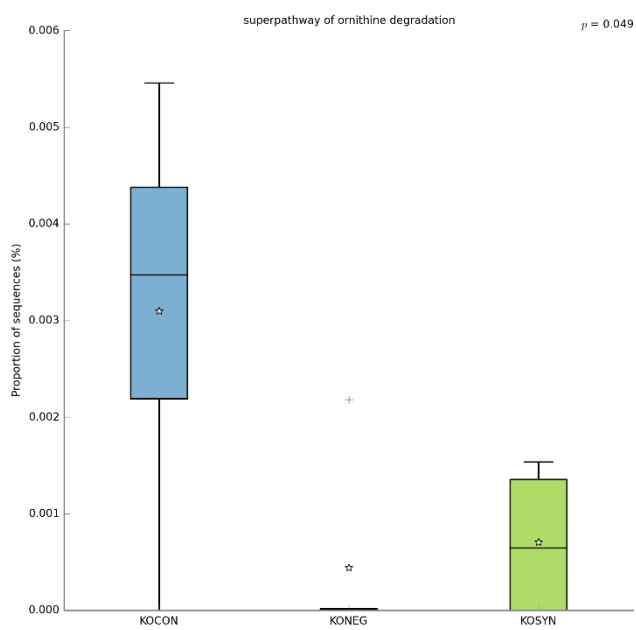
Functional level box plot chart profile between the groups KONEG, KOCON, and KOSYN.

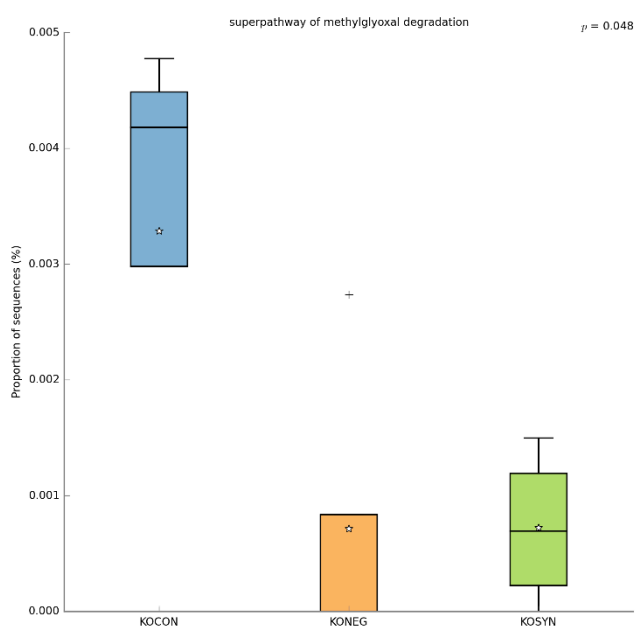
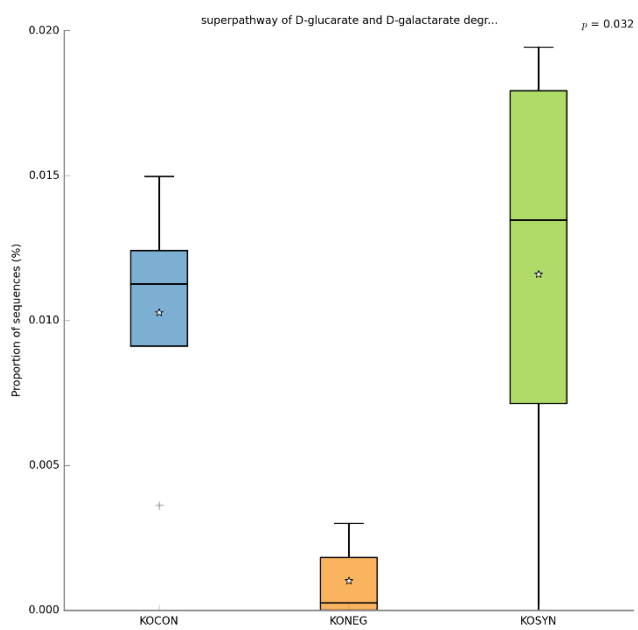












5. GENERAL CONCLUSIONS

The synbiotic formulation VSL#3 and PBY showed more benefits in a colorectal carcinogenesis model when compared to probiotic VSL#3 alone. Synbiotic reduced the incidence of CRC precursor lesions and the expression of genes related to carcinogenesis, improved the inflammatory intestinal response, reduced oxidative stress, stimulated the production of short-chain fatty acids, reduced the activity of the enzyme β -glucuronidase, and improved intestinal barrier function.

Bacterial genera present in the synbiotic formulation increased significantly in the intestinal microbiota of the animals, proving the synbiotic's ability to modify the microbial structure. We also observed an increase in SCFA, products of the fermentation of prebiotics present in PBY.

There was also the enrichment of several functional metabolic pathways of the microbiota. Although little is known about these microbial pathways, our results confirmed the influence of symbiotic on the metabolism pathways of carbohydrates, proteins, and vitamins, possibly associated with the colorectal carcinogenesis process.

In the colitis-associated cancer model, our findings were more discrete, although some benefits were also observed. The microbiota of this model was characterized by a low diversity and, despite advances in metagenomic sequencing techniques, little is known about the structure of the microbiota of these animals.

In conclusion, the synbiotic VSL#3 and PBY proved to be safe in the experimental conditions studied and potential use for prevention of colorectal carcinogenesis and in the progression of CAC. Finally, understanding the dynamic changes of the microbiota from health to disease can assist in the development of diagnostic tools based on the fecal microbial structure, and targeting interventions aimed at balancing the microbiota.

6. ATTACHMENT

Attachment 1

Applied Microbiology and Biotechnology
<https://doi.org/10.1007/s00253-020-10863-x>

GENOMICS, TRANSCRIPTOMICS, PROTEOMICS



Synbiotic VSL#3 and yacon-based product modulate the intestinal microbiota and prevent the development of pre-neoplastic lesions in a colorectal carcinogenesis model

Bruna Cristina dos Santos Cruz¹ · Vinicius da Silva Duarte² · Alessio Giacomini² · Viviana Corich² · Sérgio Oliveira de Paula³ · Lilian da Silva Fialho⁴ · Valéria Monteze Guimarães⁵ · Célia Lúcia de Lucas Fortes Ferreira⁶ · Maria do Carmo Gouveia Peluzio¹

Received: 10 June 2020 / Revised: 6 August 2020 / Accepted: 26 August 2020
 © Springer-Verlag GmbH Germany, part of Springer Nature 2020

Abstract

Colorectal cancer is a public health problem, with dysbiosis being one of the risk factors due to its role in intestinal inflammation. Probiotics and synbiotics have been used in order to restore the microbiota balance and to prevent colorectal carcinogenesis. We aimed to investigate the effects of the probiotic VSL#3® alone or in combination with a yacon-based prebiotic concentrate on the microbiota modulation and its influence on colorectal carcinogenesis in an animal model. C57BL/6J mice were divided into three groups: control (control diet), probiotic (control diet + VSL#3®), and synbiotic (yacon diet + VSL#3®). The diets were provided for 13 weeks and, from the third one, all animals were subjected to induction of colorectal cancer precursor lesions. Stool samples were collected to evaluate organic acids, feces pH, β-glucuronidase activity, and microbiota composition. The colon was used to count pre-neoplastic lesions and to determine the cytokines. The microbiota composition was influenced by the use of probiotic and synbiotic. Modifications were also observed in the abundance of bacterial genera with respect to the control group, which confirms the interference of carcinogenesis in the microbiota. Pre-neoplastic lesions were reduced by the use of the synbiotic, but not with the probiotic. The protection provided by the synbiotic can be attributed to the modulation of the intestinal inflammatory response, to the inhibition of a pro-carcinogenic enzyme, and to the production of organic acids. The modulation of the composition and activity of the microbiota contributed to beneficial changes in the intestinal microenvironment, which led to a reduction in carcinogenesis.

Key points

- Synbiotic reduces the incidence of colorectal cancer precursor lesions.
- Synbiotic modulates the composition and activity of intestinal microbiota.
- Synbiotic increases the abundance of butyrate-producing bacteria.

Keywords Gut microbiota · Probiotic · Prebiotic · Synbiotic · Colorectal cancer

Introduction

Colorectal cancer (CRC) is a public health problem worldwide, with 1.8 million new cases and almost 861,000 deaths reported

in 2018 (IARC 2019). Colorectal carcinogenesis is characterized by a series of morphological changes of the intestinal epithelium, with the formation of precursor lesions of CRC, such as aberrant crypt foci (ACF), which can progress to invasive adenomas and carcinomas (Calderwood et al. 2016; Armaghany et al. 2012). The ACF study has become an important marker for understanding the pathogenesis of CRC and represents a challenge for cancer screening and surveillance in the early stages, in addition to being proposed to identify new chemopreventive agents (Newell and Heddle 2004).

Sporadic CRC, that is, not associated with heredity, is diagnosed in approximately 70 to 87% of the cases, indicating the existence of other important risk factors for the

Electronic supplementary material The online version of this article (<https://doi.org/10.1007/s00253-020-10863-x>) contains supplementary material, which is available to authorized users.

✉ Bruna Cristina dos Santos Cruz
 brunacruz09@yahoo.com.br

Extended author information available on the last page of the article

Published online: 09 September 2020

Springer

Attachment 2











Received: 8 November 2020 | Revised: 18 February 2021 | Accepted: 20 February 2021

DOI: 10.1111/1750-3841.15690

HEALTH, NUTRITION, AND FOOD

Food Science WILEY

Evaluation of the efficacy of probiotic VSL#3 and synbiotic VSL#3 and yacon-based product in reducing oxidative stress and intestinal permeability in mice induced to colorectal carcinogenesis

Bruna Cristina dos Santos Cruz¹  | Luís Fernando de Sousa Moraes²  | Leticia De Nadai Marcon¹  | Kelly Aparecida Dias¹  | Leonardo Borges Murad³  | Mariáurea Matias Sarandy⁴  | Lisiane Lopes da Conceição¹  | Reggiani Vilela Gonçalves⁵  | Célia Lúcia de Luces Fortes Ferreira⁶  | Maria do Carmo Gouveia Peluzio¹ 

¹ Nutritional Biochemistry Laboratory, Department of Nutrition and Health, Universidade Federal de Viçosa - UFV, Viçosa, Minas Gerais, Brazil

² Experimental and Dietetic Nutrition Laboratory, Department of Nutrition - Federal University of Pernambuco - UFPE, Recife, Pernambuco, Brazil

³ Brazilian National Cancer Institute, Rio de Janeiro, Brazil

⁴ Department of General Biology, Universidade Federal de Viçosa - UFV, Viçosa, Minas Gerais, Brazil

⁵ Experimental Pathology Laboratory, Department of Animal Biology, Universidade Federal de Viçosa - UFV, Viçosa, Minas Gerais, Brazil

⁶ Institute of Biotechnology Applied to Agriculture & Livestock (Bioagro), Universidade Federal de Viçosa - UFV, Viçosa, Minas Gerais, Brazil

Correspondence

Bruna Cristina dos Santos Cruz, Nutritional Biochemistry Laboratory, Department of Nutrition and Health, Universidade Federal de Viçosa - UFV, Viçosa, Minas Gerais 36570-900, Brazil.
Email: brunacruz09@yahoo.com.br

Previous address(es) [If research was conducted at a different affiliation than that listed above].

Abstract: The objective of the present study was to evaluate the effect of probiotic VSL#3 isolated or associated with a yacon-based product (synbiotic) on oxidative stress modulation and intestinal permeability in an experimental model of colorectal carcinogenesis. Forty-five C57BL/6J mice were divided into three groups: control (standard diet AIN-93 M); probiotic (standard diet AIN-93 M and multispecies probiotic VSL#3, 2.25×10^9 CFU), and synbiotic (standard diet AIN-93 M with yacon-based product, 6% fructooligosaccharides and inulin, and probiotic VSL#3, 2.25×10^9 CFU). The experimental diets were provided for 13 weeks. The probiotic and the yacon-based product showed antioxidant activity, with the percentage of DPPH radical scavenging equal to $69.7 \pm 0.4\%$ and $74.3 \pm 0.1\%$, respectively. These findings contributed to reduce hepatic oxidative stress: the control group showed higher concentration of malondialdehyde (1.8-fold, $p = 0.007$ and 1.5-fold, $p = 0.035$) and carbonylated protein (2-fold, $p = 0.008$ and 5.6-fold, $p = 0.000$) compared to the probiotic and synbiotic groups, respectively. Catalase enzyme activity increased 1.43-fold ($p = 0.014$) in synbiotic group. The crypt depth increased 1.2-fold and 1.4-fold with the use of probiotic and synbiotic, respectively, compared to the control diet ($p = 0.000$). These findings corroborate the reduction in intestinal permeability in the probiotic and synbiotic groups, as measured by the percentage of urinary lactulose excretion (CON: $0.93 \pm 0.62\%$ × PRO: $0.44 \pm 0.05\%$, $p = 0.048$; and CON: $0.93 \pm 0.62\%$ × SYN: $0.41 \pm 0.12\%$, $p = 0.043$). In conclusion, the probiotic and synbiotic showed antioxidant activity, which contributed to the reduction of oxidative stress markers. In addition, they protected the mucosa from damage caused by chemical carcinogen and reduced intestinal permeability.

Practical Application: The relationship between intestinal health and the occurrence of various organic disorders has been demonstrated in many

Attachment 3

Food Research International 137 (2020) 109721



Contents lists available at ScienceDirect

Food Research International

journal homepage: www.elsevier.com/locate/foodres

Use of the synbiotic VSL#3 and yacon-based concentrate attenuates intestinal damage and reduces the abundance of *Candidatus Saccharimonas* in a colitis-associated carcinogenesis model

Bruna Cristina dos Santos Cruz^{a,*}, Lisiane Lopes da Conceição^a, Tiago Antônio de Oliveira Mendes^b, Célia Lúcia de Luces Fortes Ferreira^c, Reggiani Vilela Gonçalves^d, Maria do Carmo Gouveia Peluzio^a

^a Nutritional Biochemistry Laboratory, Department of Nutrition and Health, Universidade Federal de Viçosa – UFV, Viçosa, Minas Gerais, Brazil

^b Department of Biochemistry and Molecular Biology, Universidade Federal de Viçosa – UFV, Viçosa, Minas Gerais, Brazil

^c Institute of Biotechnology Applied to Agriculture & Livestock (Bioagro), Universidade Federal de Viçosa – UFV, Viçosa, Minas Gerais, Brazil

^d Department of Animal Biology, Universidade Federal de Viçosa – UFV, Viçosa, Minas Gerais, Brazil

ARTICLE INFO

Keywords:
Synbiotic
Colitis
Colorectal cancer
Inflammatory bowel disease
Gut microbiota
Dysbiosis

ABSTRACT

Individuals with inflammatory bowel disease are at high risk of developing colitis-associated cancer; thus, strategies to inhibit disease progression should be investigated. The study aimed to explore the role of the synbiotic (probiotic VSL#3® and yacon-based concentrate) in a colitis-associated carcinogenesis model. IL-10^{-/-} mice were induced to carcinogenesis with 1,2-dimethylhydrazine and divided into two experimental groups: control and synbiotic. Manifestations of colitis, colon histology, expression of antioxidant enzymes, production of organic acids and intestinal microbiota were evaluated. The use of the synbiotic showed benefits, such as the preservation of intestinal architecture, increased expression of antioxidant enzymes and the concentration of organic acids, especially butyrate. It was also observed different microbial community profiles between the groups during the study. Together, these factors contributed to mitigate the manifestations of colitis and improve intestinal integrity, suggesting the potential benefit of the synbiotic in intestinal diseases.

1. Introduction

Individuals with inflammatory bowel disease (IBD), which includes ulcerative colitis (UC) and Crohn's disease (CD), are at higher risk of developing colorectal cancer (CRC) (Zheng & Jiang, 2016). Colitis-associated carcinogenesis (CAC) is the main complication of IBD in humans (Richard et al., 2018; Wang, Hua, et al., 2019; Wang, Li, et al., 2019) and is directly related to chronic inflammation (Potack & Itzkowitz, 2008). The risk for developing CRC is particularly relevant in patients with long-standing IBD involving at least 1/3 of the colon, and starts approximately 7 years after diagnosis, increasing linearly

thereafter (Clarke & Feuerstein, 2019; Zhou et al., 2019). For the UC, the cumulative risk of CRC is 2% at 10 years, 8% at 20 years and 18% at 30 years. The overall prevalence of CRC is shown to be 3.7% in patients with UC and 5.4% in patients with pancolitis (Eaden, Abrams, & Mayberry, 2001).

Although the mechanisms of association between IBD and carcinogenesis are not completely understood, it is believed that the malignant process is enhanced by the time, extent and severity of tissue inflammation (Herszenyi, Barabás, Miheller, & Tulassay, 2015). Chronic inflammation is responsible for the increase of a variety of pro-inflammatory cytokines, such as tumor necrosis factor (TNF),

Abbreviations: IBD, inflammatory bowel disease; CRC, colorectal cancer; CAC, colitis-associated cancer; PBY, yacon-based product; DSS, dextran sulfate sodium; TNBS, trinitrobenzene sulfonic acid; FOS, fructooligosaccharides; HPLC, high performance liquid chromatography; DMH, 1,2-dimethylhydrazine; CFE, food efficiency; SCFA, short chain-fatty acid; DAI, disease activity index; TNF, tumor necrosis factor; UC, ulcerative colitis; CD, Crohn's disease; MDA, malondialdehyde; CP, carbonyls protein.

* Corresponding author at: Department of Nutrition and Health, Universidade Federal de Viçosa, Avenida P.H. Rolfs, Campus Universitário S/N, Viçosa, MG CEP: 36570-900, Brazil.

E-mail addresses: brunacruz09@yahoo.com.br (B.C.S. Cruz), lisianelopes@yahoo.com.br (L.L. Conceição), tiagomendes@yahoo.com.br (T.A.O. Mendes), clferrei@ufv.br (C.L.L.F. Ferreira), reggiani.goncalves@ufv.br (R.V. Gonçalves), mcgpeluzio@gmail.com (M.C.G. Peluzio).

<https://doi.org/10.1016/j.foodres.2020.109721>

Received 6 April 2020; Received in revised form 22 July 2020; Accepted 9 September 2020

Available online 25 September 2020

0963-9969/© 2020 Elsevier Ltd. All rights reserved.